Summer 2021

The effects of rigid polyurethane foam as a confinement material on breaching charge detonations

Nathan Franz Paerschke-O'Brien

Department:

THE EFFECTS OF RIGID POLYURETHANE FOAM AS A CONFINEMENT MATERIAL ON BREACHING CHARGE DETONATIONS

by

NATHAN FRANZ PAERSCHKE-O'BRIEN

A THESIS

Presented to the Graduate Faculty of the

MISSOURI UNIVERSITY OF SCIENCE AND TECHNOLOGY

In Partial Fulfillment of the Requirements for the Degree

MASTER OF SCIENCE IN EXPLOSIVES ENGINEERING

2021

Approved by:

Dr. Kyle Perry, Advisor
Dr. Paul Worsey
Dr. Phil Mulligan

ABSTRACT

The effects of a rigid polyurethane foam used as a confinement material on four types of breaching explosives were tested, focusing on the changes in shockwave peak pressures, detonation load compression forces, and brisance cratering abilities. The Plate Dent testing procedure was modified to incorporate a load cell force sensor, and two air overpressure sensors were included adjacent to the blast to quantify each test result. The testing variables focused on the polyurethane foam cure times and thickness volumes around the breaching explosives to determine the breaching charges' optimal energy output capabilities when confined by the foam material. The rigid foam confinement increased the compression forces and brisance cratering abilities of all four tested explosives types as the foam cure times were extended and foam confinement radius increased. A reduction in the positive peak blast pressure was noted as the foam confinement material was increased. An increase in the peak blast pressure and compression force occurred when the polyurethane foam cure times were extended. When confined by the polyurethane foam, the average compression force was increased by 483% and the average Plate Dent depths were increased by 26.4%. The average blast peak pressure of a polyurethane foam confined detonation was 10% less than an unconfined detonation. This study's findings show how a breaching charge confined by polyurethane foam would provide a more damaging blast force to a structure while reducing the blast exposure to the breaching team performing the explosive breach.

ACKNOWLEDGMENTS

I would like to begin by thanking my committee members for all their time and efforts to help me accomplish my goals. My advisor, Dr. Kyle Perry, provided me an autonomous research methodology that allowed me to learn the essentials of a research study and was always readily available to correct my path when I become lost. Dr. Paul Worsey provided an endless wealth of knowledge and understanding of the explosive field that opened my mind to ample research possibilities. Dr. Phillip Mulligan refined my knowledge of the research process and focused on what questions I wanted my research to answer.

Next, I want to thank those often overlooked but essential for completing studies being completed. Dewayne Phelps of Missouri Science and Technology provided me with countless material resources and excellent connections to subject matter experts. My undergraduate research advisors, Dr. Tim D'Andrea and Dr. James Ayers, for providing me the foundations of my scientific knowledge and fueling my passion for science.

Finally, I want to thank my family for supporting me through all my crazy ambitions and goals to better myself. I would not have been able to make it to where I am without all your encouragement. To my son Cooper, thank you for coming into my life and giving me the ultimate reason never to allow myself to quit or to accept failure. I will always do everything in my power to assure a boundless future for you.

TABLE OF CONTENTS

Page

APPENDICES

LIST OF ILLUSTRATIONS

Page

LIST OF TABLES

Page

NOMENCLATURE AND ABBREVIATIONS

Symbol	Description
aka	Also known as
AN	Ammonium nitrates
ANNM	Ammonium nitrate nitromethane
BNC	Bayonet Neill-Concelman
C-4	Composition 4 explosive
CJ	Chapman-Jouguet
Dia.	Diameter
ft	Foot or feet
i.e.	In example
in	Inch or inches
lb.	Pound or pounds
lbf	Pound force
min	Minute or minutes
ms	Millisecond
NM	Nitromethane
oz	Ounce
P	Pressure
PETN	Pentaerythritol tetranitrate explosive
PPE	Personal protective equipment
psi	Pounds per square inch

RDX	1,3,5-trinitro-1,3,5-triazine explosive
RPF	Rigid polyurethane foam
s	Second
SOP	Standard operating procedure
t	Time
TBI	Tramatic brain injury
TexPak	Diethylenetriamine,8,11 explosive
V	Volts

1. INTRODUCTION

1.1. BACKGROUND

As conflicts between nations have continued to arise, the constant fighting among humanity has historically escalated to the war raging around the planet; thus, the improvement to wartime tactics has been ever evolving. The increase in population and the expanding urbanized development of countries have led to the transformation from rural-focused battles to guerilla-style fighting within urban environments. The progression in warfare tactics has modernized troops into developing and executing new interdiction tactics for enemy combatants embedded into urban populaces. The new guerilla wartime tactics often require troops to enter urban structures to hunt their enemies and generate breaching tactics (Marques, 2014).

Breaching of a structure is required when the breaching team needs access but cannot gain access without force. The technique of using an explosive to breach the building was historically the last resort because of the higher risks associated with handling and detonating the energetic material. Explosive breaching has been primarily used in urban environments, often with the uncertainty about what threats were waiting on the other side of the door. An explosive breach allows for a rapid entry into the structure and temporarily stuns the enemy combatants possibly waiting on the other side.

The explosives chosen for explosive breaching have traditionally been highly destructive yet lightweight for the breacher's carrying comfort. Breaching explosives and tactics have undergone alterations limiting shockwaves to ensure safety for the breaching team members in the proximity when explosives are detonated. A high-pressure shockwave

can result in traumatic brain injuries (TBI) or other possible health concerns (Kamimori, 2017) for a breaching team member.

This research aimed to evaluate the use of polyurethane spray foam as a confining material for high explosives charges by assessing the compression forces, shockwave peak pressures, and brisance cratering abilities for four types of high explosives that could be used for explosive breaching. The study focused on evaluating the explosive abilities when confined by polyurethane foam and compared the results to baseline charges with no foam. This research was designed to determine the explosive's performance changes when confined by rigid foam material to identify possible improvements to existing explosive breaching techniques. The experiment's testing was done in three rounds of testing. The first round of testing focused on analyzing the variables of confinement versus nonconfinement and the effects of extended foam cure time of four standard types of breaching explosives (C-4, DetaSheet, KineStik, and TexPak). The second round of testing studied the effects of variable foam thicknesses using smaller C-4 charges.

The testing for this research was designed to identify high explosives' critical parameters crucial for effective explosive breaching. The parameters of the explosives chosen were shockwave pressure, impulse, impact force, and brisance. These parameters were chosen to measure the different forces that would be applied when an explosive was detonated. The impact force and brisance would concentrate on evaluating the applied forces to the structure. The shockwave pressure and impulse would focus on the forces applied to the surrounding blast site that a breaching team would have to endure. Each explosive parameter required neccassary testing to establish a baseline measurement for each of the four breaching charge products selected. The baseline tests used explosives

detonated in an unconfined state and were the standard to compare the confining foam's variable effects.

1.2. LITERATURE REVIEW

The literature review for this study was set on determining previous research focused on the effects of high explosives confined by rigid polyurethane foam material. This literature review also was designed as an encompassing introduction of all the variant background understanding that led up to this study.

1.2.1. Breaching. The primary reason for breaching is to gain forceable access to a structure that was currently secured and inaccessible. Certain pertinent factors determine the physical and mechanic force level of a breach. These factors include noncombatants' presence, the need for stealth operations, the materials and tools at hand, and other determining force factors that a breacher needs to account for before choosing an appropriate force level. The structural material at the location which the breach would occur would also relate to the breaching technique required. If the access points were made up of a weaker material, a less forceful breaching method would be implemented, whereas a fortified structure would require a more aggressive technique (Lupoae M. , 2017).

The chosen force level of a breach determines which of five methods of breaching will be implemented. Breaching techniques focus on identifying the weak points of a location, such as doors or windows, and forcefully gaining access by physically damaging the weak point enough to obtain entry. Access could be achieved by breaking critical structural components on the desired access point, such as hinge points or lock points (Figure 1.1), to make the securing features fail.

The force levels of breaching a structure have resulted in current practices of breaching. A low force level breach, such as lock picking, ramming, or prying, is known as a mechanical breach (Figure 1.2). These less forceful breaching levels are typically used when access to breaching equipment is limited or when stealth is required. Although these low force breaching levels appear simplistic in logic, they need trained professionals to be appropriately implemented (United States of America. CA Patent No. 8794597B1, 2014).

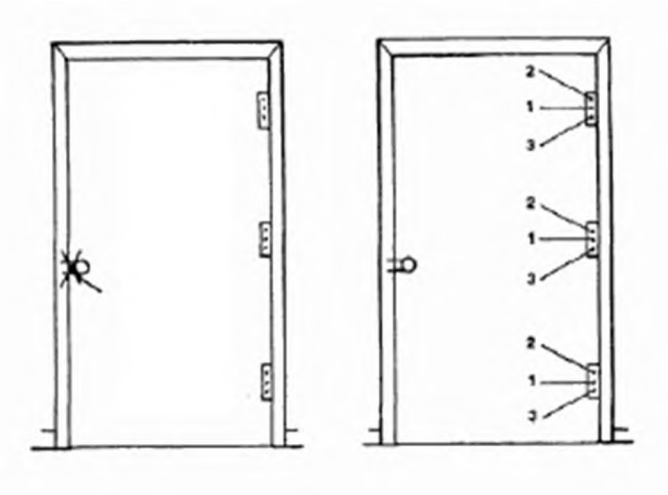

Figure 1.1. Structural weak points that are targeted for breaching operations (Department of the Army, 2006).

Another technique of breaching is called thermal breaching. This technique involves using an exothermic chemical reaction, such as an oxy-acetylene torch or thermite, to melt through the door and gain access to the desired structure (Figure 1.3). The thermal breaching method is effective against metal blockades, but this technique is time demanding due to the length of time required to cut through the metal barricade. Thermal breaching has been widely used by the military and law enforcement agencies worldwide due to its reliability and overall effectiveness against almost all structural materials.

Figure 1.2. Mechanical breach of a structure's door by use of a ram (Ranum, 2013).

Figure 1.3. A thermal breach being performed using an exothermic torch to cut a metal door handle (Cantrell, 2020).

Hydraulic breaching is performed like a mechanical breach, but instead of brute force to enter a structure, hydraulic breaching uses hydraulic pressure from a hydraulic actuator to separate the door from its frame (Figure 1.4). Both methods reduce a door frame's structural integrity and allow a door to be removed by exploiting the weak attachment points. This forcible entry style is a standard method in fire rescue operations and civilian law enforcement operations due to the minimal damaging effects on the individuals inside the structure.

Figure 1.4. A hydraulic breach tool being used to expand a door frame outward to the point of breaking to allow entry into the building (Hansen, 2017).

A more rapid and forceful level of breaching is known as ballistic breaching (Figure 1.5). A ballistic breaching technique uses a projectile accelerated from a weapon to damage the structure. Commonly, ballistic breaching of doors uses a buckshot shotgun to be fired multiple times at a door handle lock or the hinge points on the door. This breaching technique provides a rapidly deployable and effective breach against wooden and nonreinforced doors. Ballistic breaching has also been defined as a larger projectile or

weapon used to breach a structure, such as a tank round or an artillery round that impacts a building (United States of America/ CO Patent No. 5883328, 1999). The major downfall of ballistic breaching would be the exposure of pressures to the breaching team from firing the ballistic weapon due to the required proximity to the breaching event and the chance of injury from fragmentation. There is also the risk of fatal injury to possible hostages or bystandersinside the structure.

Figure 1.5. A ballistic breach demonstration of a cut-off shotgun being used to damage a door lock enough to gain access (TACTICAL-LIFE.COM, 2007).

The final technique of breaching to be considered is explosive breaching. This technique requires the highest force level breaching technique and is viewed as the most dangerous (Figure 1.6). Explosive breaching requires detonating an energetic material to weaken the target structure to gain access (Akers, Breaching of Triple-Brick Walls: Numerical Simulations , 2007). This method is technical and requires expert knowledge to

be implemented correctly but has proven effective on almost all structural materials (Cantrell, 2020). This style of breaching technique was the foundation of the investigation of this research.

Figure 1.6. United States Marines demonstrate an explosive breach using a linear shape charge centered on a wooden door (Long, 2013).

Explosive breaching is when a high explosive charge is detonated on the structure's point to gain a forceful access point. This technique requires an expert breacher to place a primed explosive directly on the proposed access point, then clear the immediate area and detonate the charge. The breaching team may immediately enter the structure through the blast's access point (Cantrell, 2020).

Explosive breaching requires breaching teams to be in proximity to the blast, allowing for a rapid entrance into the structure to eliminate the threats inside. The proximity could put the breaching crew in harm's way of experiencing overpressures and possible shrapnel from the blast occurring close to them. Several countermeasures have been previously implemented to protect the breaching team, such as body armor and blast shields. Other techniques have been longer lead-in wires to the detonator or extended delay-time fuses to allow the breaching team the ability to gain a greater distance from the blast (Hetherington, 1994).

Exposure to the blast waves of explosive breaching has adverse health effects on the exposed breaching teams. Results of proximity to the blast waves have been reported to cause Traumatic Brain Injuries (TBI), loss of hearing abilities, and systematic effects on the autonomic nervous, vascular, and immune systems (Committee on Gulf War and Health: Long-Term Effects of Blast Exposures; Board on the Health of Select Populations; Institute of Medicine, 2014). When an explosive detonation occurs, extreme gas pressures expand into the blast site location due to the tremendous amount of energy released. The human body's vulnerability to these elevated air pressures has been limited by implementing personal protective equipment (PPE) and greater distances from the blast site. The breachers need to be close to the beach location to rapidly enter the structure following the explosion, thus making breaching teams performing explosive breaches vulnerable to increased health risks. A substantial part of this study evaluated the changes in blast peak pressure intensities at a close distance to the blast site to determine if the polyurethane confined detonations produced safer breaching environments for the breaching teams to conduct tactical operations.

Composition 4 (C-4) or comp-four is a common explosive in both military and industrial fields. The C-4 used in this testing consisted of 91% plastic explosive 1,3,5-trinitro-1,3,5-triazine (RDX) bonded with a polyisobutylene binder (Figure 1.7) that allowed the material to be molded and shaped but would not fall apart easily. The mouldability and high-brisance capability of C-4, along with its other powerful explosive properties from a high detonation velocity, has made C-4 useful for demolition and breaching (Janssen, 2011).

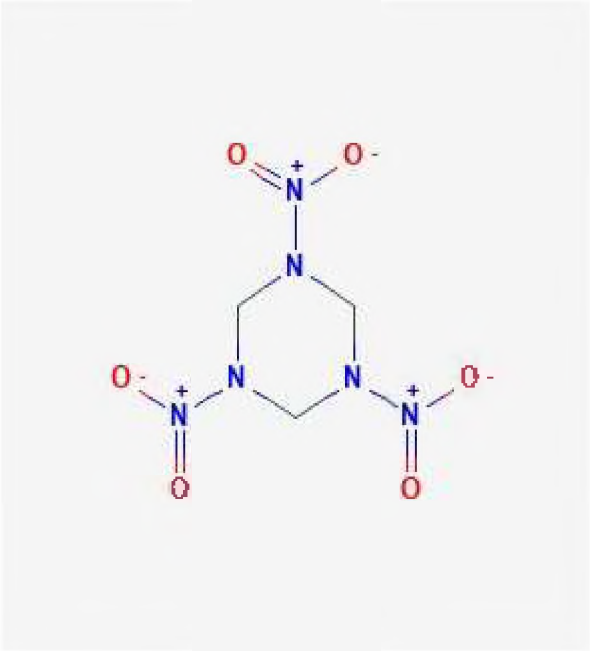

Figure 1.7. Chemical structure depiction on RDX (National Center for Biotechnology Information, 2021).

C-4 has been a common high explosive used for the explosive breaching technique. A C-4 breaching charge consists of a block of the energetic material molded together beforehand, with the block's size being determined by the structure that was planned on

being breached. The explosive block could be wrapped in a thin but durable plastic to help sustain molded shape and assist with environmental wear. At the breaching site, the breacher could insert a detonator through the plastic and imbedded into the C-4 material. This primed charge may then be attached to the breach point by wedging it securely or adhering to the explosive with double-sided tape. The breaching team would clear the relative blast site and detonate the charge to enter the structure (Elbeih, 2019).

Another common breaching charge explosive is known as DetaSheet. DetaSheet explosives are rubberized explosives made of pentaerythritol tetranitrate (PETN), nitrocellulose, and a binding agent (Figure 1.8). PETN, a nitrate ester compound, is insoluble in water resulting in an explosive that is highly water-resistant (Chemring Energetics UK Limited, 2007). This explosive is typically manufactured into twelve-inch wide, quarter-inch thick, and twenty-feet rolls cut down to operational sizes. DetaSheet is a cap-sensitive, energetic material capable of powerful detonating capabilities (Cooper, 1996).

DetaSheet is a standard selection for explosive breaching because of its demolition abilities and relatively lightweight. DetaSheet has been considered one of the more powerful and more brisant explosives available for demolition uses (Janssen, 2011). A breaching charge of DetaSheet can contain two, six-inch by twelve-inch rectangular strips of the quarter inch-thick material that were stuck together by taping the edges together. A double-sided tape may be applied to one side of the charge, and a detonator could be inserted between the two strips of explosive. The assembled breaching device could then be stuck to a breach point and detonated by the breacher in charge.

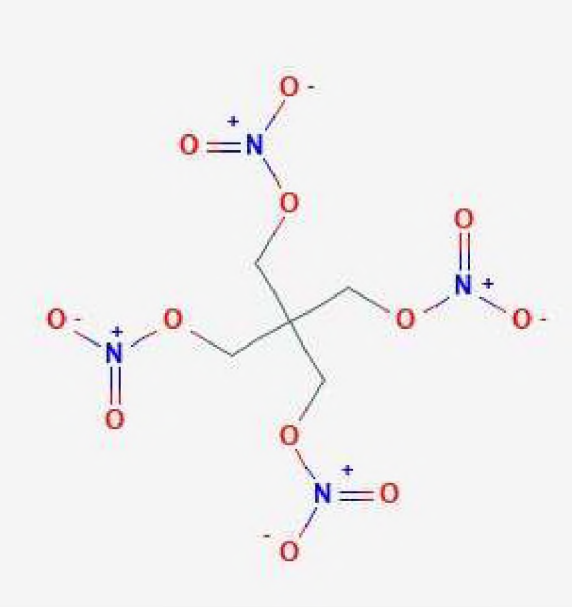

Figure 1.8. Chemical structure depiction of PETN (National Center for Biotechnology Information, 2021).

A KineStik charge is a binary charge that consists of ammonium nitrate (AN) products in one vessel and nitromethane (NM) in another vial. When the two products are separate and not mixed, they are less sensitive and not considered high explosive material. The AN alone is regarded as an oxidizer, and the NM is classified as a flammable liquid. When the AN and the NM are combined into a single vessel, ANNM, the two components become more sensitized and are classified as a high explosive. This binary explosive makes transport and handling of the energetic material safer. The KineStik binary explosive has vital detonation attributes that would make it ideal for explosive breaching usage (Bureau of Alcohol Tabacco and Firearms, 2014).

A KineStik explosive as a breaching charge allows the breaching team to transport and store the individual materials sealed in their respective vessels. When the breaching team was ready to use them, the team may insert the NM into the AN vessel and shake the

material until a consistent color is shown throughout the transparent container. Then, the breaching team would insert a blasting cap into the vessel's designed detonator well and adhere the charge to the structure with tape or wire. They would then clear the area and detonate the explosive to gain the necessary entry into the building.

Another binary explosive that has been introduced to the market of effective breaching charges is TexPak. This fully liquid two-part explosive comprises a mixture of diethylenetriamine and concentrated nitromethane (Figure 1.9). Like the KineStik binary explosive, the TexPak system is non-explosive when unmixed and classified as a corrosive and oxidizer. However, when the two parts are mixed, they fall into a 1.1 explosive classification. The TexPak system has beneficial attributes over the KineStik system as the TexPak charge is a fully liquid system that allows for instantaneous mixing and use. The KineStik system of Ammonium Nitrate solid prills and liquid nitromethane requires extensive mixing and reaction time to become a homogenous combination compared to the TexPak system.

The TexPak binary explosive manufactured by Tripwire Incorporated was designed specifically for tactical blasting operations. The two vials of liquid material are made to be one-third pound weight charges when mixed. The plastic canister comes equipped with a built-in blasting cap holding point to expedite the time requirements for priming the charge. The TexPak system can be primed with either a detonator or detonating cord and can be lodged into place or taped to a door's weak point that was being breached. The team would then retreat to a safe distance and then detonate the charge to access the structure.

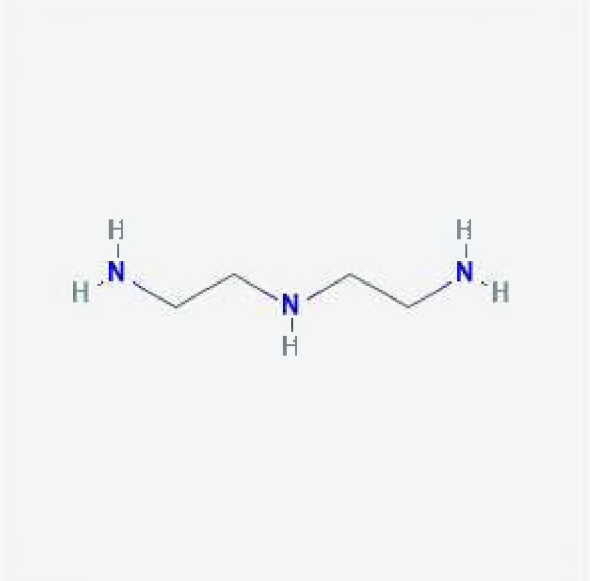

Figure 1.9. Chemical structure depiction of diethylenetriamine (National Center for Biotechnology Information, 2021).

1.2.2. Confinement of an Explosive. The understanding that when an explosive is detonated, the first law of thermodynamic immediately becomes relevant as energy is never created or destroyed. The energy stored in an explosive material is converted directly from chemical potential energy into kinetic energy forces. Following the second law of thermodynamics concerning entropy, the conversion of energy can never be 100%. A detonation's kinetic energy is less than the initial potential energy of an explosive due to energy loss to thermal and sound energy (Atkins, 2010). This energy loss means that a blast's energy would immediately become less than its initial potential value and would continue to dissipate as the kinetic energy expanded into the surrounding environment. In an open-air explosion of an explosive, the blast energy expands equally in all directions away from the point of detonation until an equilibrium of the system is reached.

The application of the first and second thermodynamics laws to an explosive blast would exploit the idea that the system's volume was limited to a closed system with boundaries that the explosion would occur. The same amount of energy in a small volume system would have a significant concentration of energy compared to the equal amount of energy in a more extensive volume system. The energy saturation would have a more substantial effect to cause destructive forces on the materials around it.

Confinement of an explosive blast is an attempt to limit the boundaries of the explosion's energy to focus the power of the explosion to cause more damage in the focused area. The blasting practice of confinement has been done to limit the blast forces from escaping the detonation point too rapidly and allowing for the blast's kinetic energy to be converted into compression and tension forces surrounding materials. This phenomenon is known as coupling of a charge and the effects to slow a blast's shock pressures to increase the chemical reaction rates occurring at the blast site.

The confinement of a charge limits the pressure rate decrease as the detonation front expanding outwards and results in a more effective chemical reaction zone of the blast. A more effective reaction zone means that an explosive's confinement makes the explosive's detonation more sustainable, thus creating a smaller confined explosive as useful as a larger unconfined explosive (Persson, 1994). The technique of explosive breaching follows the same aspects as industrial surface blasting of boulders. Boulder blasting uses high explosives to fracture and break the large rock into smaller, more manageable pieces. Licensed blasters use a technique called mud capping or adobe. These blasting techniques require an explosive charge to be placed on a boulder's surface and covering the charge with a mud casing (Figure 1.10). A charge detonated against a boulder's body allows four

breakage mechanisms to occur: shock wave transfer, sustained gas pressures, relief gas expansion bending, and flexural failure resulting in fractures (Ezekiel Enterprises, LLC), (Konya, 1990).

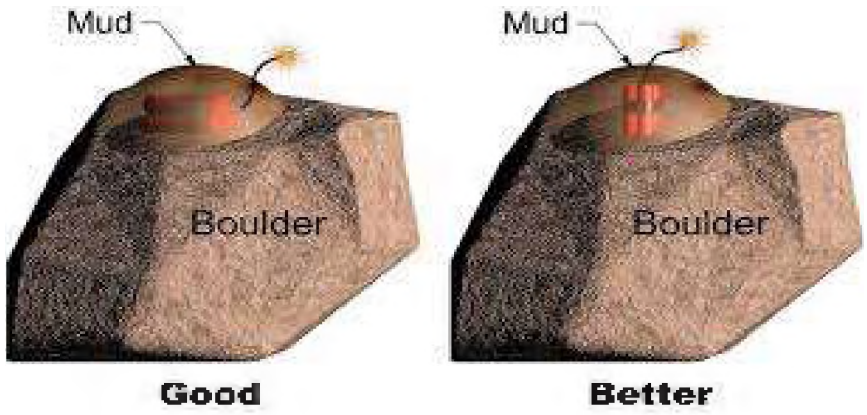

Figure 1.10. Placement of explosive charges relative to a boulder's surface using mud capping techniques (Ezekiel Enterprises, LLC).

The detonation shock wave is understood to be the weakest and least damaging mechanism from the blast. The shock wave causes microfractures to occur on the material's surface, but no significant damages occur. Sustained gas pressures from the high explosive detonation cause substantial damage to the material's surface by causing radial fractures to expand throughout the material. The radial fracturing causes splits throughout the material and weakens the sustainability of the material. The relief of the extreme gas pressures is an essential damaging mechanism to assist with the sustained gas pressure mechanism. The relief works in a perpendicular function to allow a bending effect of the material and further breakage of the material. Without the relief, the sustained gas pressures result in the blast cratering the material's surface instead of breaking the material's internal composition. The final mechanism, flexural failure, allows the material to push towards a free face and away

from the blast energy. The bending away from the blast location flexes the material until the material reached its maximum sustainable tolerance and then breaks the material apart.

Explosive confinement for boulder blasting by mud capping technique would amplify the blasts' damaging effects. The mud encasement limits the amount of blast energy that would escape the surrounding environment and directs the energy towards the boulder's surface (Figure 1.11). An unconfined charge's detonation would not have any substantial damaging effects. The blast energy would be lost to the surrounding air environment because of the energy following the least resistant path. An unconfined charge would result in a small cratering effect against the boulder, whereas a mud capped confined charge would have directed blast energy and more damaging mechanisms.

The last three mechanisms of a material's structural failure due to an explosive's detonation, such as boulder blasting, are the same mechanisms recognized in explosive breaching. A door or wall would experience radial fracturing from excess gas pressures, which would be amplified when the gas pressures reached the relief points of the opposite side of the door or wall. The final mechanism, flexural failure, would also be highly sought after in explosive breaching techniques. This mechanism would result in the wall or door bending inwards away from the blast point and result in an entry point into the structure.

Explosive breaching would be further related to commercial mining's understanding of coupling and uncoupling of charges in borehole blasting due to the same expectations of the physical outputs of the detonation of the explosives (Cevizci, 2013). In rock blasting, an explosive is loaded into a drilled borehole and detonated to fracture and weaken the material into smaller pieces. The explosive forces are transferred from the detonation point into the surrounding environment in material tension and compression

forces. These applied forces create excessive strain on the material, whether a rock face in a quarry or a door on a structure, which makes extreme shock wave loading energy that results in the material failure. The material's failure results in the required breakage of the material (Knepper, 2014).

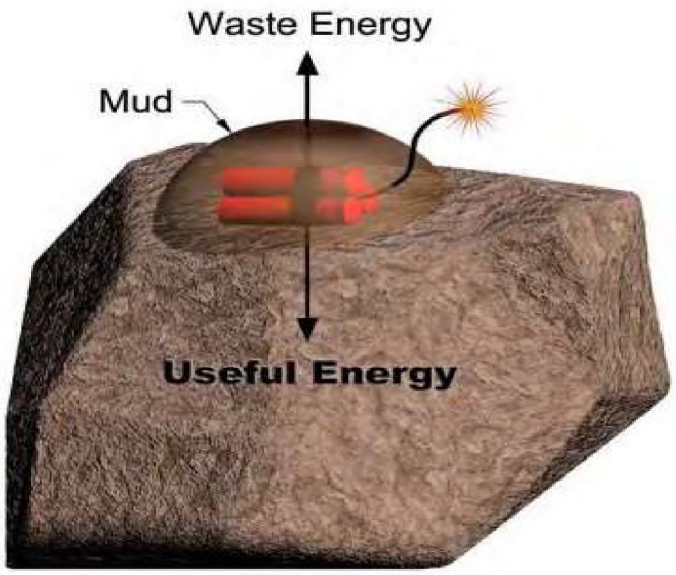

Figure 1.11. The effect of directing the blast energy of a charge by mud capping (Ezekiel Enterprises, LLC).

An explosive has been described as having the ability to apply six types of forces to a material's surface to cause damaging effects. Those six forces were tensile, unconfined compressive, confined compressive, confined shear, triaxial torsion, and triaxial loading. The comparison between unconfined and confined compression forces was chosen as the testing focus of this study. The understanding that with the confinement of an explosive, lateral energy forces' expansion could be limited, and the compression forces become more significant than an unconfined detonation (Persson, 1994). The more bonded and

interlocking the material is, the more influential the material would be to sustain the blast pressure and confine the blast (Feldgun, 2016). This study's initial testing addressed an unconfined comparison versus a confined explosive force using polyurethane foam material as the confinement material. This testing was designed to evaluate the work being done by the charge's detonation on the surrounding environment. The first round of testing also assessed the bonding and interlocking effects of the polyurethane foam by varying the foam's cure times to evaluate changes in the blast forces.

Previous testing for breaching charge evaluation has focused on such variables as structural material strengths and required explosive weights for adequate damage to successful breach (Akers, 2007). Another testing has focused on the effects blasting has on the breaching teams being close to the detonation and possible relations to traumatic brain injuries (Kamimori, 2017). Only one other relevant study was found that focused strictly on evaluating the effects of a breaching charge's performance when confined by a solid-state material (Lupoae M. , 2011). The study analyzed the possibility of water being used as a confinement material during an explosive breach. The water confinement breaching resulted in the water itself assisting in damaging effects by creating a cutting effect on the test breaching surface. The water jet resulted from the confinement water being accelerated by the detonation velocity of the breaching charge. The accelerated water system would prove useful damaging structural material requiring breaching but would possibly become a fragmentation hazard for the breaching team nearby. The effect of a cutting material jet formation would not be expected when testing the polyurethane foam material due to the density difference.

While the understanding that a denser inert confinement material would be a more useful material in limiting the blast forces' escape, the optimal thickness levels of a confinement material are unknown. This study's secondary testing focused on evaluating the polyurethane foam material's minimal thickness levels required to indicate a change in blast forces due to confinement. While the secondary testing would not determine a maximum amount of confinement material that may influence the detonation pressures to optimize the blast, the results would indicate a rate at which the confinement thickness affected the explosions. The confining material was evaluated for its effectiveness in changing the detonation forces of various explosive blasts.

1.2.3. Plate Dent Test. The analysis of an explosive's ability to perform damaging effects onto a given surface has historically been conducted to determine the explosive's strength level. Testing procedures, such as the crater dimension analysis of near-surface explosives (Cooper H. F., 1976) or the measurement of underwater explosive detonations test (Yancik, 1970), would be used to determine how an explosive would react when confined by a material and the effects that the blast would have on the surrounding area. Other explosive testing procedures, such as the lead block test (Snelling, 1912) or the cylinder compression test (TRZCINSKI, 2001), evaluated an explosive's relative strength by assessing the work done when the detonation of the explosive occurs. The plate dent test has been a simple and relatively affordable procedure that would allow for an explosive's strength to be evaluated and related to the chemical reaction's energy. The plate dent test procedure published by Los Alamos Scientific Laboratory (Pimbley, 1980) illustrated the plate dent test to be a quick and reliable way to analyze the relationship between an explosive's ability to impact a crater onto a steel witness plate's surface to the

detonation pressures. This procedure calls for a cylindrical shape charge to be detonated directly on a steel plate thick enough that the steel plate would not bend or warp but instead have a crater dent imprinted on the detonation surface (Figure 1.12). The resulting dent in the steel's surface would then be quantified by measuring the dent's depth (Figure 1.13) and then related to the explosive detonation pressure. This relationship demonstrated an explosive's ability to damage a material's surface within proximity to the detonation.

In the field of explosive breaching, an explosive's damaging effects to a material's surface would need to be known and understood to ensure that the proper explosive was used for the appropriate material to allow for a successful breach to be achieved. This understanding made the Plate Dent test the chosen testing procedure for this study's evaluation of a breaching charge's detonation pressure or brisance ability. Brisance of an explosive has been used historically to describe an explosive's ability to shatter or break a material such as steel, concrete, or any hard surface material (Persson, 1994).

This obsolete understanding of brisance has been modernized and updated as a relationship understanding between the of the Chapman-Jouget pressure (CJ pressure) or detonation pressure of an explosive relates the cratering ability of the explosive to the detonation pressures (Janssen, 2011), (Persson, 1994). While publications and studies exist that focus on calculating and testing for accurate brisance measurements and relating these values to the detonation pressure of the explosives to other explosives (Licht, 2000), this study was focused on determining the changes of brisance. This study was not focused on the determination of the exact brisance of the tested explosives compared to the previously published brisance's of explosives.

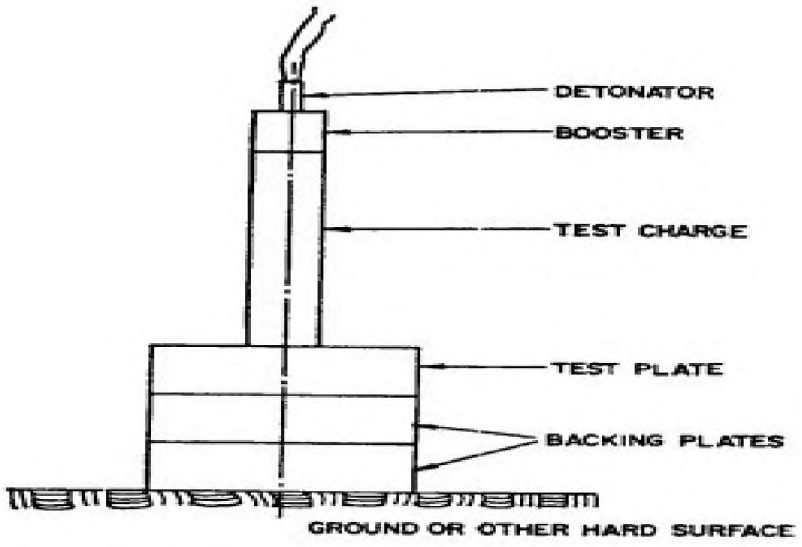

Figure 1.12. Sideview of original Plate Dent experiment test charge assembly (Pimbley, 1980).

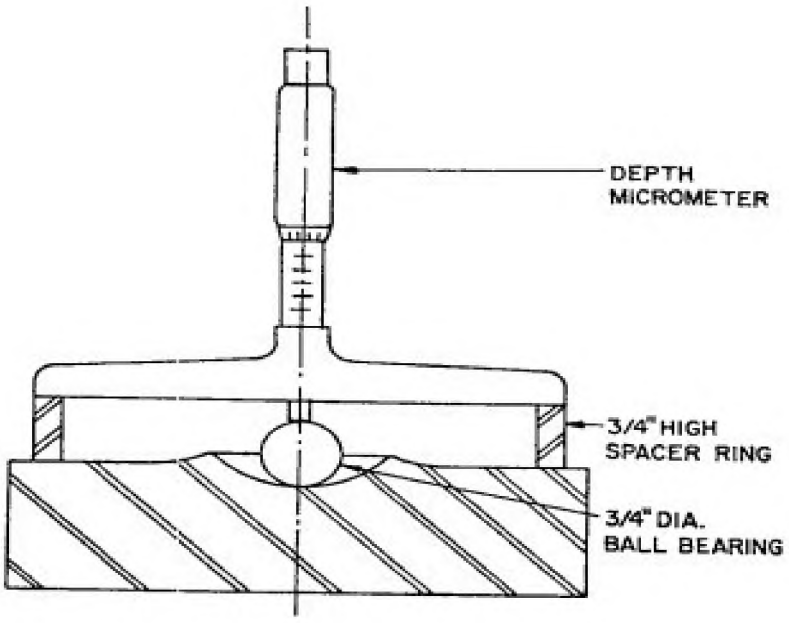

Figure 1.13. Measurement of Plate Dent experiment witness plate after test charge detonation (Pimbley, 1980).

1.2.3.1. Modifications of the Plate Dent test procedures. Although the Plate Dent testing procedure described by (Pimbley, 1980) provided an effective way to determine an explosive's brisance ability, the Plate Dent test did not incorporate modern scientific instrumentation. This limitation did not allow users to fully understand all the forces that an explosive was expelling when detonated. For this experiment, a few modifications to the prescribed Plate Dent procedure were performed to maximize the amount of data collected from a single detonation.

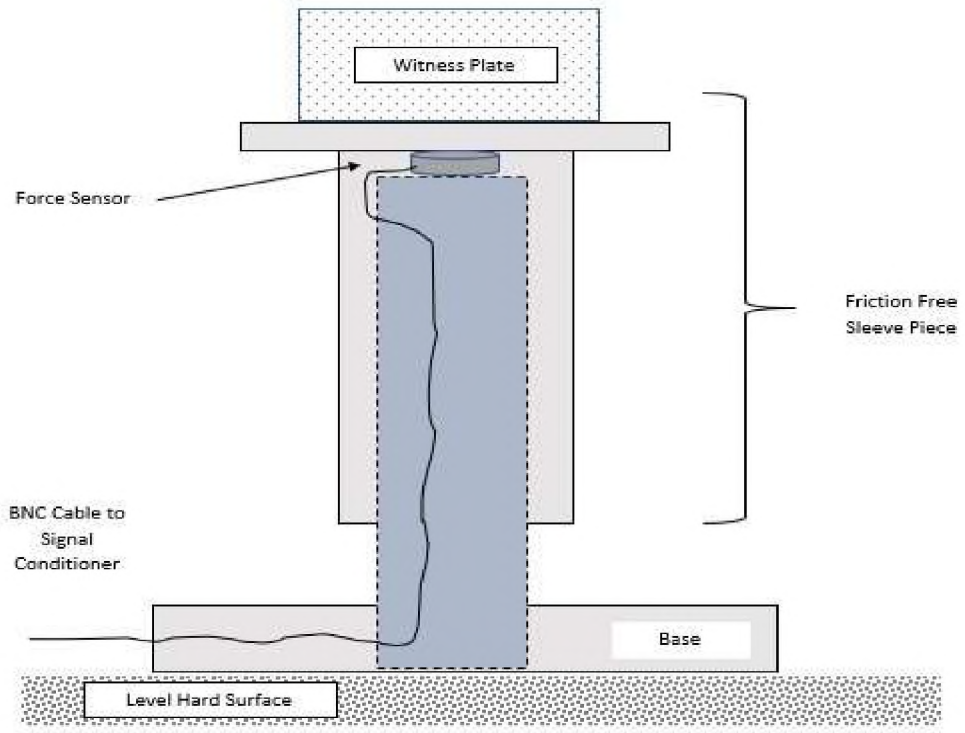

Figure 1.14. Fabricated steel platform device to house force sensor below test blasts of Plate Dent test.

The first modification incorporated a force load-cell sensor to measure the compressive strength produced by the explosive charge. The inclusion of this

instrumentation required the fabrication of a device that would securely protect the sensor from the blast wave but allow for the test plate's free motion to move. This realization led to the design and creation of the load cell housing structure (Figure 1.14). This device allowed for a secure platform for the Plate Dent test plate to be secured to a frictionless device that would transfer the blast's kinetic energy to the load cell sensor's compression forces to be recorded and analyzed. The new device provided all the needed testing requirements for analyzing an explosives force on a surface, with adequate protection of the instrumentation from the blast.

The final modification to the original Plate Dent procedure was to eliminate the requirement of testing and relating the explosives to TNT as a standard. The experiment was designed to determine relative changes in blast properties by utilizing polyurethane foam as a confining material. This experimental testing was not intended to focus on analyzing CJ pressures and comparing previously published data but strictly on the changes of the peak shock wave pressures, impact force, and brisance abilities of the selected explosives when confinement variables were altered.

1.2.3.2. Scientific instrumentation. The modifications from the (Pimbley, 1980) Plate Dent test procedure allowed for scientific blasting data to be incorporated into the explosive testing. The improvements would ultimately make a single detonation of an explosive capable of obtaining four data points (two pressures, a compression, and a Plate Dent depth) describing the blast versus a single data point. The testing procedure changes made each test more beneficial to determine if the polyurethane foam changes the blast effects' blast effects and makes testing more economical.

As in most modern-day experiments, scientific instrumentation was implemented to record accurate and repeatable data points. In the event of testing the physical parameters of explosives that occur almost instantaneously, the selected instrumentation needs to be capable of recording the needed data points within milliseconds of the detonation occurring. Blasting instrumentation typically use Piezoelectric quartz materials that transfer the input force to an output voltage. These instruments are professionally calibrated and maintained to ensure the experimental results were accurate and justifiable.

Once the instrument and a relative voltage is detected, the blast's force is outputted, the voltage needs to be processed through a signal conditioner. A signal conditioner will clean the voltages and eliminated possible signal noise interference. After the signal conditioner, the voltage needs to be recorded and stored by a data collection processor or a Data Trap.

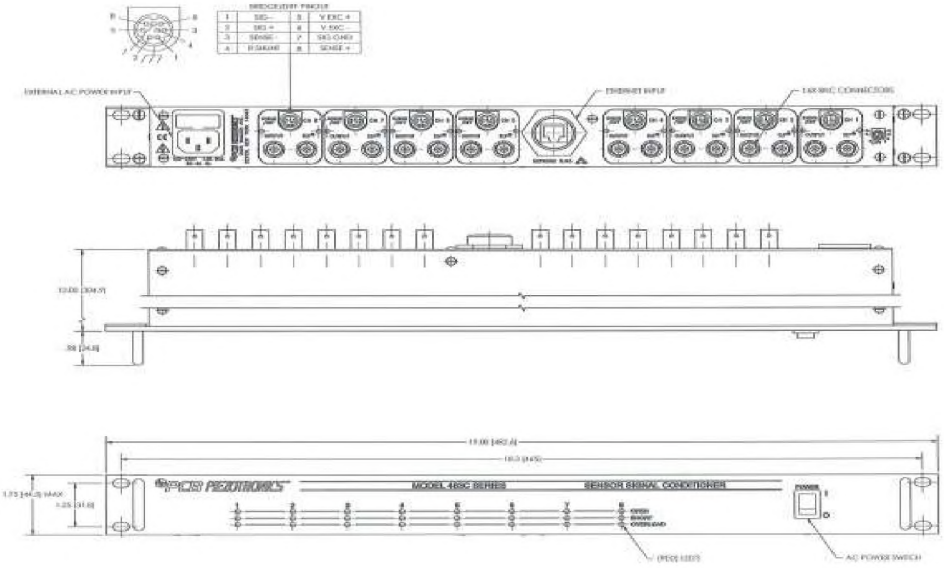

Figure 1.15. Diagram of Sensor Signal Conditioner unit used for testing (PCB Piezoelectonic , 2020).

A data acquisition system, such as an MREL Data Trap II, is commonly used in the blasting industry to monitor and record a blast's physical parameters. A Data Trap continually monitors the output signal from a signal conditioner (Figure 1.15) before the explosion occurs. Once an explosion occurs, the instrumentation would experience an increase or decrease in the instrument's output voltage, and the Data Trap could begin recording the data (Figure 1.16).

Figure 1.16. Data Acquisition System (DAS) unit manufactured by MREL used for data collection while testing (MREL Group of Companies Limited, 2021).

A standard instrument for determining an explosive's shock wave pressure is a pressure transducer. The two most familiar blasting pressure transducers are a pencil probe and a flush mount. The flush mount pressure transducer (PCB Piezoelectronics, 2020) can

be threaded into a steel plate and used to record pressures inside a sealed tank, such as a blast chamber (Figure 1.17).

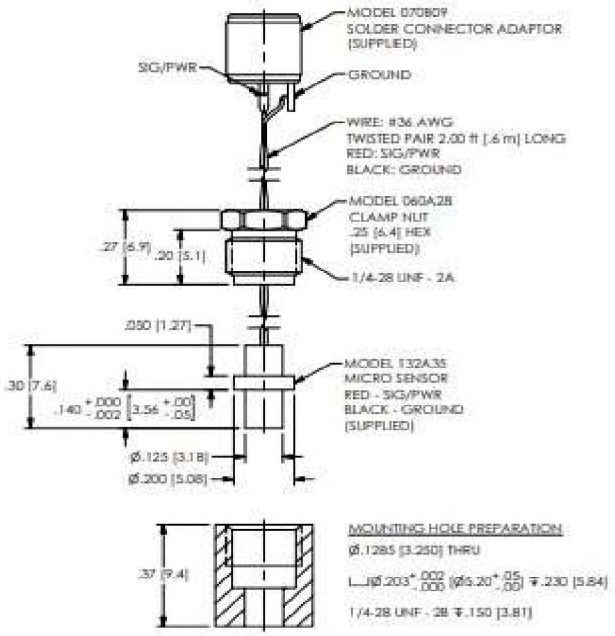

Figure 1.17. Flush-mount pressure transducer specification drawing (PCB Piezoelectronics, 2020).

A pencil pressure probe (Figure 1.18) is designed to be directed at an open environment detonation point and encounter the blast's shockwave as it passed by the instrument. One side of the pressure probe has a force sensor that transforms the pressure applied to the sensor's surface area to a corresponding voltage. Both pressure instruments can measure the force applied to the sensor and output a relative voltage to be recorded and analyzed.

Understanding a spherical shockwave front meant that although the probes were not in direct line with each other, the fact they had identical distances from the detonation

site would mean they would experience approximately the same pressures of the shockwave (Figure 1.19). This understanding allowed the collected experimental probe data to reflect roughly the same pressure values. Both probes would have been placed at similar distances from the detonation point to simulate the shockwave pressures that a breaching team would experience in a side-on stacked breach. The collected data would help evaluate if the polyurethane foam confinement material had any effects that may affect the breaching team.

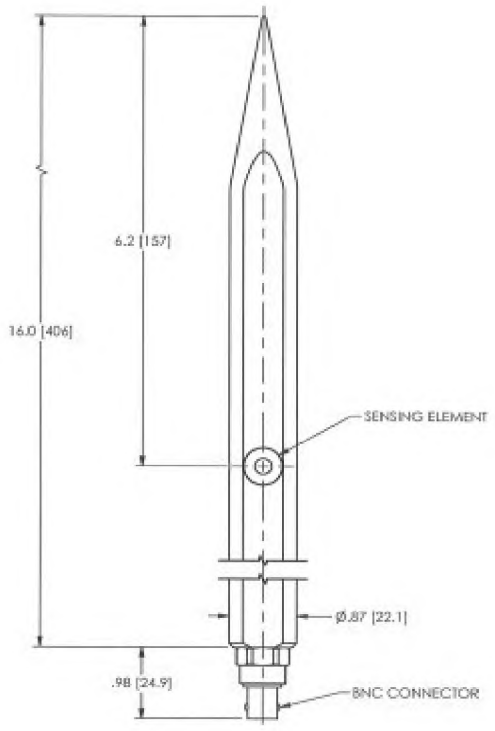

Figure 1.18. Diagram side view of piezoelectric pressure transducer selected for testing (PCB Piezoelectronics, 2020).

Understanding a spherical shockwave front meant that although the probes were not in direct line with each other, the fact they had identical distances from the detonation

site would mean they would experience approximately the same pressures of the shockwave (Figure 1.19). This understanding allowed the collected experimental probe data to reflect roughly the same pressure values. Both probes would have been placed at similar distances from the detonation point to simulate the shockwave pressures that a breaching team would experience in a side-on stacked breach. The collected data would help evaluate if the polyurethane foam confinement material had any effects that may affect the breaching team.

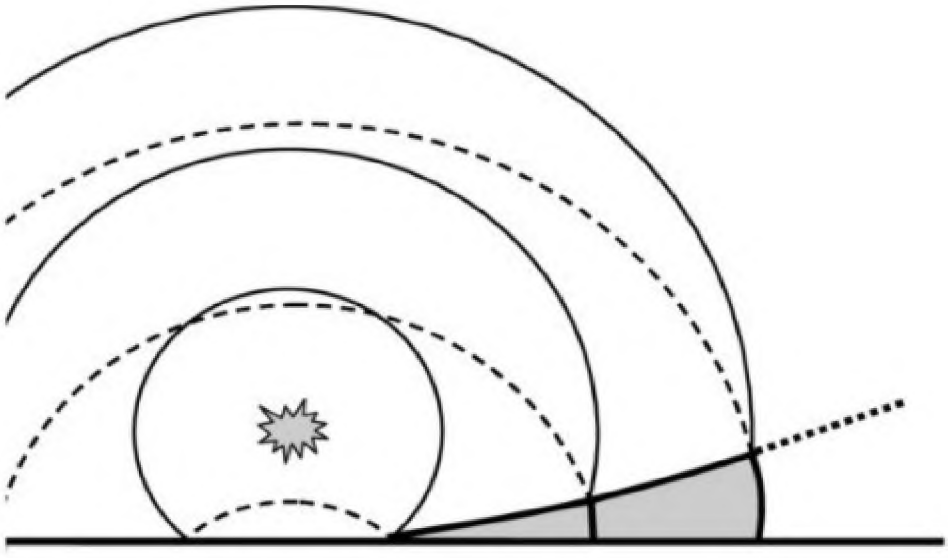

Figure 1.19. An illustration of a spherical blast wave as it expands away from the detonation site (Wunderli, 2014).

A force load-cell sensor is a scientific instrumentation capable of measuring compression and tension forces (PCB Piezoelectonics, 2020). The sensor's applied forces are converted into recorded output voltage and used to determine the sensor's load (Figure 1.20). This instrumentation is not typically exposed directly to the blast of an explosion but

more to determine the amount of kinetic energy applied to a point. This force is measured in tension, a pulling force, connecting the sensor at either side and stretching the sensor, or a compression force, by placing the sensor between two points and pushing the sensor ends towards each other.

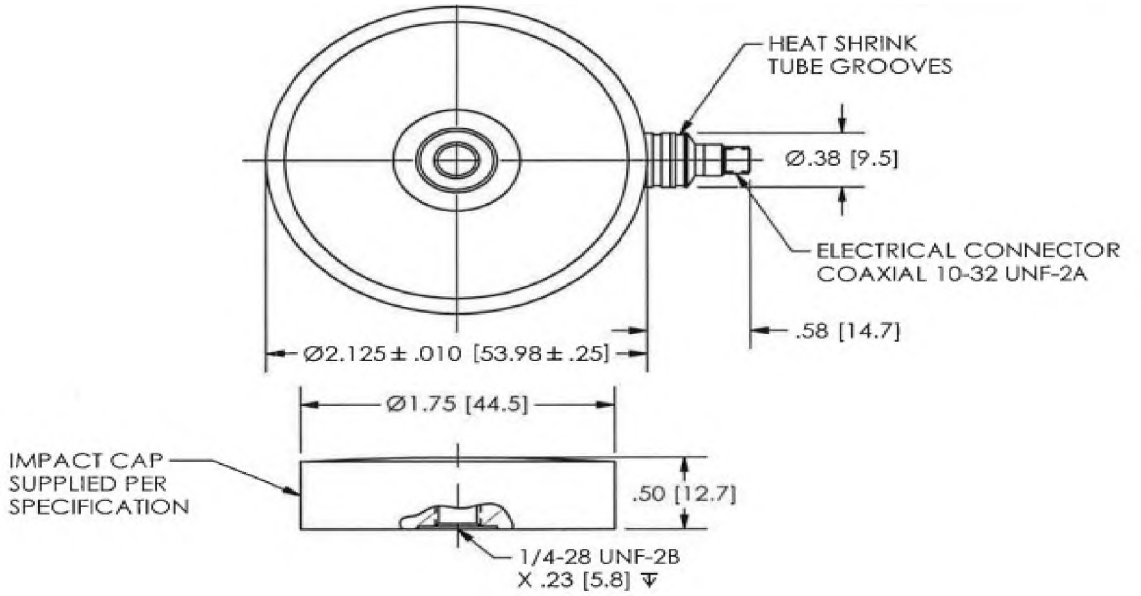

Figure 1.20. Specification illustration of the piezoelectric compression force load-cell chosen for experimental testing (PCB Piezoelectonics, 2020).

1.2.4. Polyurethane Foam. The polyurethane foam's attributes and physical properties made it an ideal candidate as a confinement material for explosive charges. Most commonly, polyurethane foam has been used as an insulation barrier in structural designs. The foam's ability to expand and fill air voids in unusual locations around pipes and wires makes it a desirable insulating product compared to other solid-state insulation. Most polyurethane foams are manufactured in an aerosol arrangement to allow for a pressurized release of the foam to be forced into tight places and distributed across large areas

efficiently, such as attics and walls. Some polyurethane foams are sold as unpressurized two-part liquid systems to be poured into the desired location, i.e., post holes or cinderblock centers, to replace concrete.

Polyurethane foam reactants consist of isocyanate and polyol resin blend polyols, which when mixed, undergo an oxidation reaction that forms Hydrazoic acid, water, and carbon dioxide products. As the organic compound's exothermic reaction occurs, the products expand and multiply the physical volume, resulting in a foam product (Figure 1.21). Once expansion has slowed, the foam surface begins to harden as the product cures. For this experiment's chosen polyurethane foam products, the manufactures reported the curing hardness levels in two phases.

Figure 1.21. A two-part liquid foam was combined and stirred to demonstrate the expanding reaction of polyurethane foam (Carpenter, 2011).

The first curing level was called “Tack-Free,” meaning the foam had been applied long enough to provide maximum protection to the surface without disruption or damage (Corrosion Pedia, 2017). The manufacture's datasheet estimated this time to be five to fifteen minutes after application of the foam. The final cure time was noted when the foam had been applied long enough that the polymer chemical reaction had reached completion

and the foam was fully set. The manufacturers estimated this full cure time to be eight hours after applying the foam (Grainger, 2020).

The polyurethane foam's attributes to expand and fill air voids within an applied area makes it an ideal material for stemming or confining a blast. The foam would be capable of filling a horizontal or vertical borehole, whereas crushed stone or water would not. Polyurethane foam has been previously tested as a confinement material for military uses as a counter to landmines (Alba, 1997). The idea of the testing was to coat the landmine field with a polyurethane foam material and allow safe passage of military vehicles across the hazardous area by either incapacitating the landmine triggering system or by confining the explosion of the landmines. The U.S. Navy's testing resulted in the findings that when the polyurethane foam was poured to certain thickness levels, blast mines' explosive effects were neutralized and made feasible for an alternative for counter-minefield option.

The Navy's Rigid Polyurethane Foam (RPF) study applied to this study following similar logic that the RPF would reduce the blast effects from one direction and direct the explosion in the opposite direction. The redirection of explosive power applied to a breaching charge would make smaller charges more damaging and explosive breaches more effective following commercial blasting's mud capping logic. The RPF confinement material would also provide additional protection to a breaching team from the blast effects by limiting the blast towards the breach site location. The RPF could also eliminate the production of any possible harmful fragmentation hazards due to the low density and

flammable material being burned up in the blast. The effects of explosives comfined by RPF could be greatly beneficial to improving an explosive breeach's force while protecting the breaching team performing the breach.

2. METHODOLOGY

2.1. POLYURETHANE FOAM AS A CONFINEMENT MATERIAL

This study focused on analyzing and determining any effects that rigid polyurethane foam (RPF) had when used as a confinement material around a breaching charge. The testing was designed to investigate the changes of compression forces, blast pressures, and brisance crater abilities on four types of explosives (C-4, DetaSheet, KineStik, and TexPak) using a modified Plate Dent procedure. The testing was focused on determining changes in peak shockwave pressure, impact compression force, and brisance abilities of a breaching charge confined by RPF compared to unconfined charges. Variables changed to determine explosive performance included foam thickness and foam cure-time (Table 2.1). The experiment test procedure was designed so that one detonation of an explosive would result in two pressure recordings, a force impact reading, and a plate dent depth.

Table 2.1. Outline of testing for Rigid Polyurethane Foam (RPF) confinement material encasing an explosive breaching charge.

	Chosen Variable	Explosives Tested	Explosive Weight (oz)	Expected Outcome
First Round	No Changes	C-4, DetaSheet, KineStik, TexPak	5.80 ±0.02	Baseline Data
Second Round	Foam Cure Time (3.5, 10, 20, 30 min)	C-4, DetaSheet, KineStik, TexPak	5.80 ±0.02	Confinement data and optimal foam cure time
Third Round	Foam Thickness	C-4	3.53 ±0.04	Optimal foam thickness

The initial testing was to collect baseline data values of unconfined charges. These unconfined charges were to collect baseline force values for each of the four types of explosives. The second round of testing focused on collecting data points of the standardized charges when confined by a spray RPF. The only change from the baseline testing was applying a 12-oz spray RPF to each charge with varying foam cure times. A data point was collected for a 3.5-, 10-, 20-, and 30-minute foam cure time for each of the four types of explosives. The goal was to determine any changes in the tested explosive parameters from the baseline due to the RPF confinement and respective cure times.

The third round of testing focused on determining an optimal RPF thickness to encase a breaching charge to maximize the desired blasting attributes. For this testing, C-4 was selected as a standardized breaching charge due to the positive results C-4 had in the previous rounds of testing. The test charges were reduced by 60% because of the outstanding RPF confinement results exceeding the instrumentation's limitations. The same modified Plate Dent procedure was used, with the only variable being the RPF thickness around each charge. Ten RPF blocks, with known varying dimensions, were tested by inserting the C-4 charge inside the RPF blocks.

The testing was not designed to compare the previously published performance properties of the chosen explosives to the experimental results. All established standard operating procedures of Missouri S&T's Experimental Mine (Department of Mining Engineering , 2017) were followed whenever handling or detonating explosive testing was performed.

2.2. SCIENTIFIC INSTRUMENTATION

The incorporation of scientific instrumentation was a vital step to collect valid data points for this study. Since a detonation occurs almost instantaneously, the use of specialized blasting instrumentation was necessary. All sensors measured the applied forces from the blast and converted them into an outputting voltage signal. The signals were passed through a signal conditioner and then recorded by an MREL data acquisition system. This advanced blasting system could capture the blast effects as they occurred and storing the data for later analysis.

The first instrument chosen to incorporate into the testing was a load-force sensor that measured the compression forces applied to the sensor. The fabrication of a sleeve-style device (Figure 1.14) to safely house the load sensor from the explosive forces but still record the work being done by the blast was needed. The sensor's cable was routed through the device and through steel-tubing to the signal conditioner to ensure no damage was done to the line. The load-cell was held centered on a lower stationary part of the sleeve device by a guide pin to ensure the sensor did not drift around on the plate. The upper non-stationary part of the sleeve device was slipped over the lower stationery. This upper non-stationary part of the device was designed to directly hold the Plate Dent test plate above the load cell sensor and slide straight downwards onto the load-cell. The upper non-stationary part of the device was built wide enough so that there were no contacting points to the lower stationary part of the device so that no friction between the two pieces would be experienced.

A pressure transducer system was incorporated into the testing design to record the shockwave pressures that the breaching charges were generating. In these experiments, two

pencil-probes pressure transducers were chosen to measure the blast's shock wave pressure forces at equal but different directional distances from the detonation point. Pressure probe one and pressure probe two were pointed at a ninety-degree angle from one another, mainly due to the underground testing facility's constraints. Since the testing was performed in an underground facility, these testing results would best be related to a breach inside of a structure, such as a building hallway entering a room, rather than an external structure breach. The pressure wave characteristics would be expected to be slightly different if performed in an open testing facility. Following (Stewart, 2013), a blast's shockwave could be understood to be spherical as it extended away from the detonation point. Both transducers were secured at heights level with the test charges.

2.3. PROCEDURE

The testing arena and instrumentation pieces were assembled as described in Figure 2.1, which shows locations and required testing equipment. The pressure sensor probes were selected to be set distance away from the detonation test site to replicate a breaching team's typical distance from the breaching location. The testing was performed to simulate a side-stack breach rather than a head-on breach. The underground testing location was equipped with only one entrance/ exit portal to improve site security during testing. The MREL Data Trap collection device and Piezo-electronic signal conditioner were located at the farthest possible point away from the blasting site, limited by the instrumentation coax cable lengths. This placement location was chosen to minimize blast forces from damaging the instrumentation. The blast site was within proximity of a ventilation fan to minimize harmful gases after the blasts occurred.

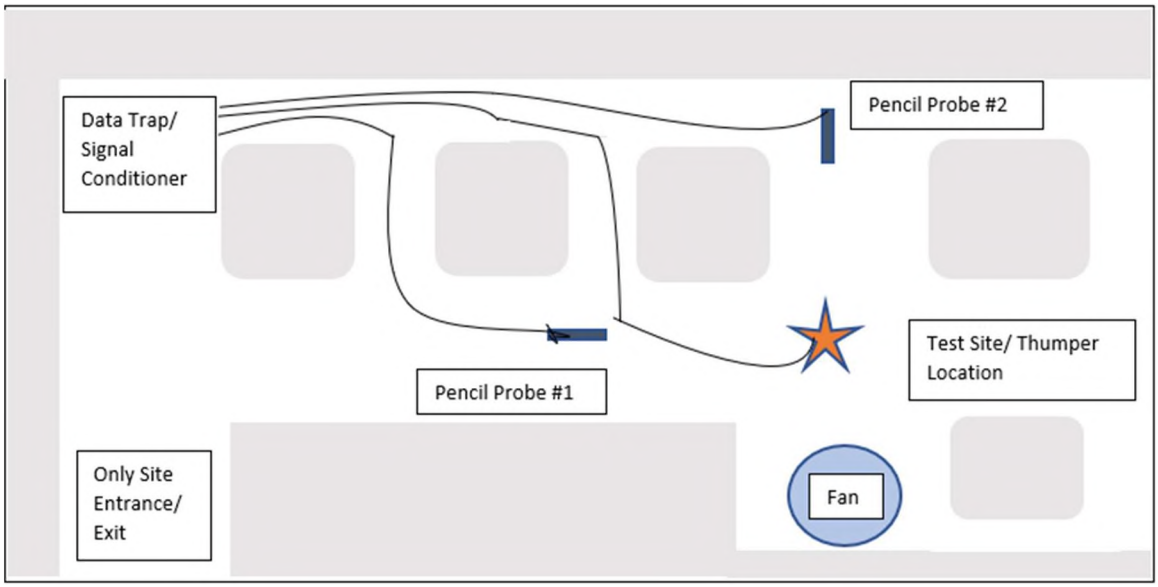

Figure 2.1. Underground testing site layout of instrumentation placement about testing detonation location. Pencil probe distances from the blast site varied on testing.

The original Plate Dent test (Pimbley, 1980) did not specify an explosive weight of the test charges but rather the dimensions of a cylindrical test charge of 1.625 inches in diameter and 8 inches tall. The unspecified weight charge was detonated by a blasting cap with a booster charge. In this experiment, the charge size was altered from a dimension limitation of the test charges to an explosive weight limitation. All the charges were still limited to 1.25-inch diameter, but the test charges' heights were varied to meet the explosive weight requirement. The Plate Dent witness plates were A36 cold rolled steel pre-cut into 6-inch square plates that measure 2-inches tall for all tests.

The experiment's desired outcome was not to compare relative explosive strength weights to one another but rather to compare the chosen breaching explosives' actual physical weight. The reasoning behind the charge's physical weight being the study's focus was to the relation to the actual weight a breach team member would endure carrying a

charge to the breach point. No boosters were used in this experiment as all the chosen explosives were cap sensitive, and a booster charge would not have always been equipped in the field. This alteration allowed the testing results to illustrate the breaching charges' capabilities as they would perform in real-life operations.

2.3.1. Unconfined Testing. Four types of breaching charges (C-4, DetaSheet, KineStik, and TexPak) were selected for testing. Three tests were performed for each of the four explosive types to determine a baseline for each of the tested explosive properties (peak shockwave pressure, compression impact force, and brisance crater ability). All explosive test charges were prepared in one-inch diameter, five-inch-tall plastic containers, or left in manufactured plastic packaging, meeting similar container dimensions. All test charges' total gross weight was set to have an explosive weight of 5.80 ± 0.02 ounces.

A prepared and pre-weighed test charge was placed in the center of a new Plate Dent steel witness plate located on top of the fabricated testing device (Figure 1.14) containing the force load-cell sensor. The use of electrical tape was implemented to secure the test charge upright on the witness plates. The tape was applied in minimal amounts to decrease any confinement changes that the tape may have caused (Figure 2.2).

An electric blasting cap was inserted into the explosive material or in the manufactured blasting cap well on the explosive container and connected to a lead-in a shot reel line. The MREL Data Trap was armed, and the testing site was cleared of all personnel. The explosive was then detonated, and auxiliary fans then ventilated the underground testing site for mandated times by the testing site's standard operating procedure (Department of Mining Engineering , 2017). Once the testing site's reestablished adequate air quality, the area was cleared safely by a qualified research member. The Plate Dent test

witness plate (example shown in Figure 2.3) was retrieved and labeled for later dent depth analysis. The sensor data collected by the MREL Data Trap was stored until testing was completed and then downloaded and analyzed using MREL Data Trap software.

Figure 2.2. Unconfined baseline test for TexPak charge using the fabricated device to protect the load-cell sensor below the blasting site directly.

Figure 2.3. Example of a Plate Dent crater on a witness plate to analyze an explosive's brisance cratering abilities.

2.3.2. Confinement Testing. The same procedure for RPF confinement testing was followed as the unconfined testing except for the foam's application. Once the 5.80 ± 0.02 oz charge was primed, an entire twelve-ounce can of spray polyurethane foam was dispensed, encasing the charge. The foam was relatively distributed around charge in the effort to cover the entirety of the test explosive (Figure 2.4). The RPF was cured for a variable amount of time (3.5-, 10-, 20-, 30-minutes) before the charge was detonated. The 3.5-minute cure time was the shortest time lapse to safely apply the RPF, secure the testing site, and detonate the charge. For the 15- and 20-minute cure time tests, an open-ended cardboard box was used to ensure no foam was spilled while waiting for the elapsed cure time to pass. The cardboard box was placed between the fabricated force sensor protection device's top platform and the bottom of the Plate Dent witness test plate.

Figure 2.4. Confinement test of TexPak 10-minute foam cure time.

Once the site was secured, and the RPF had cured for the prescribed amount of time, the test charge was detonated, and ventilating would occur. After air quality was deemed safe, the Plate Dent test plate was collected and labeled for later analysis for dent depth and dent radius. The sensor data collected by the MREL Data Trap was stored until testing was completed and then downloaded and analyzed using MREL Data Trap software. This confinement procedure was repeated for each of the four cure times (3.5, 10, 15, 20 minutes) for each of the four types of explosives (C-4, DetaSheet, KineStik, TexPak), totaling sixteen confinement trials.

2.3.3. Volumetric RPF Testing. Ten variant size mold canisters were selected with a ranging diameter from 2 to 18 inches (Figure 2.5). The molds were filled at least halfway with a mixed two-part liquid RPF resin and allowed to fully cure for 48-hours compared to the manufacture's specification cure time of twelve hours. The mold canisters were then removed with care not to damage the surface of the RPF. A 1.25-inch diameter, 5-inch-deep hole was drilled into the center of each of the cured foam blocks (Figure 2.6). The shortest measurement from the foam's outer edge to the drilled hole's edge was measured by a digital caliper and recorded as the RPF radius for each block.

At the explosive testing location, a change in the testing arena set up was made of the pressure transducer probes' locations compared to the previous testing. Instead of the pressure probes being equidistant from the blast location, the probes were placed at varying distances. One pressure probe was placed at ten-feet from the blast site, and the other pressure probe was placed at fifteen- feet from the blast site. The pressure probe placement change was done so that the positive peak pressures' effects could be analyzed as the blasting site's distance increased to determine changes in the explosion effects a breaching

team would experience. C-4 was selected as a standardized breaching charge due to the positive results the C-4 explosive had in the previous rounds of testing. The C-4 charges were reduced from 5.80 ± 0.02 oz. to 3.53 ±0.04 oz. for this round of testing because of the outstanding RPF confinement results exceeding the force load-cell sensor's instrumentation limitations in the second round of testing. The same modified Plate Dent procedure from the unconfined testing was used, with the only variable being the RPF thickness around each charge.

Figure 2.5. Ten rigid polyurethane foam blocks cast with variable dimensions used for volumetric confinement analysis.

The same procedure was used as the unconfined baseline tests apart from using a reduced C-4 charge and the RPF blocks confining the charges. Each RPF block was prepared individually by inserting a primed 3.53 ±0.04 oz., C-4 charge into the block's

previously drilled hole. The block was then placed directly on a fresh Plate Dent witness plate with the C-4 test charge centered on the witness plate. If needed, the foam block was secured firmly to the witness plate using tape. The same testing procedures were then followed until all ten RPF blocks were tested, ensuring to label each witness plate properly after each test for later analysis of plate dent depth and dent radius. The sensor data collected by the MREL Data Trap for the volumetric confinement testing were stored until testing was completed and then downloaded and analyzed using proper MREL Data Trap software.

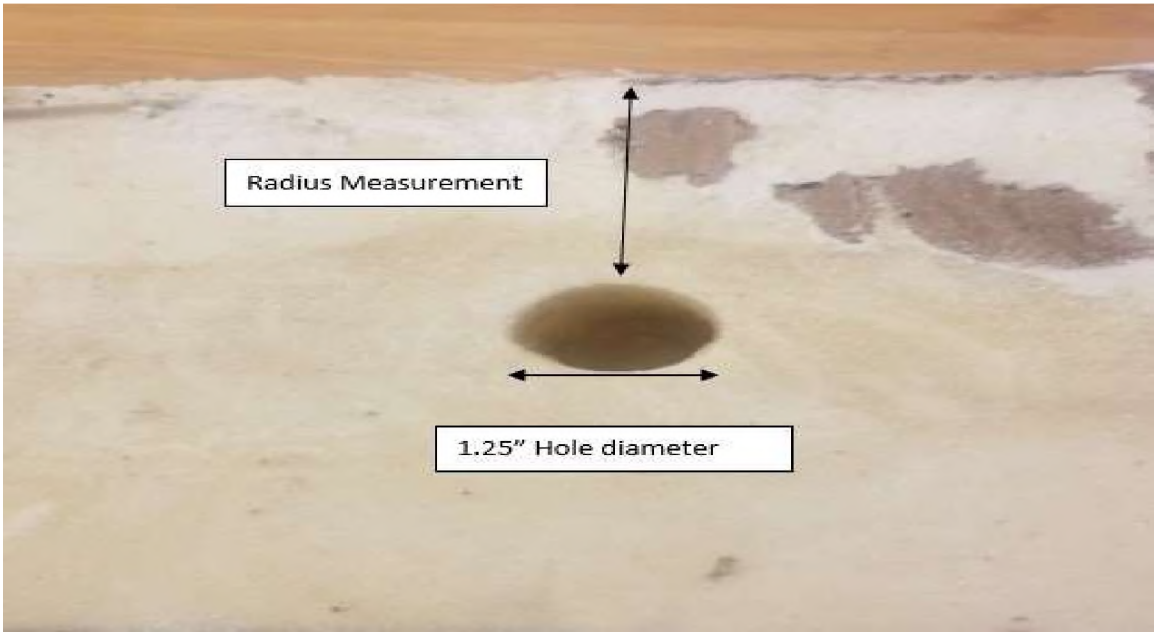

Figure 2.6. Rigid polyurethane foam block drilled hole diameter and block radius measurement.

2.3.4. An Example of a Single Test Charge Blast. An empty pre-weighed plastic test canister was tightly filled with 5.80 ± 0.02 ounces of C-4 material. A shunted electronic blasting cap was inserted in the top of the test charge at least three-quarters of the blasting

cap length and ensuring actual contact with the C-4 material by packing the explosive material around the blasting cap. The assembled test charge was then carefully placed on the center of a new steel witness plate centered on top of the fabricated device (Figure 1.14) containing the compression force load-cell. The testing instrumentation was verified to be in working conditions by demonstrating status lights on the piezoelectric signal conditioner, which did not indicate a short or open in the circuit. The MREL Data Trap was armed by pushing the "Next Test" button, followed by pressing the "Arm" button. This arming sequence was verified by the MREL Data Trap illuminating a red light labeled "Armed." All personnel secured the testing area, and each trial detonation followed the S&T's Experimental Mine standard operating procedure for underground blasting (Department of Mining Engineering , 2017). After the blast, auxiliary fans then ventilated the blast site for approximately fifteen minutes before anyone reentered the detonation location. Once a safe air quality was reestablished and deemed non-hazardous by the blaster in charge, the area was inspected for the test charge's proper detonation. The witness plate of the test charge detonation was collected and labeled adequately for analysis later. The instrument data collected by the MREL Data Trap was stored until testing was completed and then downloaded and analyzed using proper MREL Data Trap software.

2.3.5. Data Analysis. After the detonation was completed, all the piezoelectric instrumentation data was collected and stored by the MREL Data Trap. The stored experimental data was downloaded from the MREL Data Trap using a software system by MREL Blasting Instrumentation called "DAS Data Acquisition Suite" (MREL Blasting Instrumentation, 2020). The software sorted the collected data by trial number. Each test was then further sorted into the corresponding channel of each instrumentation sensor.

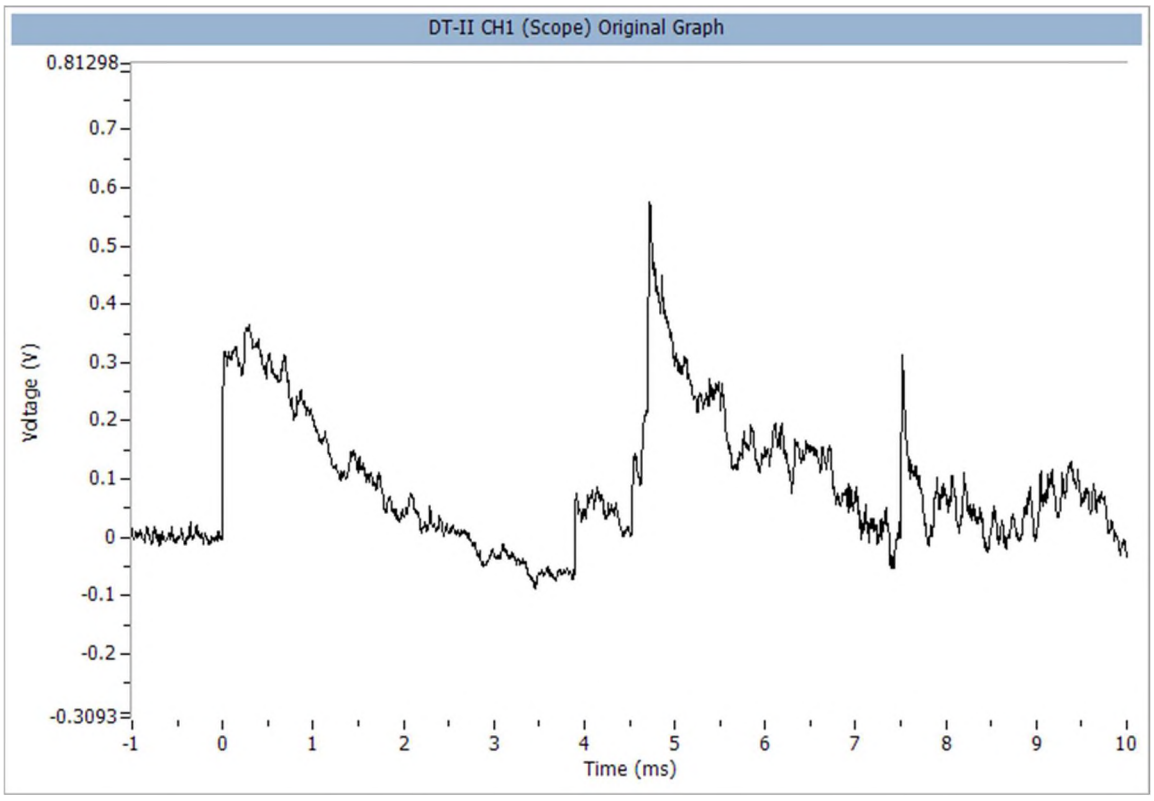

Figure 2.7. Raw data graph of voltage recorded during TexPak baseline test by channel one pressure transducer sensor.

The data collected by each instrument was displayed in a channel-specific graph (Figure 2.7) with recorded instrument voltage (V) on the y-axis and time (ms) on the x-axis. The MREL software was then used to apply the appropriate unit conversion to the data collected using calibration sheets for each respective instrument. The pressure sensors data was converted from volts (V) to pounds per square inch (psi). The compression force sensor data was recorded in volts (V) and converted into pound-force (lbf). The MREL software then displayed the test data in the proper unit graphs (Figure 2.8). The positive peak pressures and the compression force for each trial could be determined and recorded for analysis.

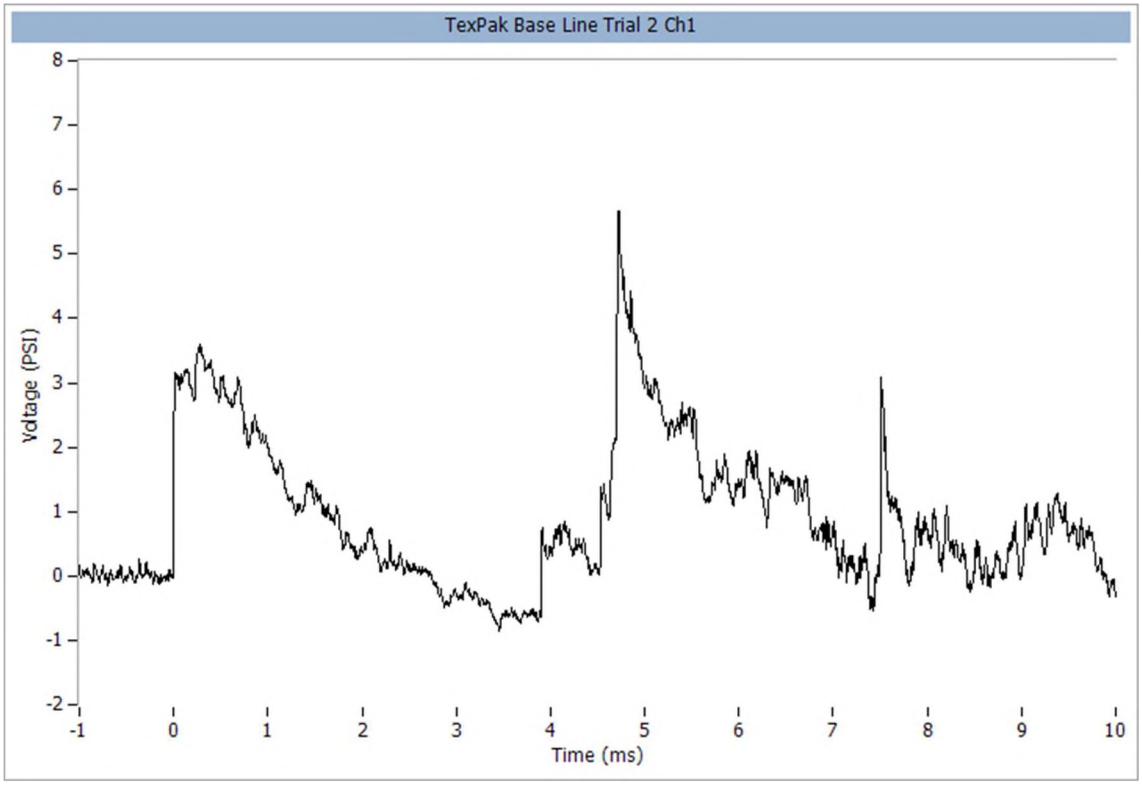

Figure 2.8. Converted data graph of pressure recorded during TexPak baseline test by channel one pressure transducer sensor.

3. TEST RESULTS

3.1. RESULTS OF BASELINE AND CURE TIME CONFINEMENT

The results found from this study were collected by the MREL Data Trap System and processed using the associated software. The Plate Dent data was manually recorded. These collected data points were consolidated into these findings.

3.1.1. Plate Dents. The Plate Dent test demonstrated the four types of explosives' brisance abilities by creating a blast crater on the six-inch square, two-inch-thick A36-steel witness plate. The crater depth was measured for each test with a digital depth gauge with a magnetic stand for stability. The depth gauge was zeroed using the witness plate's undamaged part, and then the deepest point of the crater was found by passing the depth gauge over the entirety of the cavity to find the most significant value measured by the depth gauge. Each test's crater radius was found by measuring the crater's greatest diameter using a digital caliper. All crater dimension values were recorded in (Table 3.1). The Plate Dent results were averaged respectfully of the three unconfined tests for each of the four explosive types to establish a baseline value.

The baseline testing results depicted the four types of tested explosives (Figure 3.1). The baseline testing showed a difference in the explosives' strengths, with the TexPak binary explosive being the most damaging explosive with a crater depth of 0.388 ± 0.005 inches. The averaged dent depth was approximately twice as deep as the DetaSheet depth (0.189 ± 0.005 in.), four times deeper than C-4 depth (0.088 ± 0.005 in.), and eighteen times more profound than the KineStik crater depth (0.021 ± 0.005 in.).

The unconfined KineStik explosives tests were unable to damage the witness plates. No dent depths were visible on the witness plate except in one of the three initial trial detonations. Several additional retrials for the KineStik baseline trials were executed, but no cratering was seen on the witness plates. This resulted in several data points for the KineStik explosive to be left undetermined.

Table 3.1. Measurements of the depths (in.) of the craters created on witness plates by the tested explosive charges.

	Baseline Average	3.5 Min. Cure	10 min. Cure	20 Min. Cure	30 Min. Cure
C-4	0.0875	0.0875	0.1011	0.1025	0.1130
DetaSheet	0.1893	0.2348	0.2515	0.3050	0.3305
KineStik	0.007	No Dent	No Dent	0.0245	No Dent
TexPak	0.3887	0.4100	0.4305	0.5100	0.6010

The tested DetaSheet charges would create good craters in the Plate Dents, but the crater dent depth and crater dent radius were noted to be inconsistent. These variations were likely due to the select loading procedure utilized for preparing the charge. The DetaSheet charges produced a swirling style crater in the test plate due to the DetaSheet being a sheet explosive and being rolled to fit into the experimental plastic charge containers (Figure 3.2). For any future testing of DetaSheet explosives using the Plate Dent test, a different loading procedures would be recommended.

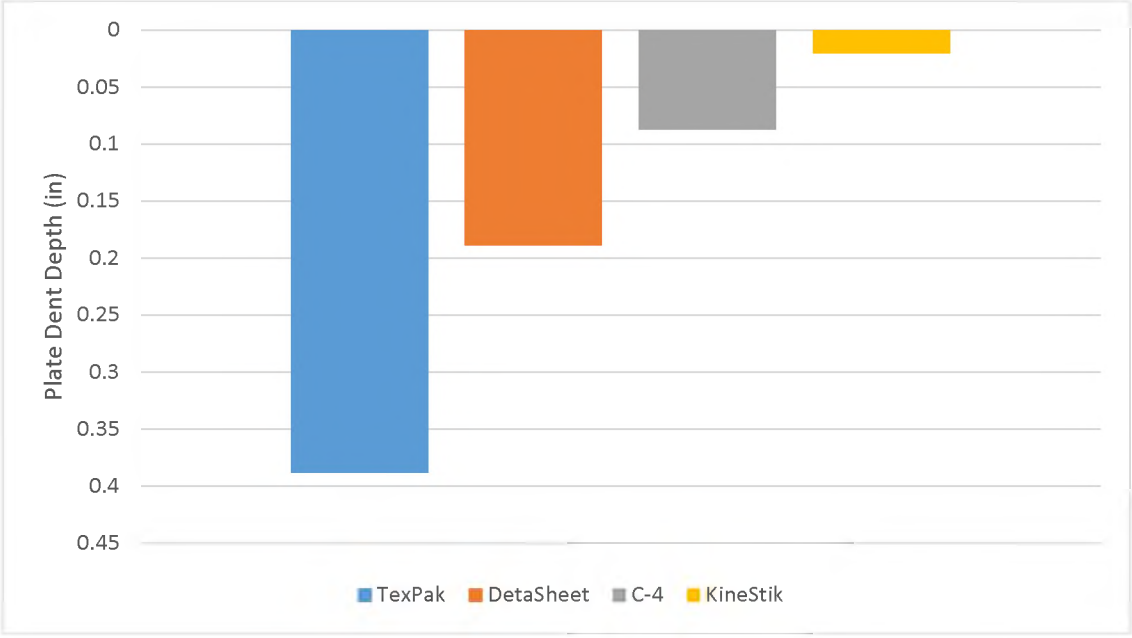

Figure 3.1. Unconfined averaged baseline Plate Dent witness Plate Dent depths of the four tested explosive types.

Figure 3.2. Unconfined DetaSheet Plate Dent baseline trial showing the inconsistency in cratering due to chosen loading procedure.

The variable cure time RPF confined detonations were evaluated the same as the unconfined detonations by measuring the crater depths (Table 3.1). The variances of cure times of the polyurethane foam confined detonations were compared to determine blast effects changes because of longer foam cure times (Figure 3.3 - Figure 3.4).

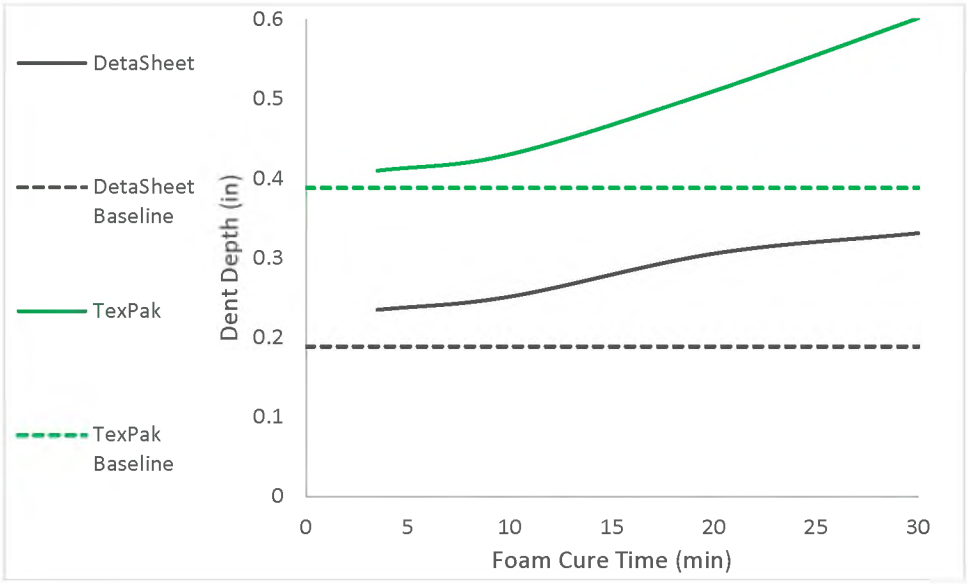

Figure 3.3. Measured Plate Dent crater depths with variable rigid polyurethane foam cure times for DetaSheet and TexPak explosives. The solid lines are the Plate Dent depths confined by variable cured foam, whereas the dashed lines are respective explosive' unconfined average Plate Dent depth.

Comparing the confining RPF dent depths with varying cure times of 3.5-, 10-, 20-, 30-minutes indicated a linear relationship for C-4 and TexPak. The C-4 dent depth increased by 29% from a 3.5-minutes cure time to a 30-minute cure time. The TexPak experienced the largest dent depth increase of 46% from a 3.5-minutes cure to a 30-minute cure time. A logarithmic rate of change was fitted for the DetaSheet dent depth as the RPF cure time increased. A 41% dent depth increase occurred by curing the confinement RPF

for 30-minutes as opposed to 3.5-minutes. The KineStik explosives could not provide appropriate data points for cratering as the only notable dent occurred on the 20-minute cure time trial. The other KineStik trials resulted in no damage done to the witness plates even after repeated attempts were performed. The three other explosives tested followed the trend that the longer the foam could cure, the deeper the dent depth was found.

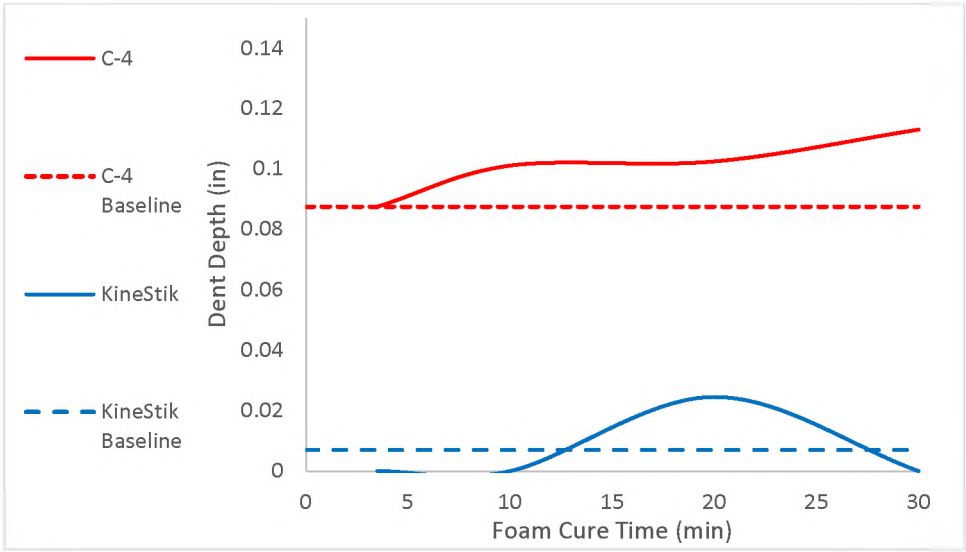

Figure 3.4. Measured Plate Dent crater depths with variable rigid polyurethane foam cure times for C-4 and KineStik explosives. The solid lines are the Plate Dent depths confined by variable cured foam, whereas the dashed lines are respective explosive' unconfined average Plate Dent depth.

3.1.2. Pressures. The shockwave peak pressures of the blast of a breaching charge needed to be determined during testing to identify the changes in pressure that a breaching team may experience in the proximity of the explosion. The four types of explosives tested, confined and unconfined by the RPF, were detonated fifteen feet from two pencil pressure probes placed perpendicular. The peak pressures recorded by both pressure probes were recorded in voltage converted to pounds per square inch (psi) by MREL software.

Table 3.2. Recorded blast pressure (psi) of unconfined and polyurethane confined detonations.

	Baseline Average	3.5 Min. Cure	10 min. Cure	20 Min. Cure	30 Min. Cure
C-4	3.7026	3.4954	3.5467	3.7121	3.8354
DetaSheet	3.6530	3.0850	3.2727	3.6100	3.6566
KineStik	1.5858	1.5162	1.6992	1.6918	1.8181
TexPak	4.6584	1.9579	2.0131	3.4403	3.7174

The four types of explosives were each detonated three times in an unconfined, free-field set-up to collect a baseline of the peak pressure expected from an open charge detonation. The unconfined explosives' positive peak pressures were averaged (Table 3.2) between the two pressure probes for each shot and compared to the other tested explosives (Figure 3.5 - Figure 3.6). This data combination was possible because the pressure probes being the same distance from the detonation site and the understanding of spherical detonation shockwaves.

A notable difference was seen between the tested explosive's peak pressures. The TexPak charges had the highest average peak pressure of 4.6585 ± 0.0001 psi, in contrast to the KineStik charges had the lowest averaged peak pressure of 1.5858 ± 0.0001 psi. This difference in peak pressure forces would be critical information for a breaching team to consider when selecting a breaching charge. This determination would be a set standard to select a safe proximity that a breaching team would need to be from the blast location to ensure minimal health risks.

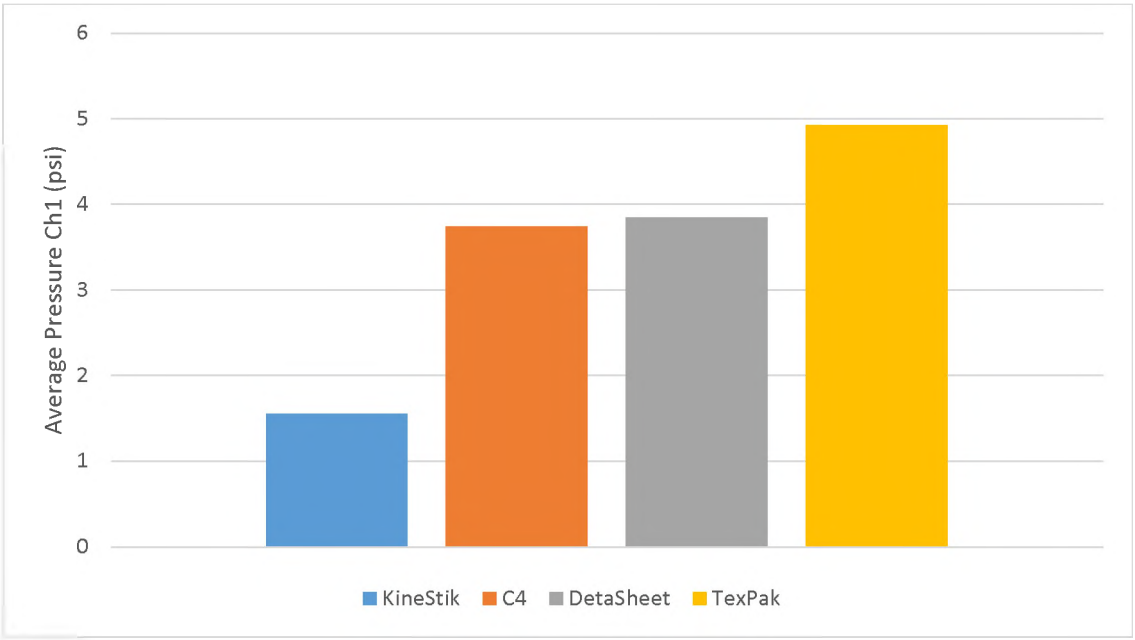

Figure 3.5. Averaged positive peak pressures were recorded at 10 feet by channel one pencil probe of unconfined explosives.

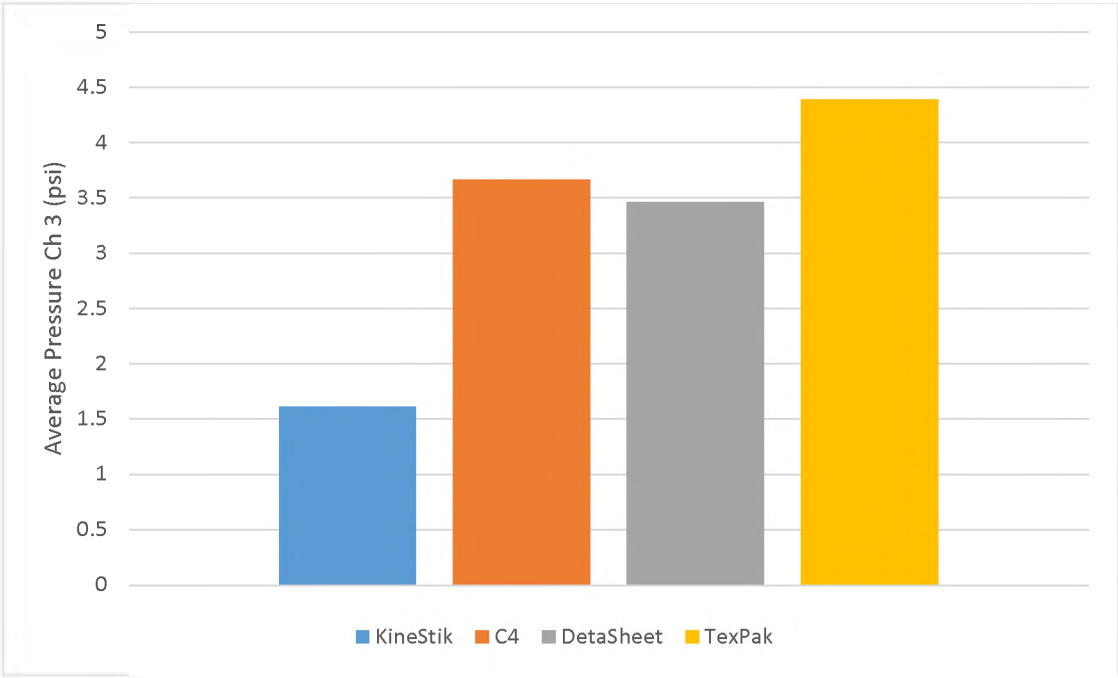

Figure 3.6. Averaged positive peak pressures were recorded at 15 feet by channel three pencil probe of unconfined explosives.

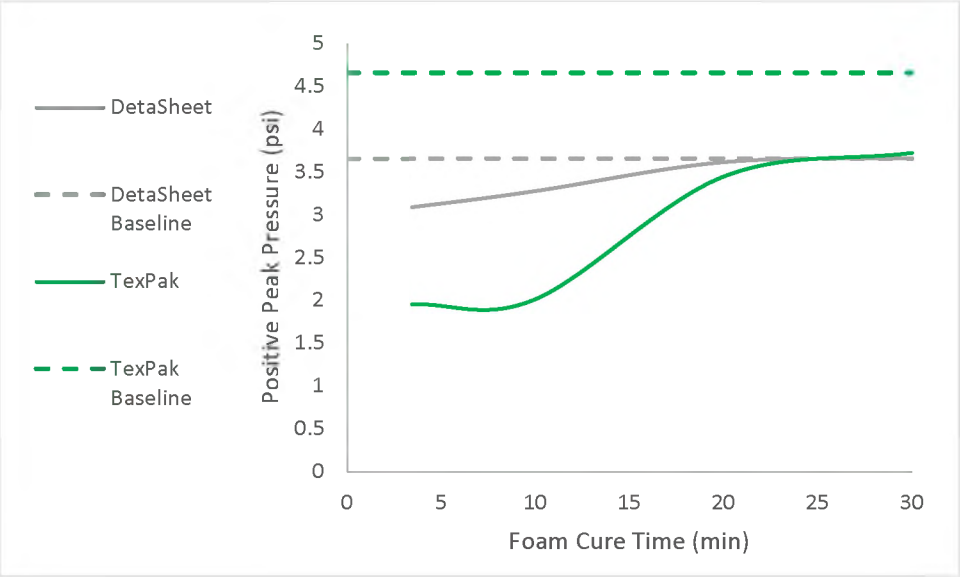

Figure 3.7. Recorded positive peak pressures with varying rigid polyurethane foam cure times for DetaSheet and TexPak explosives. The solid lines are the peak pressure confined by variable cured foam, whereas the dashed lines are respective explosive' unconfined average peak pressures.

The RPF peak pressures with varying cure times were averaged between the two pressure probes and the relative tested explosives' peak pressures. The collected data (Figure 3.7 - Figure 3.8) showed the effects of the breaching charges' peak pressures when the RPF was used as a confinement material. An increase in positive peak pressure was determined by confining the tested explosives compared to the unconfined tested explosives. The polyurethane foam's cure time indicated that the longer the cure time, the blast pressure increases. The tested variable of the polyurethane foam cure time also indicated that the longer the RPF around the test charges could cure, the greater the peak pressure would be recorded. The cure time would be limited by the amount of time that a breaching team had to perform a safe and effective breach.

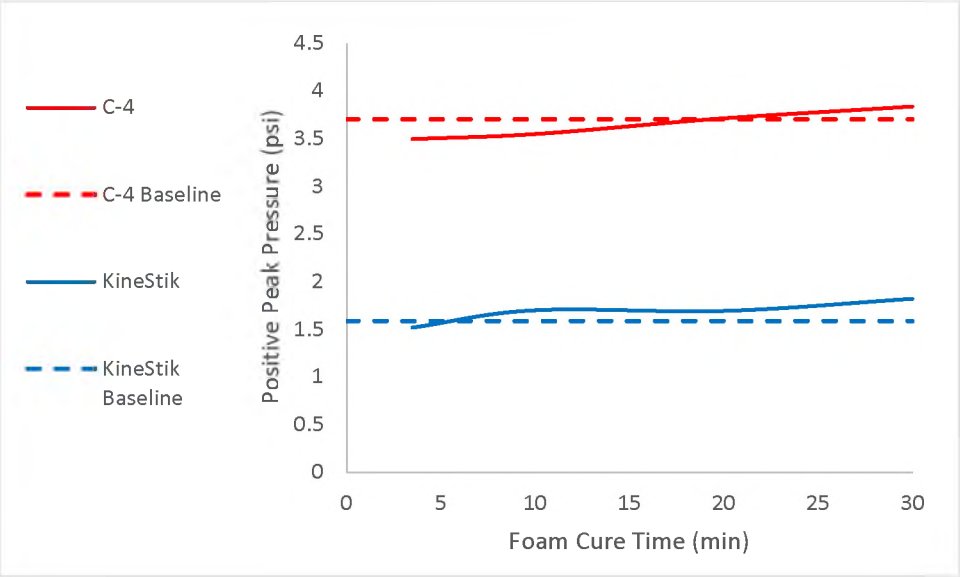

Figure 3.8. Recorded positive peak pressures with varying rigid polyurethane foam cure times for C-4 and KineStik explosives. The solid lines are the peak pressure confined by variable cured foam, whereas the dashed lines are respective explosive' unconfined average peak pressures.

The theory for this trend was that by extending the amount of time between application of the foam, and before the charge was detonated, the RPF confinement material would have different levels of curing. RPF cures from the outside, inwards as the organic cyanate group reacts with water in the surrounding air. This reaction establishes a cured harden-surface and uncured inner sub-structure. The longer that RPF cured, the harder the inner sub-section became. By detonating a charge inside of this diaphragm-like, partially cured RPF structure, the shockwave expands outwards, passing through the uncured RPF and striking the more solid outer surface of the RPF. This interaction would result in reflected shockwaves until the RPF surface was broken and the shockwave pressure could escape into the surrounding open-air environment.

Another measurement derived value considered in this testing was the positive phase impulse (Table 3.3). The positive phase impulse of a shockwave is the area under the positive phase of the pressure versus time waveform. For this experiment, the positive impulse values were found by transferring the MREL pressure data for each trial into a data plotting software capable of integrating the area under each positive peak curve. The integral was set from the peak pressure spike to the first point that the pressure returned to ambient pressure value (x-axis).

Table 3.3. Measured positive phase impulse (psi*ms) for unconfined and variable rigid polyurethane foam cure-time confinement material for four types of explosives.

	Baseline Average	3.5 Min. Cure	10 min. Cure	20 Min. Cure	30 Min. Cure
C-4	2.692	7.529	7.51	7.055	7.408
DetaSheet	2.465	8.377	7.524	7.647	7.903
KineStik	1.655	3.748	4.054	3.916	4.07
TexPak	2.694	9.732	10.867	11.192	11.651

The positive phase impulse was seen to increase all four types of tested explosives (Figure 3.9 - Figure 3.10). This increase of positive impulse would indicate that the application of RPF would increase the amount of impulse force that a breaching team would encounter by using this purposed technique of breaching compared to conventional unconfined charge techniques. This effect on the breaching team could be harmful to the breaching team and may present unwantful blast forces to the breaching team. Further research into this possible risk would be suggested.

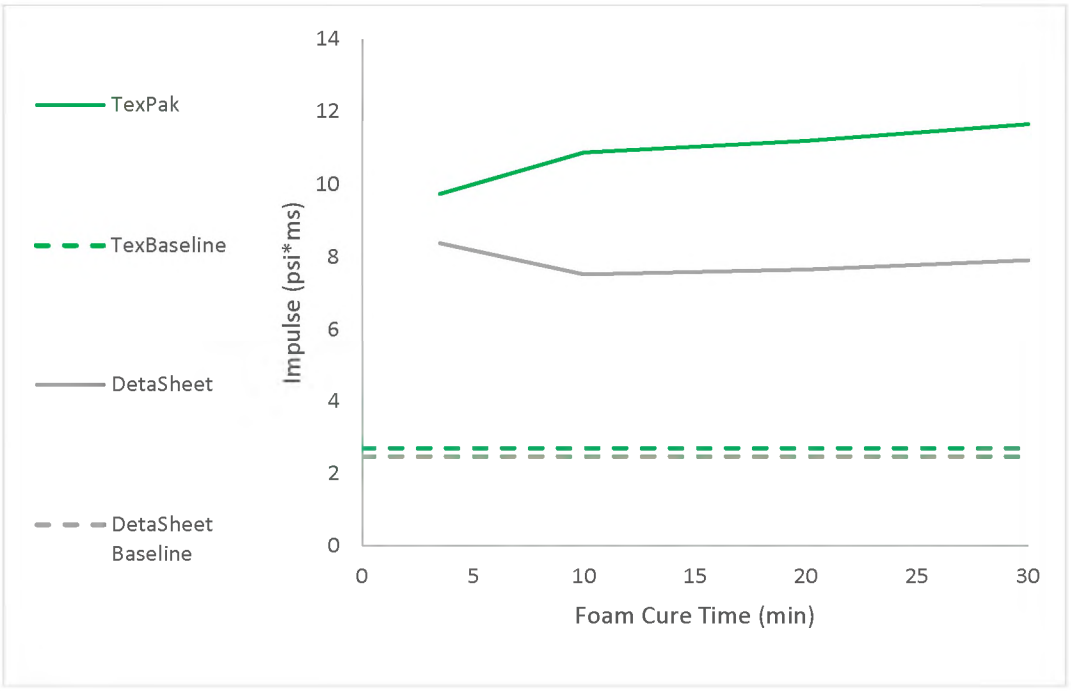

Figure 3.9. Positive phase impulse changes for TexPak and DetaSheet explosives as rigid polyurethane foam confinement material cure-time was extended. The dashed line indicated unconfined baseline positive phase impulse for respective explosive types.

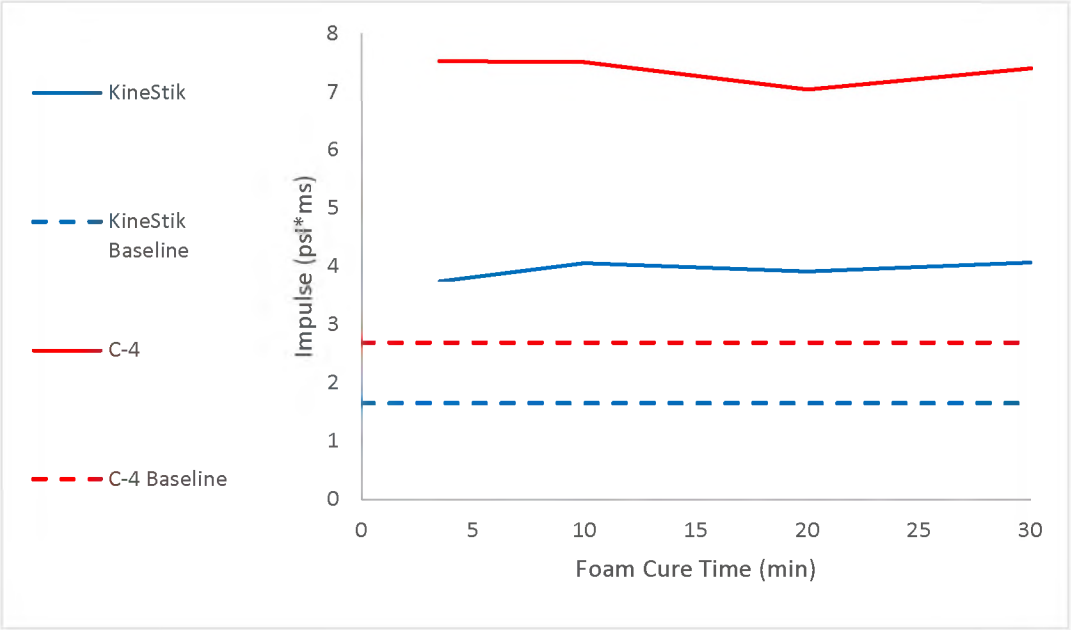

Figure 3.10. Positive phase impulse changes for C-4 and KineStik explosives as rigid polyurethane foam confinement material cure-time was extended. The dashed line indicated unconfined baseline phase impulse for respective explosive types.

Table 3.4. Measured duration of first positive phase of shockwave (ms) for unconfined and variable rigid polyurethane foam cure-time confinement material for four types of explosives.

	Baseline Average	3.5 Min. Cure	10 min. Cure	20 Min. Cure	30 Min. Cure
C-4	2.96	3.14	3.09	2.97	2.86
DetaSheet	3.33	2.78	2.84	2.75	2.67
KineStik	2.32	2.18	2.84	2.72	2.99
TexPak	3.08	3.13	3.51	3.36	3.43

The duration of the first positive phase of the pressure shockwave was determined by analyzing the data outputted by the pressure transducers. The time at which pressure initially spiked was subtracted from the time at which the pressure transitioned from a positive pressure to a negative pressure. This value was recorded in milliseconds (ms) in Table 3.4.

3.1.3. Compression Forces. Implementation of a load-cell force sensor into the testing made it possible to analyze compression forces that a breaching charge applies to a surface that the charges were detonated against. The load-cell provided applied work values of a breaching charge as it converted chemical potential energy into kinetic energy.

During the first round of unconfined charge testing, a baseline compression force value was collected for each of the four types of tested explosives. These baseline values were obtained by performing three unconfined detonations of the explosives directly above the load-cell sensor (Table 3.5).

Table 3.5. Recorded compression forces (lbf) of unconfined and polyurethane confined detonations

	Baseline Average	3.5 Min. Cure	10 min. Cure	20 Min. Cure	30 Min. Cure
C-4	3,561	24,780	74,070	103,900	103,900
DetaSheet	5,523	3,215	3,491	1,726	3,009
KineStik	3,059	3,721	12,150	65,180	66,820
TexPak	83,210	49,540	66,650	74,770	92,490

A large difference in pound-force was seen when comparing the four tested explosives' unconfined baseline values. The TexPak unconfined compression forces were seen to be approximately ten times greater than the other tested explosives. The KineStik explosives were seen to apply the weakest compression forces. The three baseline values were averaged together respectfully to establish a relative compression force value for each type of explosive detonated in an open-air, unconfined environment (Figure 3.11).

The tested breaching charges' detonations demonstrate the compression force changes when confined by the varying cure time RPF (Figure 3.12 - Figure 3.13). The C-4, KineStik, and TexPak explosives followed a logarithmic trend that best described the relationship between the variated RPF cure time and the foam's confined blast compression forces. The load-cell recorded a rapid increase in compression forces for these three types of explosives between the 3.5-minutes and the 20-minute cure time points. At the 30-minute cure time, a flattened trend line indicated that the compression forces reached their respective maximum values for each of the three explosives. A logarithmic trend of these three explosives would suggest that an optimal cure time for the RPF confinement material

would be 20-minutes to maximize compression forces but minimize cure time. The DetaSheet explosives presented an irregular trend line that would suggest that the compression forces of the DetaSheet explosives were unaffected by the RPF confinement material (Figure 3.12 - Figure 3.13).

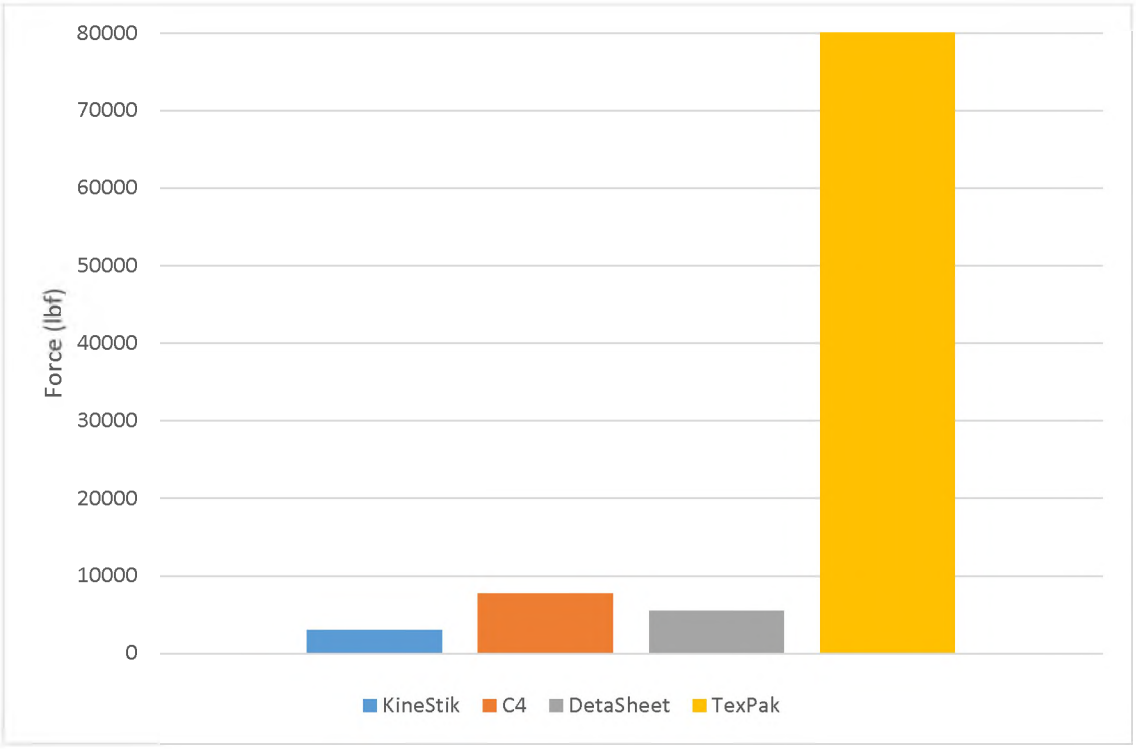

Figure 3.11. Average recorded compression forces of unconfined baseline tests measured by the load cell sensor.

The tested breaching charges' detonations demonstrate the compression force changes when confined by the varying cure time RPF (Figure 3.12 - Figure 3.13). The C-4, KineStik, and TexPak explosives followed a logarithmic trend that best described the relationship between the variated RPF cure time and the foam's confined blast compression forces. The load-cell recorded a rapid increase in compression forces for these three types

of explosives between the 3.5-minutes and the 20-minute cure time points. At the 30-minute cure time, a flattened trend line indicated that the compression forces reached their respective maximum values for each of the three explosives. A logarithmic trend of these three explosives would suggest that an optimal cure time for the RPF confinement material would be 20-minutes to maximize compression forces but minimize cure time. The DetaSheet explosives presented an irregular trend line that would suggest that the compression forces of the DetaSheet explosives were unaffected by the RPF confinement material (Figure 3.12 - Figure 3.13).

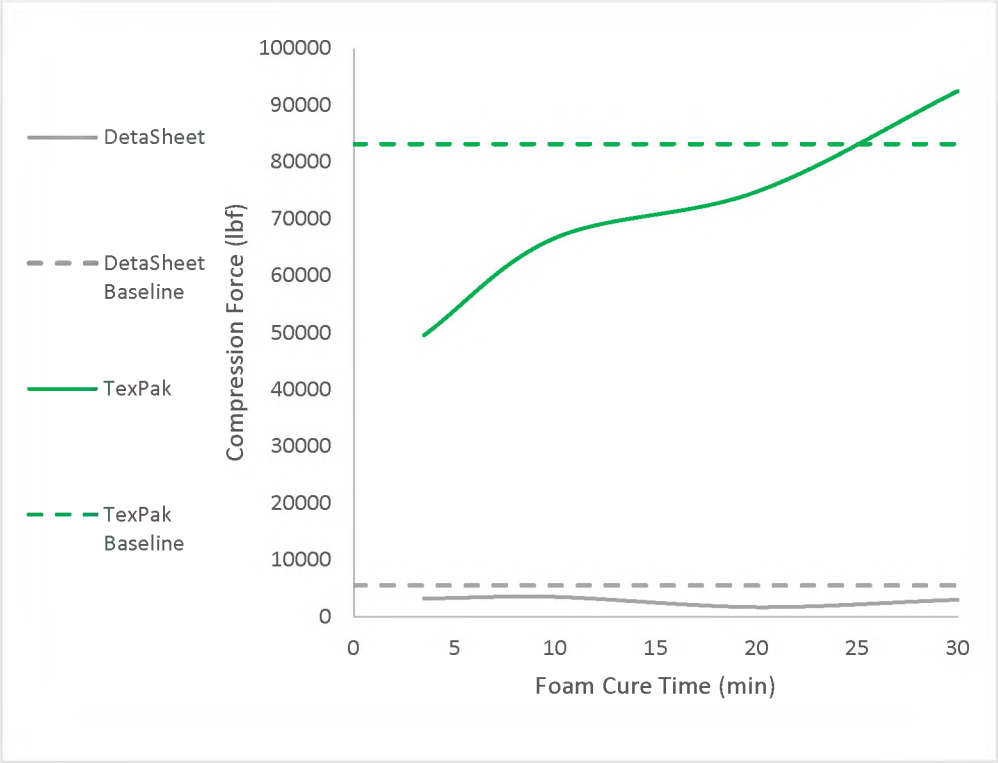

Figure 3.12. Recorded compression forces with varying rigid polyurethane foam cure times for DetaSheet and TexPak explosives. The solid lines are the compression forces confined by variable cured foam, whereas the dashed lines are respective explosive' unconfined average peak pressures.

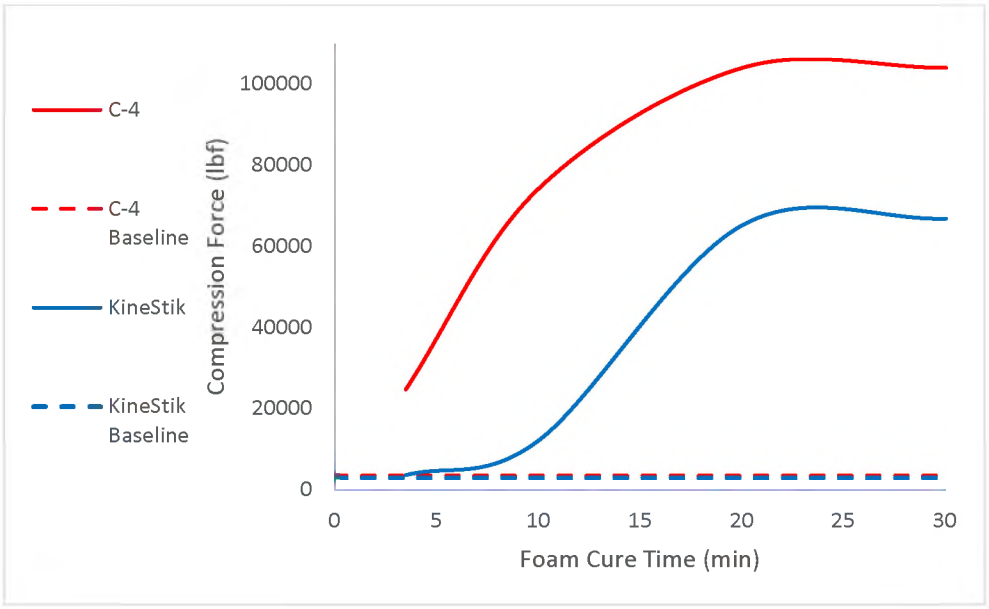

Figure 3.13. Recorded compression forces with varying rigid polyurethane foam cure times for C-4 and KineStik explosives. The solid lines are the compression forces confined by variable cured foam, whereas the dashed lines are respective explosive' unconfined average peak pressures.

3.2. RESULTS OF VOLUME TESTING OF CONFINEMENT MATERIAL

The purpose of the third round of testing was to focus on quantifying the changes of a breaching charge's blast effects because of increasing confinement material (Table 3.6). The testing procedures followed the same as unconfined baseline testing from the first round of testing with a few modifications. The first change of procedure was that only one explosive was tested. C-4 was chosen due to it being the most used as a military explosive for breaching. The second procedure change was that the explosive weight was reduced from 5.80 ± 0.04 ounces to 3.53 ± 0.04 ounces. This alteration was due to the C-4 confined testing results maxing out the load cell sensor's upper limitations. The procedure's last change was that the pressure sensors were spaced apart at ten feet and fifteen feet instead

of both sensors at fifteen feet. This modification was to measure the blast wave pressures at different distances that a breaching team might experience from the blast location.

3.2.1. Plate Dents. The crater dent depths of the reduced C-4 explosive indicated a linear relationship between the foam radius and the witness plate's dent depth. The increase in the polyurethane confinement dimension increased Plate Dent depth (Figure 3.14). This same linear relationship existed when the foam radius and the dent diameter were compared. The increase of the confinement foam material surrounding the explosive detonation resulted in a rise in the crater diameter (Figure 3.15).

Table 3.6. Values of recorded data from ten trial detonations of 3.53 ± 0.04 oz of C-4 with variable polyurethane foam radius dimensions.

Trial #	Foam Radius (in)	Probe I (psi)	Probe II (psi)	Duration (ms)	Force Sensor (lbf)	Dent Depth (in)	Dent Diameter (in)
Average Baseline	0	6.854	3.721	1.78	1,354	0.058	1.435
1	0.459	6.761	3.677	1.82	1,384	0.059	1.434
2	0.825	7.412	4.603	1.84	1,663	0.063	1.460
3	0.786	5.145	4.452	1.77	1,143	0.070	1.417
4	2.092	5.090	4.761	1.83	28,550	0.065	1.483
5	1.998	4.909	5.851	1.89	18,970	0.067	1.493
6	1.945	5.663	4.717	1.79	14,460	0.070	1.470
7	3.074	4.186	3.311	1.81	29,060	0.085	1.532
8	4.456	3.528	2.605	1.78	25,340	0.087	1.598
9	4.608	3.058	2.485	1.83	41,540	0.088	1.523
10	6.255	2.316	1.905	1.81	34,510	0.093	1.645

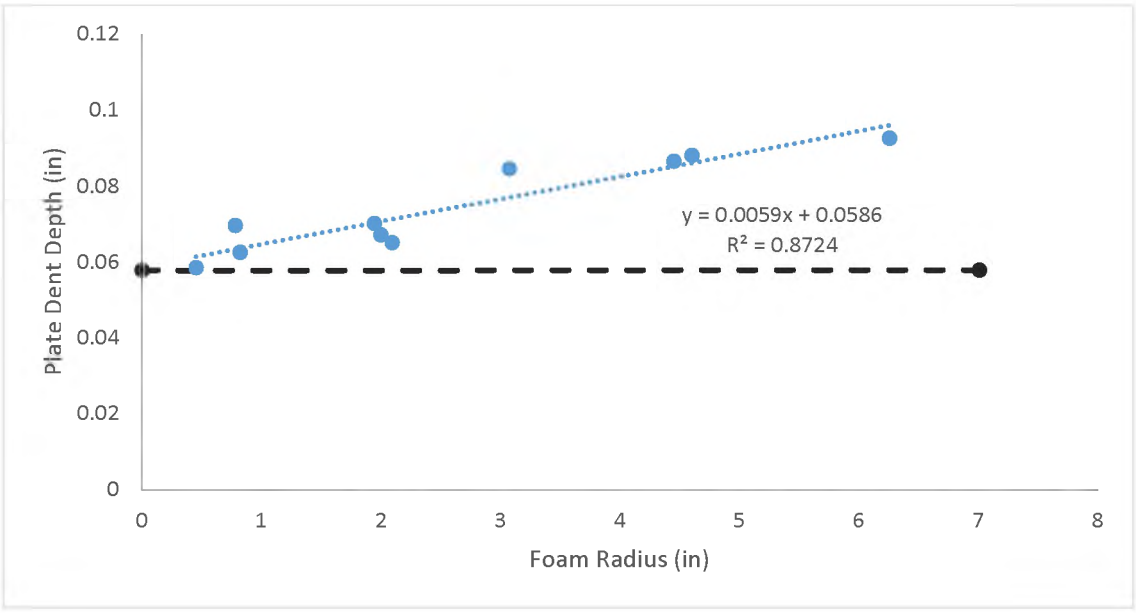

Figure 3.14. The Plate Dent crater depths results from ten trial detonations of 3.53 ± 0.04 oz. of C-4 with variable polyurethane foam radius dimensions. The dashed line indicates the average Plate Dent depth of three unconfined trials of the same weight C-4 charge.

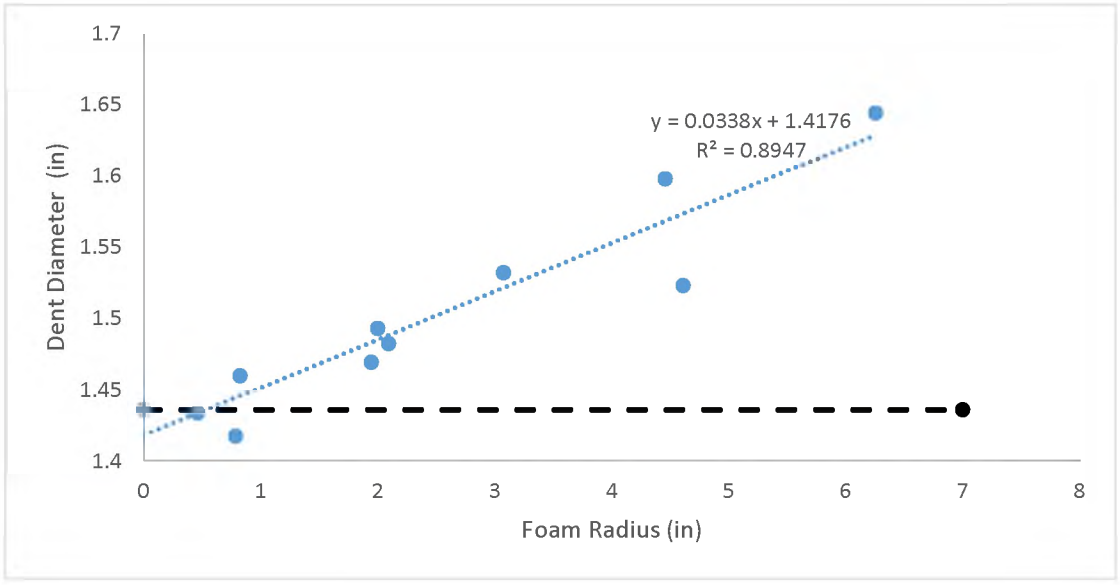

Figure 3.15. The Plate Dent crater diameter results from ten trial detonations of 3.53 ± 0.04 oz. of C-4 with variable polyurethane foam radius dimensions. The dashed line indicates the average Plate Dent depth diameter of three unconfined trials of the same weight C-4 charge.

3.2.2. Pressures. The positive peak pressures of the volumetric testing performed were analyzed in the same manner as previously done in the baseline and foam cure time testing. The raw testing data collected by the MREL Data Trap was processed through the MREL software and converted from voltage to proper pressure units. The pressure data from the farthest pressure probe from the blasting site shows a decreasing exponential trend as the RPF confinement material volume was increased, and the positive peak pressure decreased (Figure 3.16).

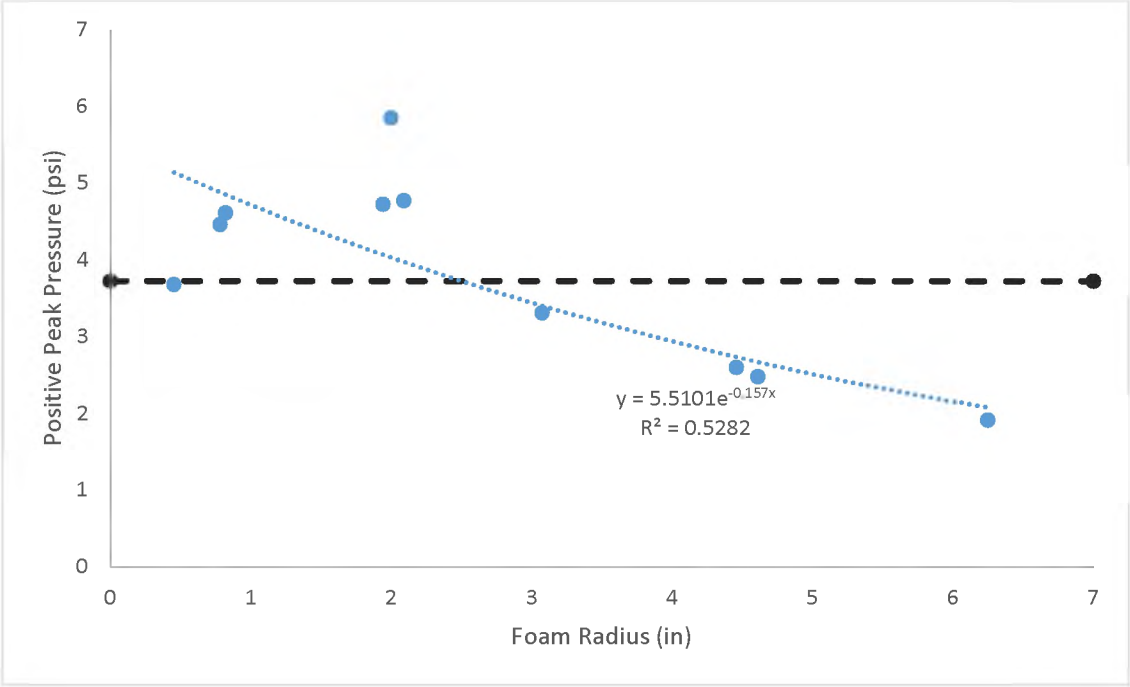

Figure 3.16. Measured positive peak blast pressures at 15-feet away from 3.53 ± 0.04 oz. of C-4 detonated with variable confinement polyurethane foam radius. The dashed line indicates the average positive peak pressure of three unconfined trials of the same weight C-4 charge.

A similar decreasing exponential trend was seen for the closer pressure transducer's data located only ten feet from the blasting site location. As the RPF blocks

increased in size, the blast pressure experienced at that distance decreased (Figure 3.17). This testing compares the peak pressures with respect to the RPF confinement volume, whereas the previous confinement testing compared the peak pressures with respect to the RPF cure time. The foam cure time was seen to increase the shockwave's peak pressures because the foam was hardening as the cure time increased. The increase of the foam confinement thickness decreased the pressures because the RPF was already hardened.

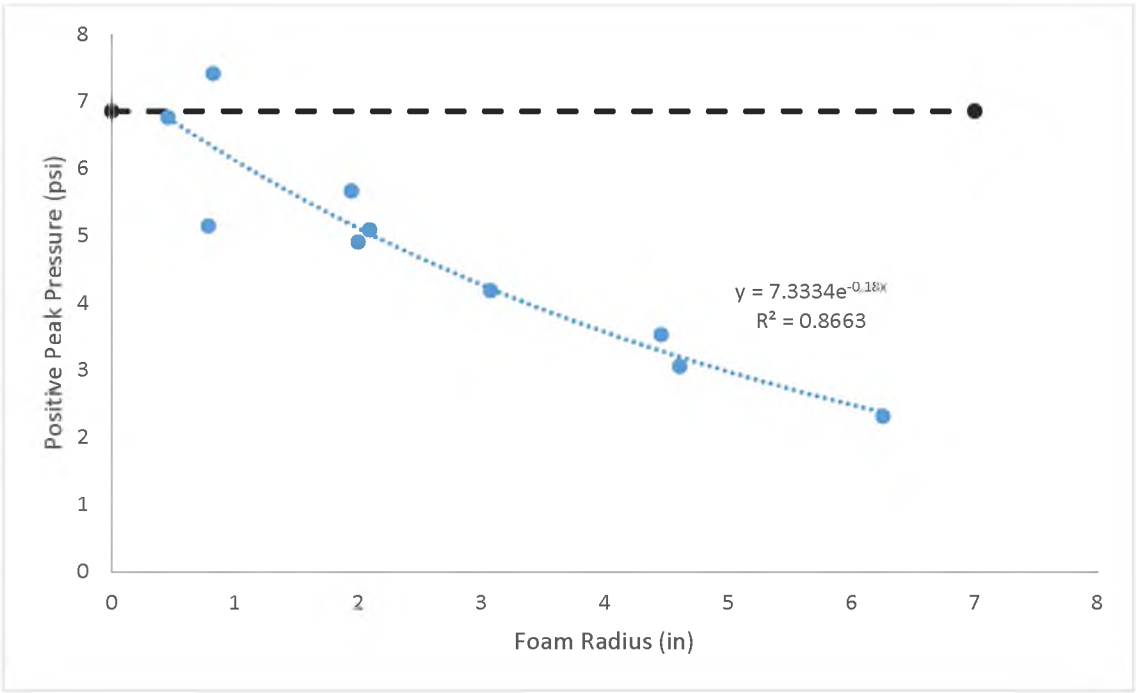

Figure 3.17. Measured peak blast pressures at 10-feet away from 3.53 ± 0.04 oz. of C-4 detonated with variable confinement polyurethane foam radius. The dashed line indicates the average positive peak pressure of three unconfined trials of the same weight C-4 charge.

The increase of a confinement material around an explosion would limit the escape of energy from the immediate blast site and direct the blast energy towards the weakest point of confinement. In the RPF volume testing case, the weakest point of confinement

was downwards towards the load sensor versus outwards towards the pressure sensors. Thus, resulting in a reduction of peak pressures and increased compression force as the RPF confinement volume increased.

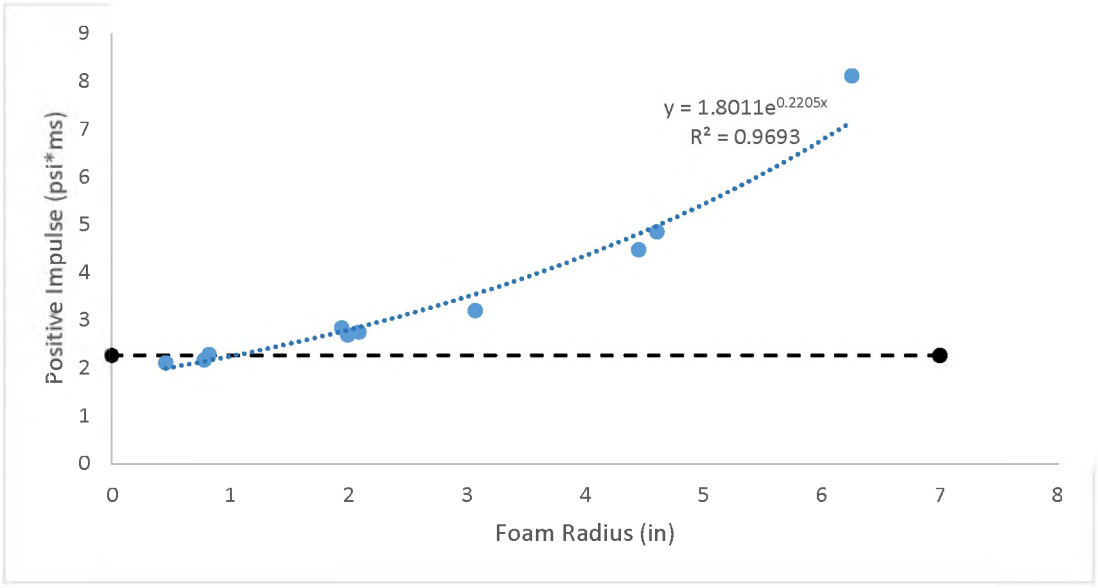

Figure 3.18. Positive phase impulse changes for 3.53 ± 0.04 oz. of C-4 explosive as rigid polyurethane foam confinement, material dimensions were increased. The dashed line indicated unconfined baseline positive phase impulse for respective explosive types.

The positive phase impulse was seen to increase exponentially as the thickness of the RPF confinement material was increased (Figure 3.18). This impulse increase would indicate that the application of RPF would increase the amount of impulse force that a breaching team would encounter by using this technique of breaching compared to unconfined charge techniques. A larger precast RPF confinement block would result in a more significant amount of positive phase impulse a blast would expel into the surrounding environment.

3.2.3. Compression Forces. The compression forces recorded by the force load cell mounted directly below the blasting test location followed an increasing logarithmic trend (Figure 3.19) opposite of the decreasing exponential trend seen in the peak pressures. The data shows that the greater the RPF radius became around a breaching charge, the more compression force strength would be recorded. The data collected by the load-cell sensor provided numerical evidence that by doubling the confinement RPF radius, the compression force of the detonation will roughly increase by 150%.

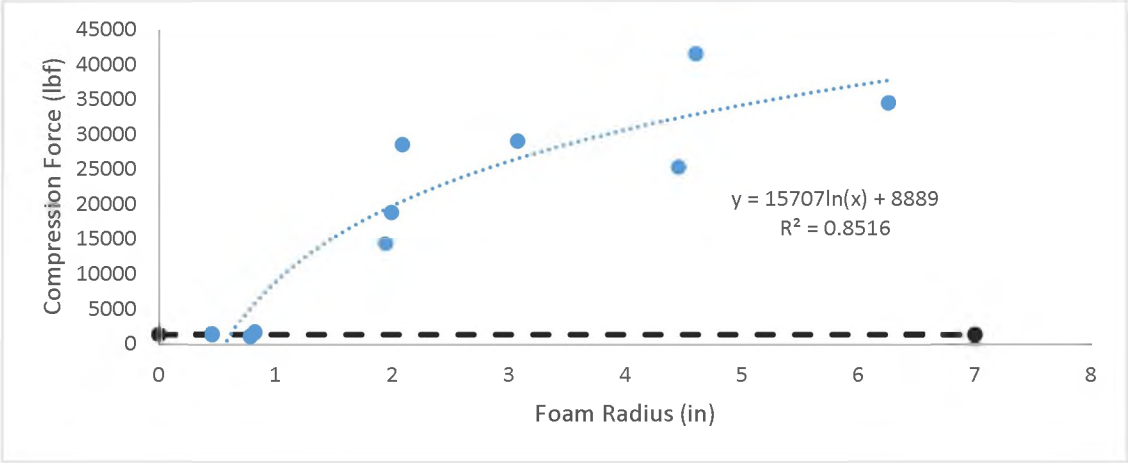

Figure 3.19. The compression forces (lbf) of 3.53 ± 0.04 oz. of C-4 detonated with variable confinement polyurethane foam radius. The dashed line indicates the average compression force of three unconfined trials of the same weight C-4 charge.

4. DISCUSSION

The data collected from the baseline testing provided average positive peak pressures, compression force capabilities, and brisance abilities of the four tested breaching charge explosives in an unconfined placement. This initial, unconfined testing demonstrated the capabilities of breaching explosives as they are currently utilized as breaching charges by placing the charge on a surface and detonating the breaching charge. The confinement testing focused on analyzing the change in a charges' explosive parameters concerning RPF cure time by illustrating that the longer the foam cured, the more damaging the charges would be. For all four of the explosive types tested, the blast effects followed a logarithmic trend. No significant change in duration of the first peak positive phase of the shockwave was noticed when comparing unconfined to RPF confined blasts. It should be noted that most of the data collected at 3.5 and 10 minutes of foam curing, the compression forces, and the shock wave pressures were seen to be less than the unconfined baseline test data. These results imply that for the polyurethane foam to be optimized as a breaching charge confinement material, the foam should be cured longer than 10 minutes to maximize the blast's damaging effects.

The final testing analyzed varying confinement radii of a fully cured RPF block that showed that the more confinement around the detonation, the greater the compression force and cratering depth. The positive peak pressure of a blast shockwave was seen to be reduced with a thicker confinement material surrounding the detonation of the breaching charges, opposite of the impulse. No significant increase in the duration of the first peak positive phase of the shockwave was noticed as the volume of the RPF confinement

material was increased. These findings imply that more RPF cast around a charge would be necessary for an explosive to demonstrate maximum blasting damage potential. The testing also provided evidence that the greater the distance a breaching team is from a blast location, the decrease in blast pressures they would experience by measuring the same blasts' pressures at a variable distance.

The real-life practicality of confining a breaching charge to maximize the blast effects and minimize the required amount of confinement raises the need to determine an optimal RPF confinement amount. The collected data would indicate that a confinement radius of two inches or more would improve a breaching charge's effects while not being so large as to be cumbersome to implement. At RPF radii beyond four inches, diminishing returns in the compression forces were seen compared to the RPF block's overall size. The curve in Figure 3.19 indicates that at two inches of RPF confinement, the compression forces were seen to have a tremendous increase from previously tested radii before the increasing logarithmic trend began to flatten out around four inches of confinement. The Plate Dent depth followed an increasing linear trend as the foam thickness increased. The shockwave pressures decreased linearly as the confinement material around the charge was increased. These two variables would indicate that the more foam around a breaching charge, the more influential the charge would be for breaching. Since the compression force data suggested an increasing logarithmic trend as the RPF material increased, this blast effect would be the limiting variable for improved breaching charge blasting.

This experiment's findings have provided data that explosive breaching charges have improved explosive properties when confined by polyurethane foam. When confined by the polyurethane foam, the average compression force was increased by 483%, and the

average Plate Dent depths were increased by 26.4%. The average blast peak pressure of a polyurethane foam confined detonation was 10% less than an unconfined detonation. The blast will have increased compression force that would be beneficial for causing more damage to the breach's entry point and destroying stronger material breaches by smaller weighted explosive charges. The breaching charge's confinement also decreased peak pressure, which would benefit a breaching team in the blast's proximity. This confinement option may reduce possible traumatic brain injuries to the breaching teams due to decreased peak pressure. Finally, the increased polyurethane foam increased brisance abilities in all four explosive types when used as a confinement material.

Further testing into advanced breaching applications of this RPF confinement would need to occur to determine this newly proposed breaching technique's optimal usage. A spray-on RPF confinement system that encased an already primed and placed breaching charge would improve the charge's blast effects and require curing time to be optimally effective. A pre-casted RPF block with an adequate confinement radius would be recommended. This application would maximize the RPF structural strength and prevent any time loss on target waiting for the RPF to cure. However, the RPF block's bulkiness and the placement technique of a confined breaching charge would need to be modified.

5. CONCLUSIONS

The use of rigid polyurethane foam (RPF) material as a confinement material for a breaching charge proved helpful in increasing the explosive charge's significant effects for a successful breach. All the explosive properties (shockwave positive peak pressure, compression force, and brisance crater ability) demonstrated an increase in desired energy output when confined by the RPF material compared to the unconfined test. The addition of a twelve-ounce spray RPF to the four types of breaching charges tested, and cured for 3.5-minutes, resulted in an average of 21% decrease in shockwave pressure, 40% increase in compression force, and 10% increase in Plate Dent depth compared to an unconfined charge. An average of 33% increase in shockwave pressure, 524% compression force, and 39% Plate Dent depth was seen when the RPF was cured to 30-minutes compared to a 3.5-minute cure time. The detonation parameters of a breaching charge were increased as the RPF cured longer before a detonation occurred.

An evaluation of varying thicknesses of fully cured RPF confinement indicated that an increase of the confinement material would increase desirable breaching effects. A 210% increase of RPF thickness around a C-4 breaching charge compared to unconfined baseline data resulted in an average of 7% decrease in positive peak pressure, a 2010% increase in compression force, and a 12% increase in Plate Dent depths. The increase of RPF thickness around a C-4 breaching charge by 610% compared to unconfined baseline data resulted in an average of 60% decrease in positive peak pressure, a 2,450% increase in compression force, and a 60% increase in Plate Dent depths. The volume of the polyurethane foam material encasing the detonations showed that the larger the

confinement radius of the fully cured polyurethane foam around the charge, the more effective and damaging the blast would be.

Overall, a breaching charge confined by rigid polyurethane foam (RPF) was more effective than an unconfined breaching charge. An RPF confined breaching charge was seen to have an increase in compression forces and brisance cratering capability compared to unconfined breaching charges. The RPF confined explosives produced a greater positive phase impulse but resulted in an overall decrease of peak positive blast pressures. The confinement of a charge with rigid polyurethane foam would be a more effective breaching technique that would result in more effective breaches and protect breaching teams better against traumatic brain injuries.

6. FUTURE WORK

6.1. FORM FACTOR AND OPTIMIZED APPLICATIONS

This study showed that a breaching charge's compression force and material cratering ability were increased, while the hazardous blast pressures were decreased by confinement of rigid polyurethane foam (RPF). A future study on how RPF could be optimally applied to real-life scenarios would need to be accomplished to optimize this study's findings. The results of this study show that a breaching charge's explosive effects would be amplified by encasing a charge in RPF before detonation but was unable to provide specific form factors of the RPF confinement material. Further research would be needed into optimal size, shape, and other physical specifications of the RPF when applied to actual breaching surfaces, such as doors and windows, compared to the Plate Dent steel surface.

6.2. PRESSURE INCREASES AS FOAM CURE TIME INCREASES

A recommended study would be suggested that further analyzed the results of the foam cure time testing. The results from this testing indicated that the longer the RPF cured, the greater the positive peak pressure would be. This finding would mean that as the foam reaction progresses towards completion, something is causing the blast pressures to build up before leaving the blast site. A future study that utilized high-speed photography and properly placed pressure transducers would help determine the physical traits resulting from the collected data found in this study about vary RPF cure times. Further analysis of the RPF confinement material on the pressure wave would include varying the pressure

transducer locations to simulate different breaching team locations. The testing would include simulating head-on breaches versus side-stack breaches as well as different distances from the blast site. The future study would also be recommended to compare this study, that simulated internal breaching scenarios, to external breaching to determine any varying results. These recommend tests would help determine the safest location of the breaching team utilizing this newly proposed breaching technique.

6.3. OTHER TYPES OF CONFINING MATERIALS

A future study into other confining material options would be incredibly beneficial for the explosive engineering community to understand how different confinement mediums alter a detonation's abilities. Understanding how confinement material affects a blast wave's physical properties would result in more efficient blasting techniques and allow for alternative confinement options in various blasting situations. This work could include a study into such confinement mediums as liquid water versus ice confinement or gelatin versus epoxy resin materials. While future studies of confinement materials would determine the effects of certain confinement materials on a blast wave, a proper understanding would be needed to apply the correct confinement material for the right blasting scenario. For example, a polyurethane spray foam may not be beneficial in a large borehole mining blast but may prove useful as a confinement material in a small underground overhead shot.

A focused study on a polystyrene foam confinement option for breaching charges would build on the work done in this experiment. This foam style would allow a breaching team to eliminate the variable cure time and application of a spray foam by having a

preassembled charge encased by a rigid foam piece. The polystyrene charge would then be rapidly set into place and detonated almost immediately compared to a polyurethane foam charge that would require charge placement and foam application, and optimal cure time.

6.4. FURTHERING THE PLATE DENT TESTING

Future studies based on this experiment would incorporate more scientific instrumentation to the classic Plate Dent procedures. While this study focused on designing an experiment that incorporated instrumentation into the Plate Dent procedure to conserve the number of trials, future research would be suggested to compare compression force values to crater dimensions. Another improvement recommended furthering the Plate Dent capabilities and accuracy would be to utilize 3-D computer modeling software to measure the witness plate craters' volumes. This modeling possibility would allow for further understandings of the effects of the blasts occurring on the steel plates.

APPENDIX A.

BASELINE DATA

The collected output data from baseline experimental testing was provided in this appendix for all trials performed. This data was collected by two pressure tranducers and a load-cell force sensor. All sensor signals were sent through a signal conditioner before being collect and stored in an MREL data accusation system. This stored data was analyzed and interpreted using MREL compatible software. The baseline testing consisted of unconfined charges detonated in an open-air environment. The data was presented in alphabetical order of explosive type tested. The order of data was further sorted in the corresponding trial number and recorded data channel number.

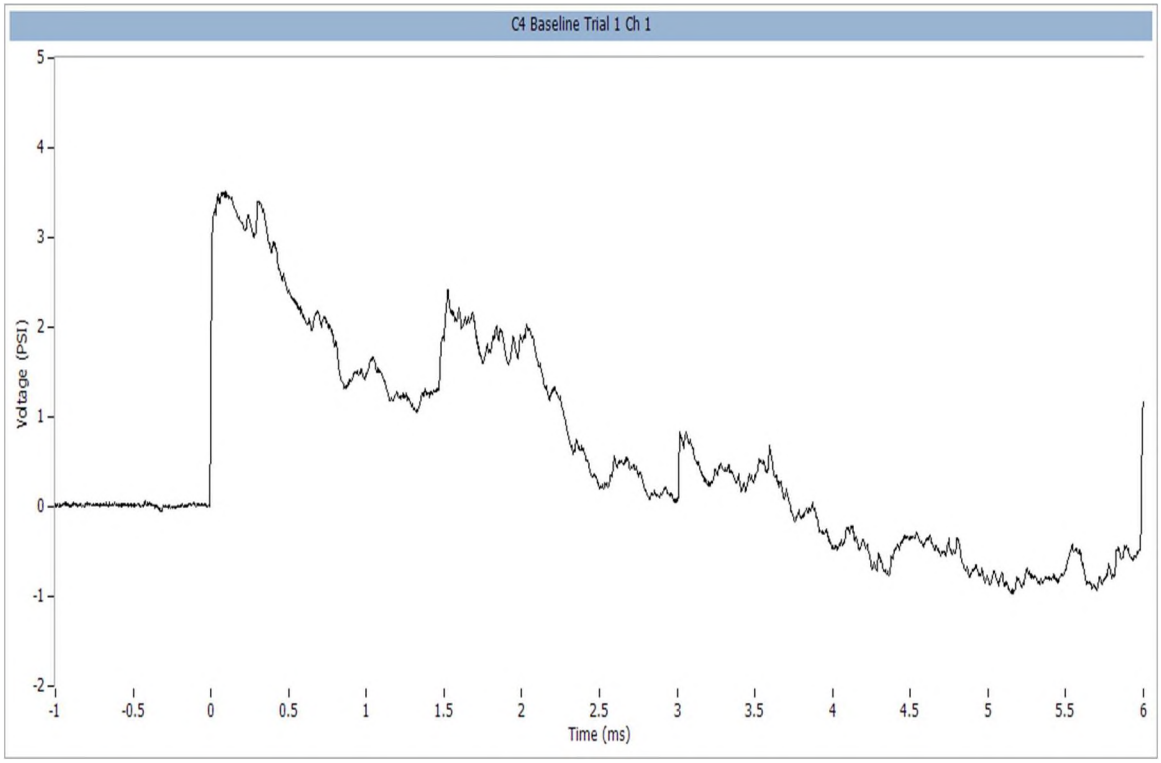

Figure A.1. C-4 baseline trial 1 channel 1 (psi).

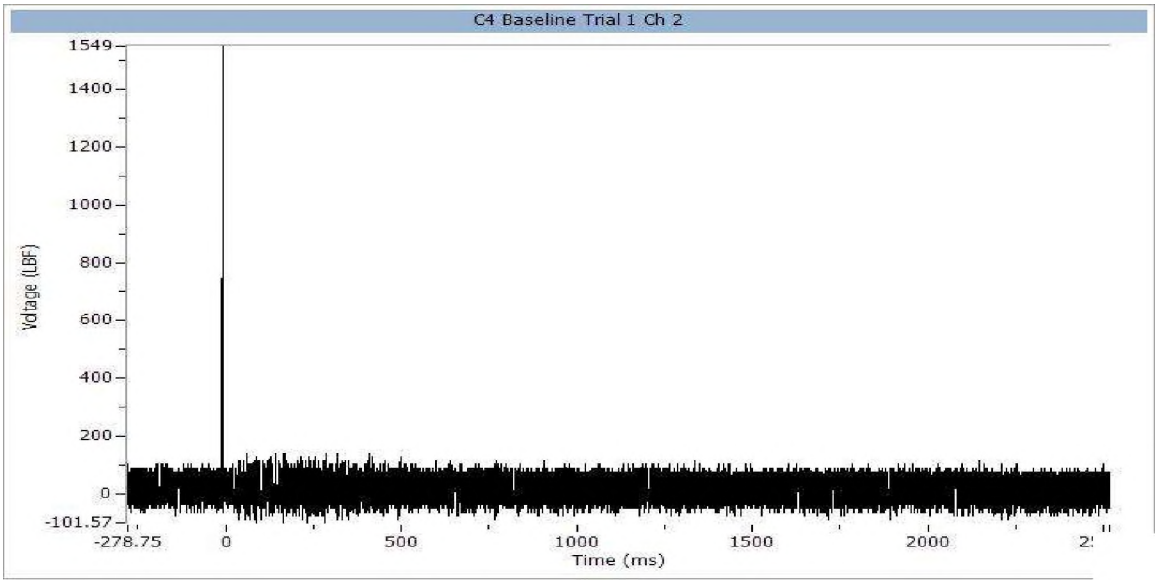

Figure A.2. C-4 baseline trial 1 channel 2 (lbf).

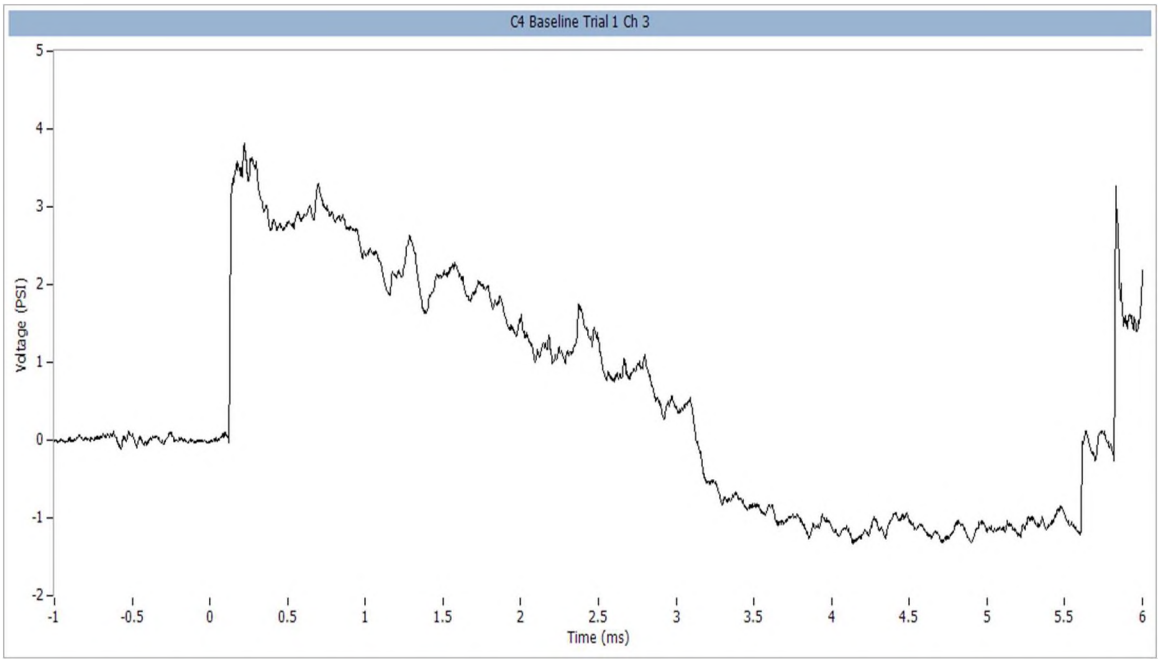

Figure A.3. C-4 baseline trial 1 channel 3 (psi).

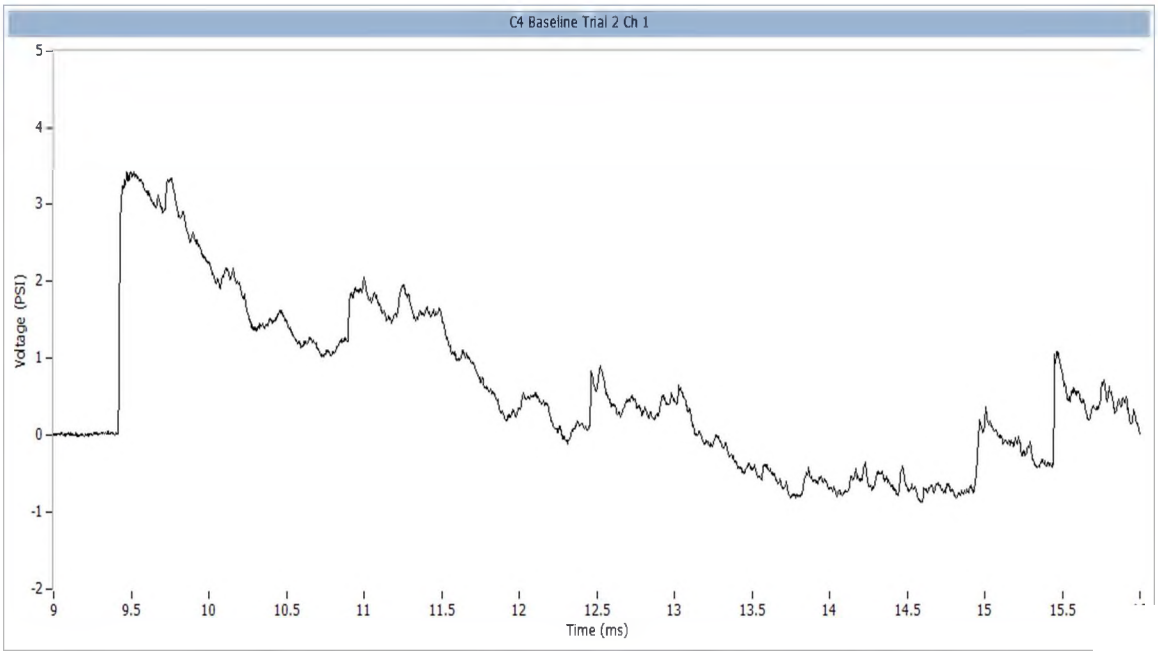

Figure A.4. C-4 baseline trial 2 channel 1 (psi).

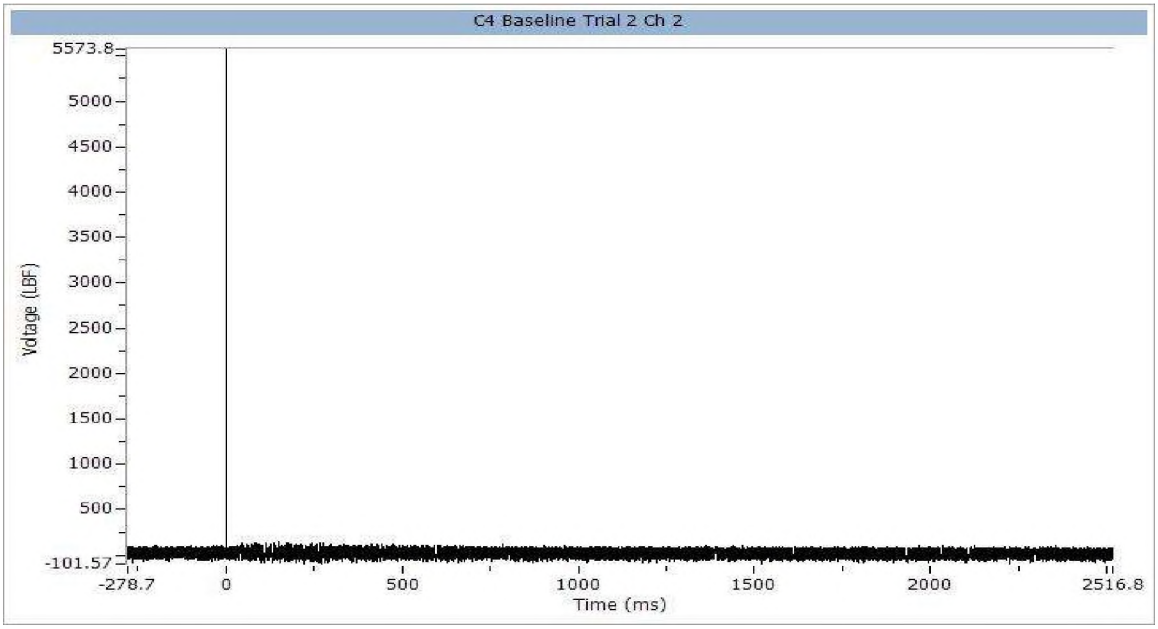

Figure A.5. C-4 Baseline Trial 2 Channel 2 (lbf).

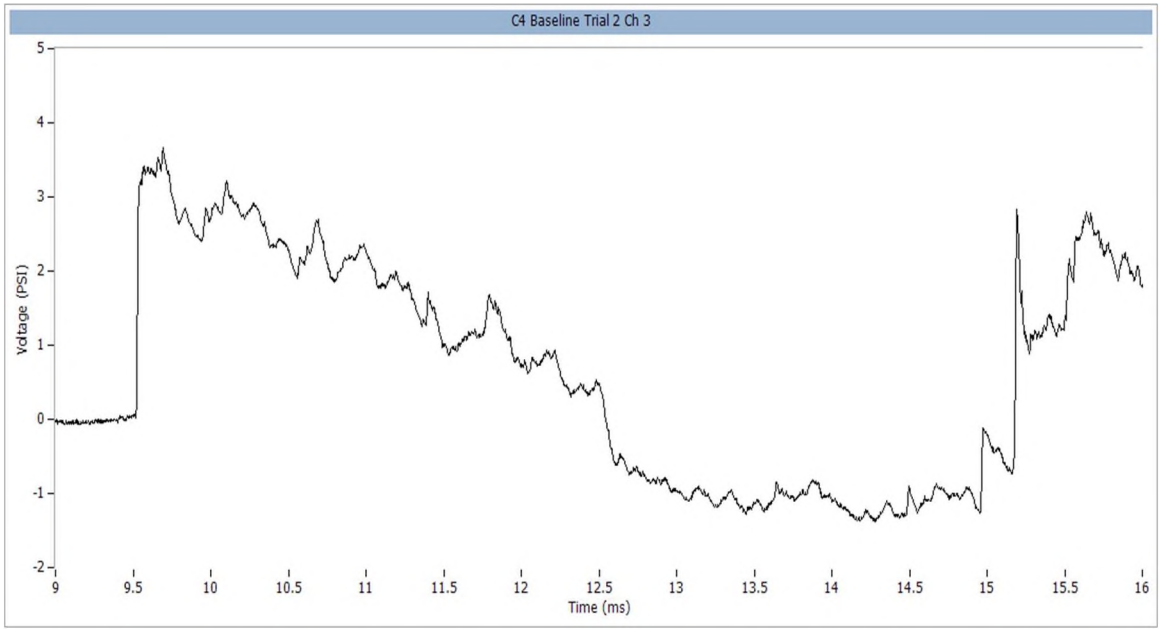

Figure A.6. C-4 baseline trial 2 channel 3 (psi).

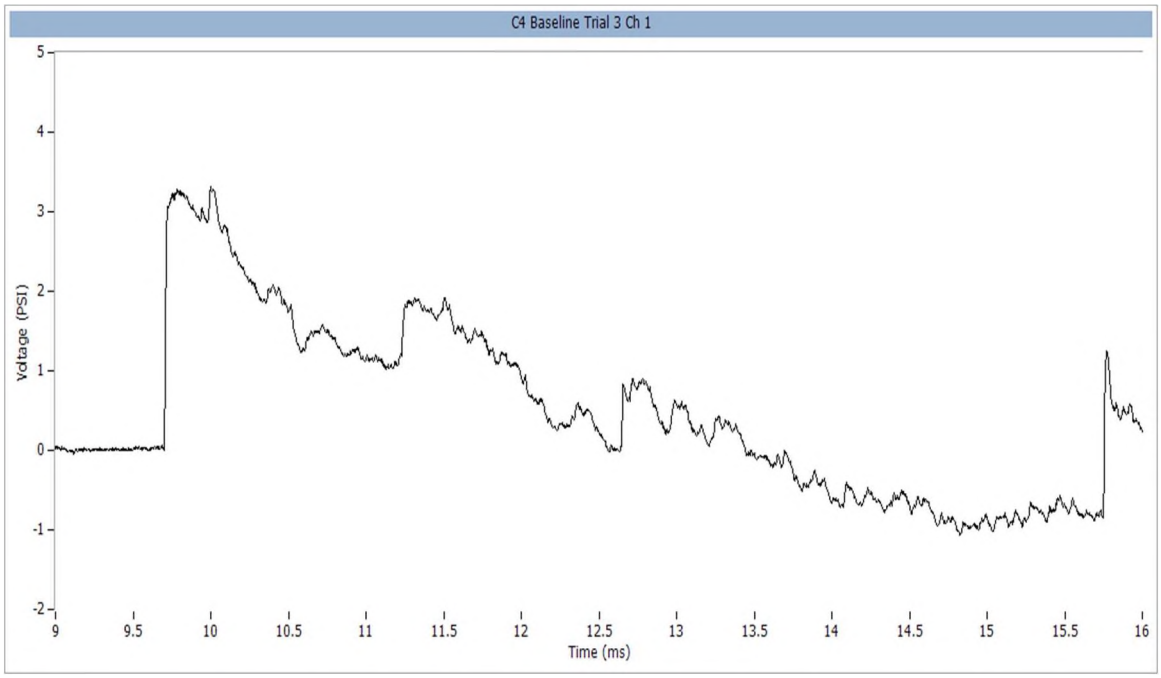

Figure A.7. C-4 baseline trial 3 channel 1 (psi).

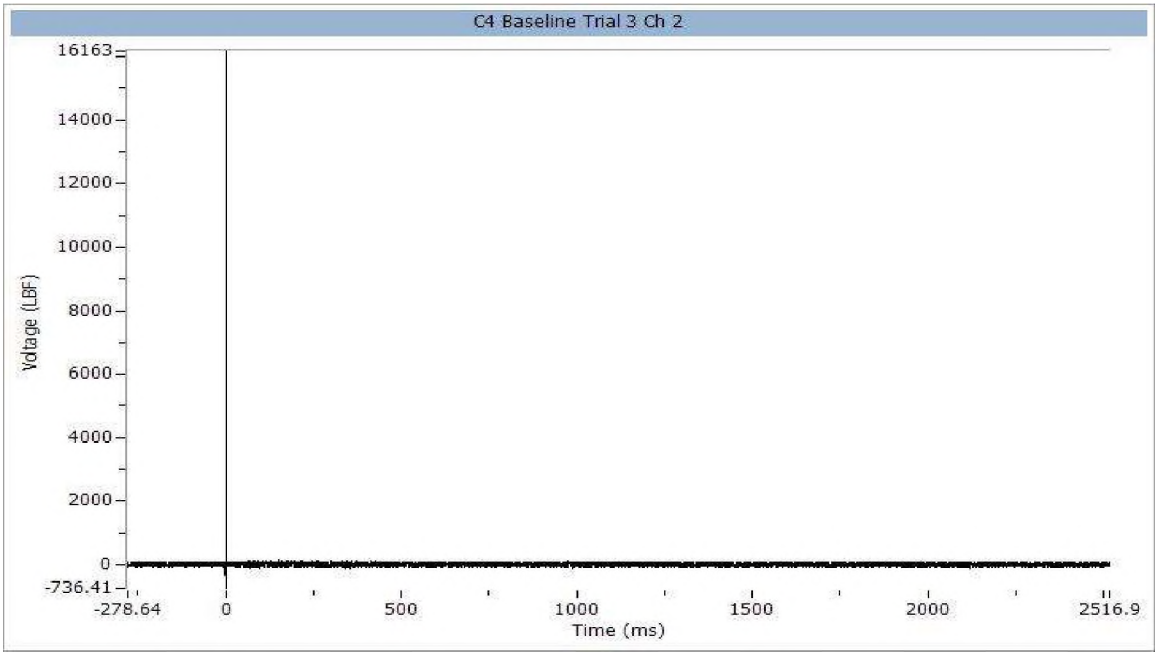

Figure A.8. C-4 baseline trial 3 channel 2 (lbf).

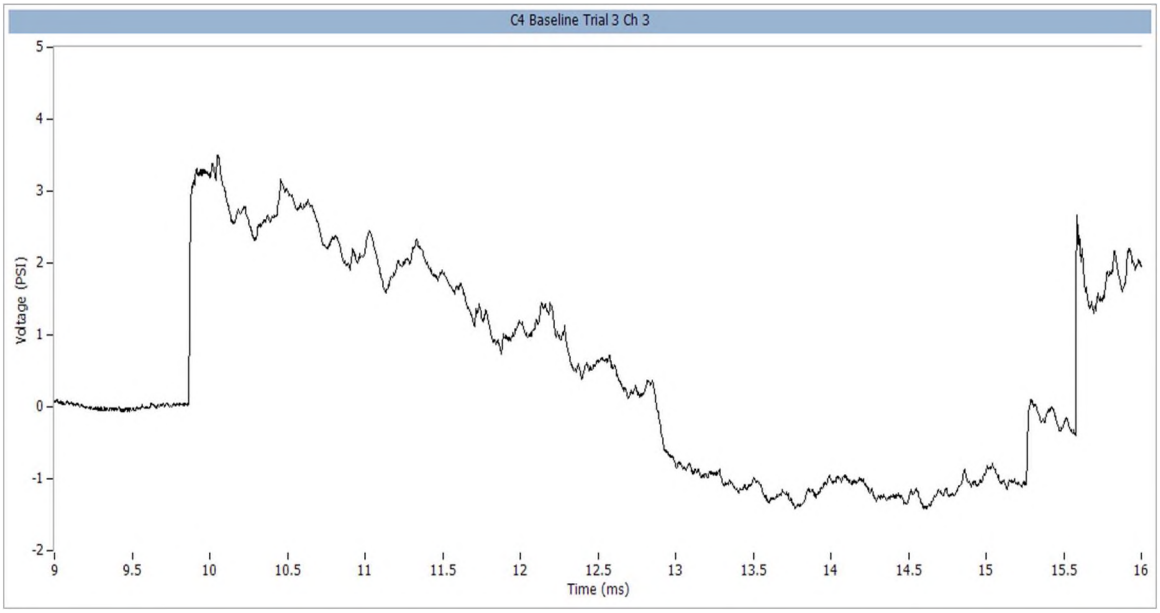

Figure A.9. C-4 baseline trial 3 channel 3 (psi).

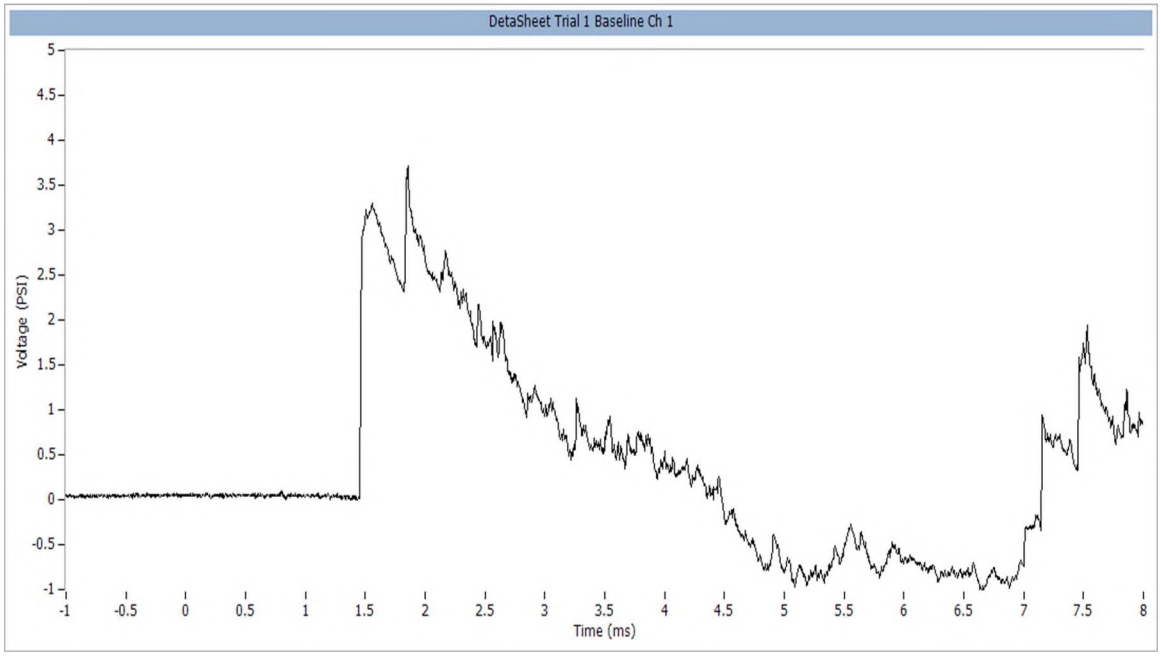

Figure A.10. DetaSheet baseline trial 1 channel 1 (psi).

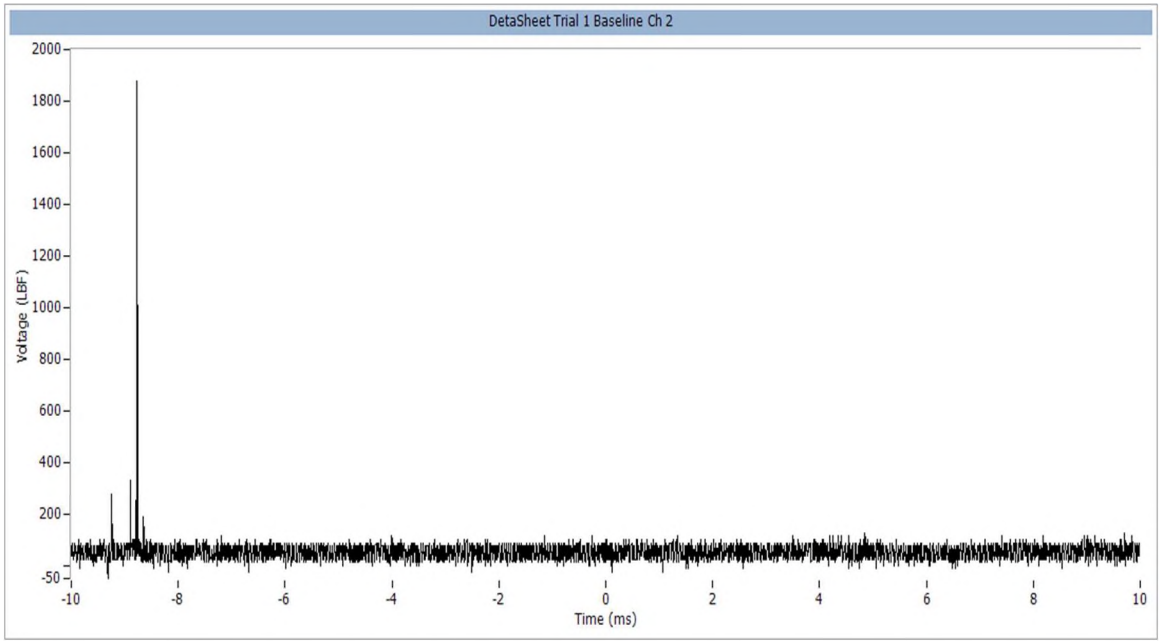

Figure A.11. DetaSheet baseline trial 1 channel 2 (lbf).

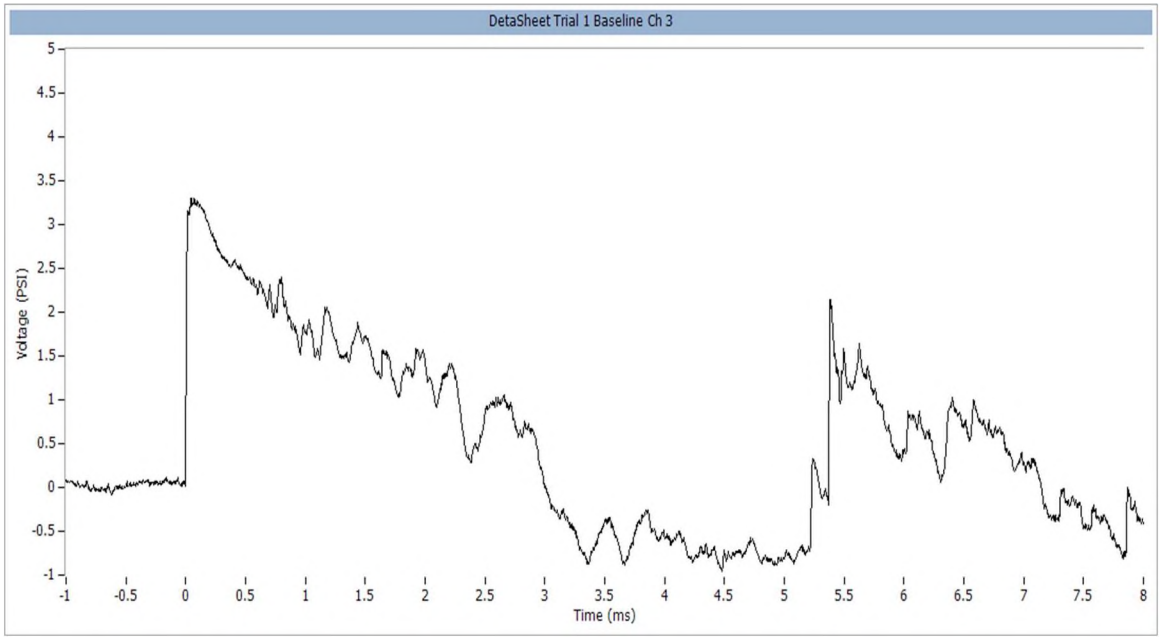

Figure A.12. DetaSheet baseline trial 1 channel 3 (psi).

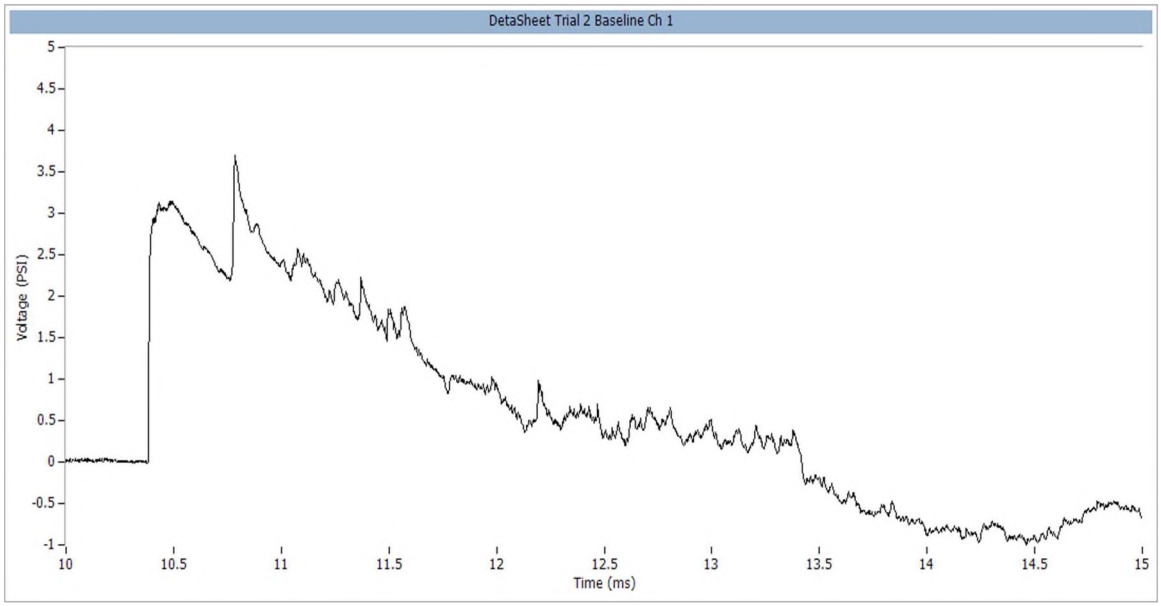

Figure A.13. DetaSheet baseline trial 2 channel 1 (psi).

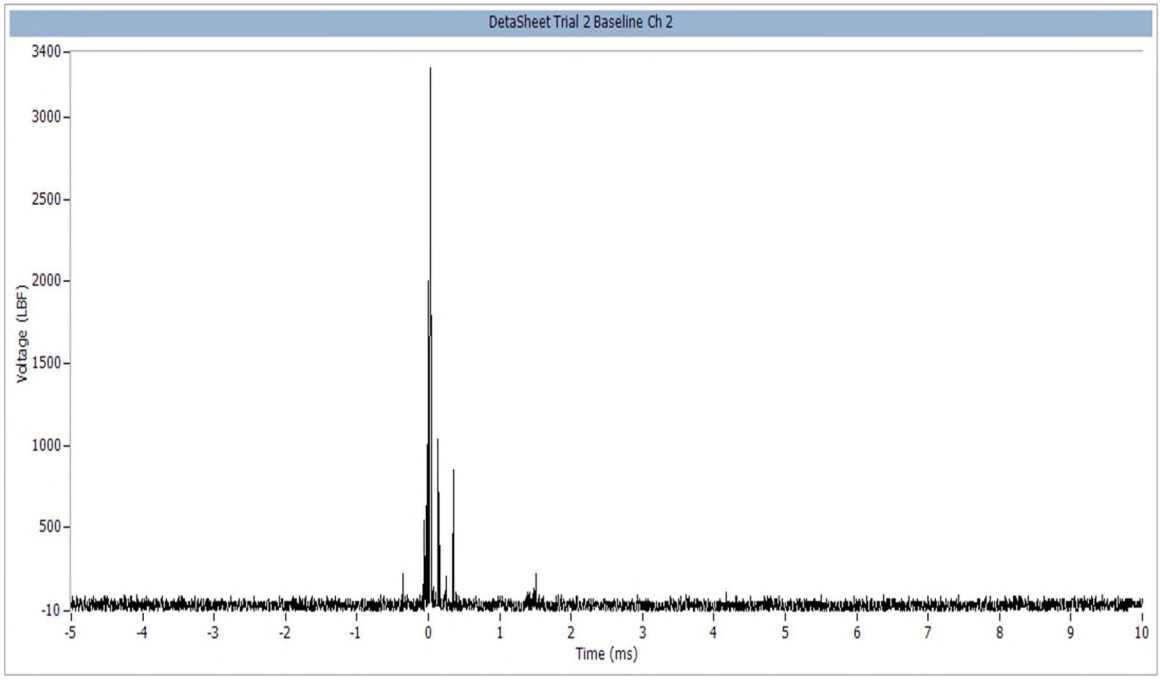

Figure A.14. DetaSheet baseline trial 2 channel 2 (lbf).

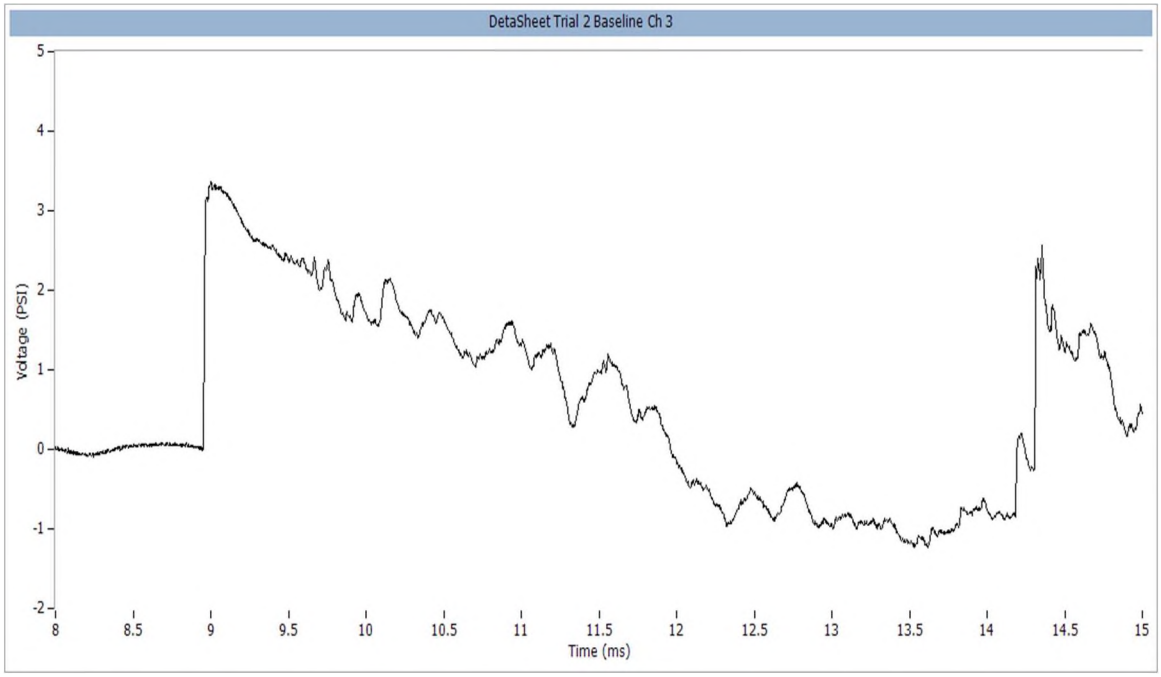

Figure A.15. DetaSheet baseline trial 2 channel 3 (psi).

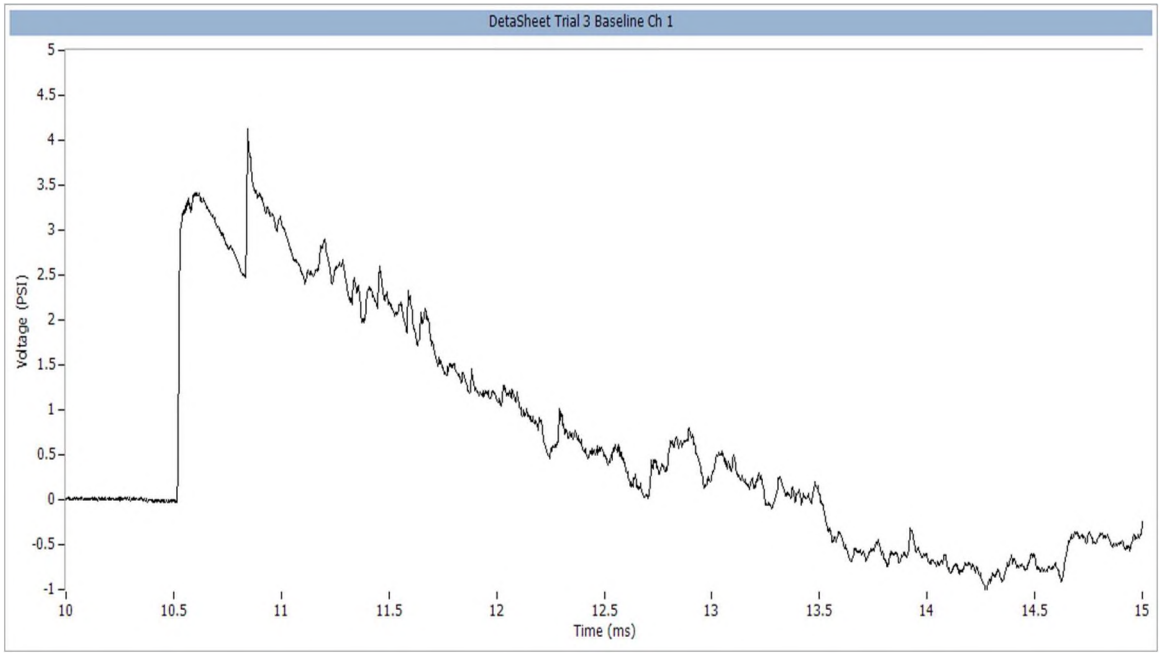

Figure A.16. DetaSheet baseline trial 3 channel 1 (psi).

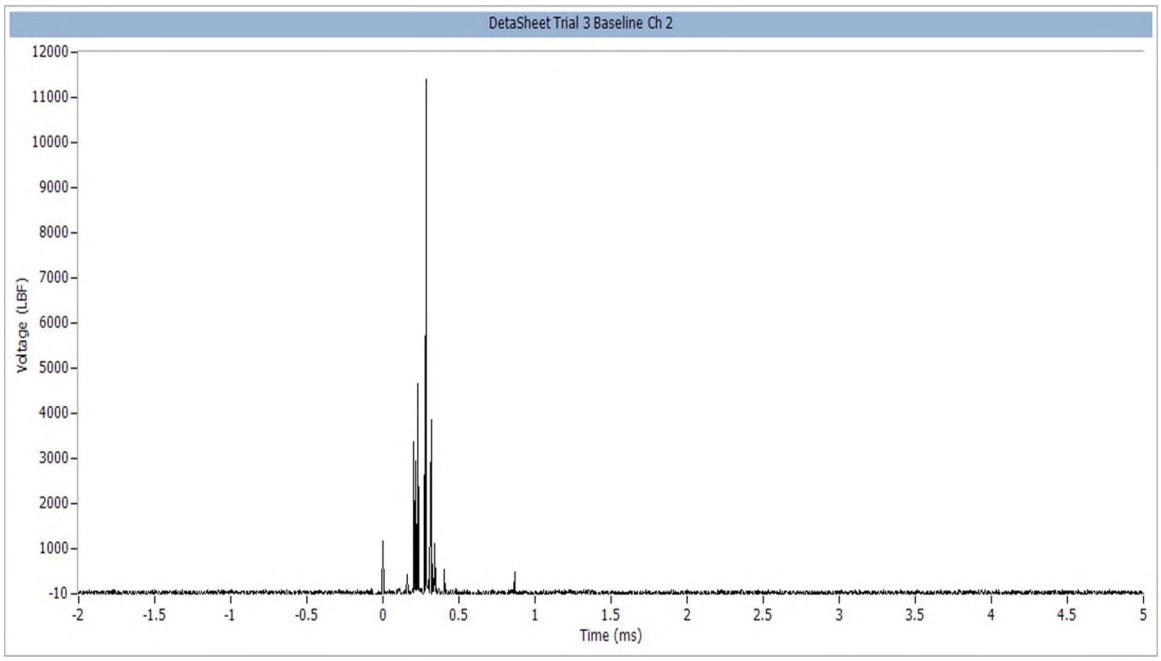

Figure A.17. DetaSheet baseline trial 3 channel 2 (lbf).

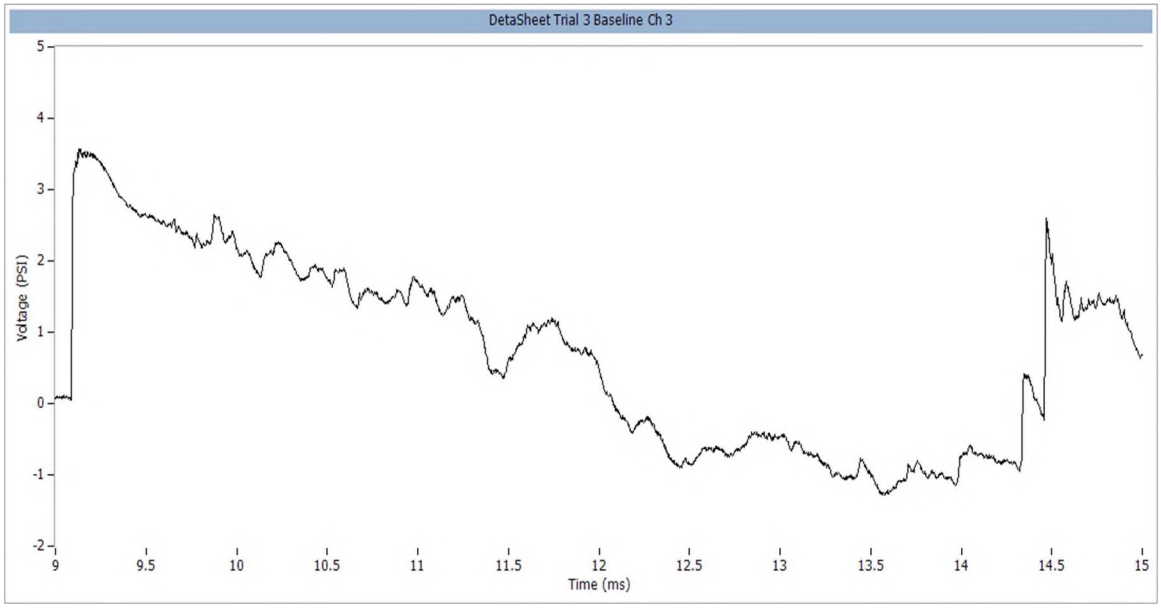

Figure A.18. DetaSheet baseline trial 3 channel 3 (psi).

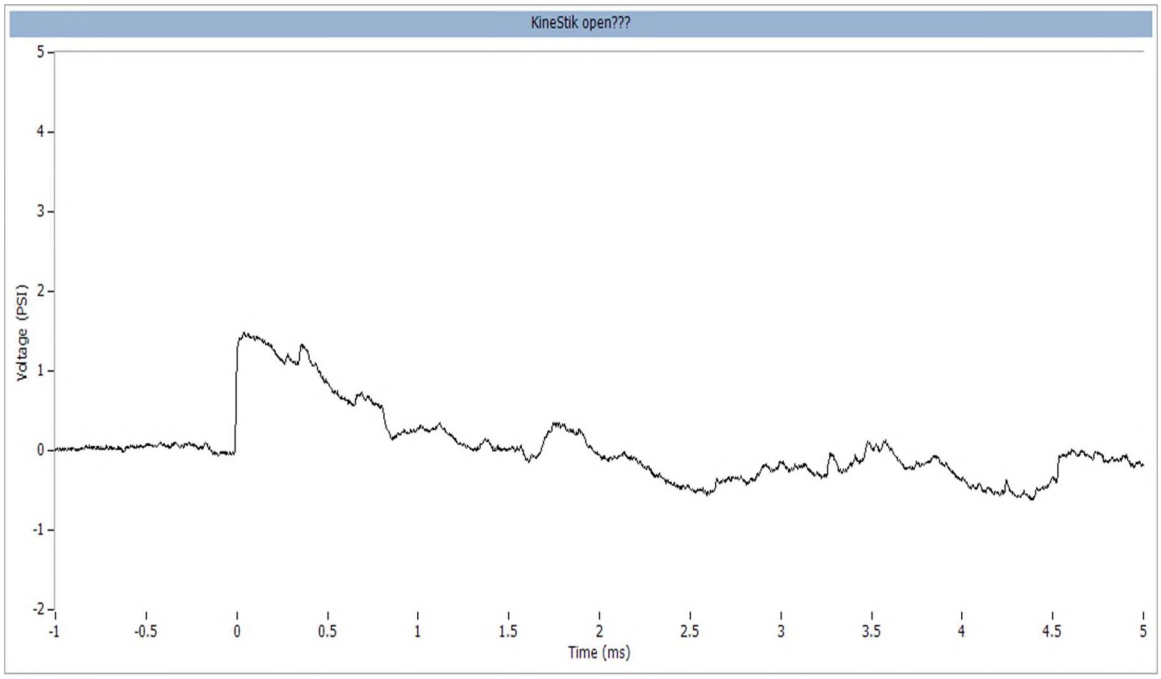

Figure A.19. KineStik baseline trial 1 channel 1 (psi).

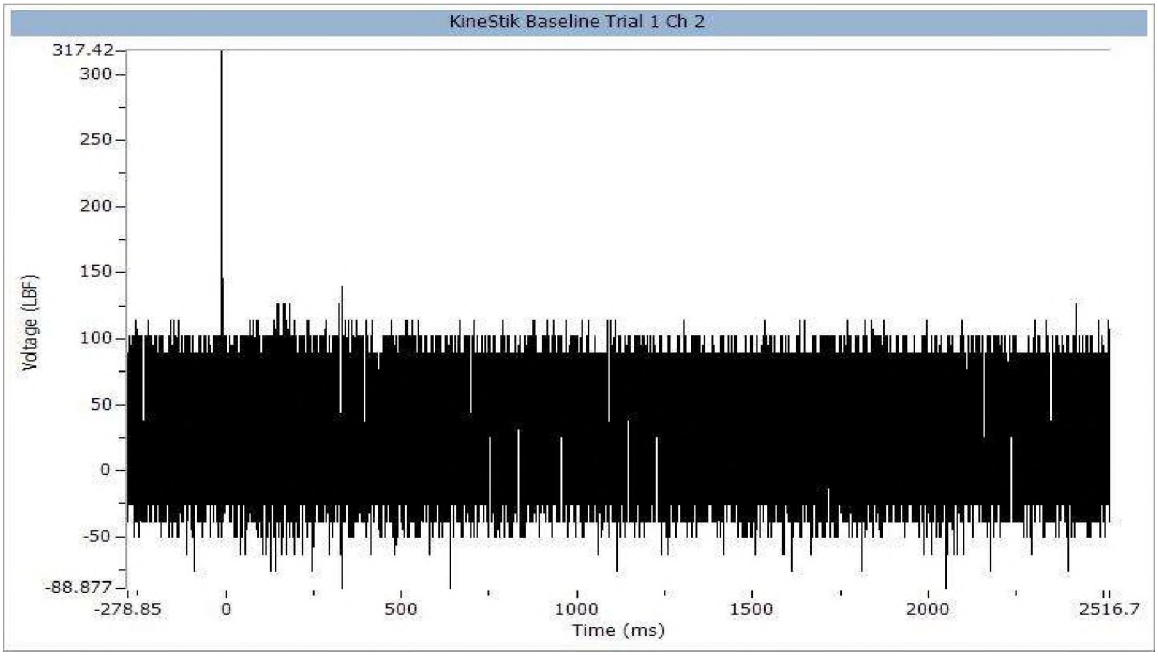

Figure A.20. KineStik baseline trial 1 channel 2 (lbf).

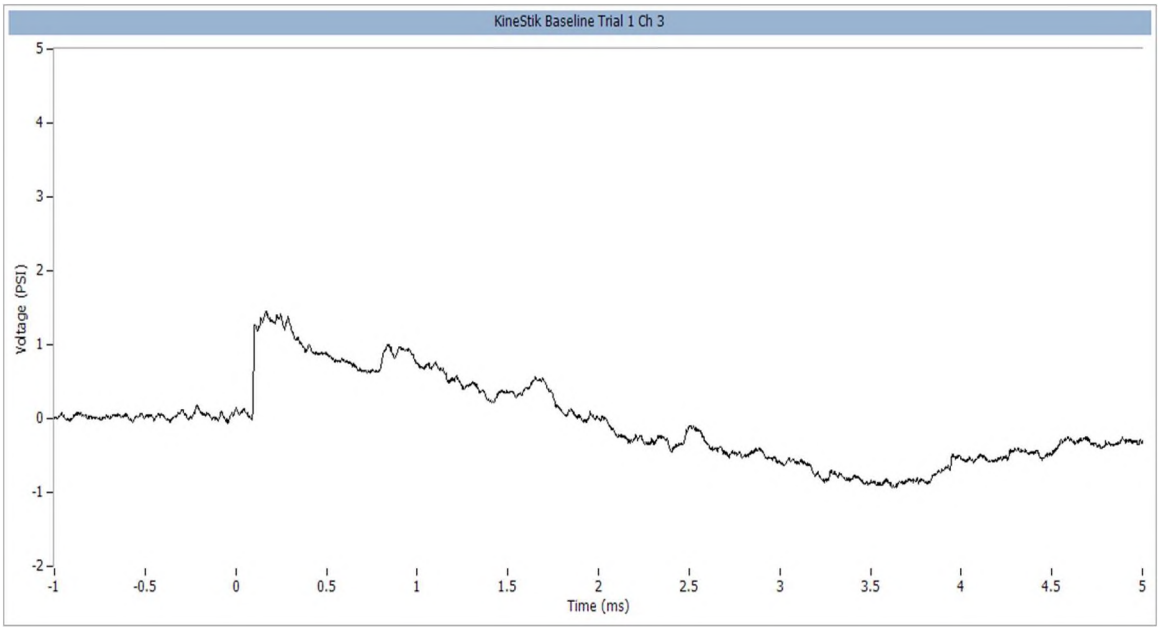

Figure A.21. KineStik baseline trial 1 channel 3 (psi).

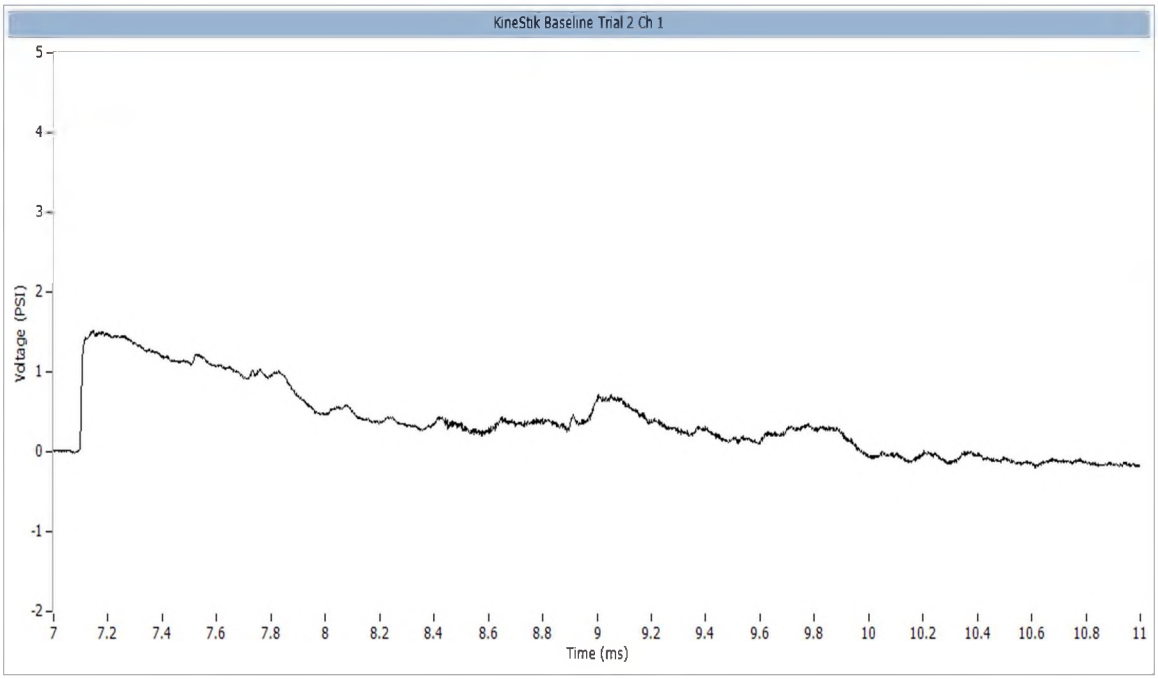

Figure A.22. KineStik baseline trial 2 channel 1 (psi).

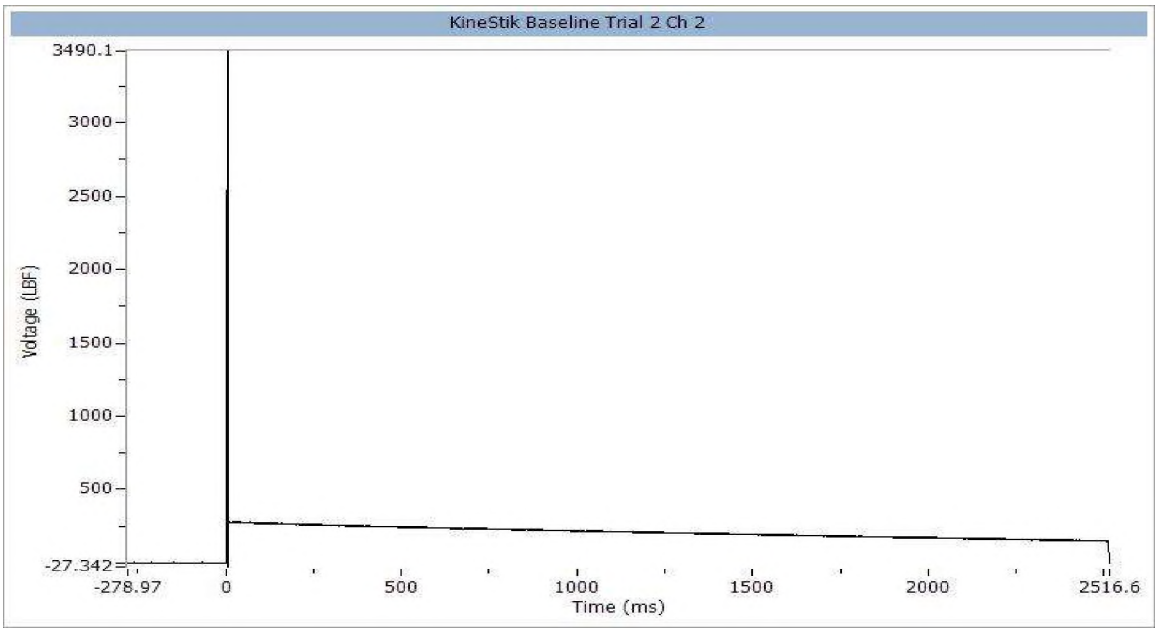

Figure A.23. KineStik baseline trial 2 channel 2 (lbf).

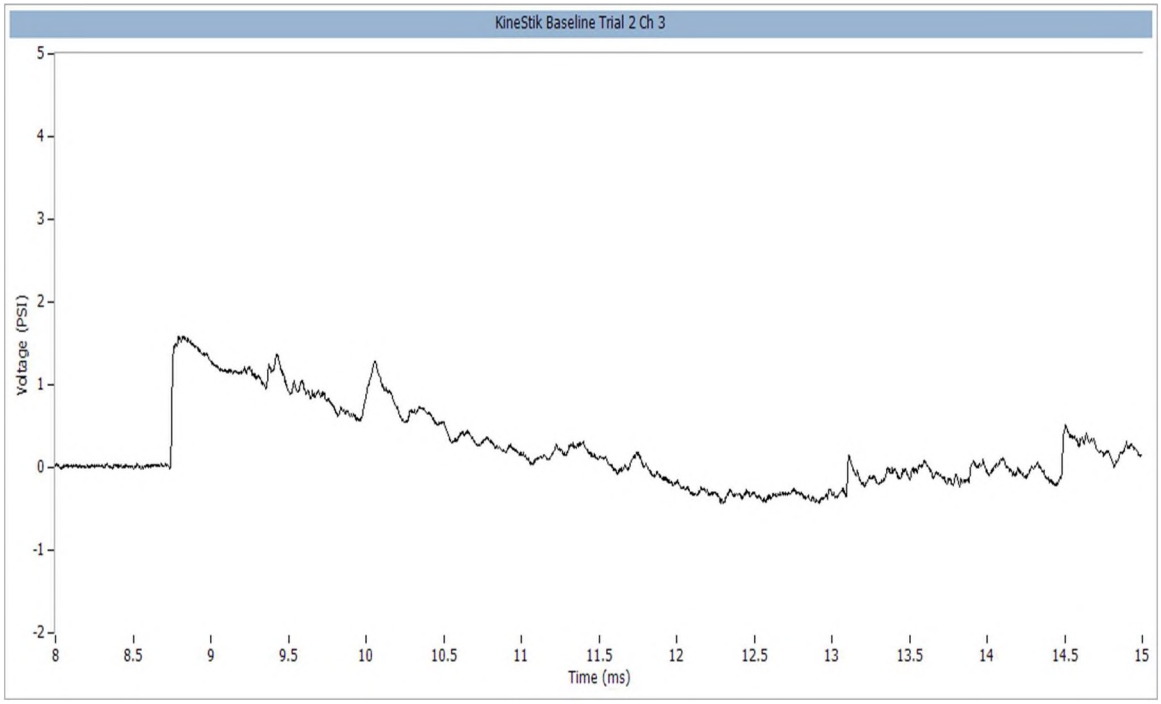

Figure A.24. KineStik baseline trial 2 channel 3 (psi).

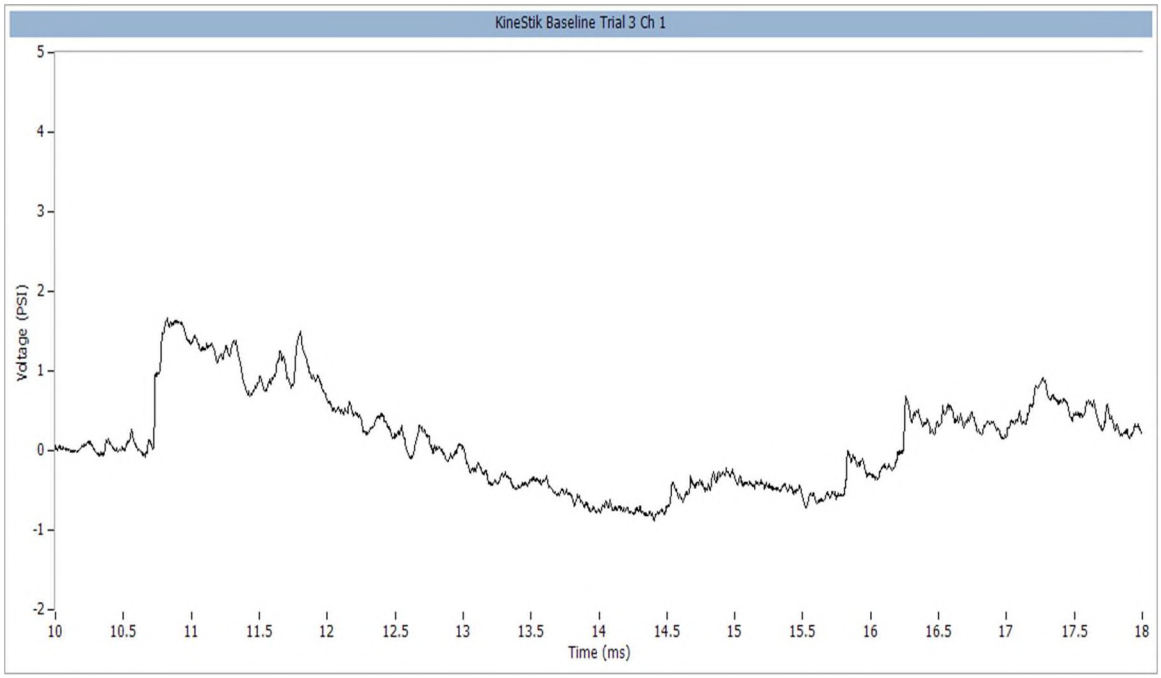

Figure A.25. KineStik baseline trial 3 channel 1 (psi).

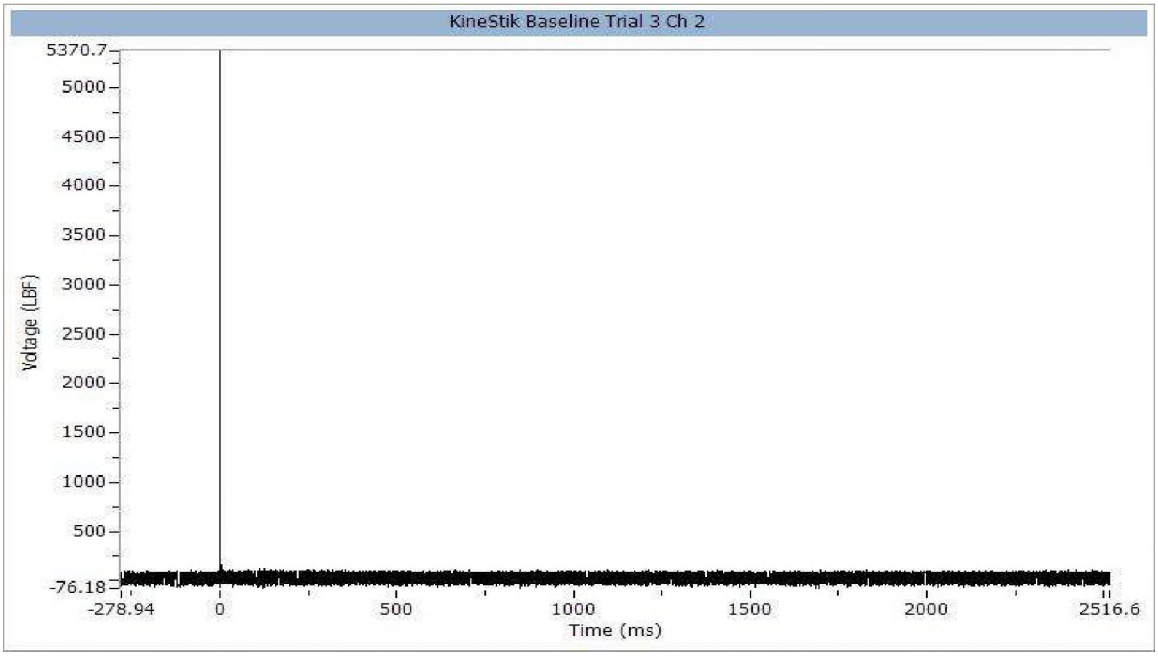

Figure A.26. KineStik baseline trial 3 channel 2 (lbf).

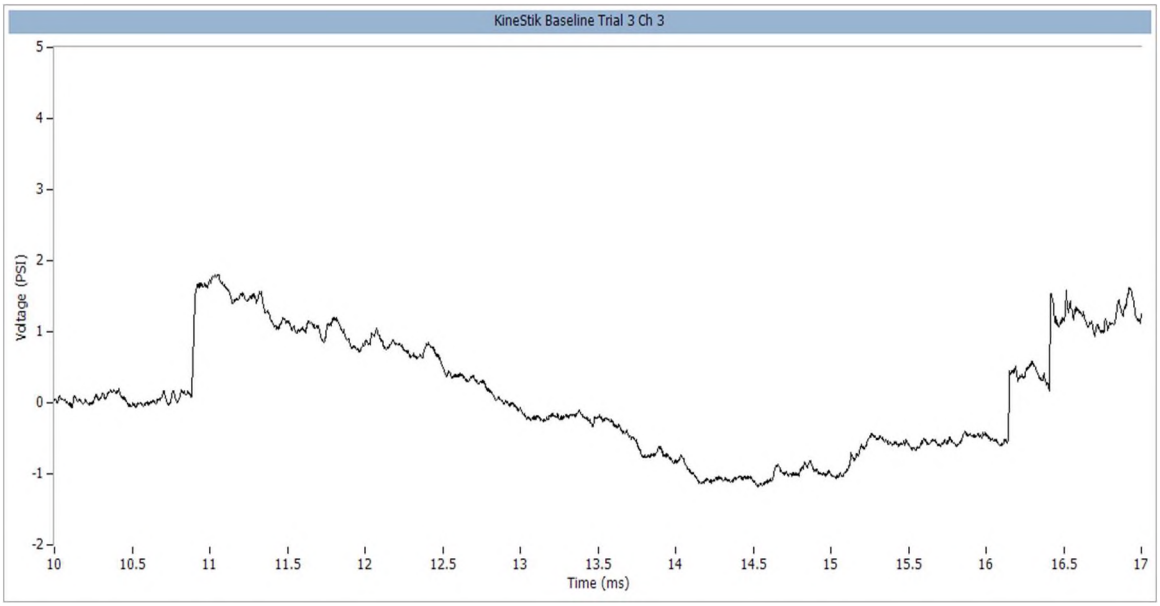

Figure A.27. KineStik baseline trial 3 channel 3 (psi).

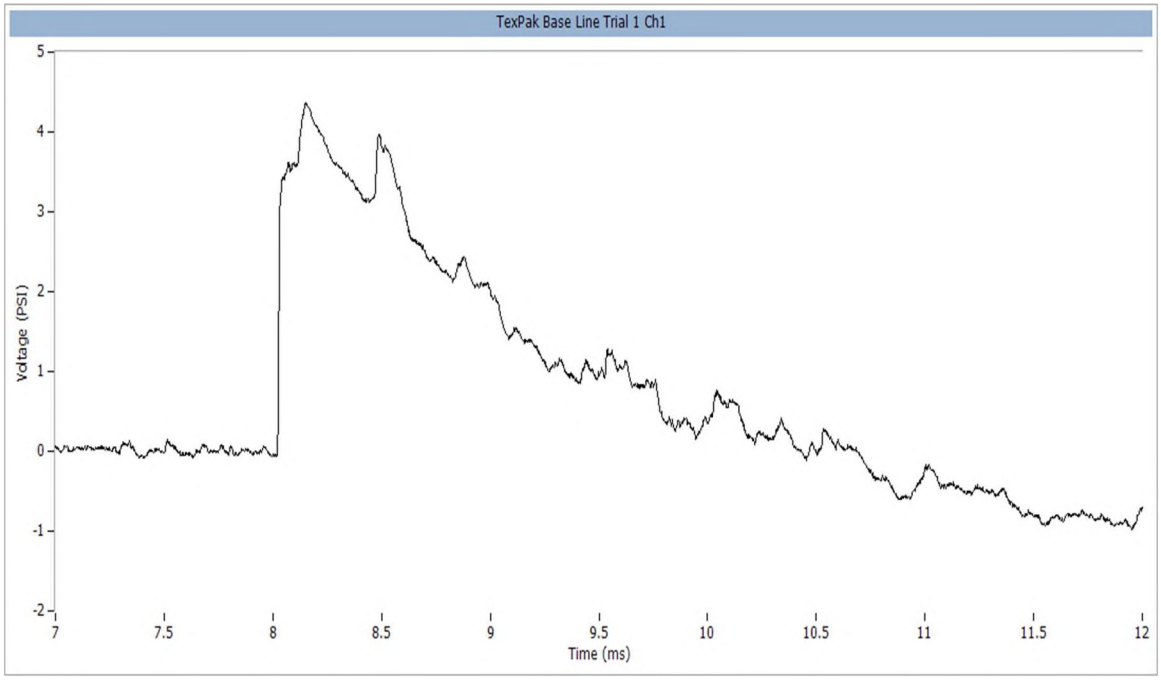

Figure A.28. TexPak baseline trial 1 channel 1 (psi).

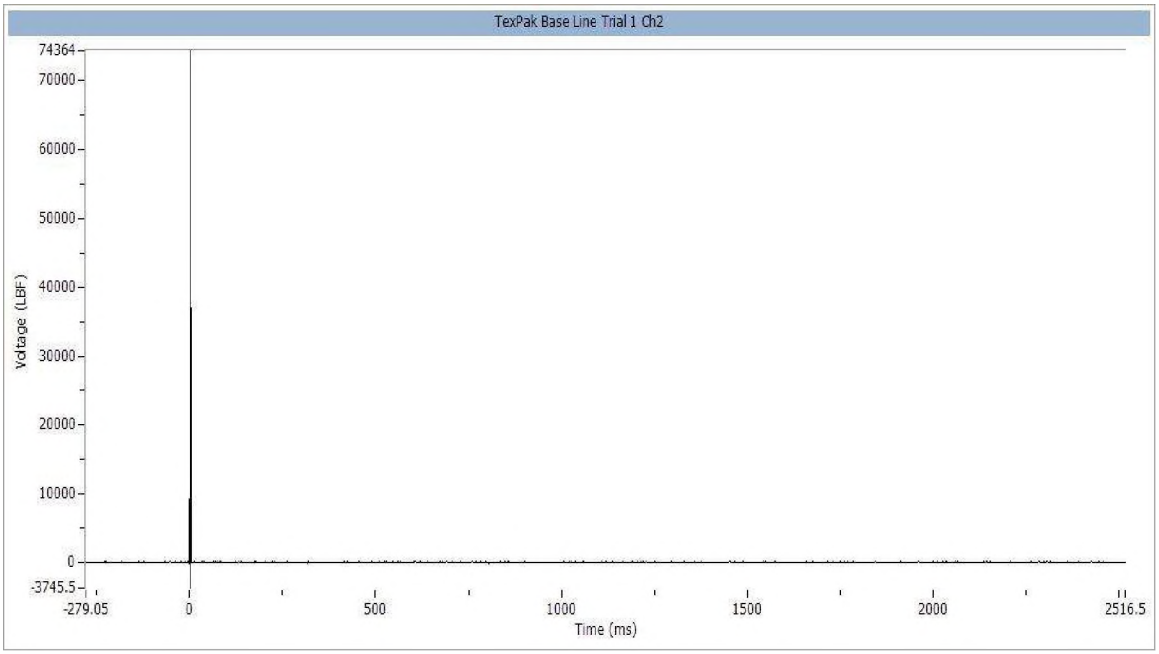

Figure A.29. TexPak baseline trial 1 channel 2 (lbf).

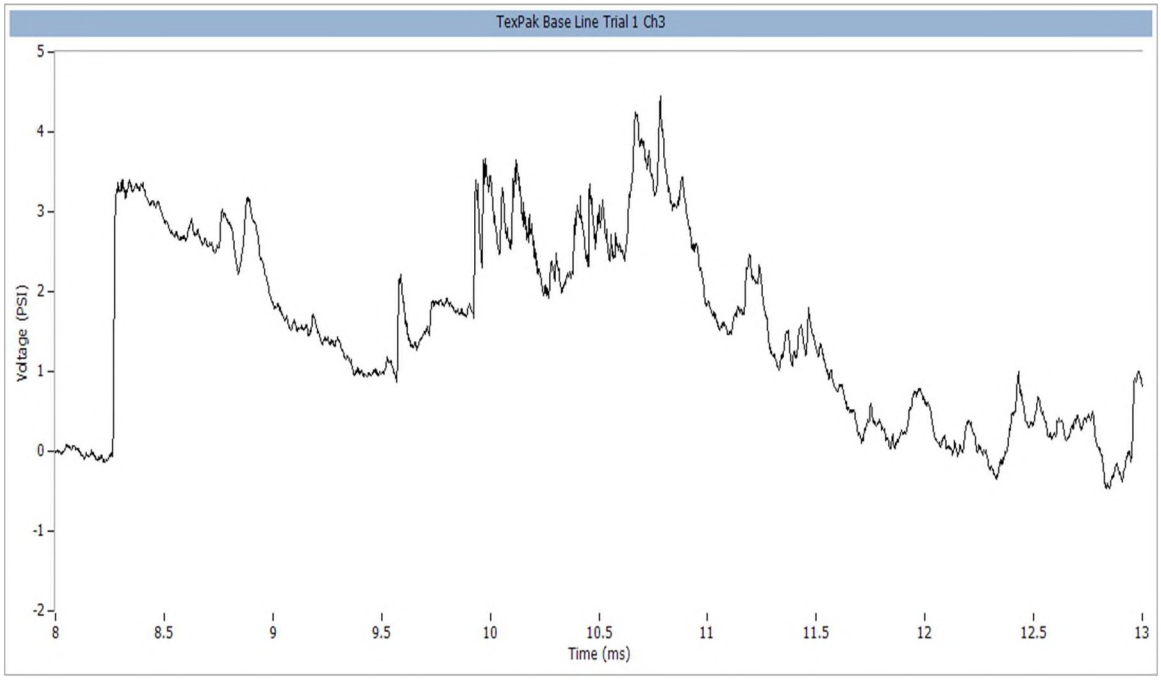

Figure A.30. TexPak baseline trial 1 channel 3 (psi).

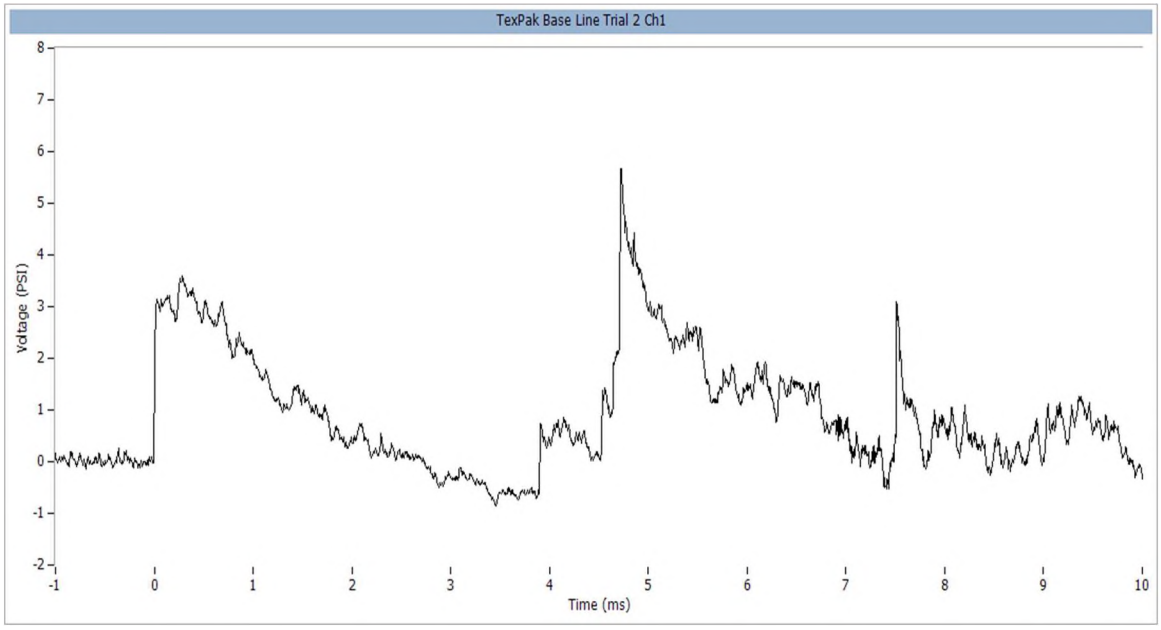

Figure A.31. TexPak baseline trial 2 channel 1 (psi).

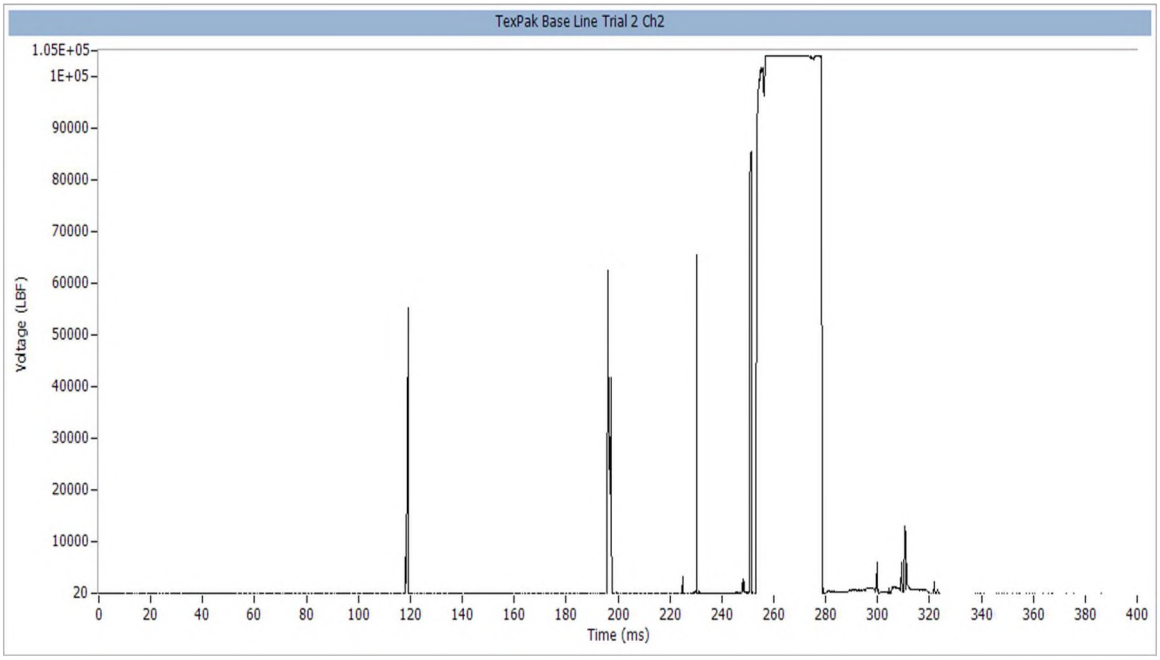

Figure A.32. TexPak baseline trial 2 channel 2 (lbf).

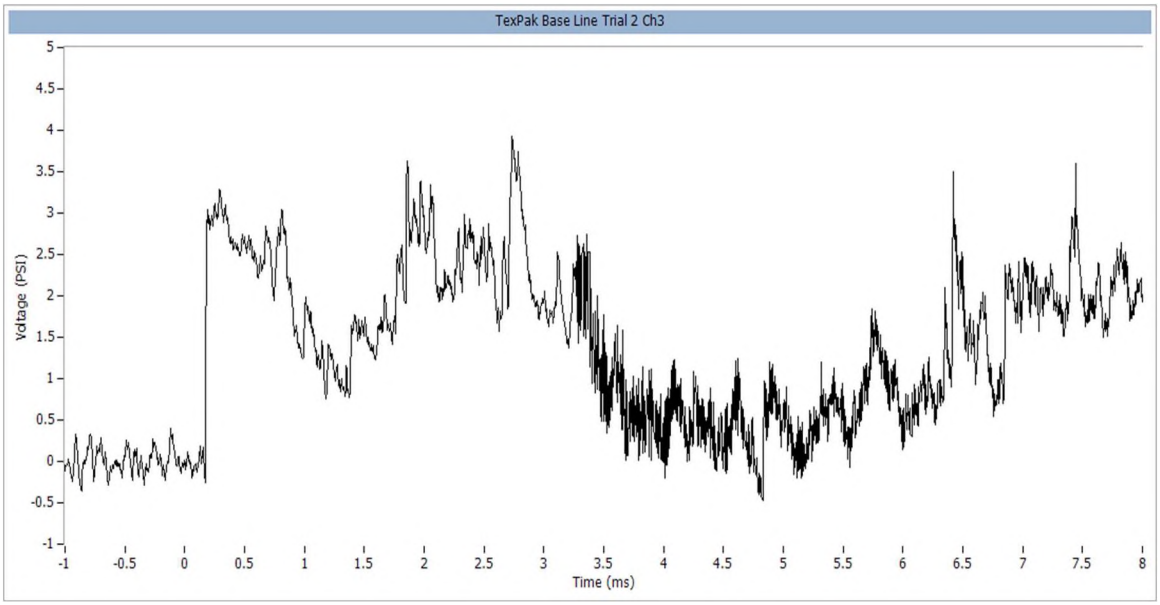

Figure A.33. TexPak baseline trial 2 channel 3 (psi).

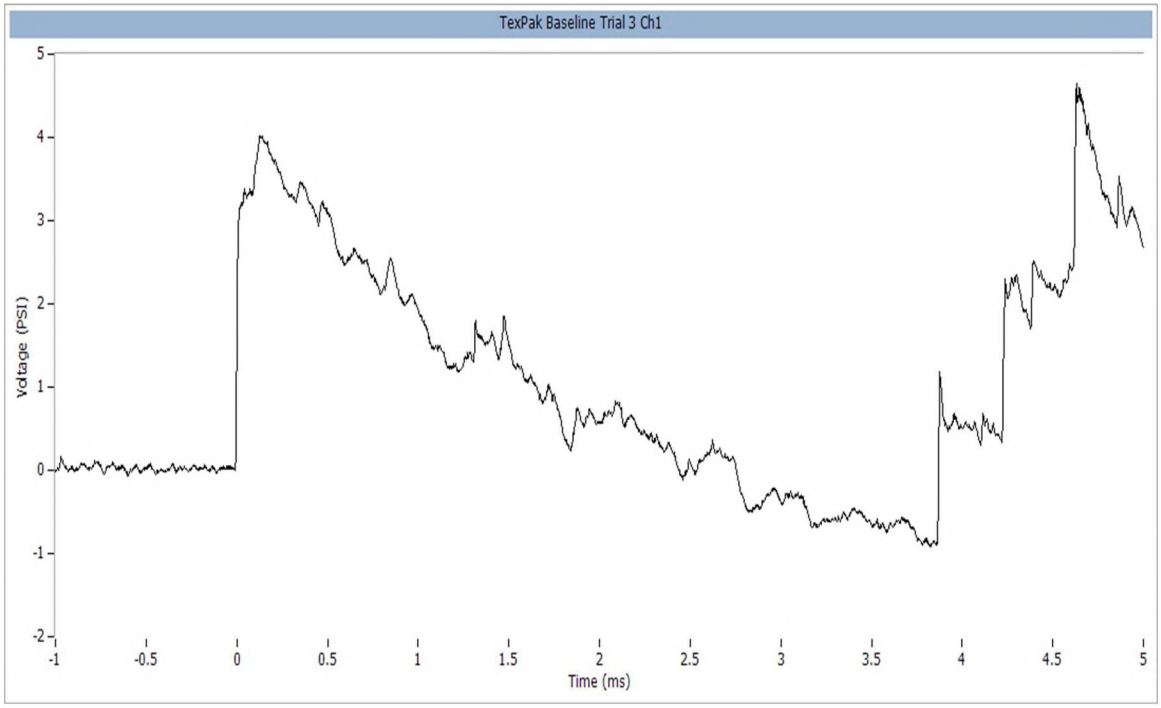

Figure A.34. TexPak baseline trial 3 channel 1 (psi).

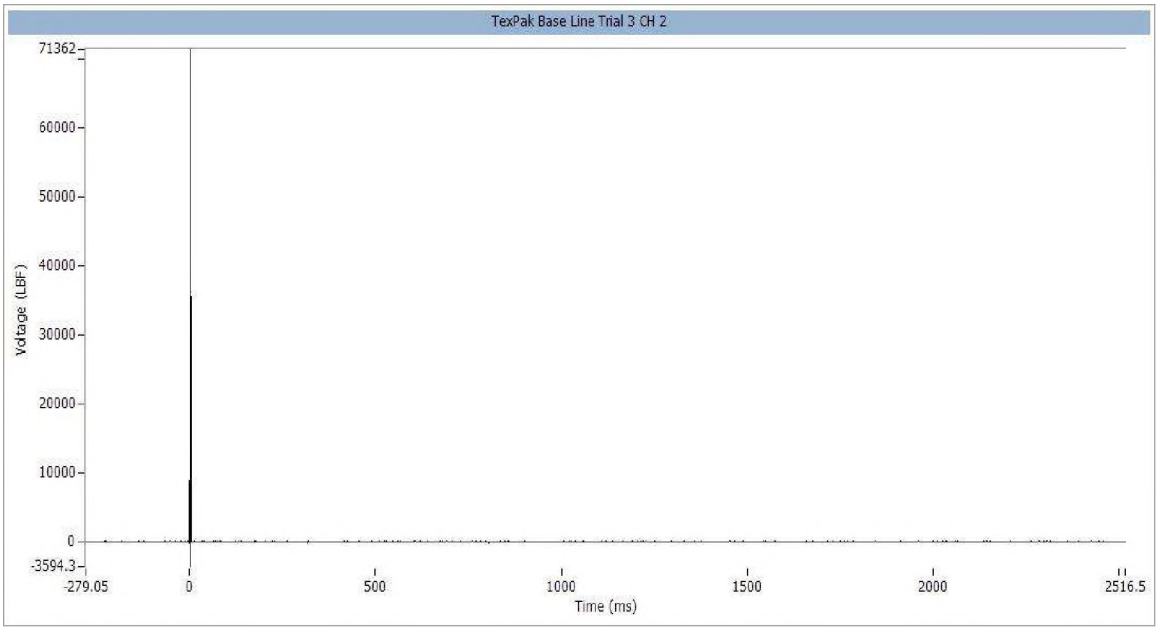

Figure A.35. TexPak baseline trial 3 channel 2 (lbf).

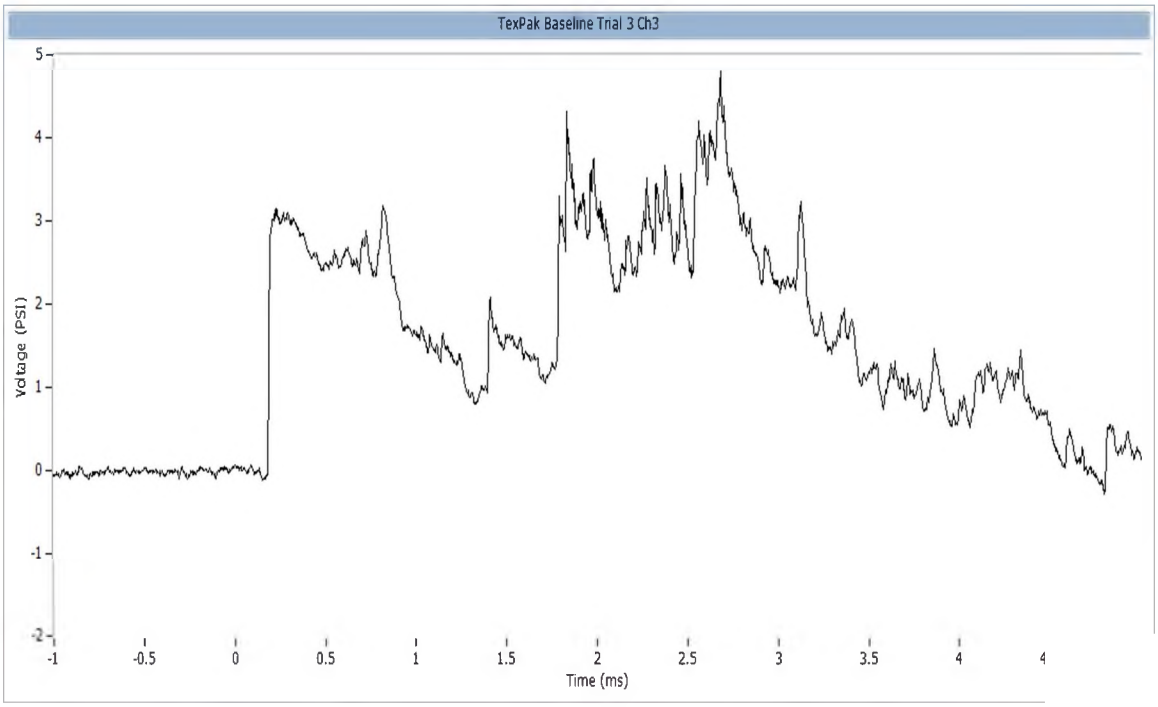

Figure A.36. TexPak baseline trial 3 channel 3 (psi).

APPENDIX B.

FOAM CURE TIME DATA

The collected output data from rigid polyurethane foam variable cure-time experimental testing was provided in this appendix for all trials performed. This data was collected by two pressure tranducers and a load-cell force sensor. All sensor signals were sent through a signal conditioner before being collect and stored in an MREL data accusation system. This stored data was analyzed and interpreted using MREL compatible software. The variable cure time testing consisted of charges detonated under the confinement of rigid polyurethane foam cured for variable time limits of 3.5-, 10-, 20-, 30-minutes. The data was presented in alphabetical order of explosive type tested. The order of data was further sorted in the corresponding trial number and recorded data channel number.

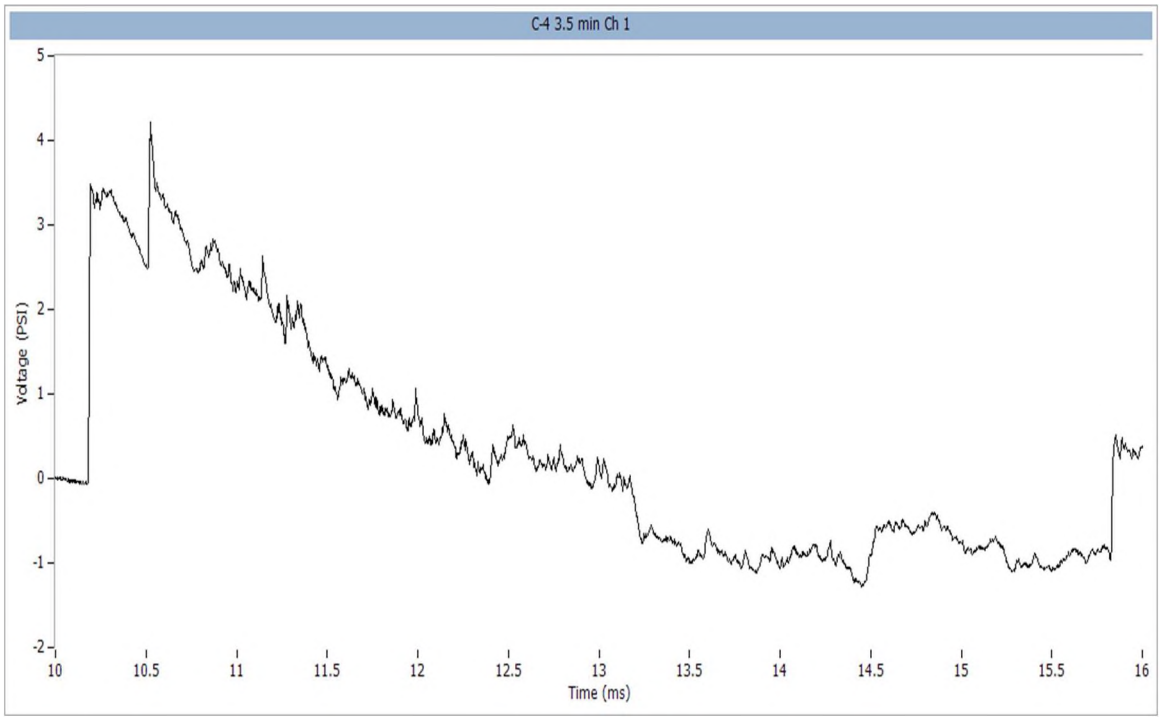

Figure B.1. C-4 3.5-minute foam cure time channel 1 (psi).

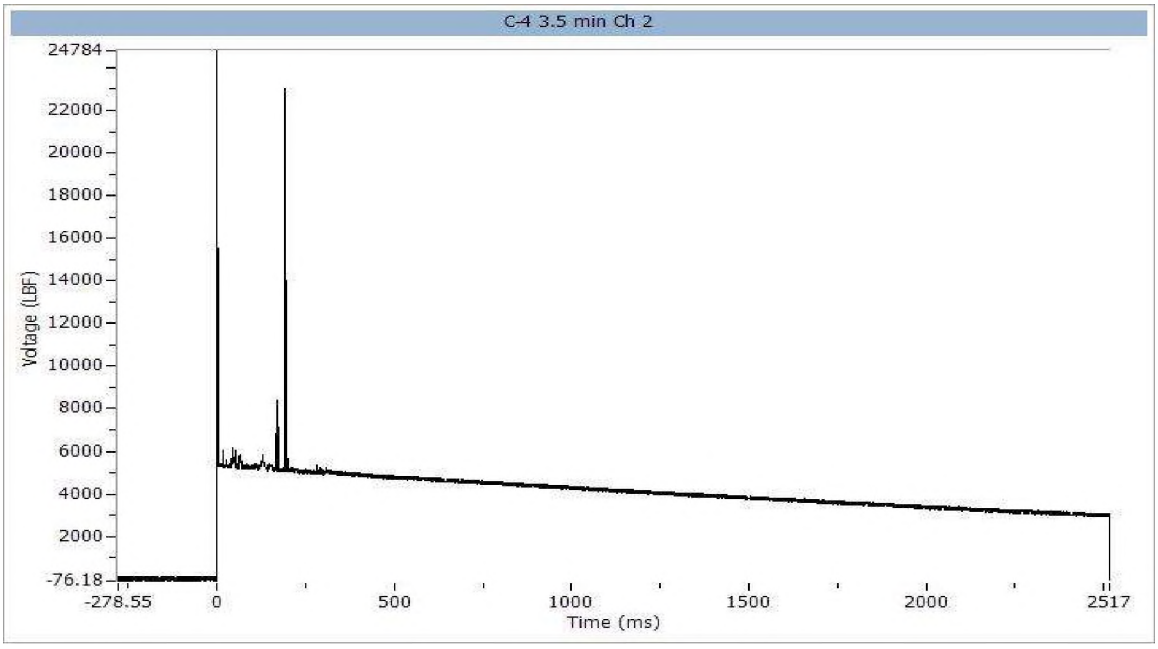

Figure B.2. C-4 3.5-minute foam cure time channel 2 (lbf).

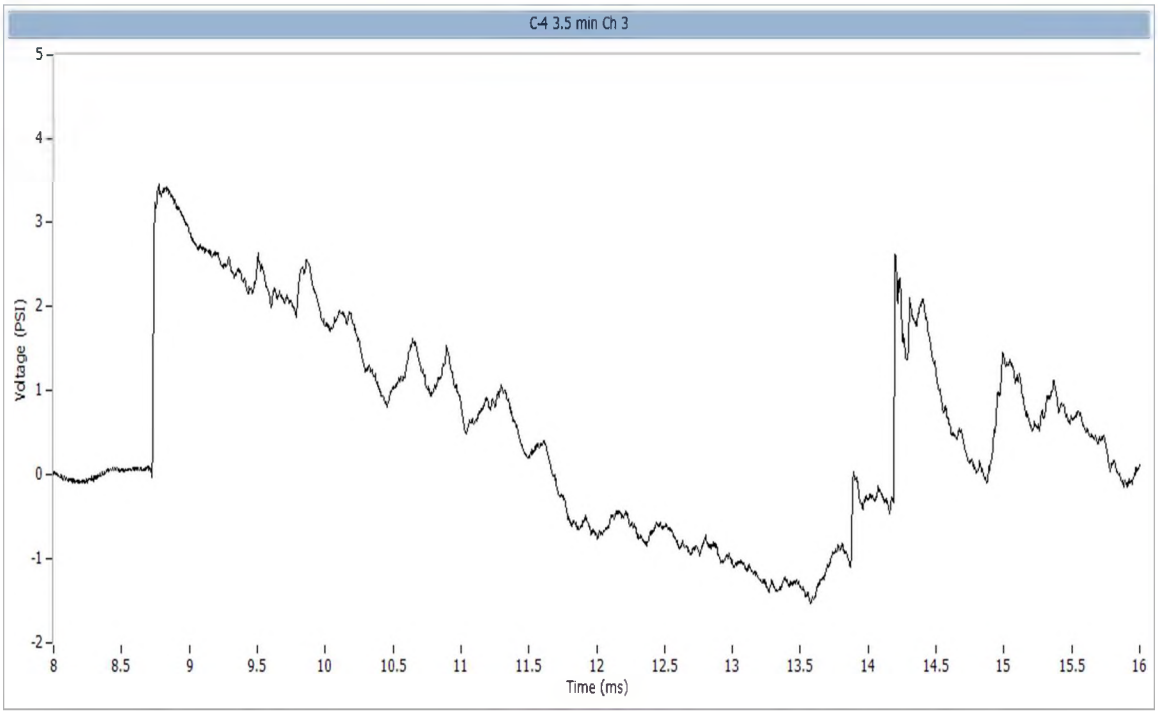

Figure B.3. C-4 3.5-minute foam cure time channel 3 (psi).

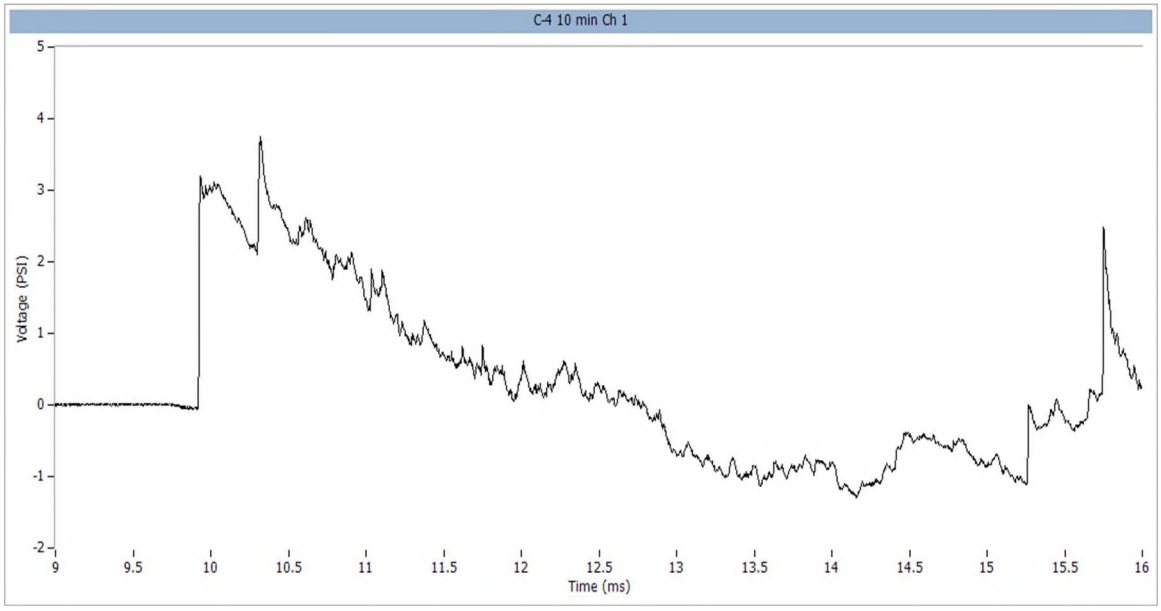

Figure B.4. C-4 10-minute foam cure time channel 1 (psi).

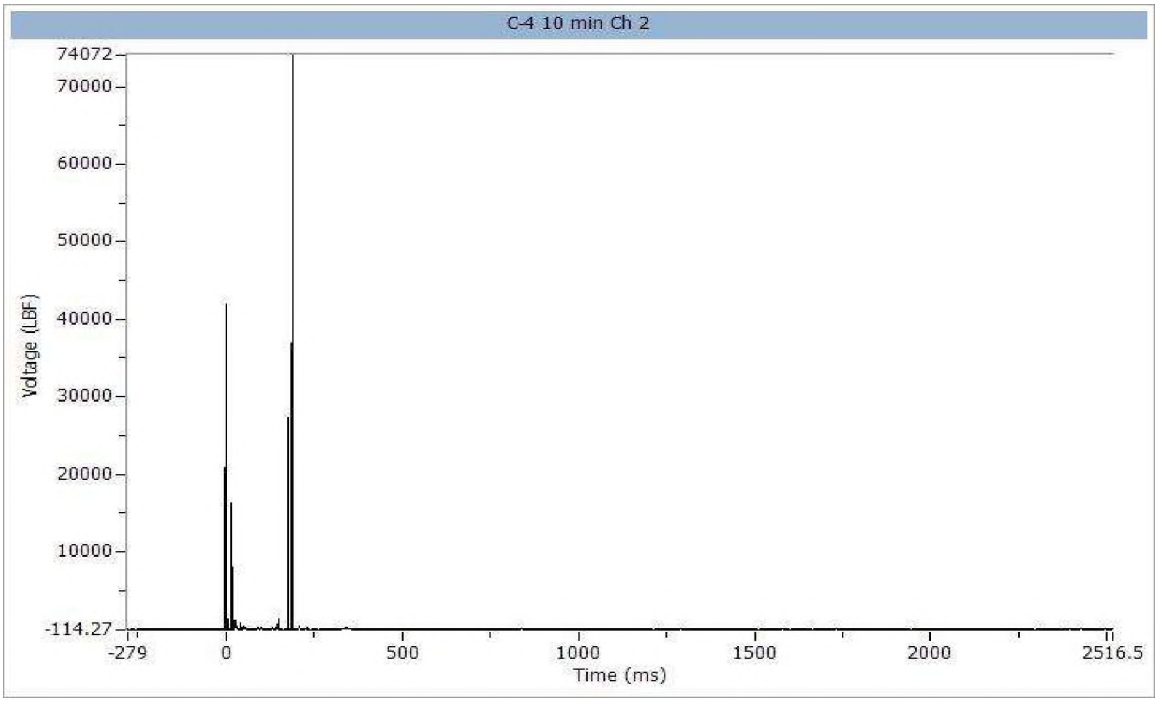

Figure B.5. C-4 10-minute foam cure time channel 2 (lbf).

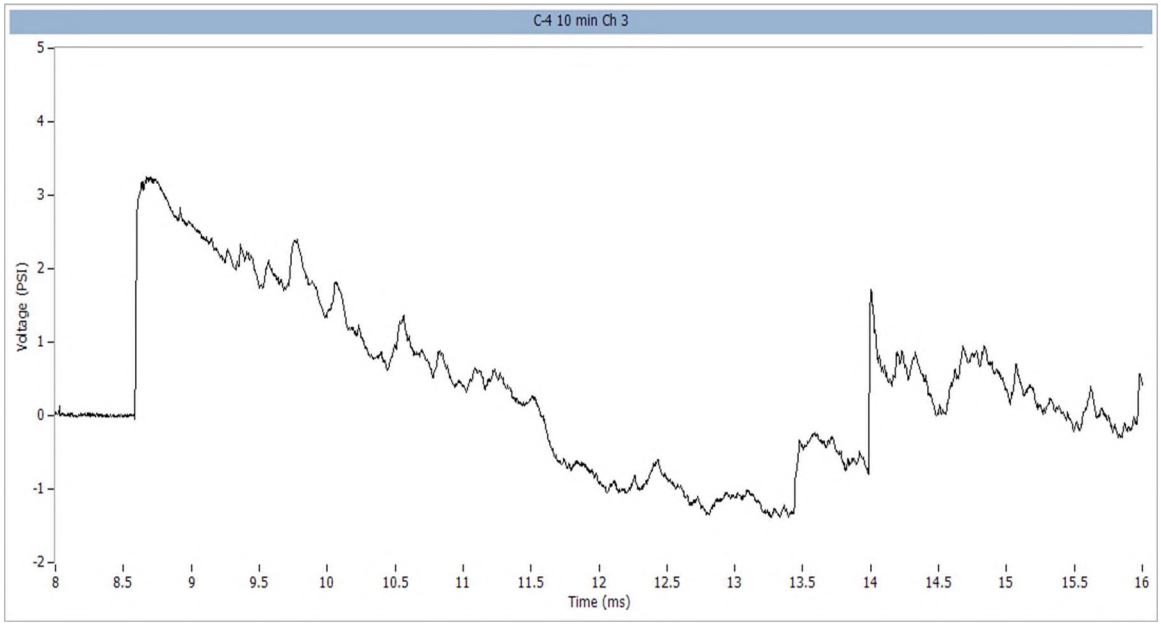

Figure B.6. C-4 10-minute foam cure time channel 3 (psi).

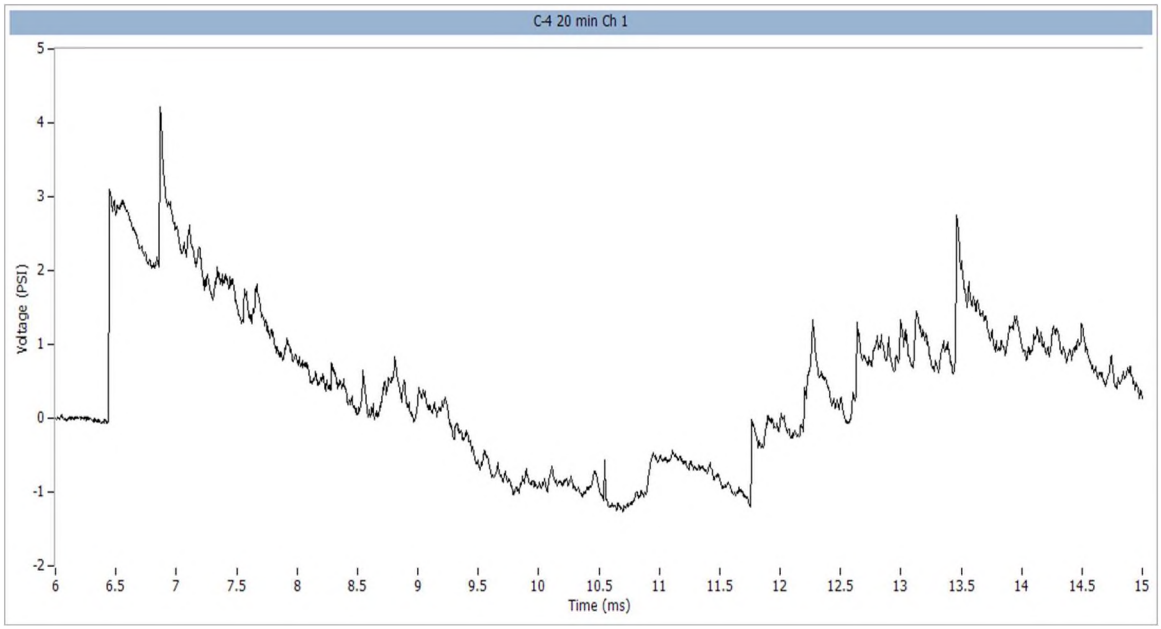

Figure B.7. C-4 20-minute foam cure time channel 1 (psi).

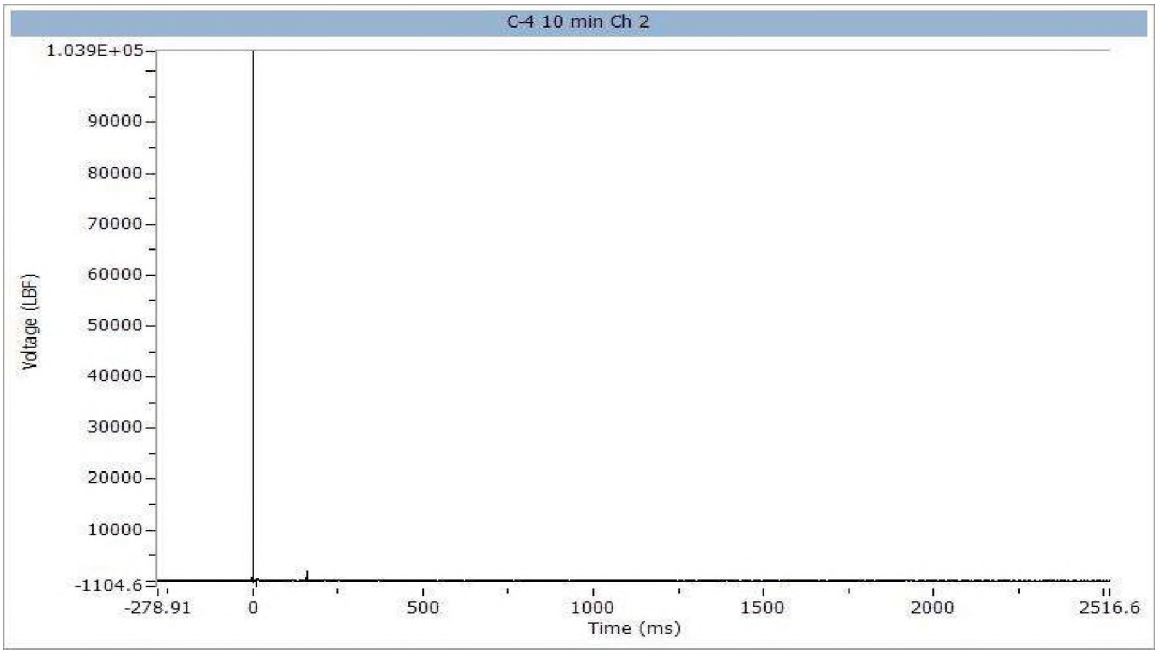

Figure B.8. C-4 20-minute foam cure time channel 2 (lbf). The plot was improperly titled "10-minute" from MREL software.

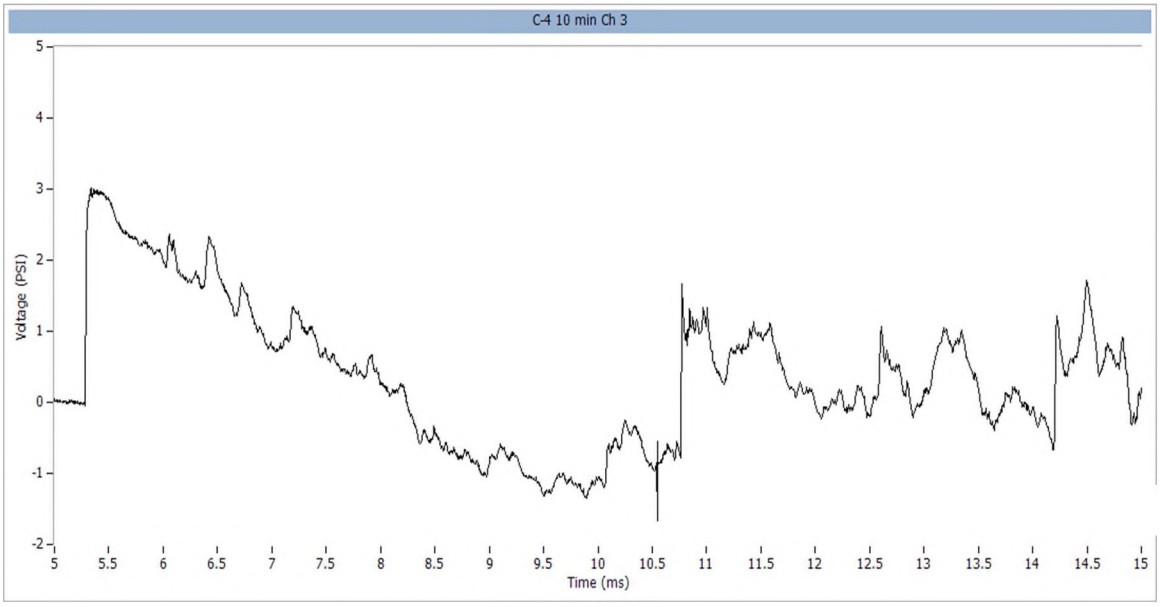

Figure B.9. C-4 20-minute foam cure time channel 3 (psi). The plot was improperly titled "10-minute" from MREL software.

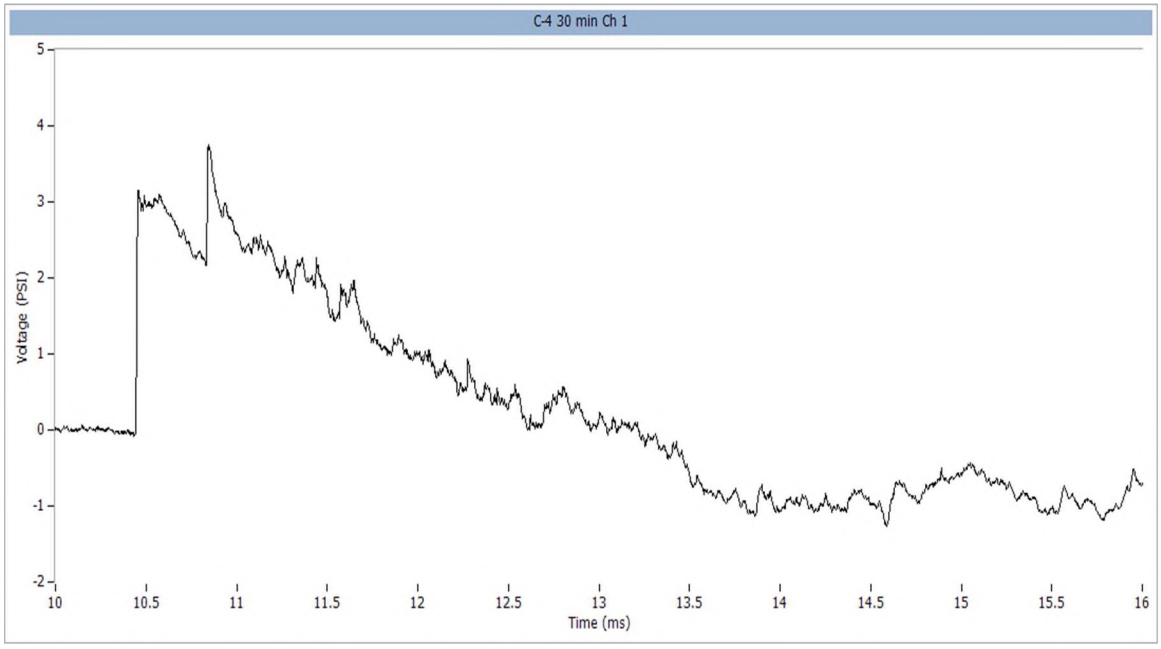

Figure B.10. C-4 30-minute foam cure time channel 1 (psi).

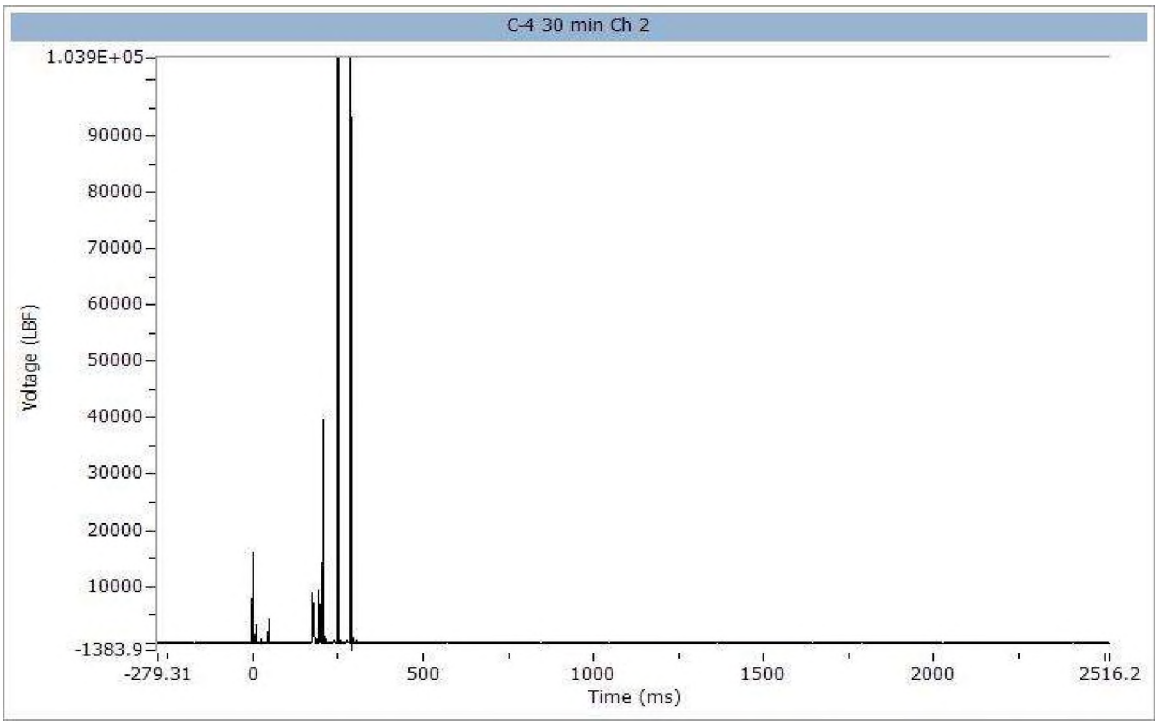

Figure B.11. C-4 30-minute foam cure time channel 2 (lbf).

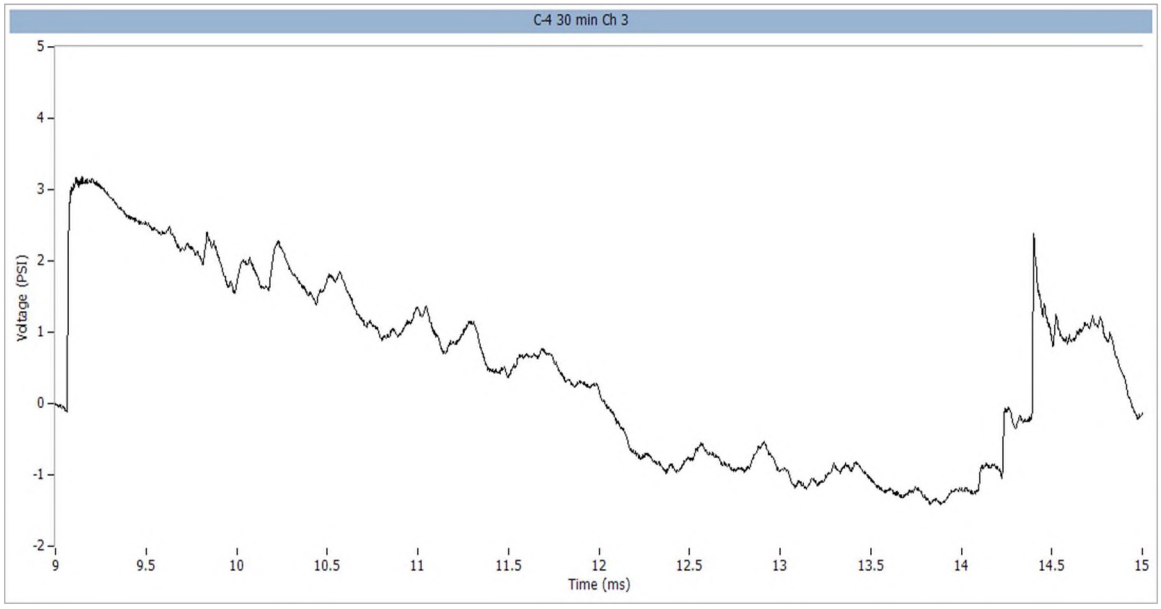

Figure B.12. C-4 30-minute foam cure time channel 3 (psi).

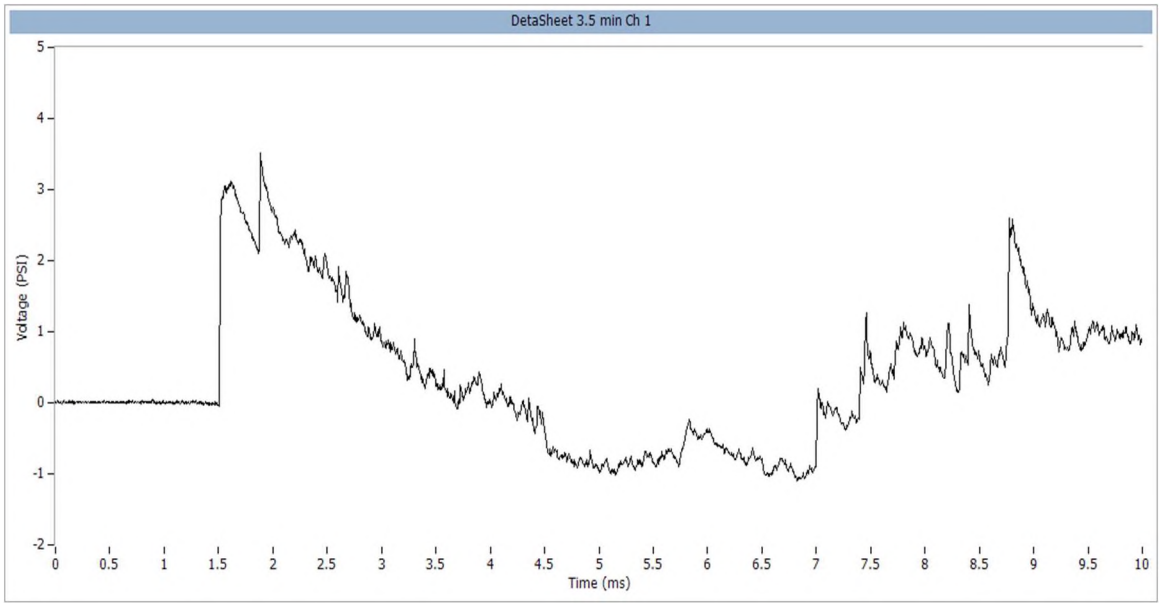

Figure B.13. DetaSheet 3.5-minute foam cure time channel 1 (psi).

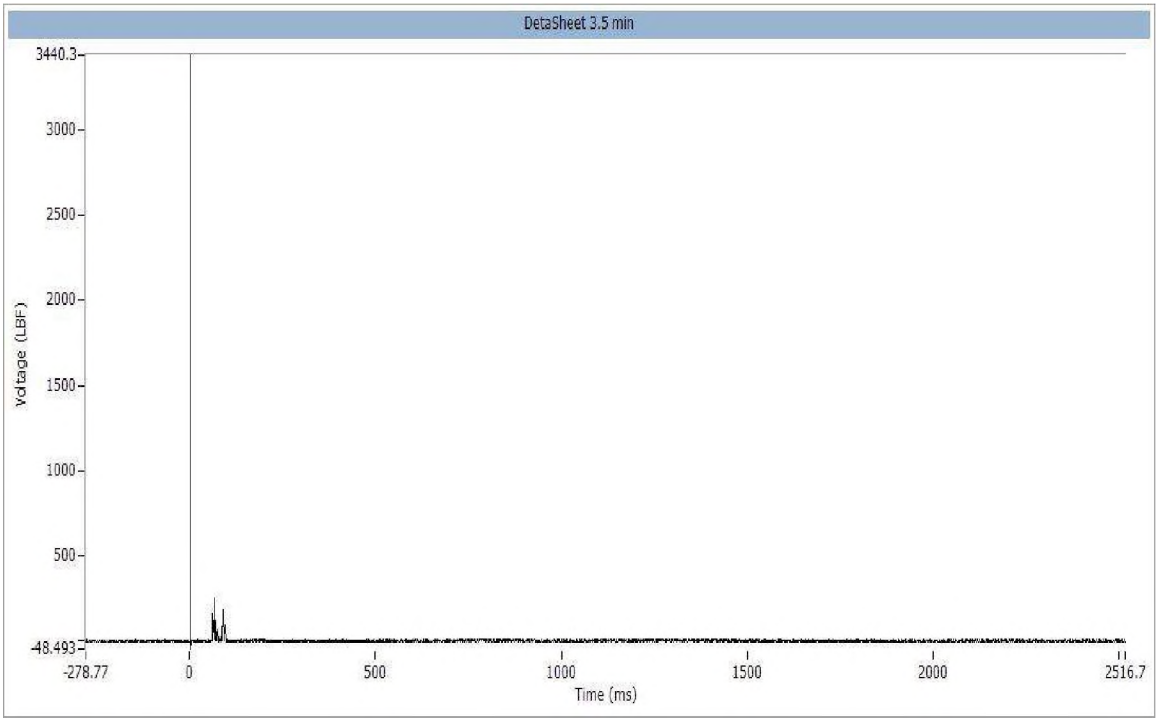

Figure B.14. DetaSheet 3.5-minute foam cure time channel 2 (lbf).

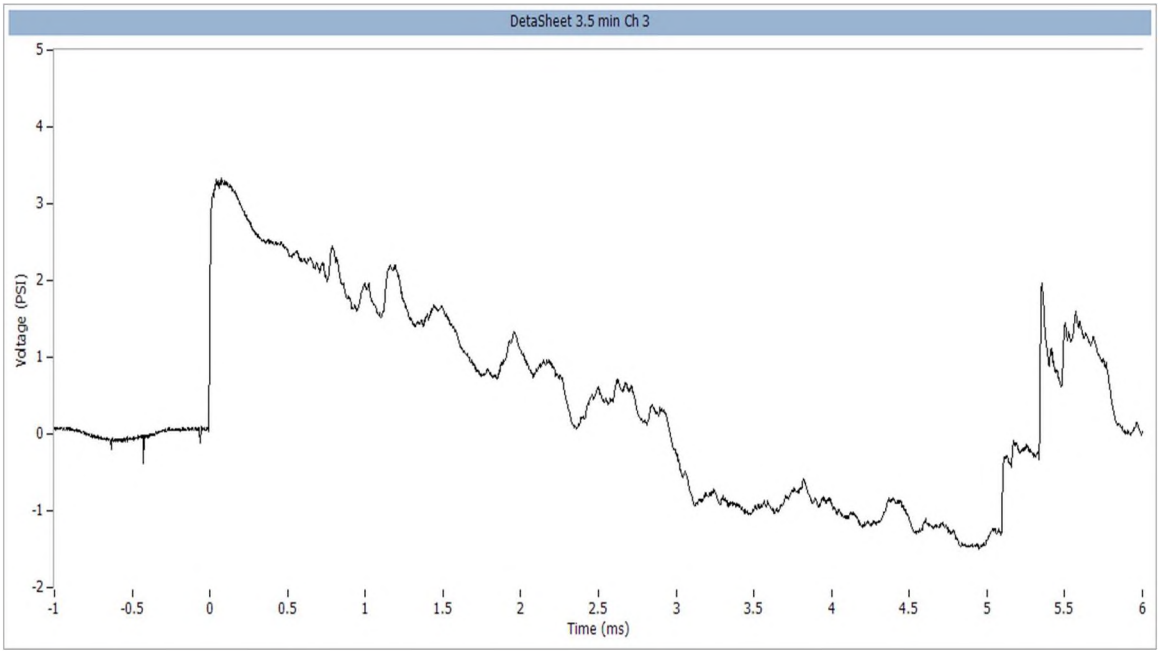

Figure B.15. DetaSheet 3.5-minute foam cure time channel 3 (psi).

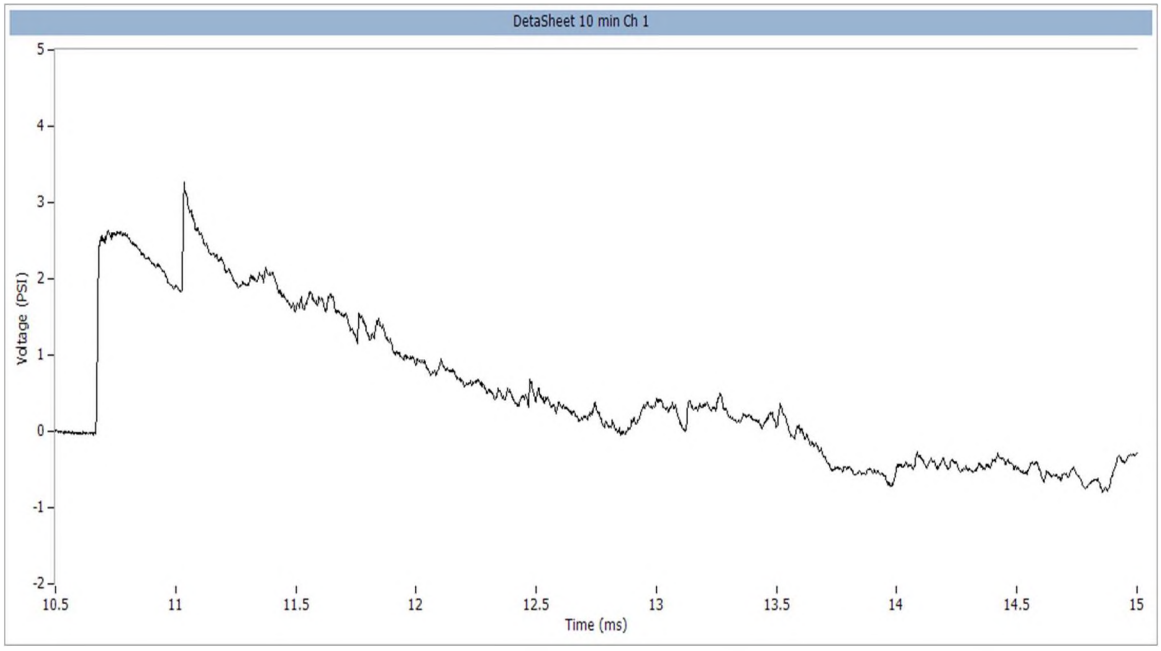

Figure B.16. DetaSheet 10-minute foam cure time channel 1 (psi).

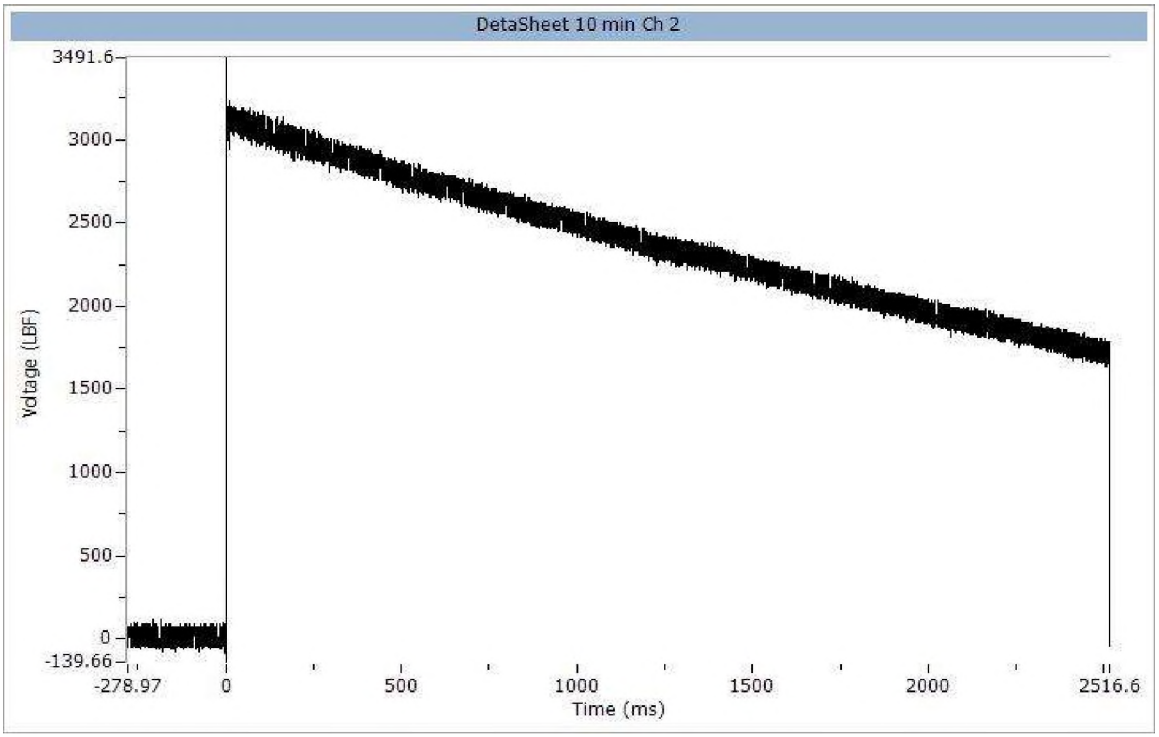

Figure B.17. DetaSheet 10-minute foam cure time channel 2 (lbf).

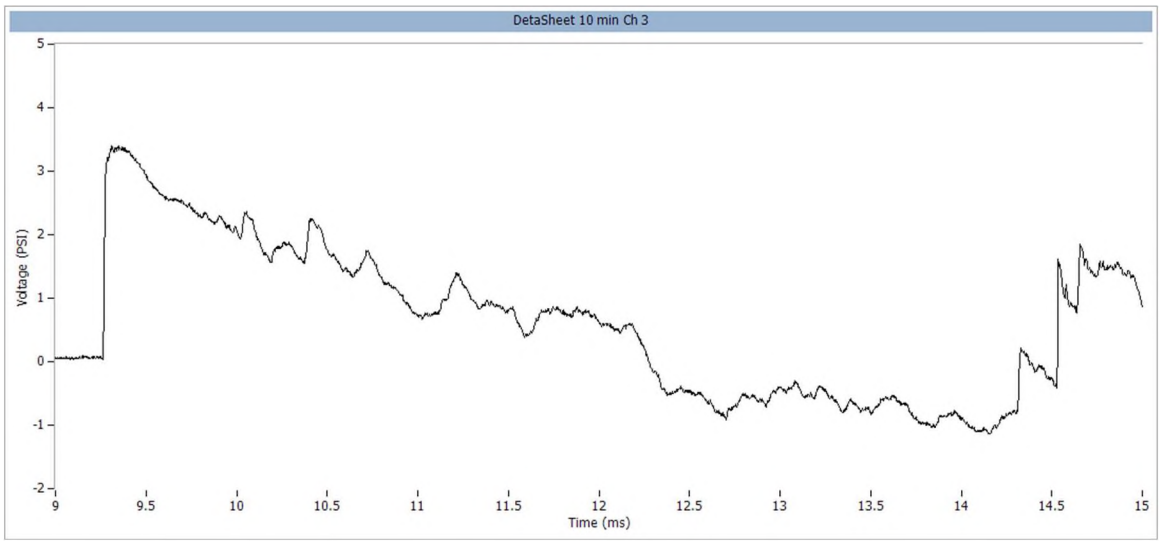

Figure B.18. DetaSheet 10-minute foam cure time channel 3 (psi).

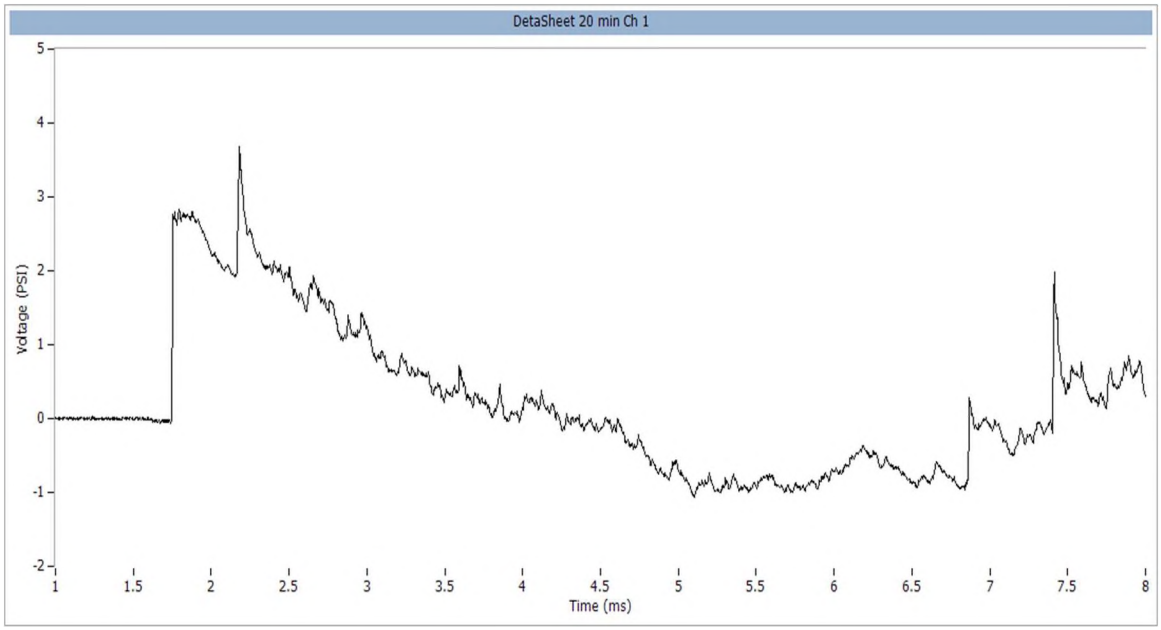

Figure B.19. DetaSheet 20-minute foam cure time channel 1 (psi).

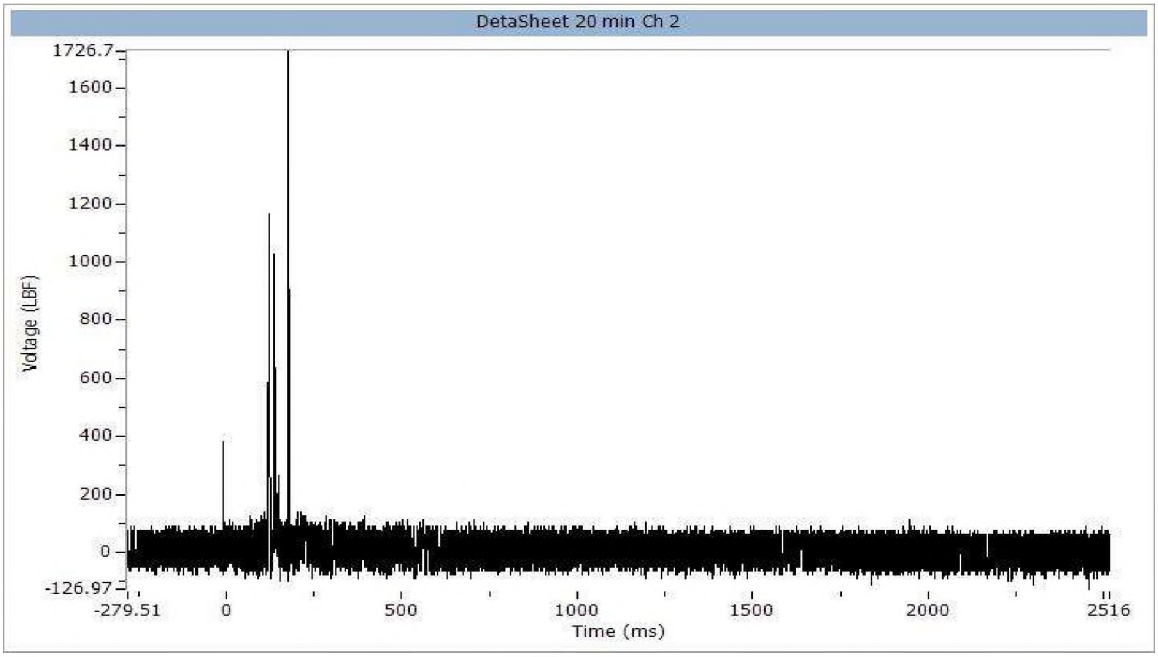

Figure B.20. DetaSheet 20-minute foam cure time channel 2 (lbf).

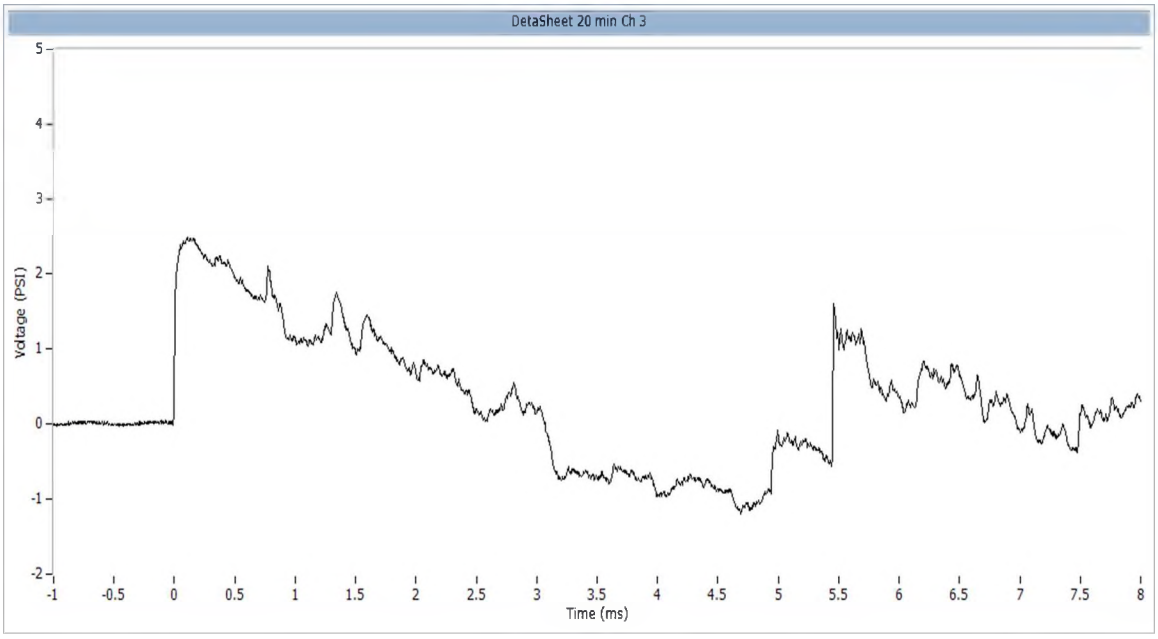

Figure B.21. DetaSheet 20-minute foam cure time channel 3 (psi).

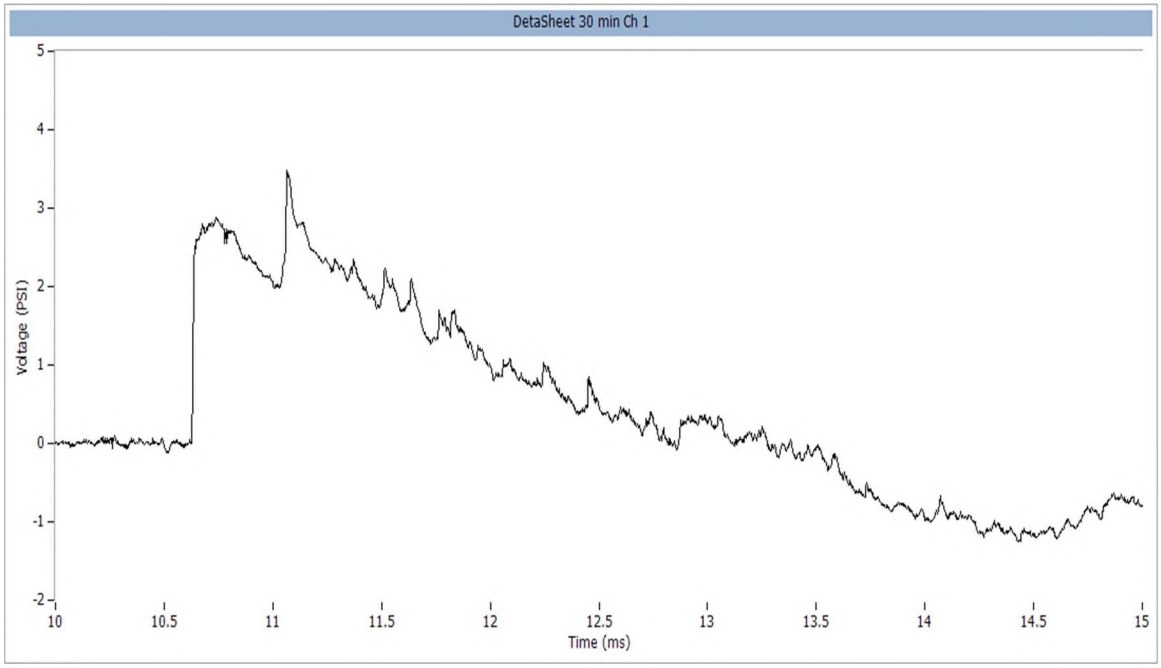

Figure B.22. DetaSheet 30-minute foam cure time channel 1 (psi).

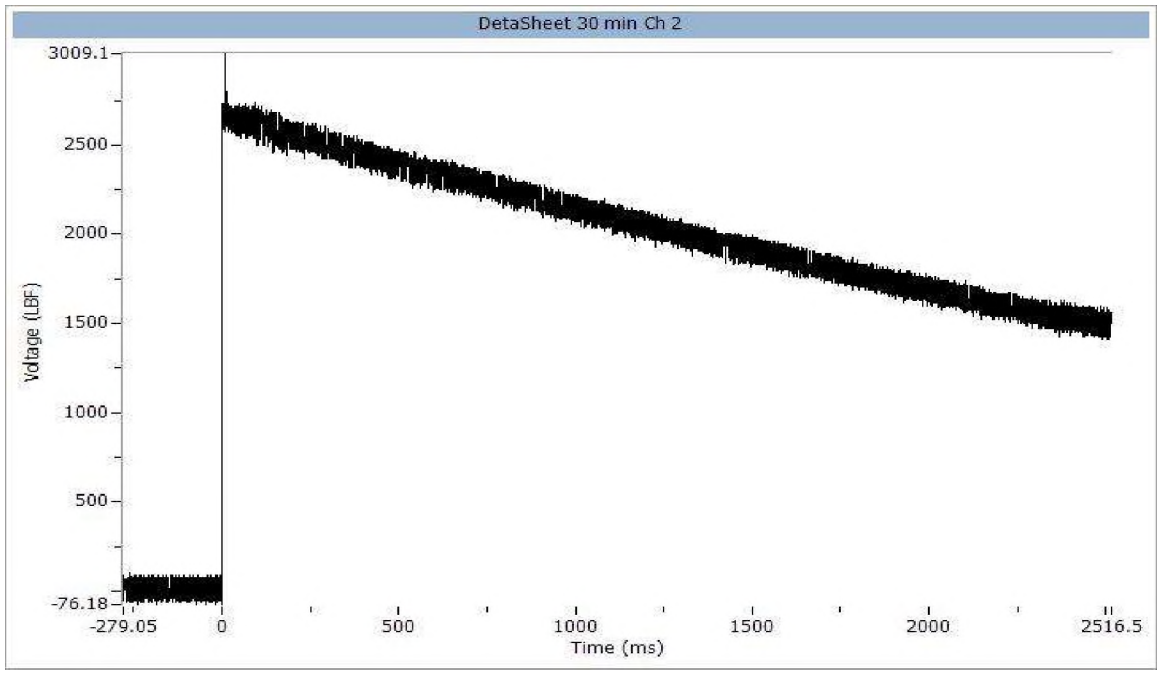

Figure B.23. DetaSheet 30-minute foam cure time channel 2 (lbf).

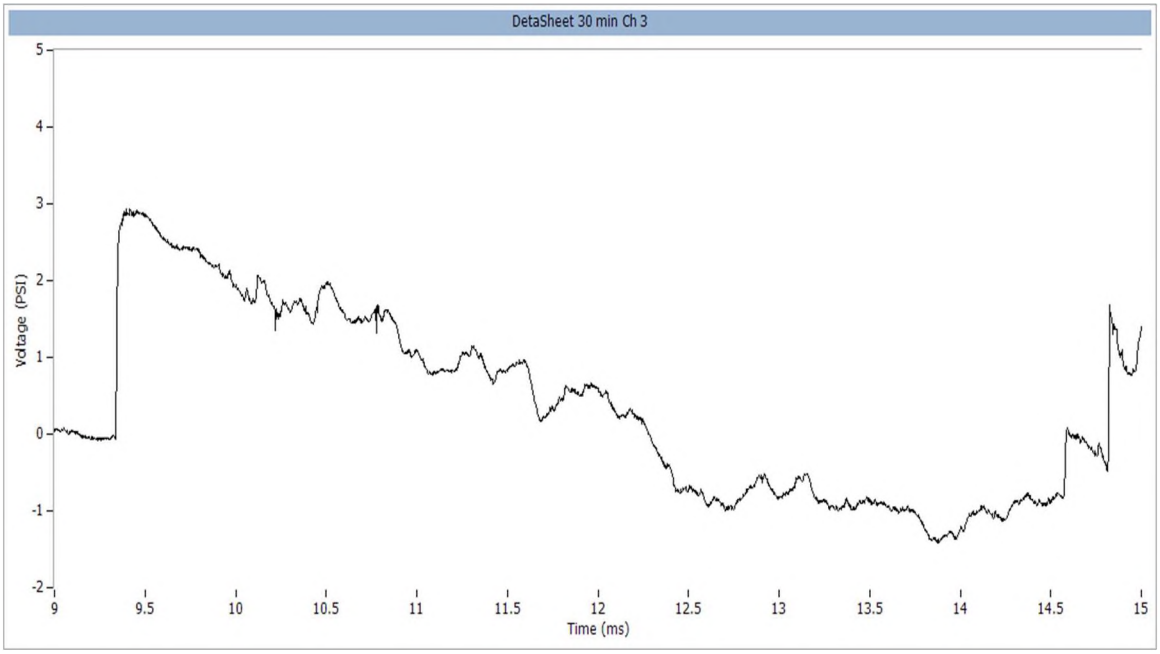

Figure B.24. DetaSheet 30-minute foam cure time channel 3 (psi).

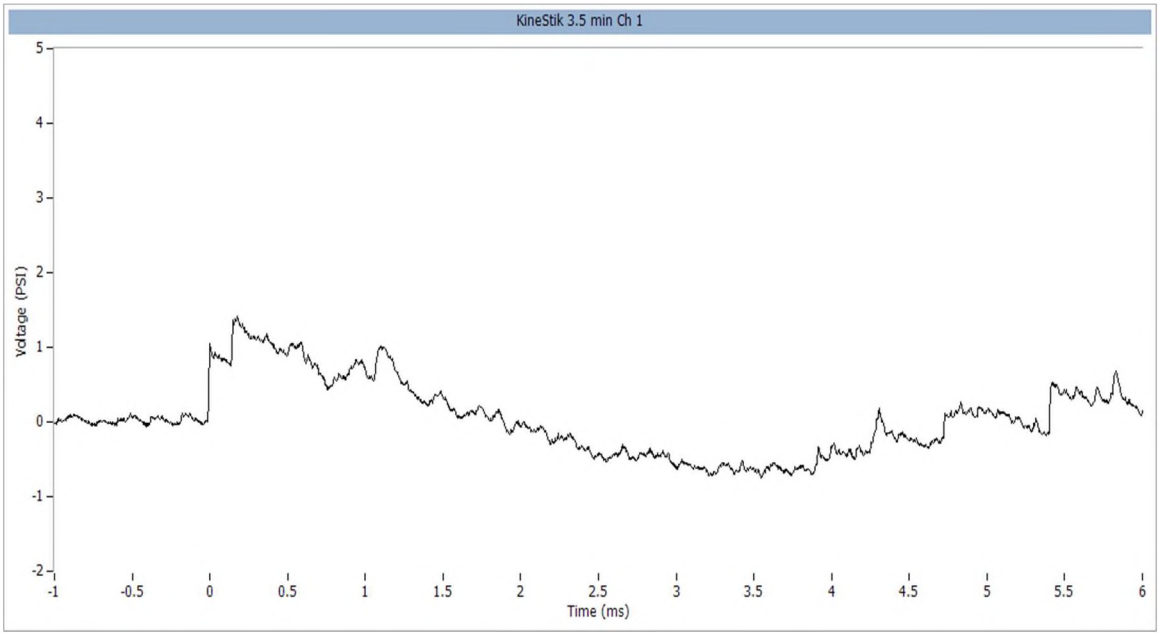

Figure B.25. KineStik 3.5-minute foam cure time channel 1 (psi).

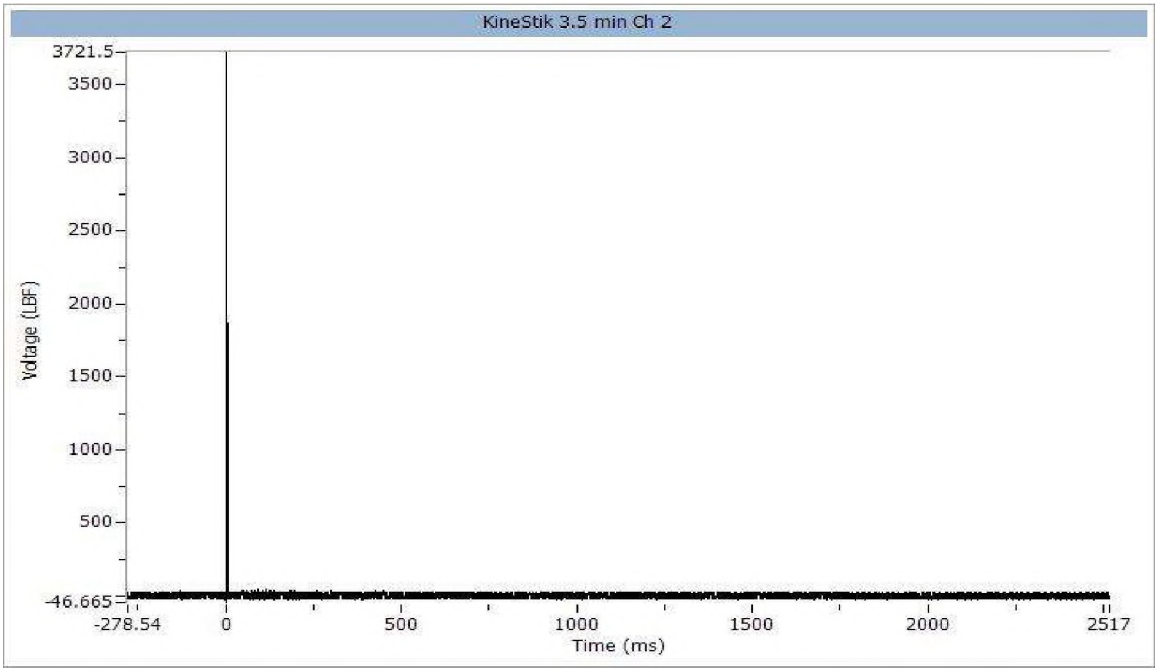

Figure B.26. KineStik 3.5-minute foam cure time channel 2 (lbf).

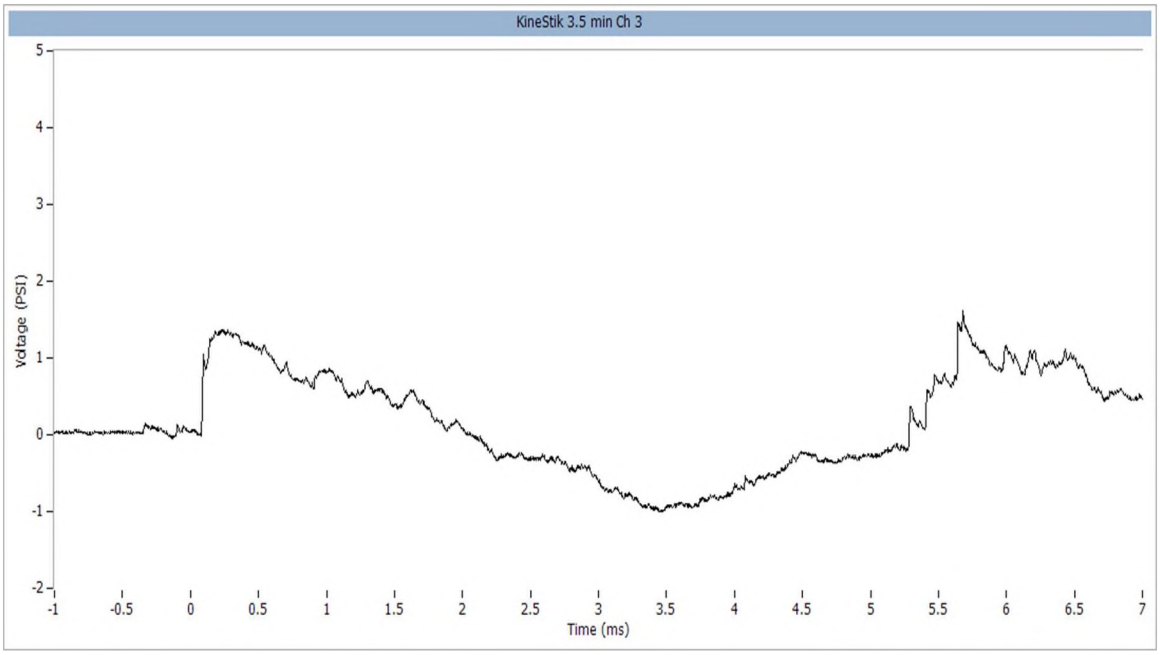

Figure B.27. KineStik 3.5-minute foam cure time channel 3 (psi).

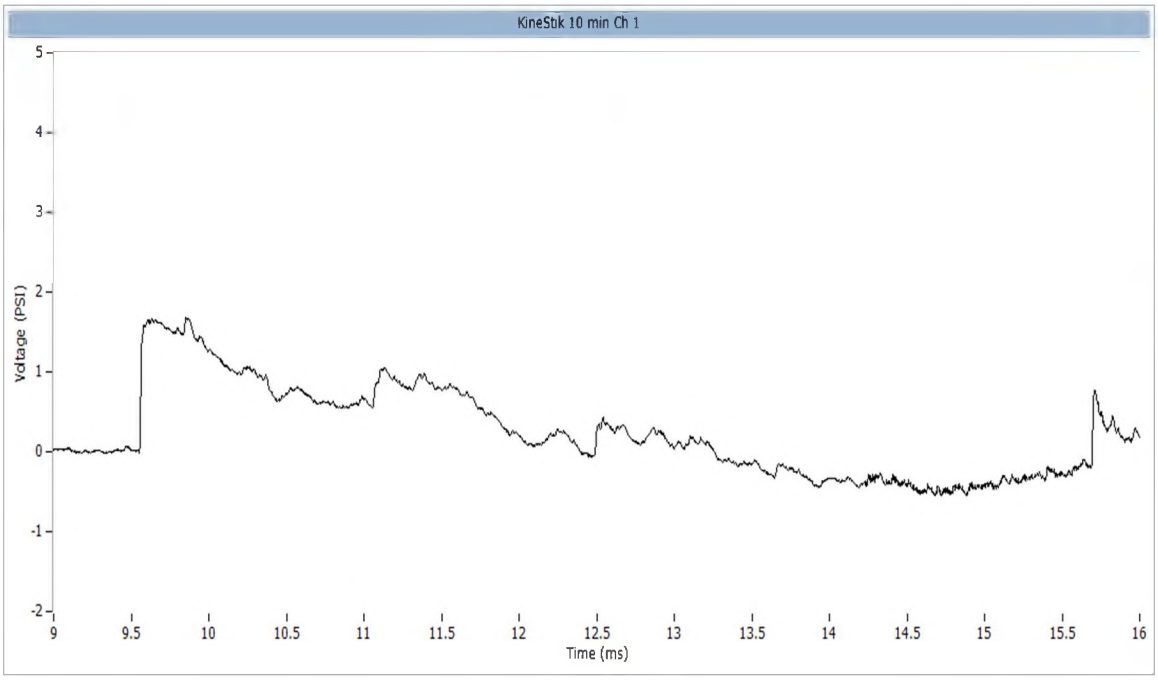

Figure B28. KineStik 10-minute foam cure time channel 1 (psi).

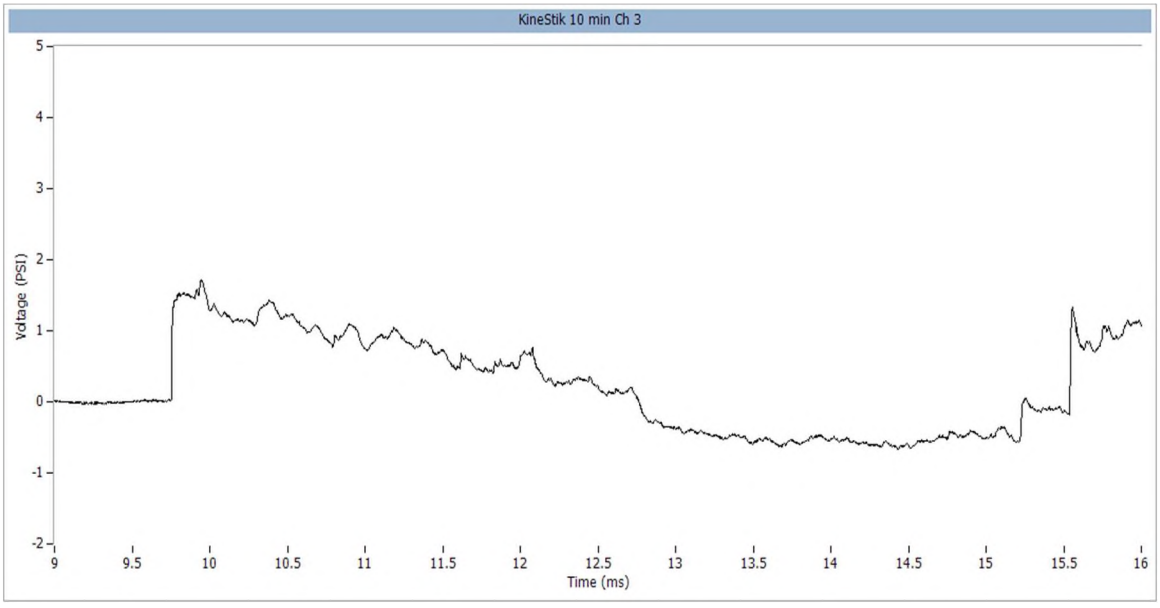

Figure B.29. KineStik 10-minute foam cure time channel 3 (psi).

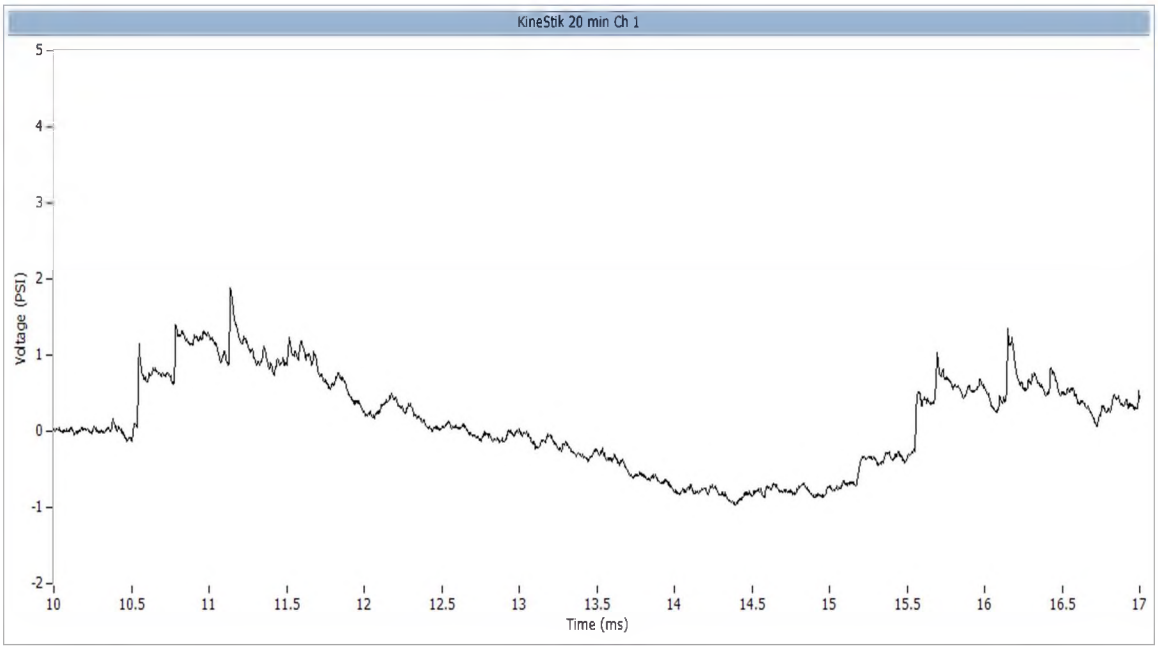

Figure B.30. KineStik 20-minute foam cure time Channel 1 (psi).

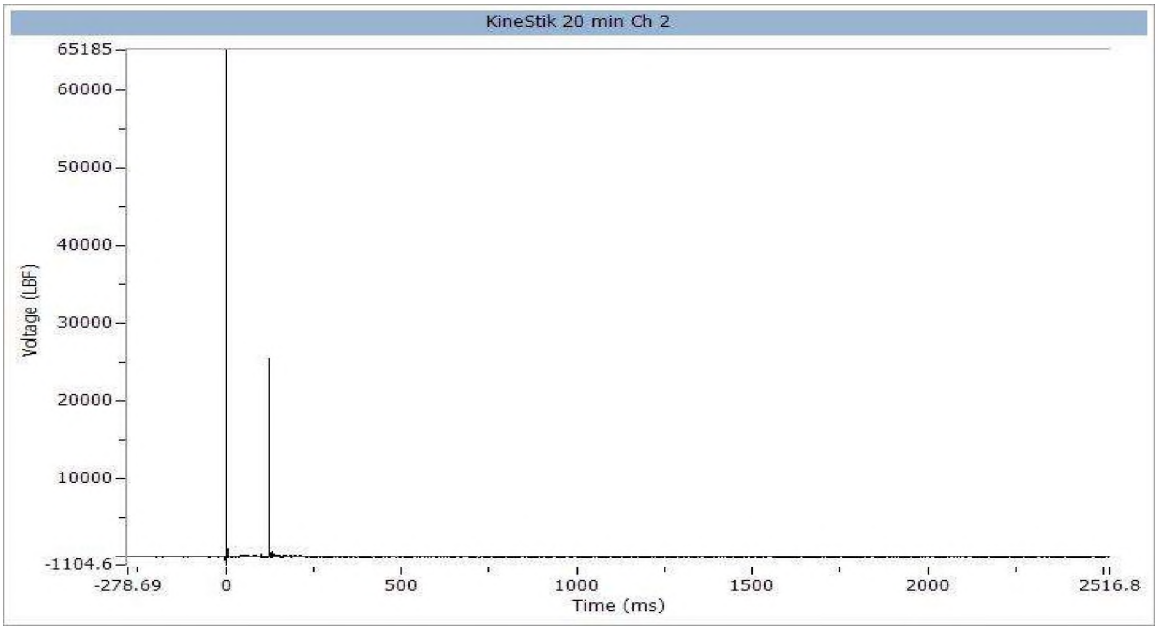

Figure B.31. KineStik 20-minute foam cure time channel 2 (lbf).

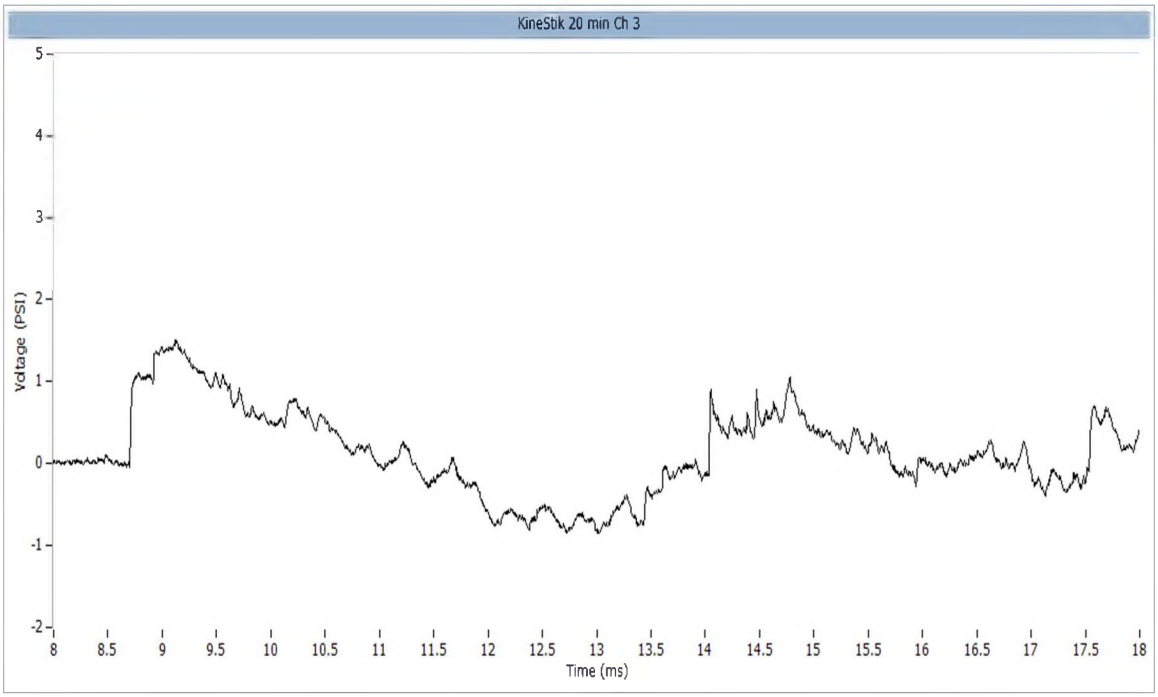

Figure B.32. KineStik 20-minute foam cure time channel 3 (psi).

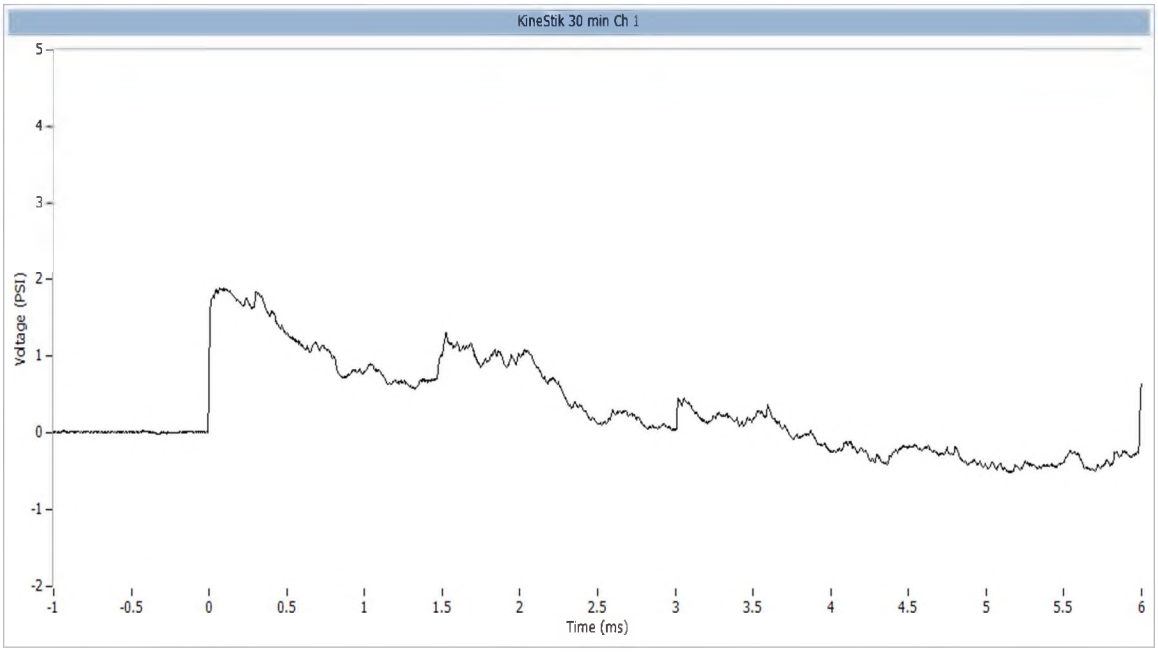

Figure B.33. KineStik 30-minute foam cure time channel 1 (psi).

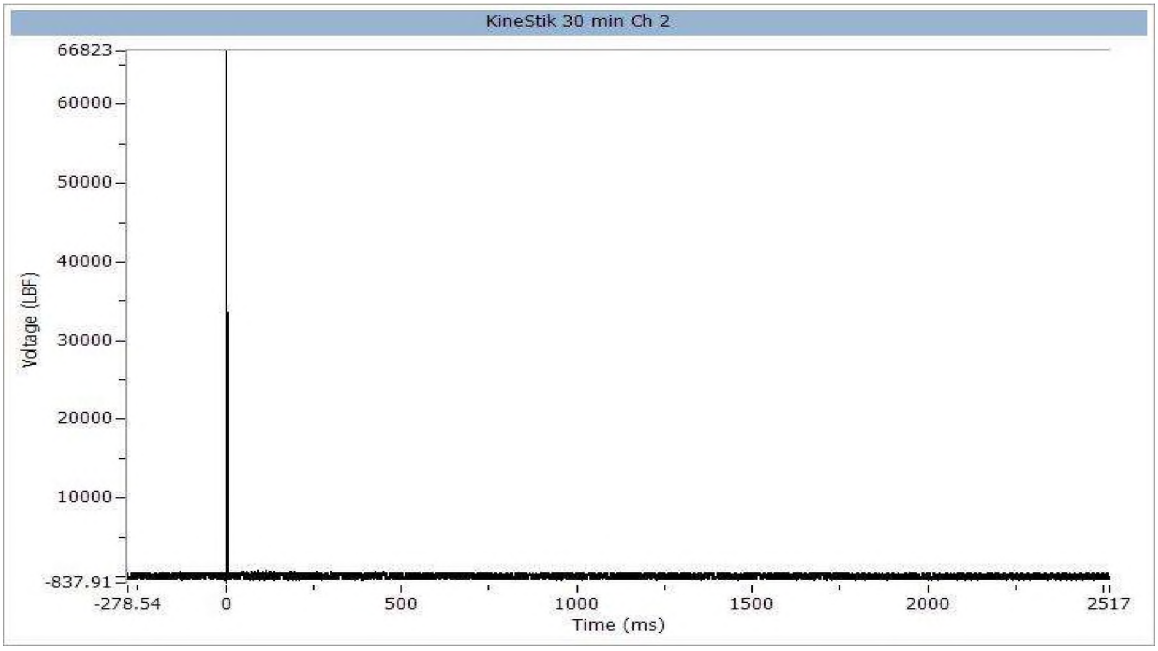

Figure B.34. KineStik 30-minute foam cure time channel 2 (lbf).

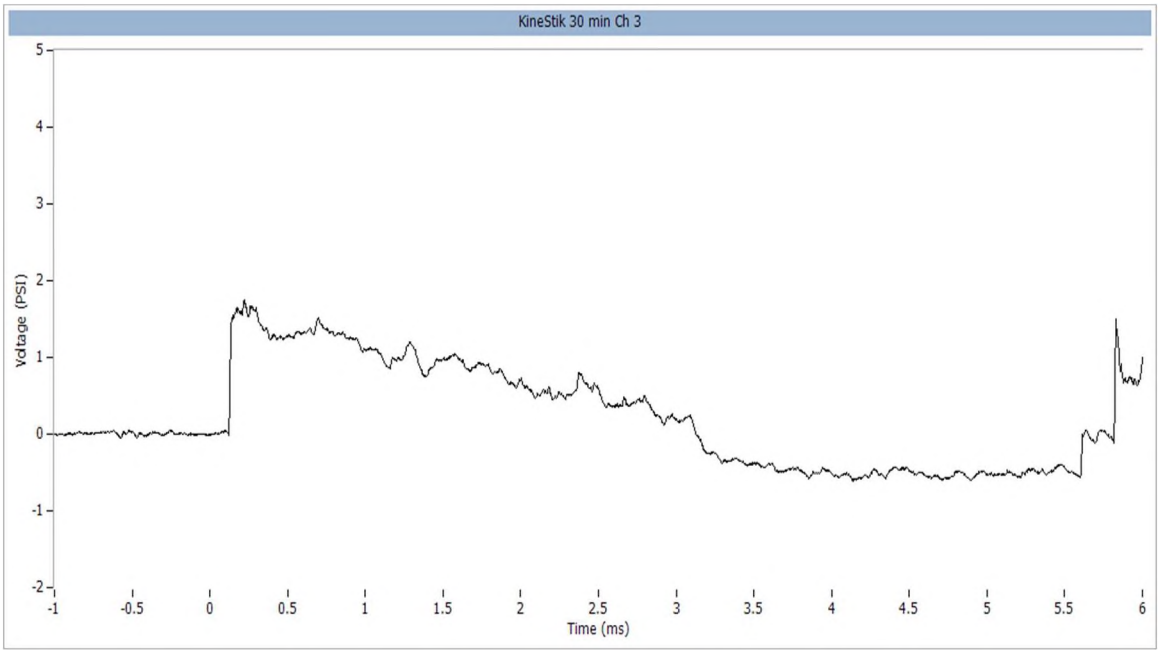

Figure B.35. KineStik 30-minute foam cure time channel 3 (psi).

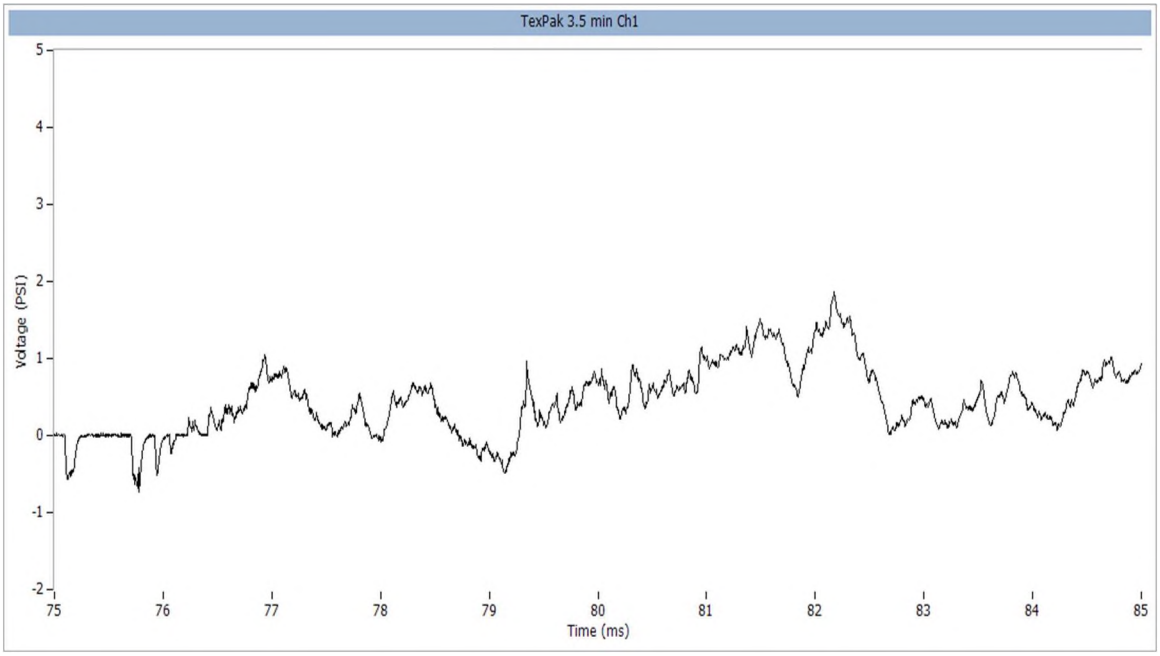

Figure B.36. TexPak 3.5-minute foam cure time channel 1 (psi).

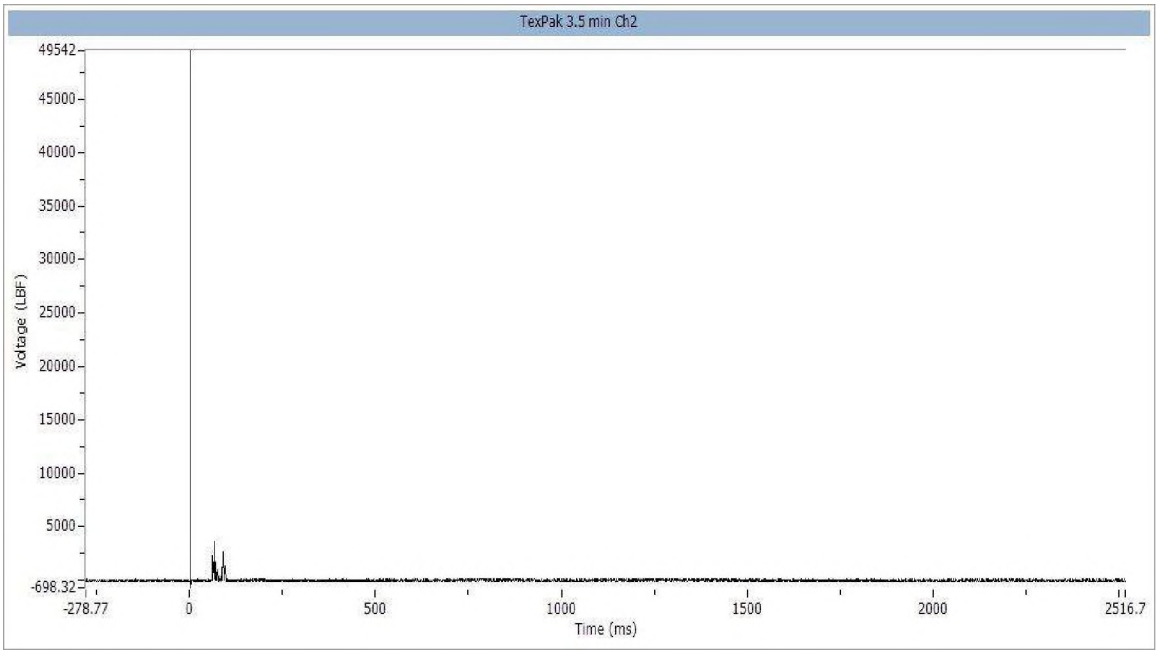

Figure B.37. TexPak 3.5-minute foam cure time channel 2 (lbf).

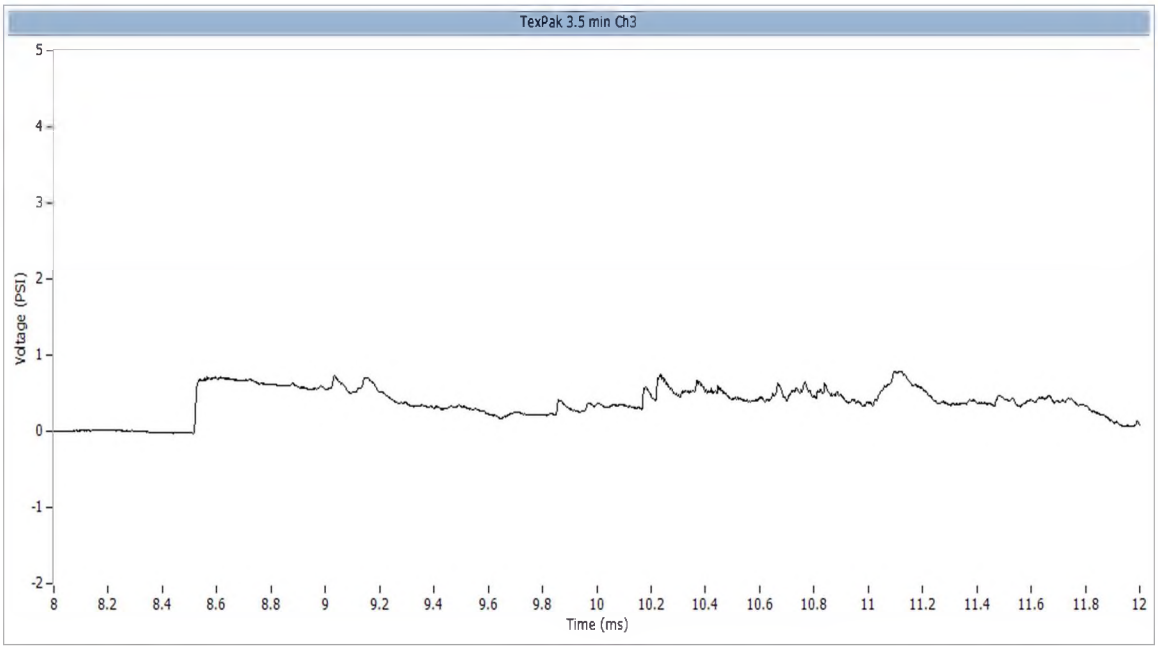

Figure B.38. TexPak 3.5-minute foam cure time channel 3 (psi).

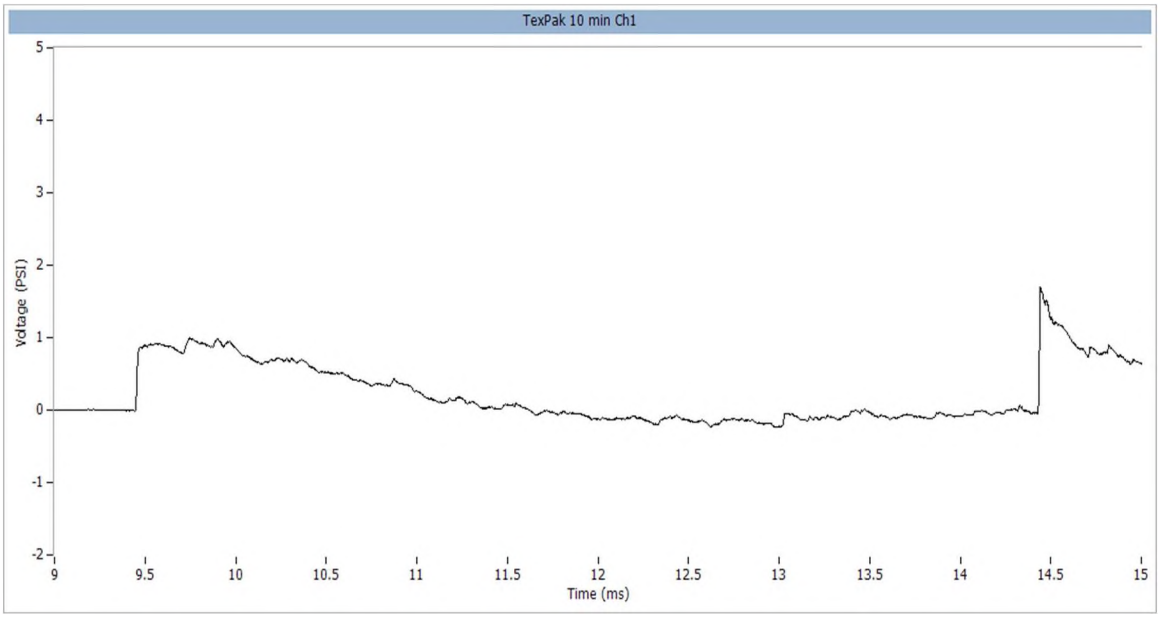

Figure B.39. TexPak 10-minute foam cure time channel 1 (psi).

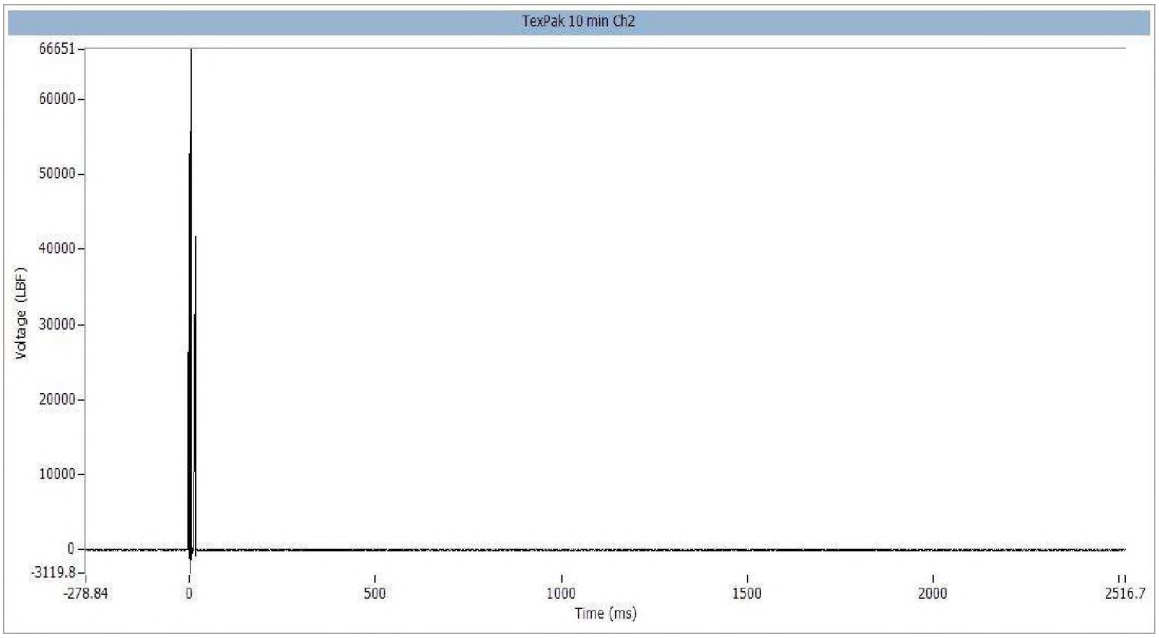

Figure B.40. TexPak 10-minute foam cure time channel 2 (lbf).

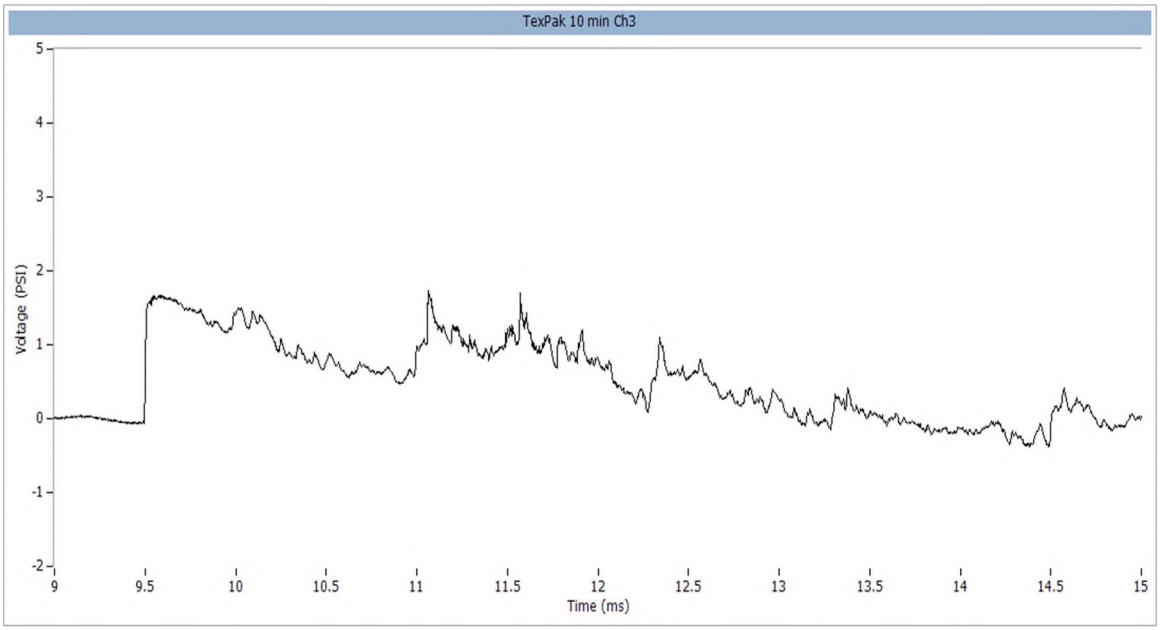

Figure B.41. TexPak 10-minute foam cure time channel 3 (psi).

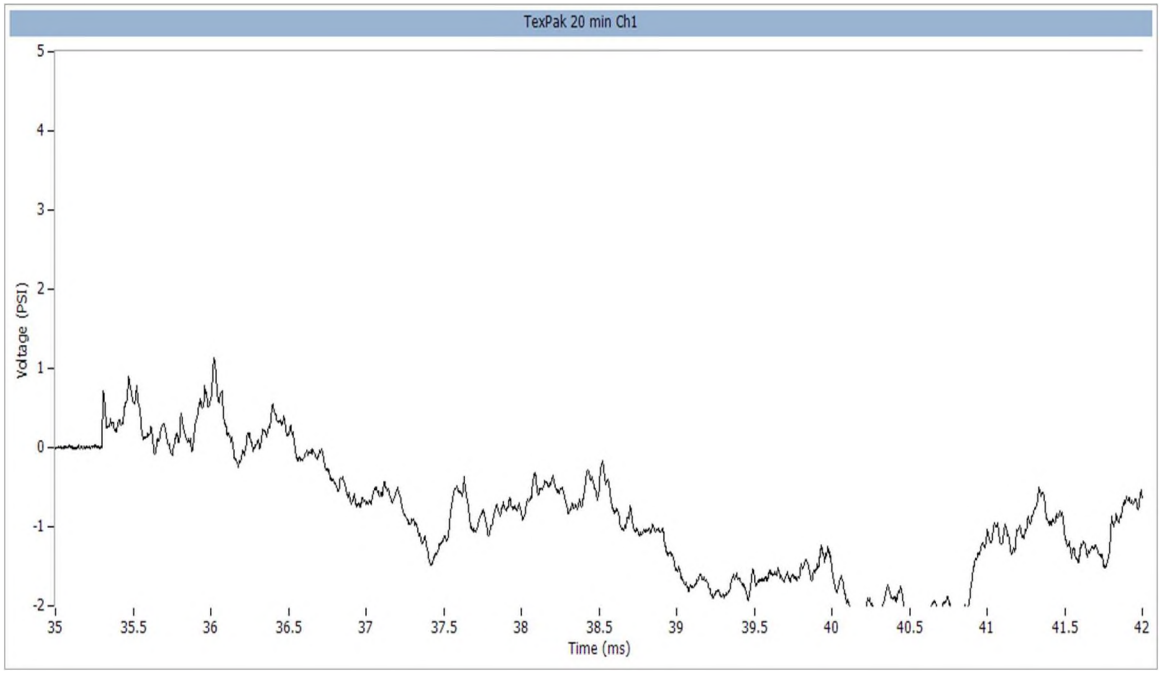

Figure B.42. TexPak 20-minute foam cure time channel 1 (psi).

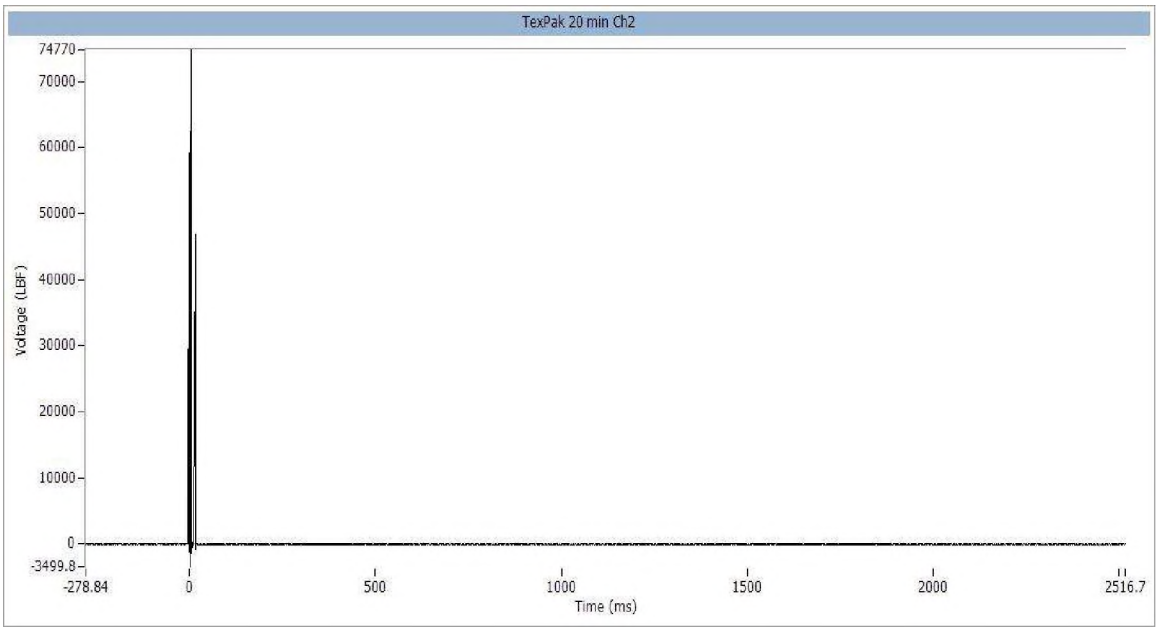

Figure B.43. TexPak 20-minute foam cure time channel 2 (lbf).

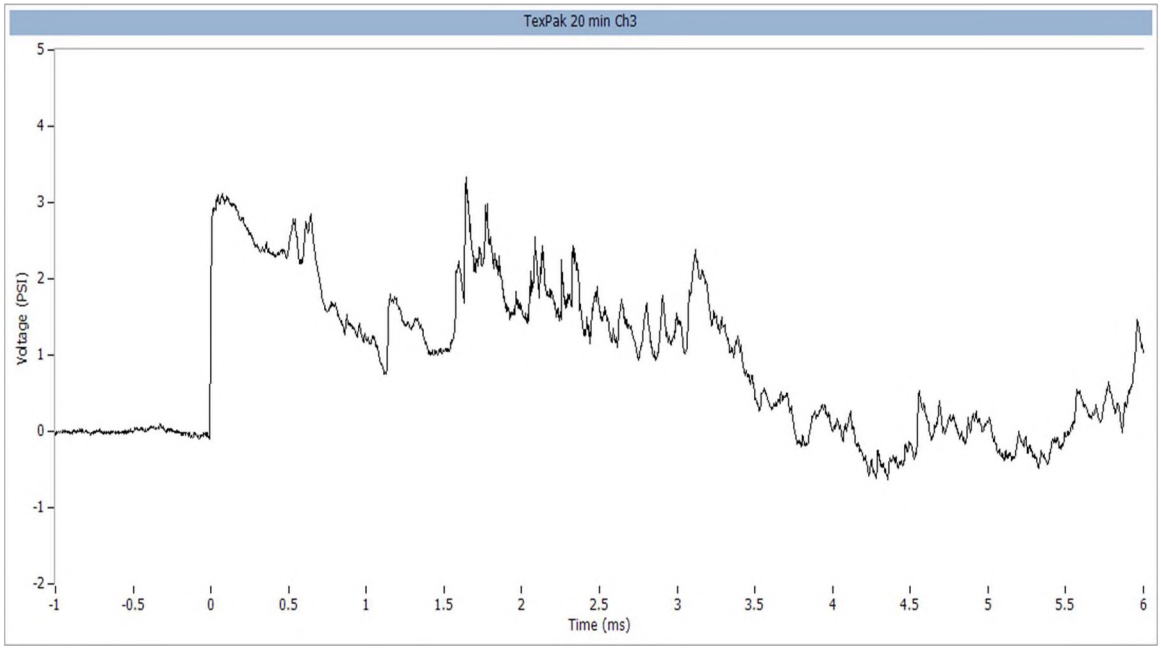

Figure B.44. TexPak 20-minute foam cure time channel 3 (psi).

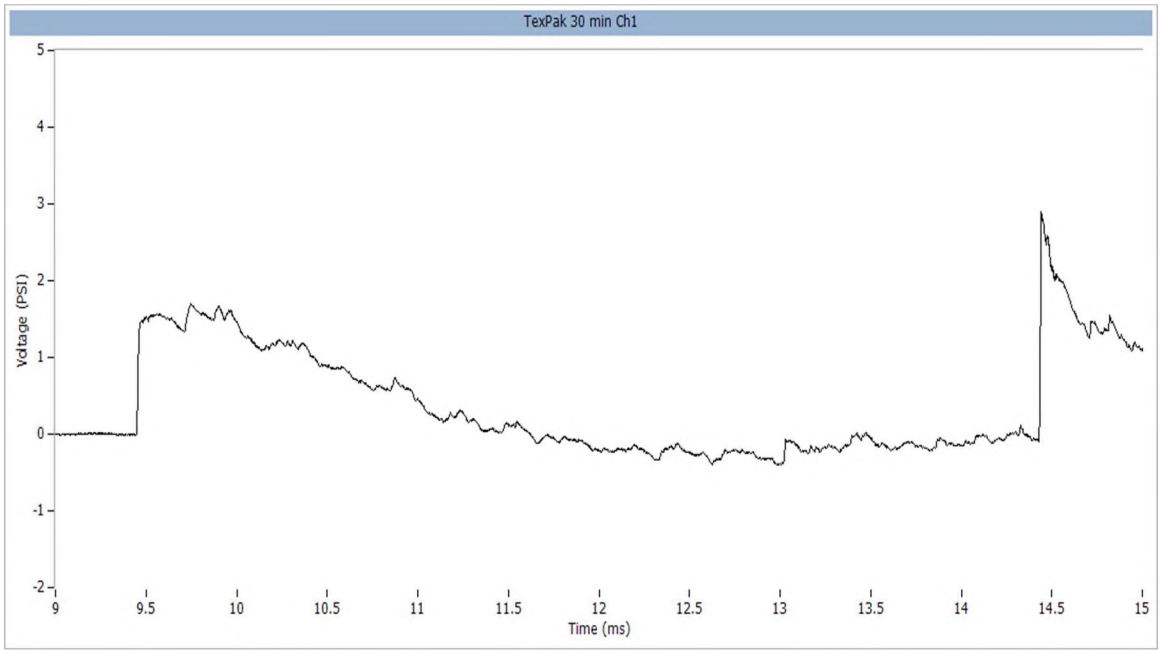

Figure B.45. TexPak 30-minute foam cure time channel 1 (psi).

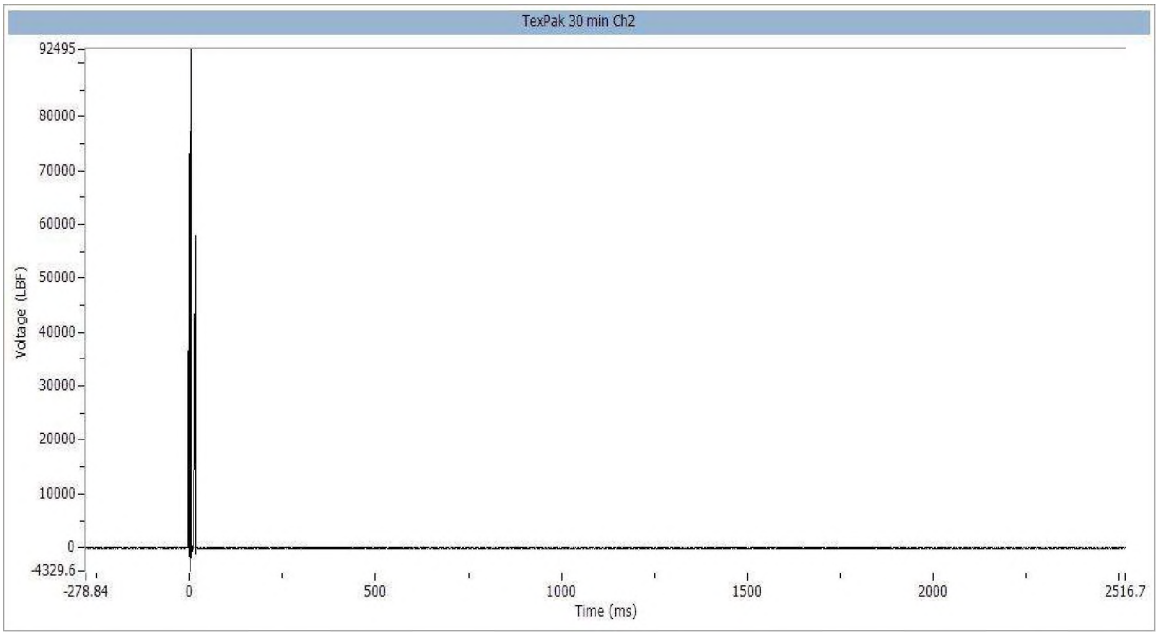

Figure B.46. TexPak 30-minute foam cure time channel 2 (lbf).

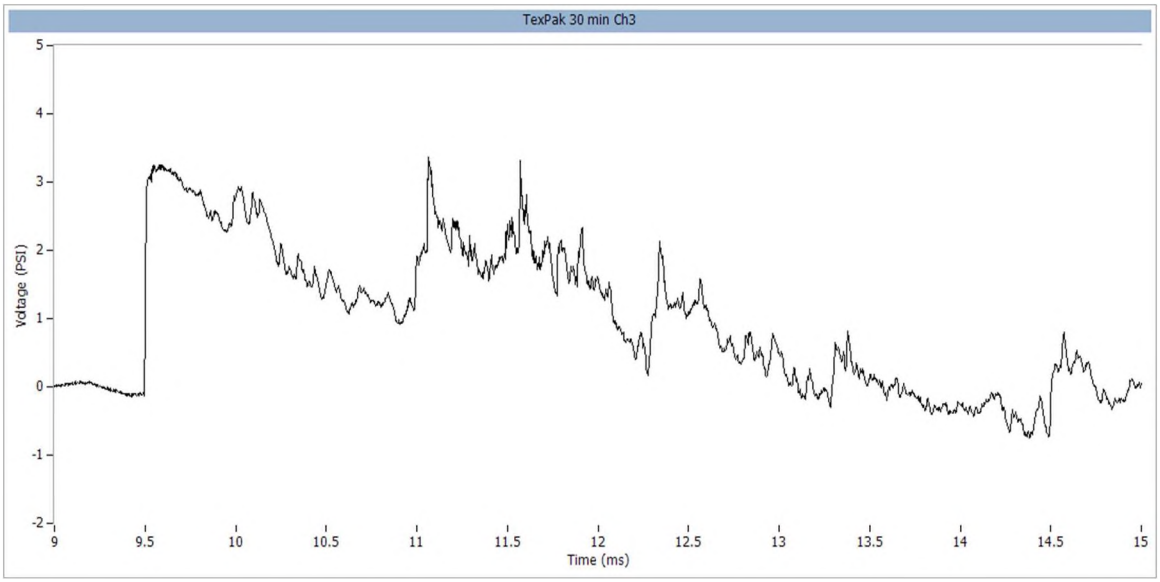

Figure B.47. TexPak 30-minute foam cure time channel 3 (psi).

APPENDIX C.

VARIABLE FOAM THICKNESS DATA

The collected output data from rigid polyurethane foam variable dimension experimental testing was provided in this appendix for all trials performed. This data was collected by two pressure tranducers and a load-cell force sensor. All sensor signals were sent through a signal conditioner before being collect and stored in an MREL data accusation system. This stored data was analyzed and interpreted using MREL compatible software. The variable dimension testing consisted of charges detonated under the confinement of fully cured rigid polyurethane foam with various radius dimensions. The data was presented in alphabetical order of explosive type tested. The order of data was further sorted in the corresponding trial number and recorded data channel number.

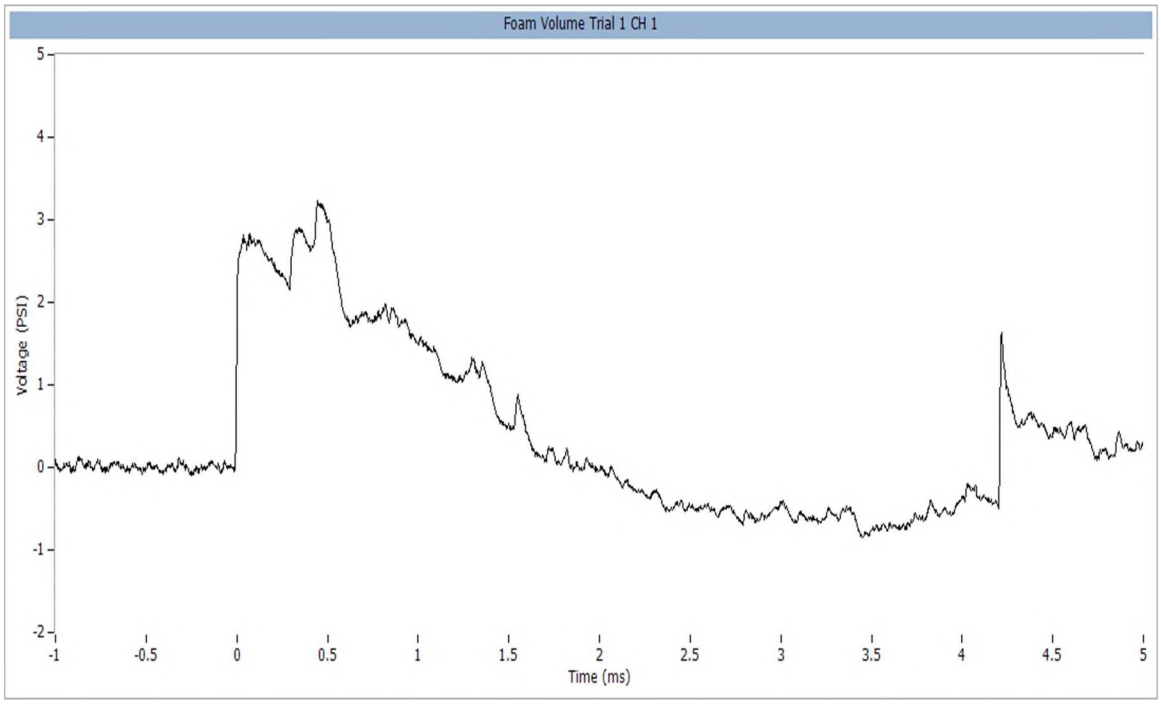

Figure C.1. Foam volume testing trial 1, channel 1 (psi).

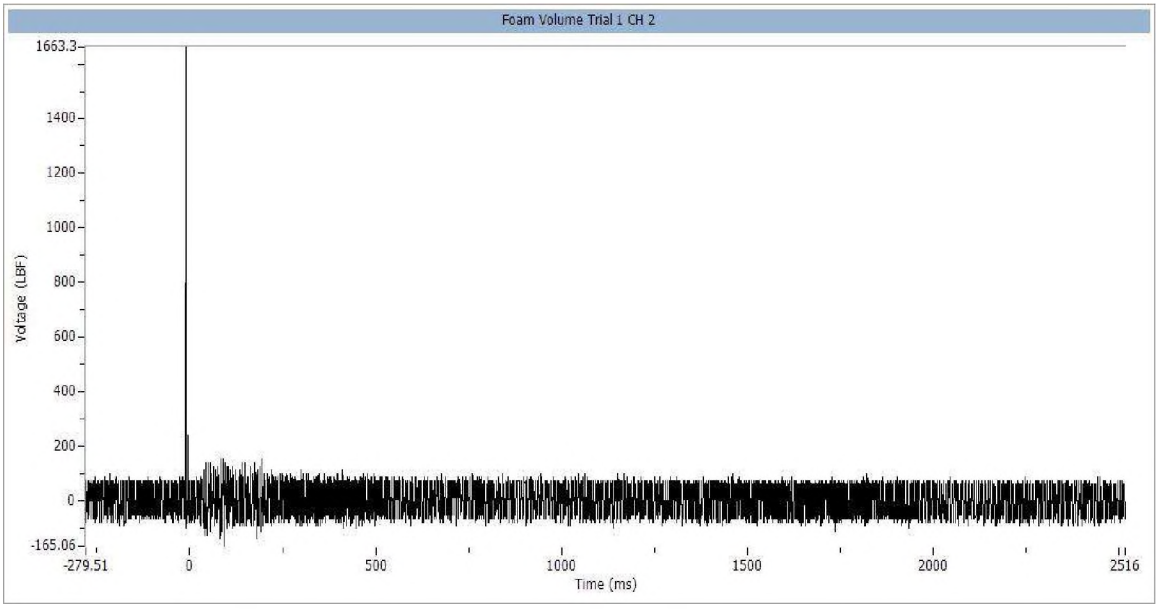

Figure C.2. Foam volume testing trial 1, channel 2 (lbf).

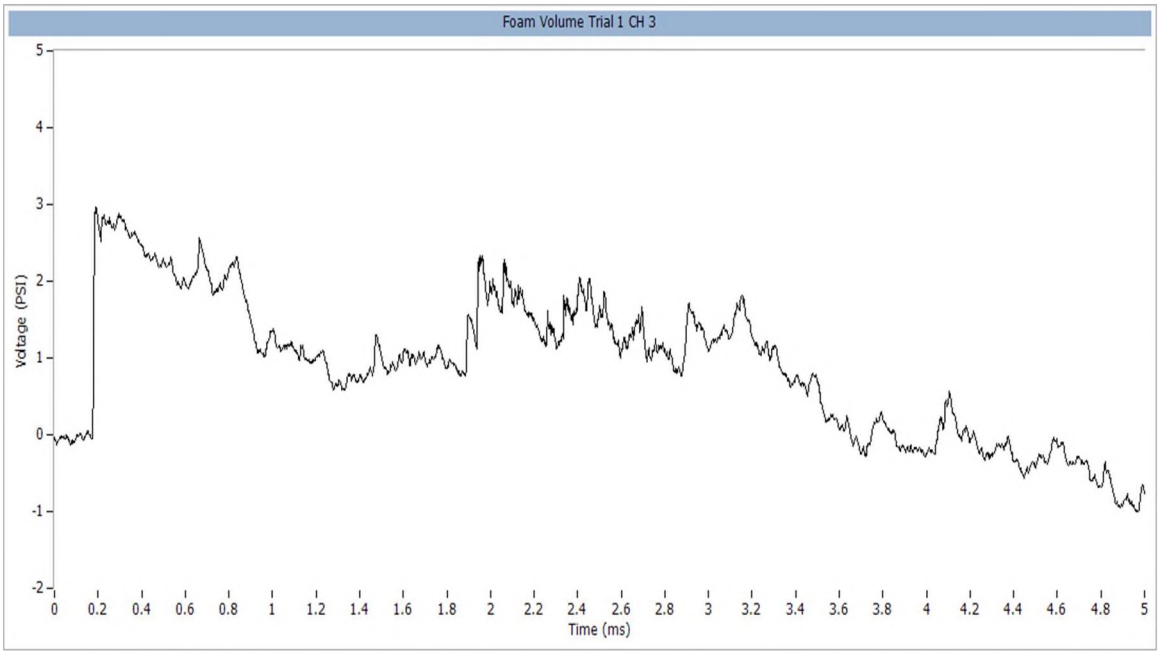

Figure C.3. Foam volume testing trial 1, channel 3 (psi).

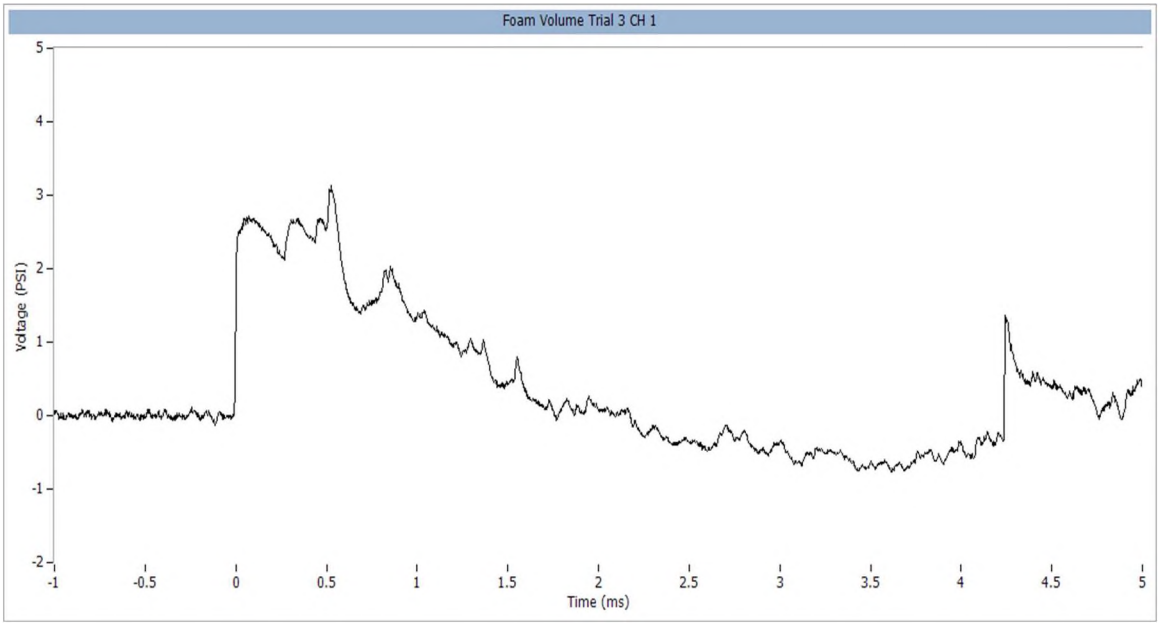

Figure C.4. Foam volume testing trial 3, channel 1 (psi).

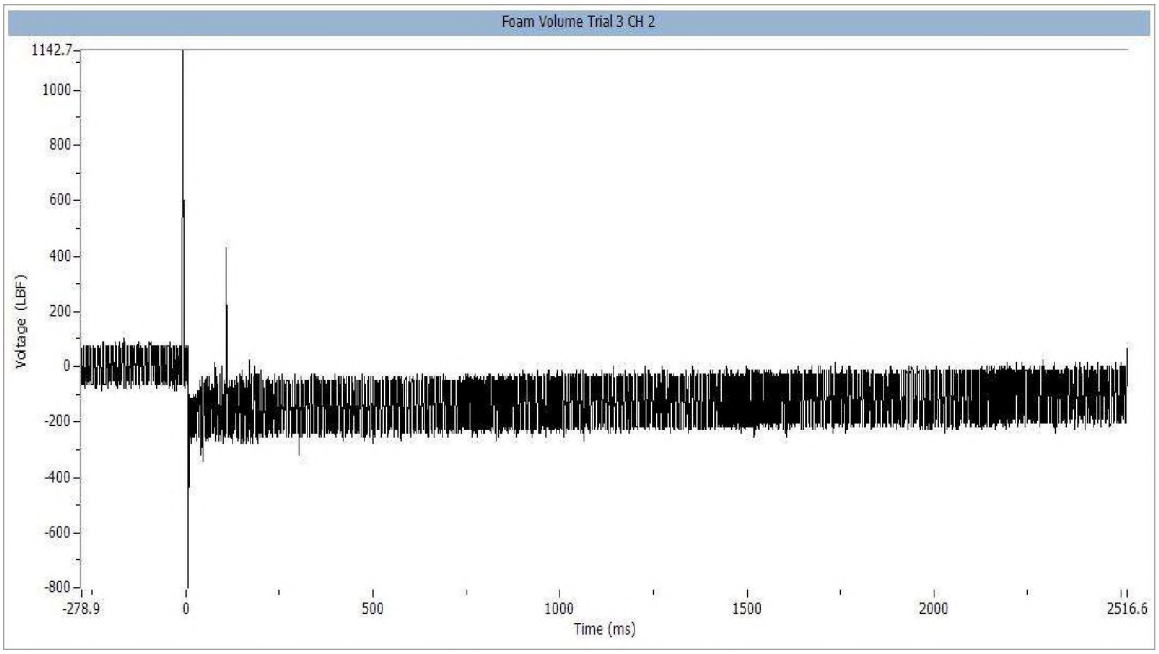

Figure C.5. Foam volume testing trial 3, channel 2 (lbf).

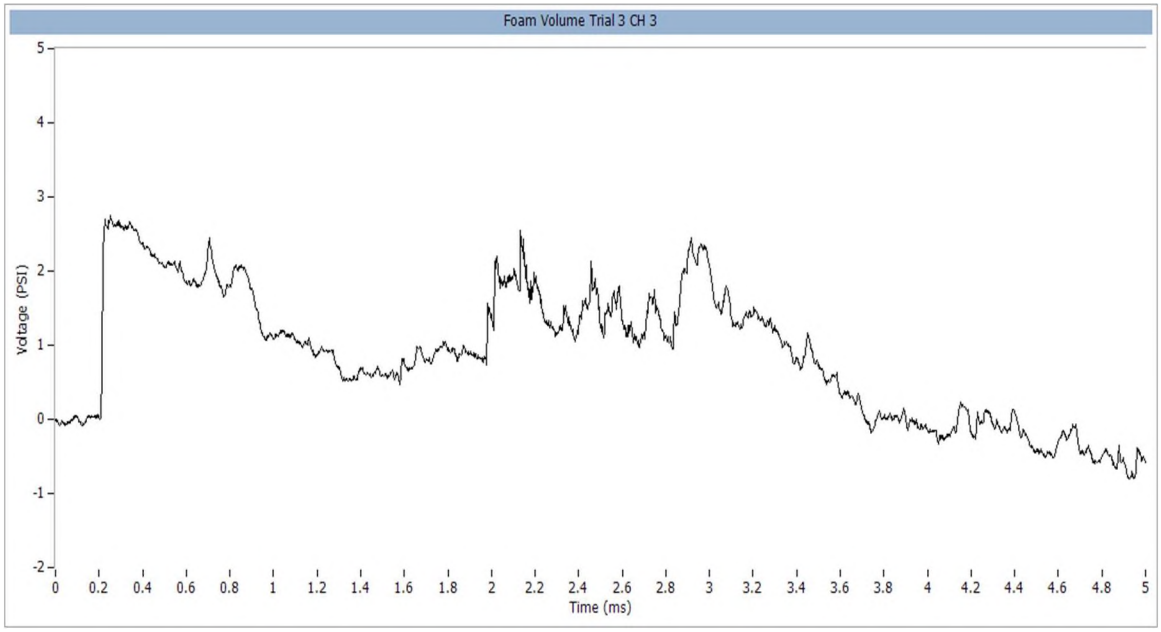

Figure C.6. Foam volume testing trial 3, channel 3 (psi).

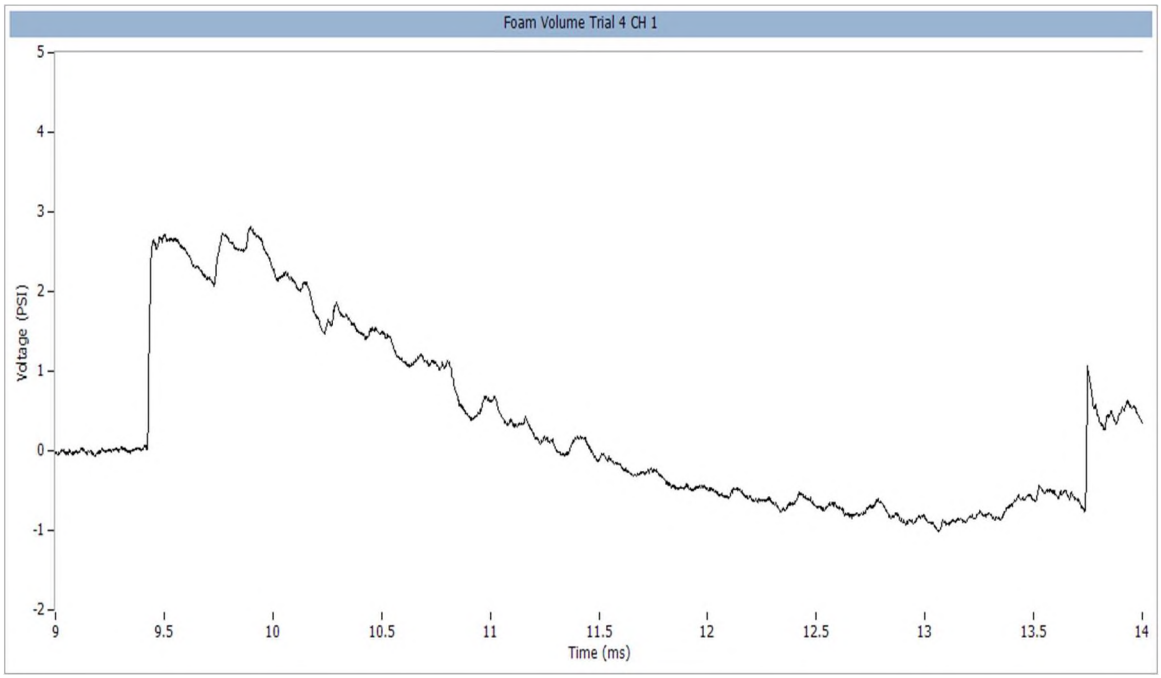

Figure C.7. Foam volume testing trial 4, channel 1 (psi).

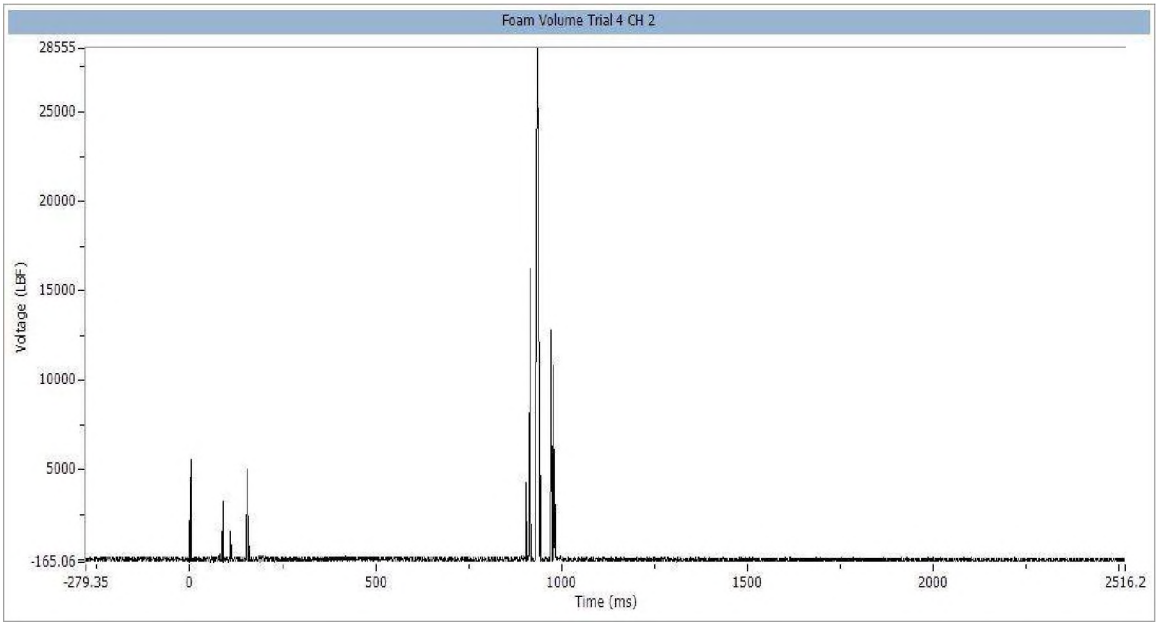

Figure C.8. Foam volume testing trial 4, channel 2 (lbf).

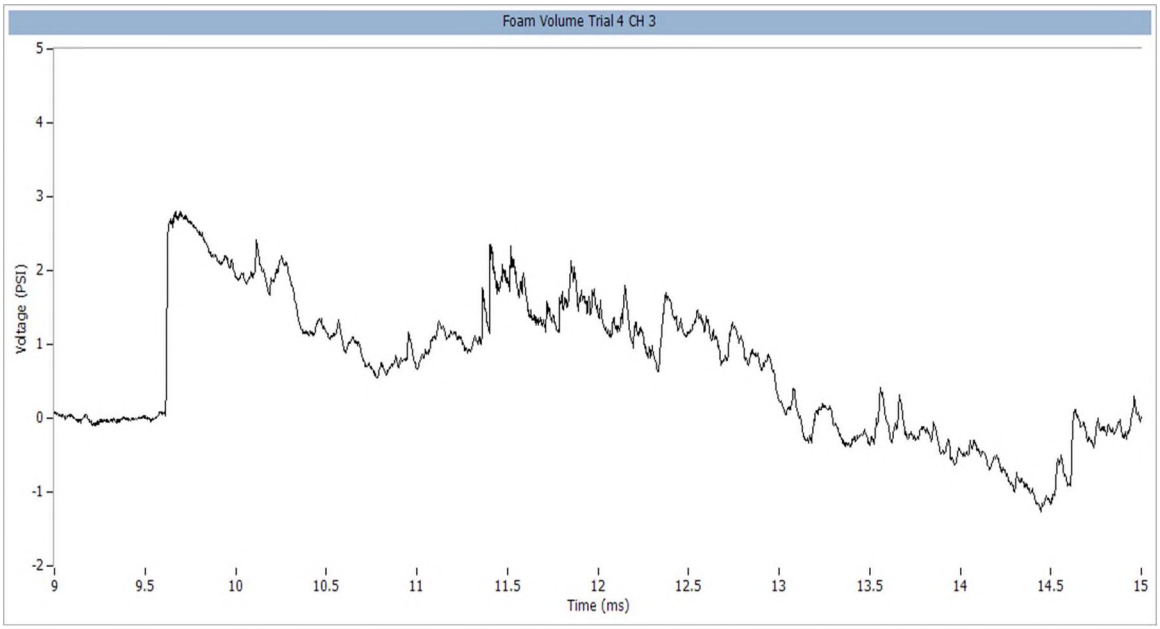

Figure C.9. Foam volume testing trial 4, channel 3 (psi).

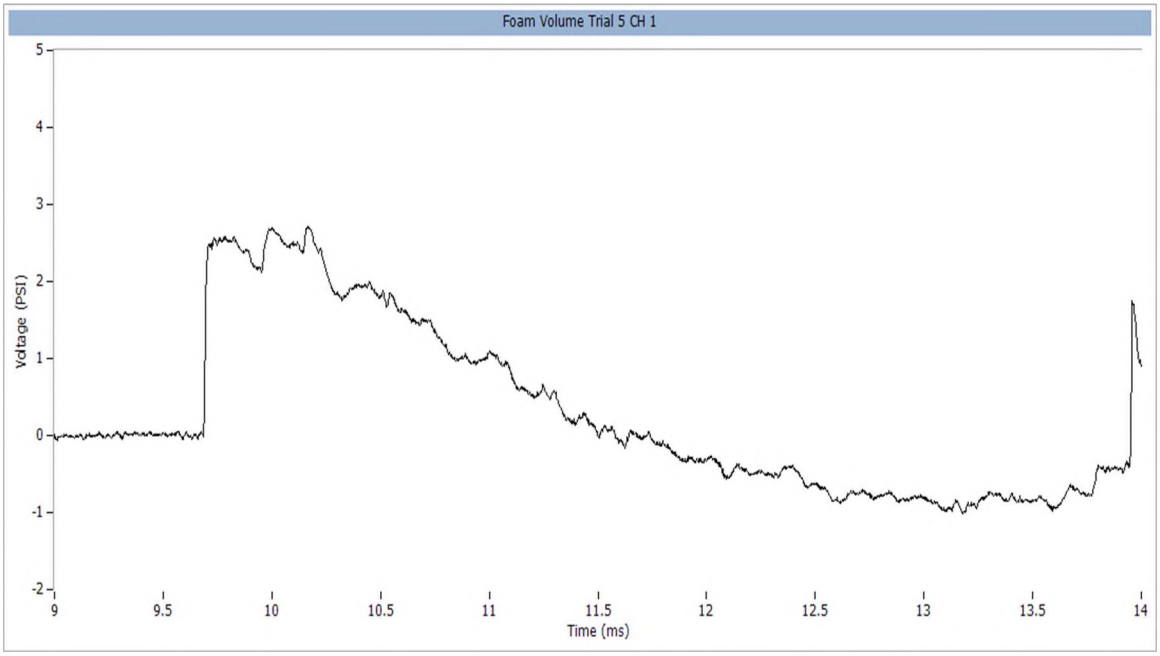

Figure C.10. Foam volume testing trial 5, channel 1 (psi).

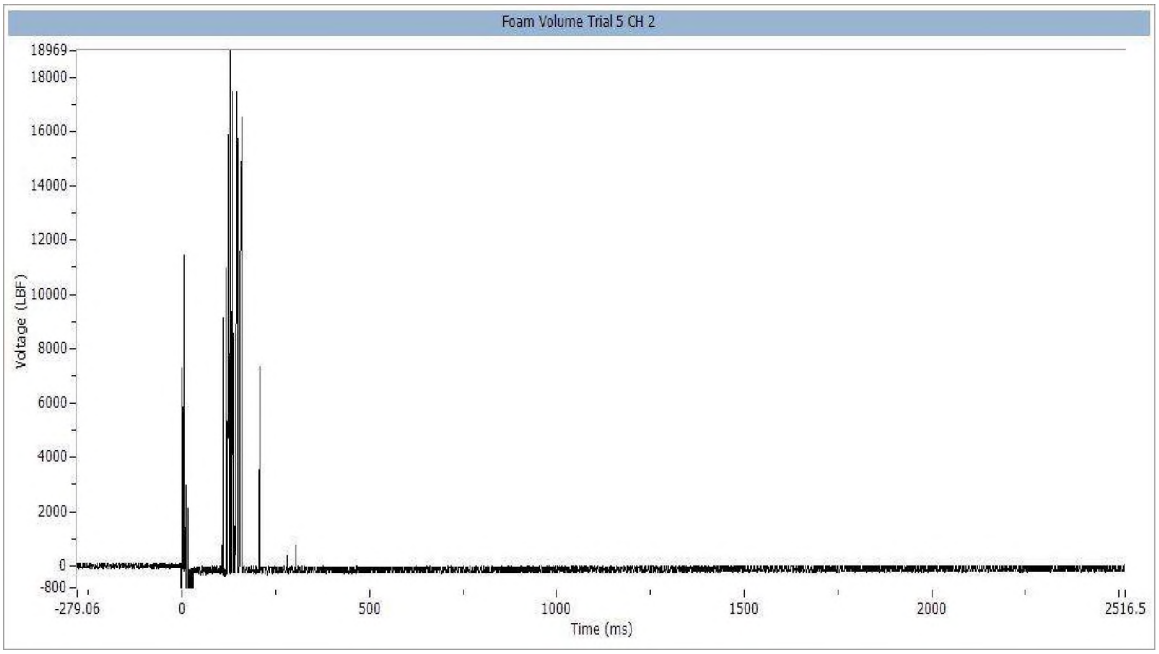

Figure C.11. Foam volume testing trial 5, channel 2 (lbf).

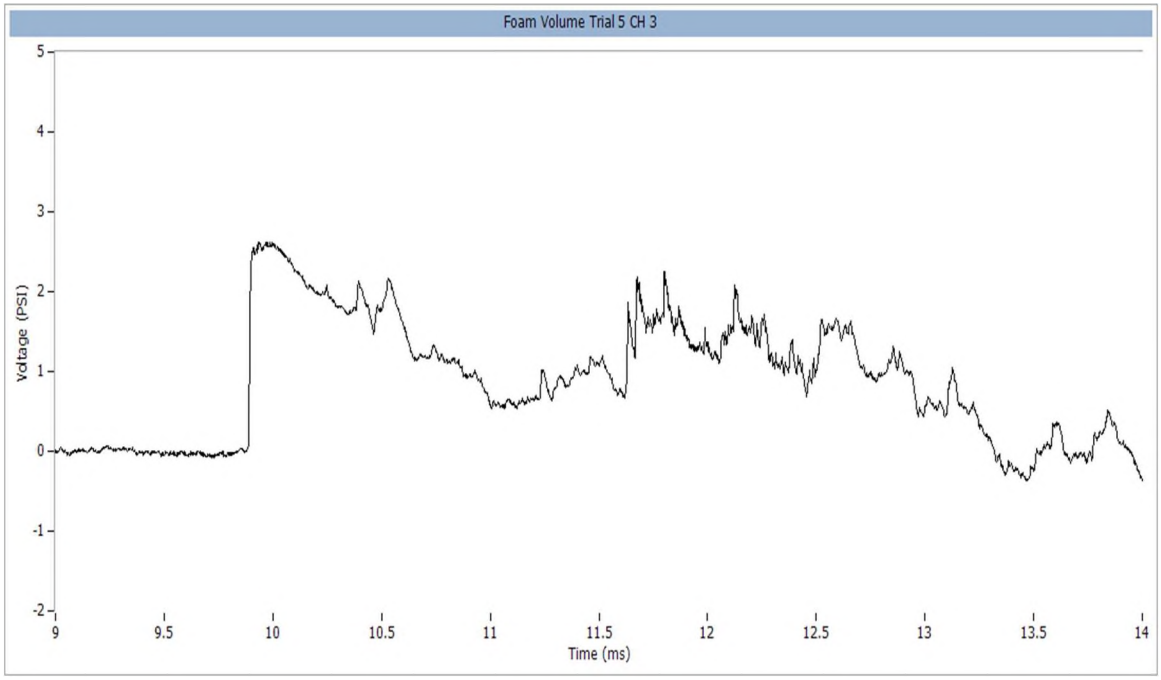

Figure C.12. Foam volume testing trial 5, channel 3 (psi).

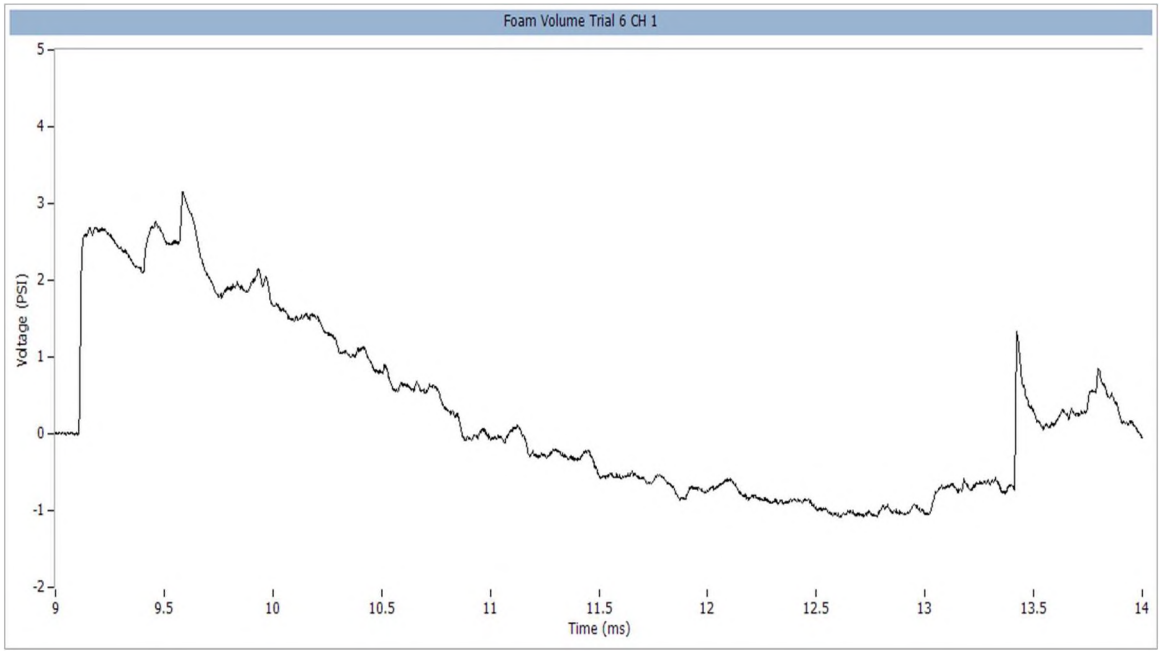

Figure C.13. Foam volume testing trial 6, channel 1 (psi).

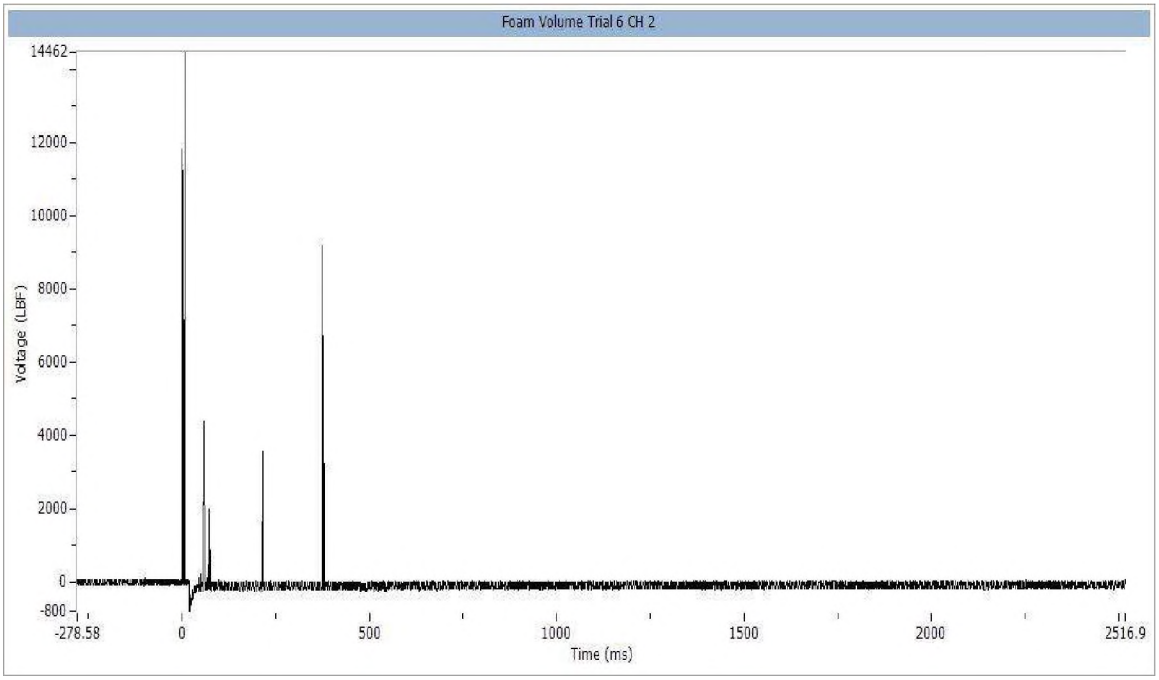

Figure C.14. Foam volume testing trial 6, channel 2 (lbf).

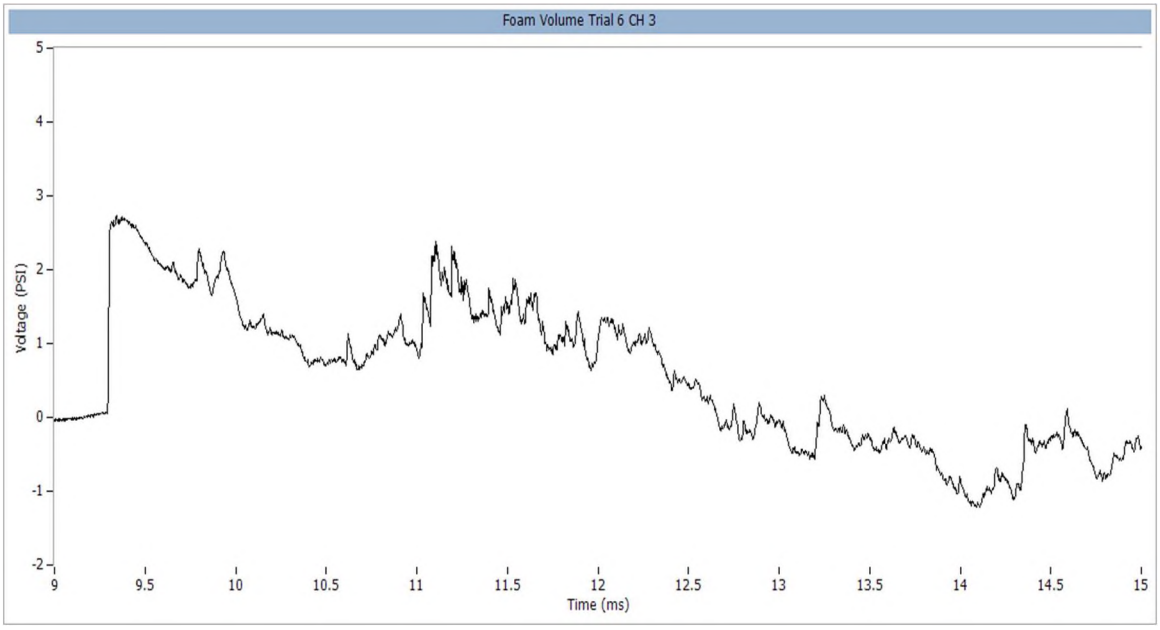

Figure C.15. Foam volume testing trial 6, channel 3 (psi).

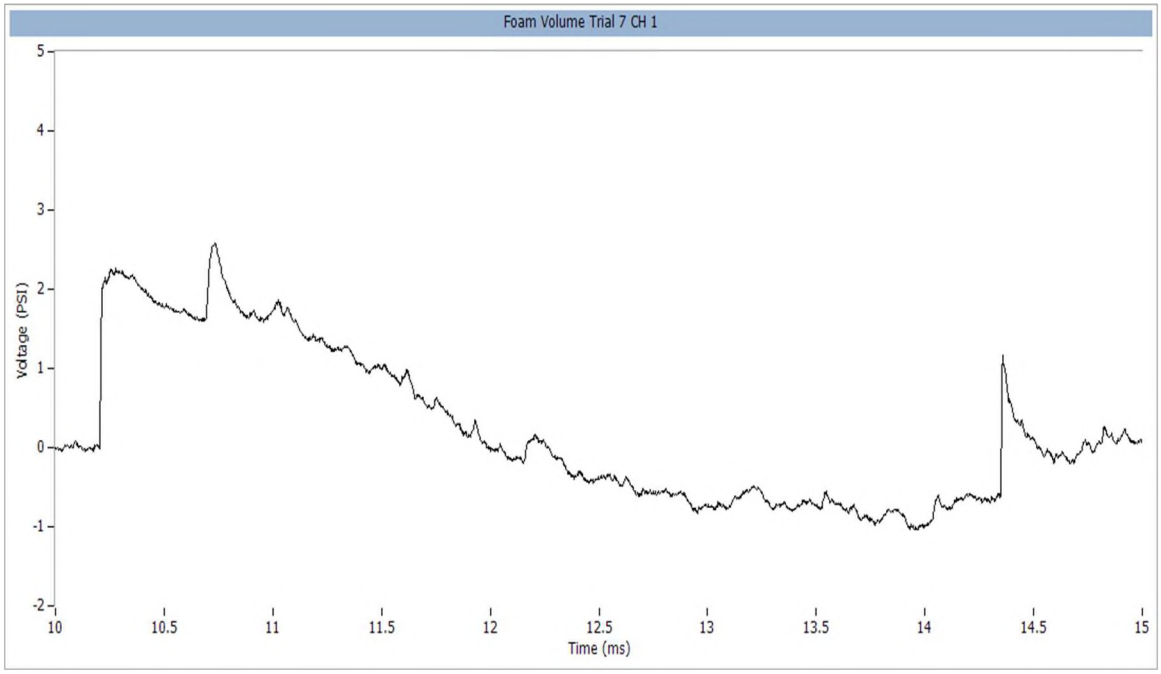

Figure C.16. Foam volume testing trial 7, channel 1 (psi).

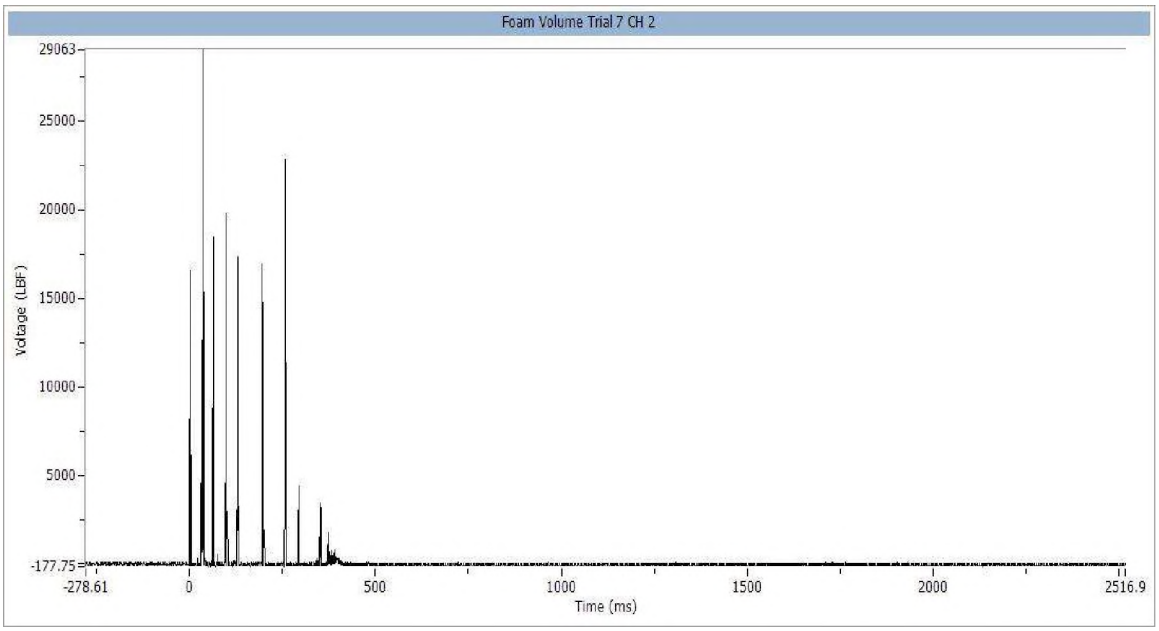

Figure C.17. Foam volume testing trial 7, channel 2 (lbf).

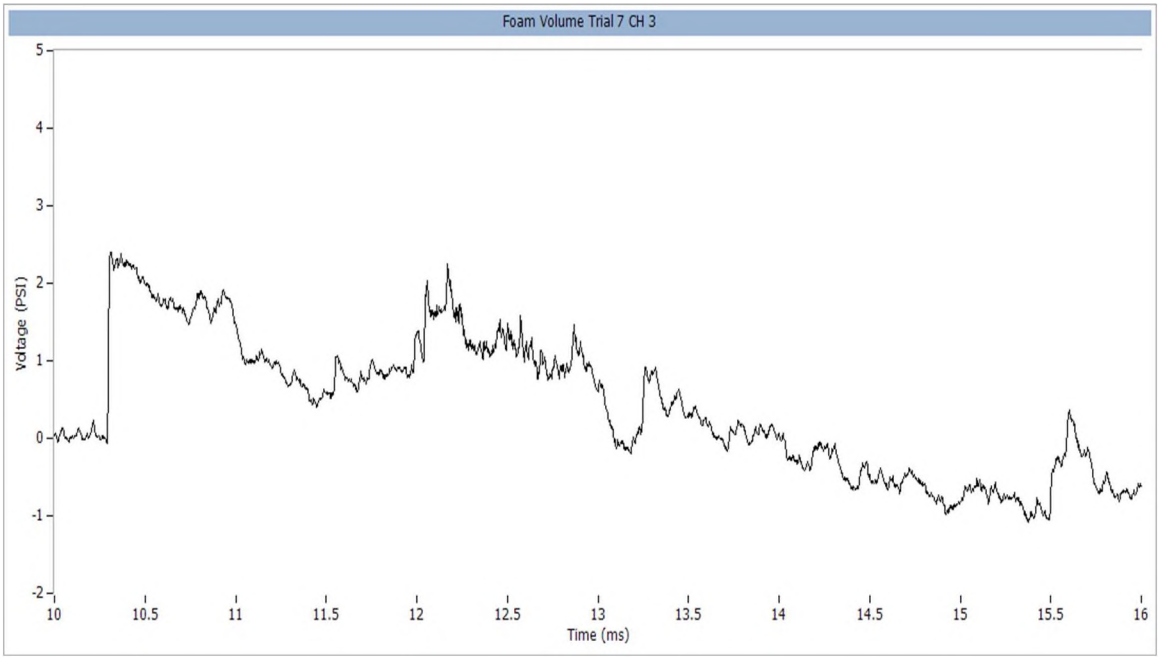

Figure C.18. Foam volume testing trial 7, channel 3 (psi).

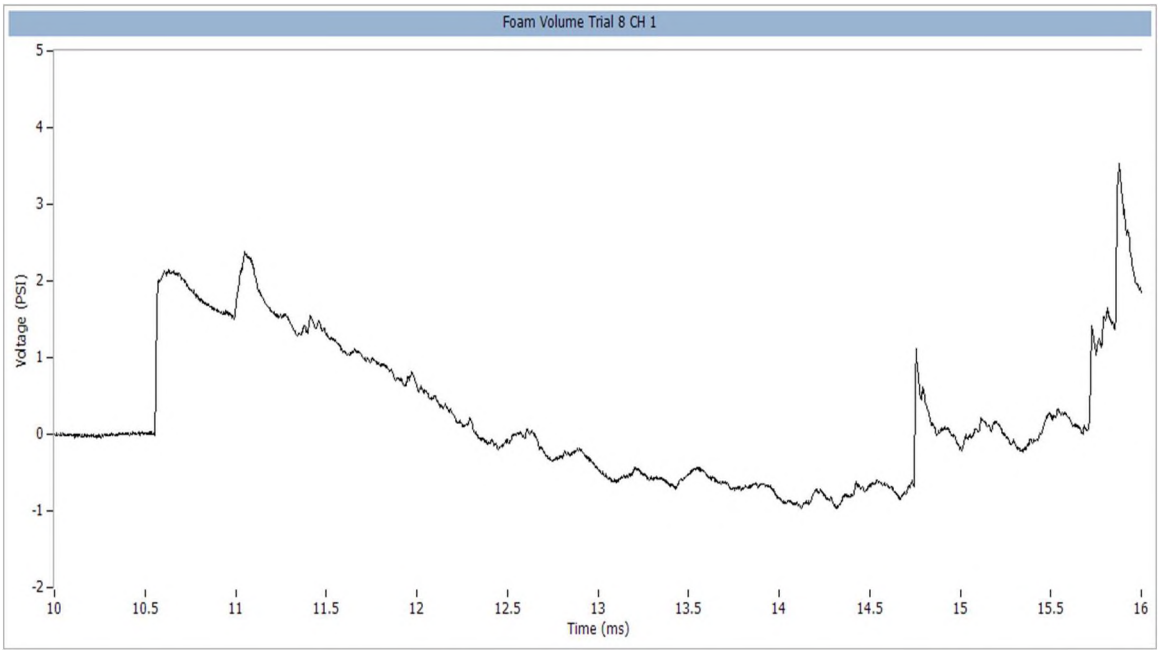

Figure C.19. Foam volume testing trial 8, channel 1 (psi).

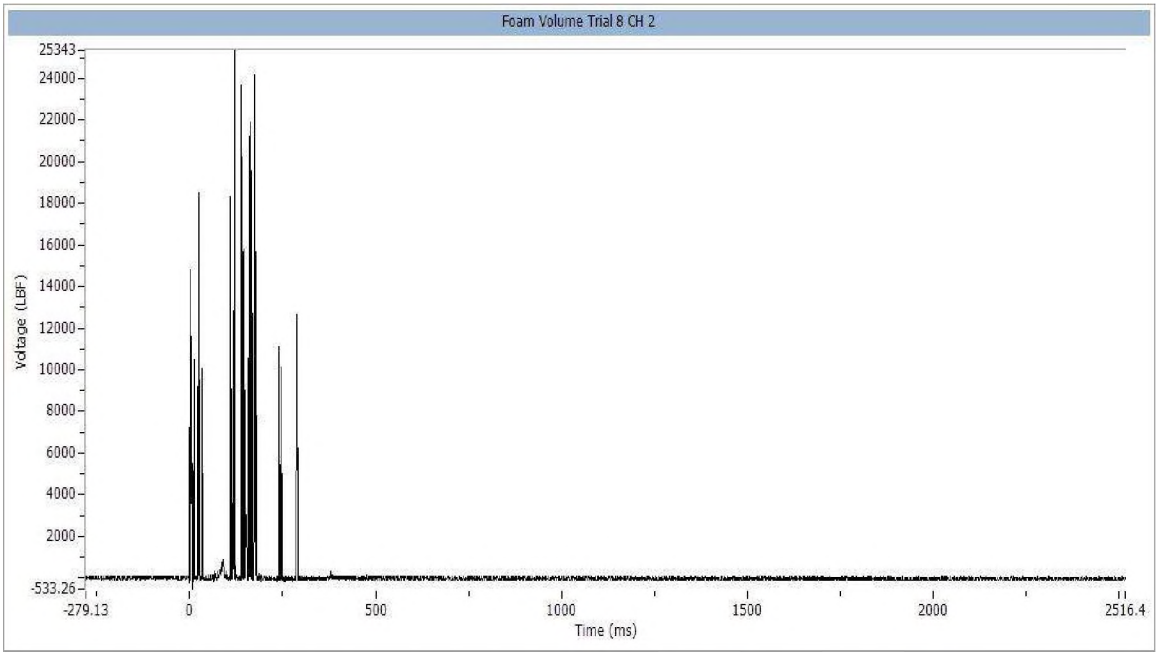

Figure A.20. Foam volume testing trial 8, channel 2 (lbf).

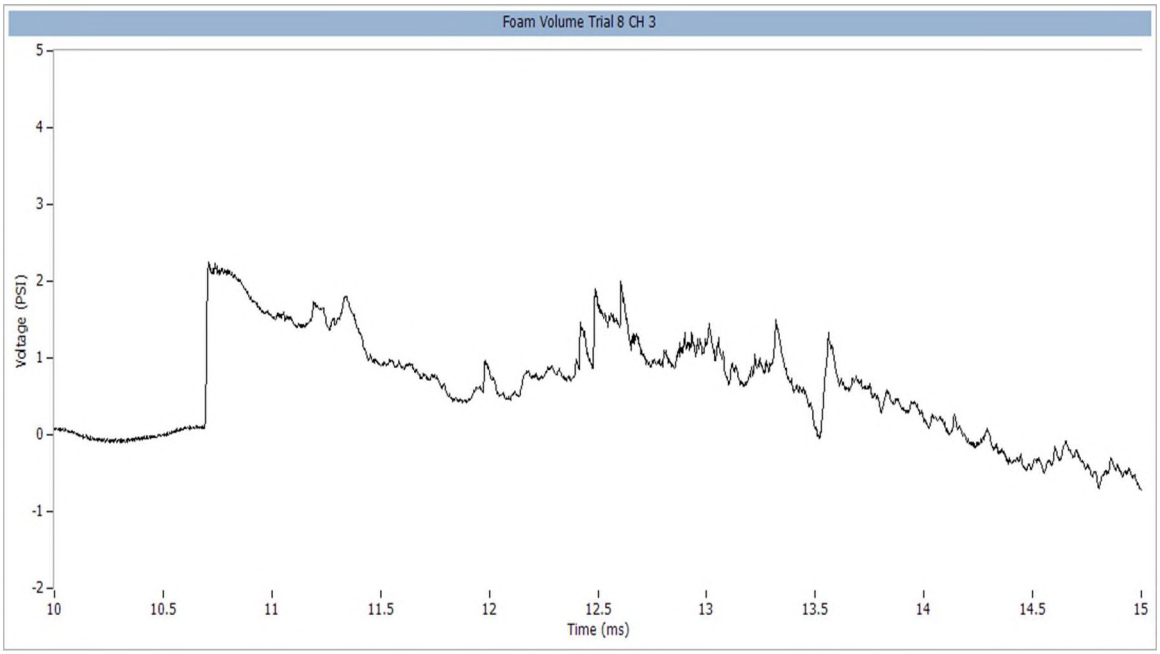

Figure C.21. Foam volume testing trial 8, channel 3 (psi).

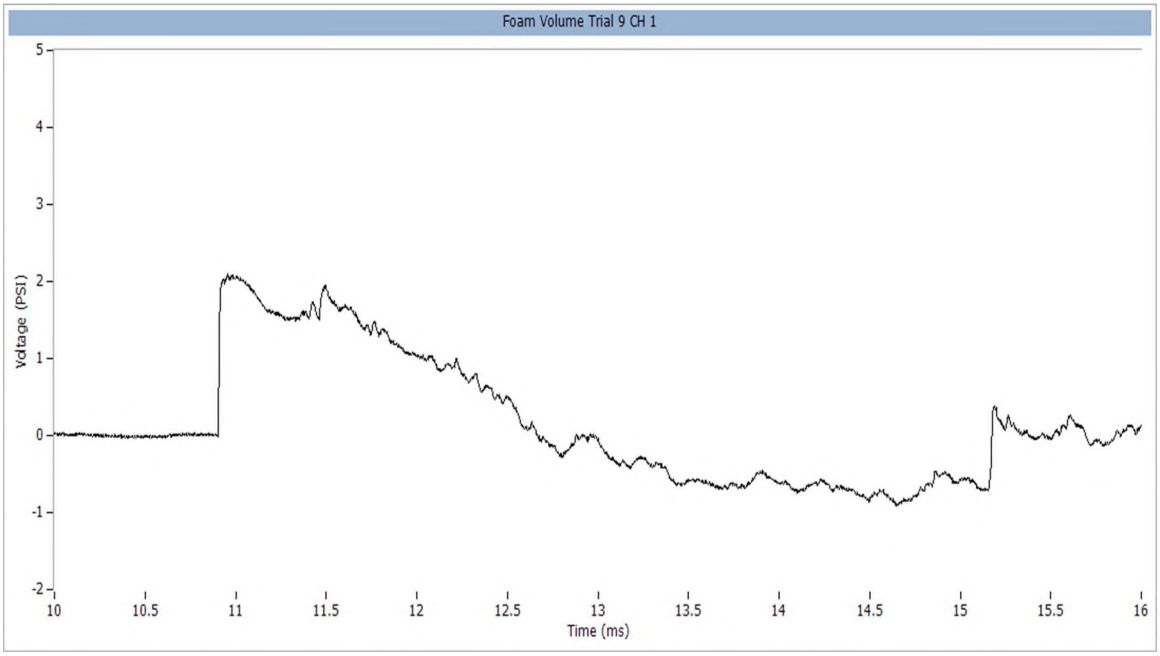

Figure C.22. Foam volume testing trial 9, channel 1 (psi).

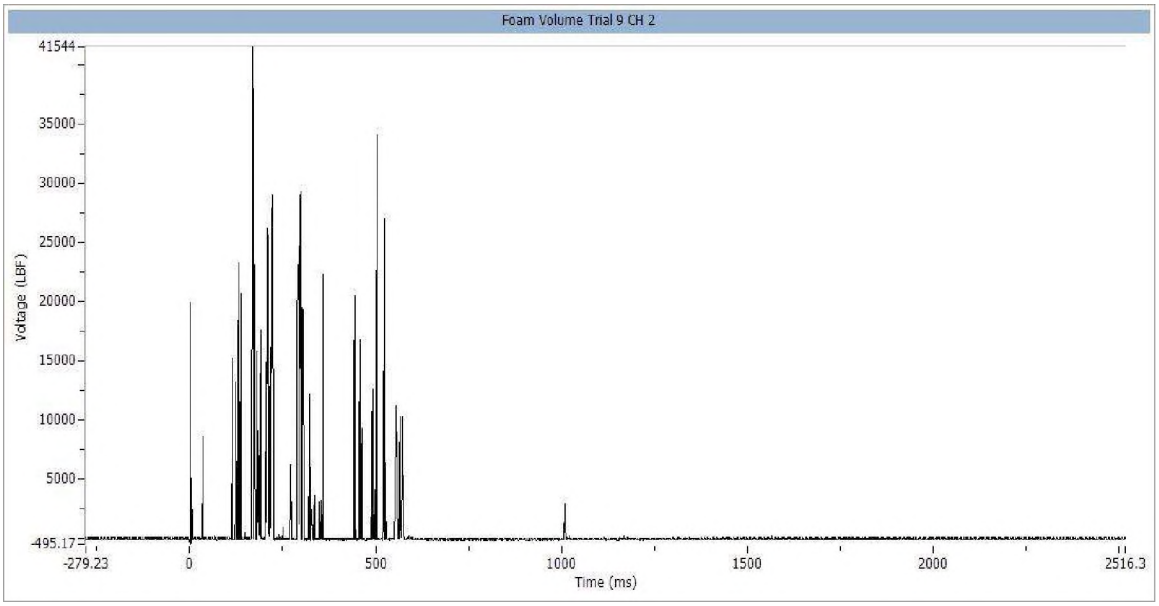

Figure C.23. Foam volume testing trial 9, channel 2 (lbf).

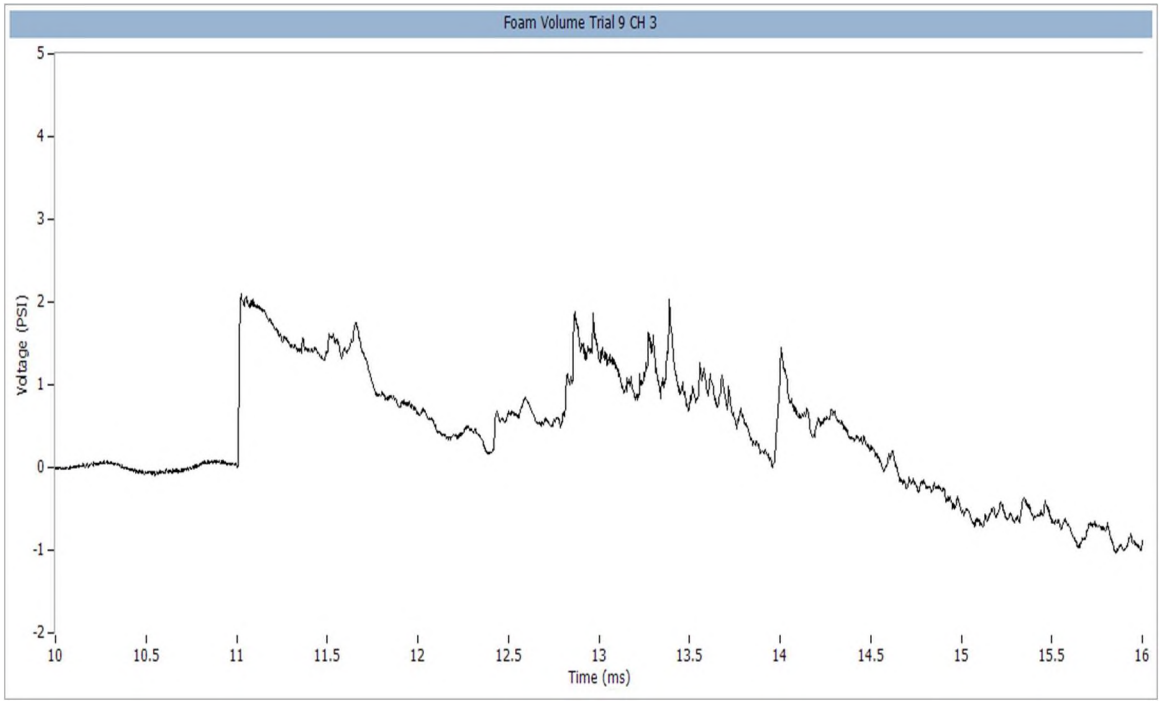

Figure C.24. Foam volume testing trial 9, channel 3 (psi).

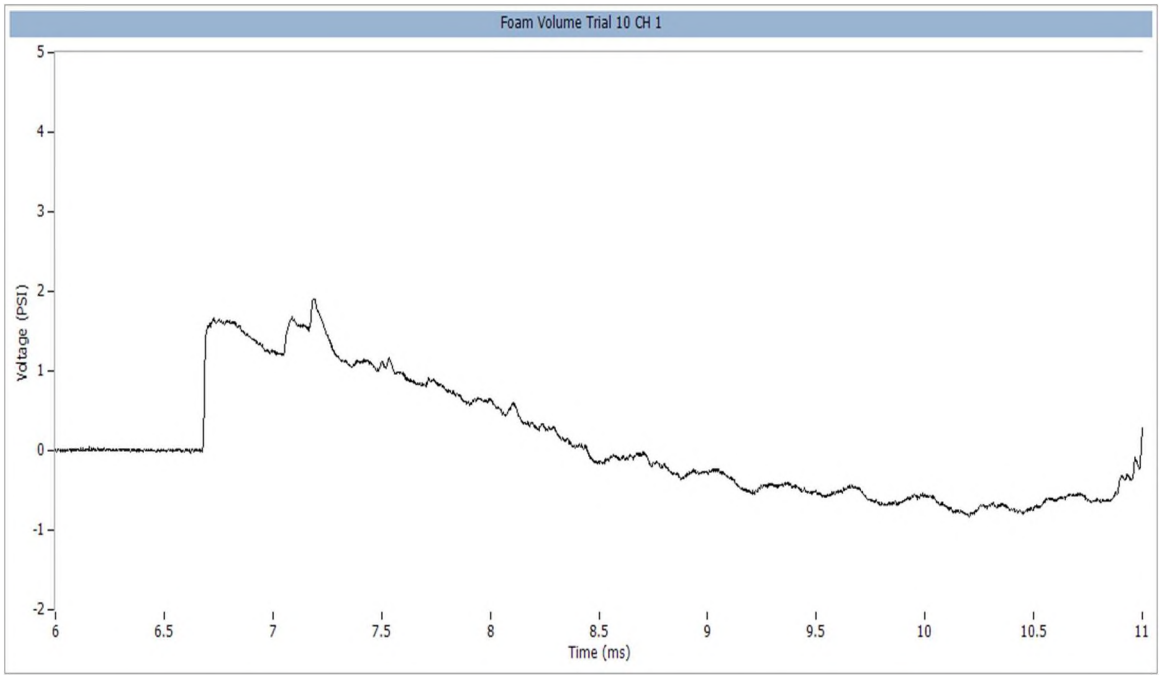

Figure C.25. Foam volume testing trial 10, channel 1 (psi).

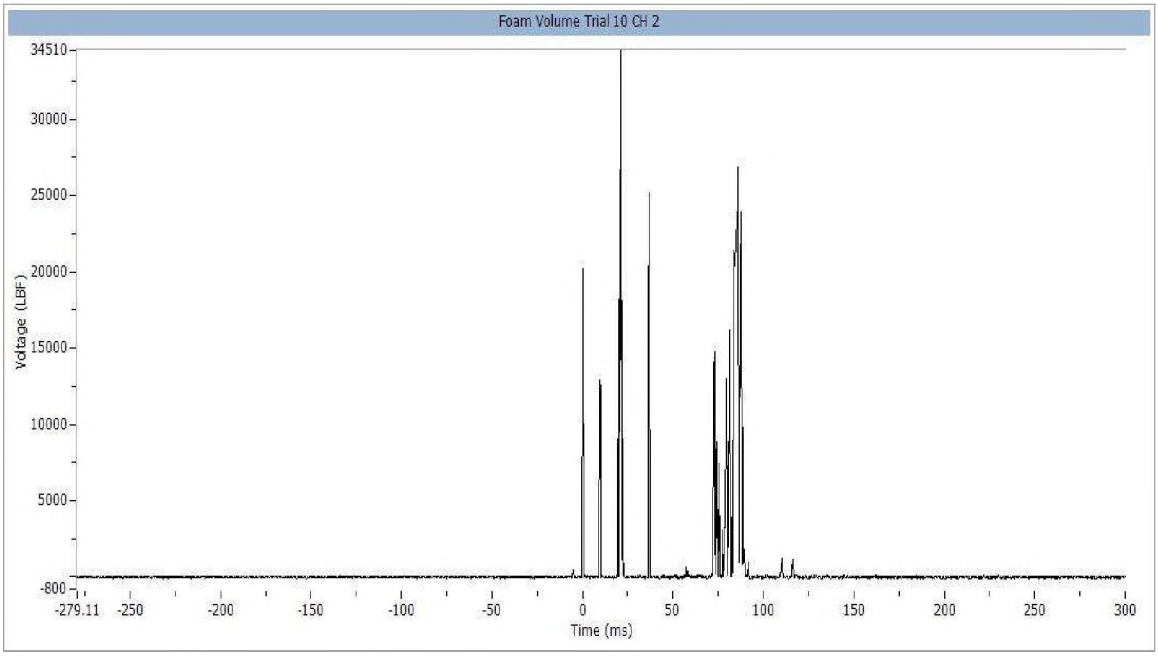

Figure C.26. Foam volume testing trial 10, channel 2 (lbf).

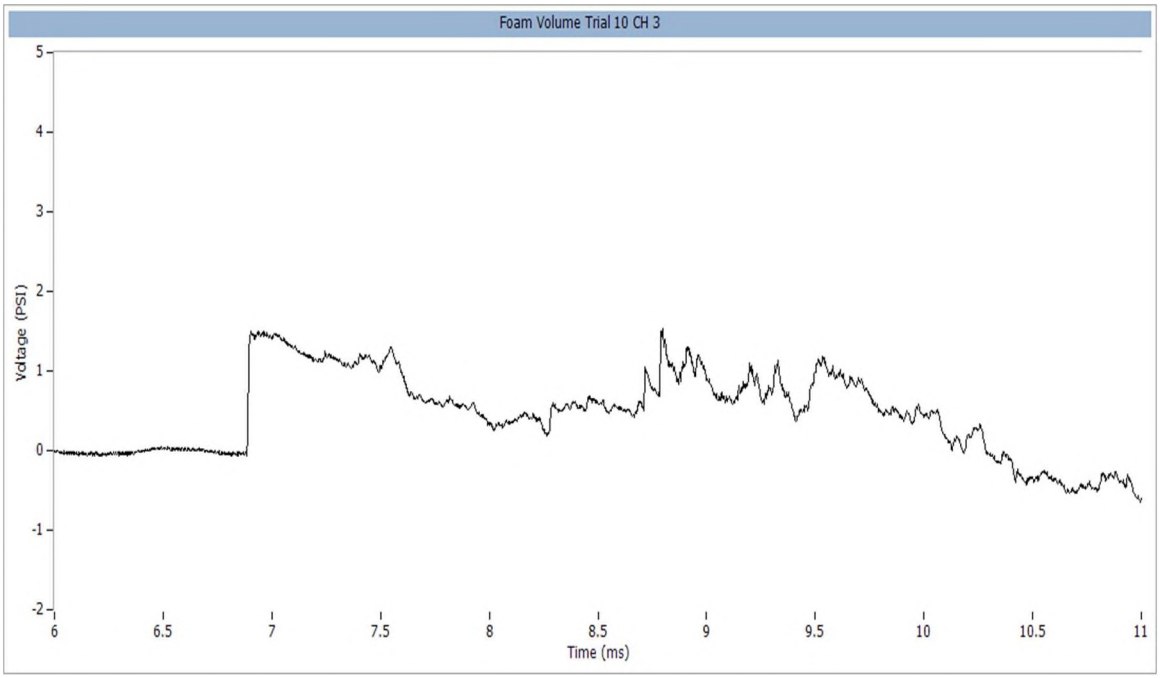

Figure C.27. Foam volume testing trial 10, channel 3 (psi).

APPENDIX D.

EXPERIMENTAL GRAPHS AND SENSOR DOCUMENTATION

This appendix contains all other pertinent experimental data, figures, and sensor calibration documentation. This data was collected by two pressure tranducers and a load-cell force sensor. All sensor signals were sent through a signal conditioner before being collect and stored in an MREL data accusation system. This stored data was analyzed and interpreted using MREL compatible software and then further analyzed using graphing software. The data were presented in order of performed testing and by alphabetical order of tested explosive type. The sensor documentation was compiled by PCB Pizeotronics.

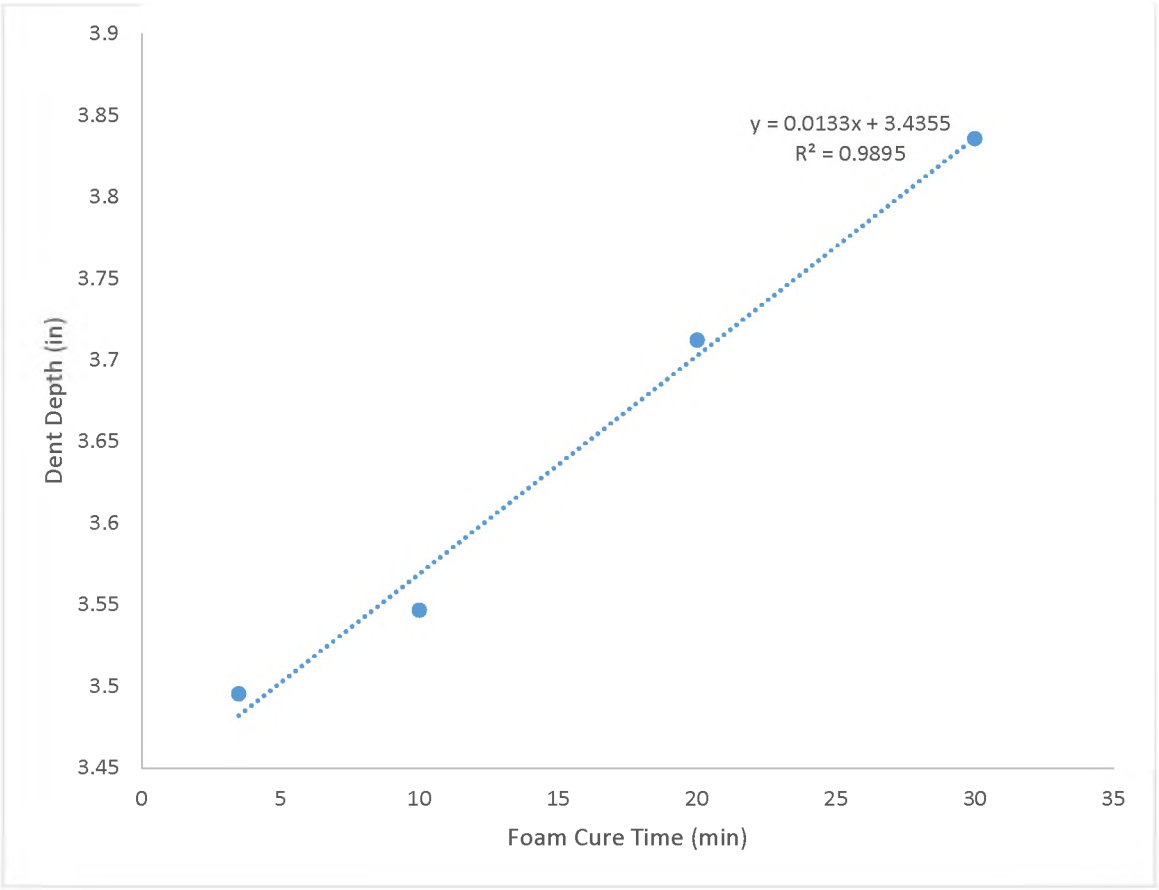

Figure D.1. C-4 Plate Dent depth on witness plate with varying cure times of rigid polyurethane foam confinement.

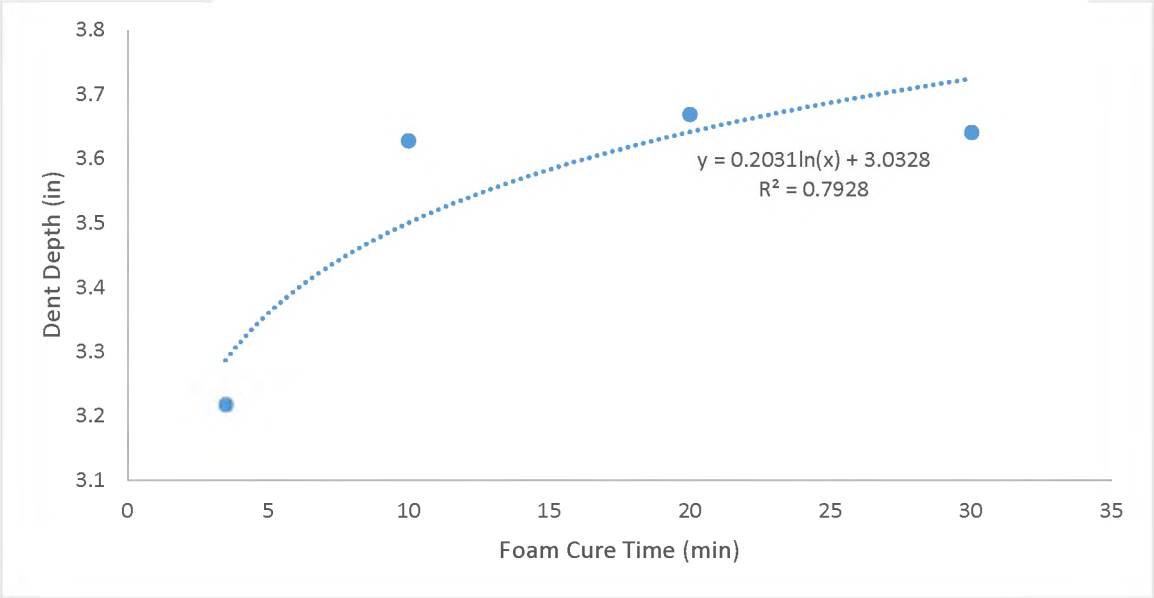

Figure D.2. DetaSheet witness Plate Dent depth versus the polyurethane-foam confinement foam cure times.

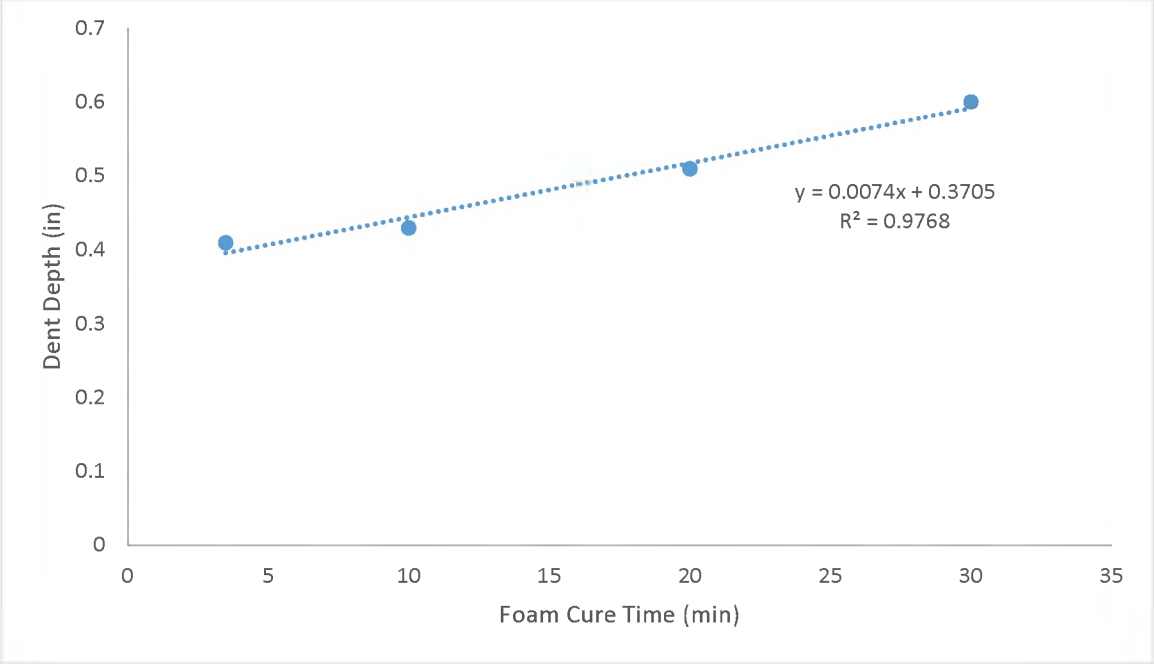

Figure D.3. TexPak witness plate dent depth versus polyurethane-confinement foam cure times.

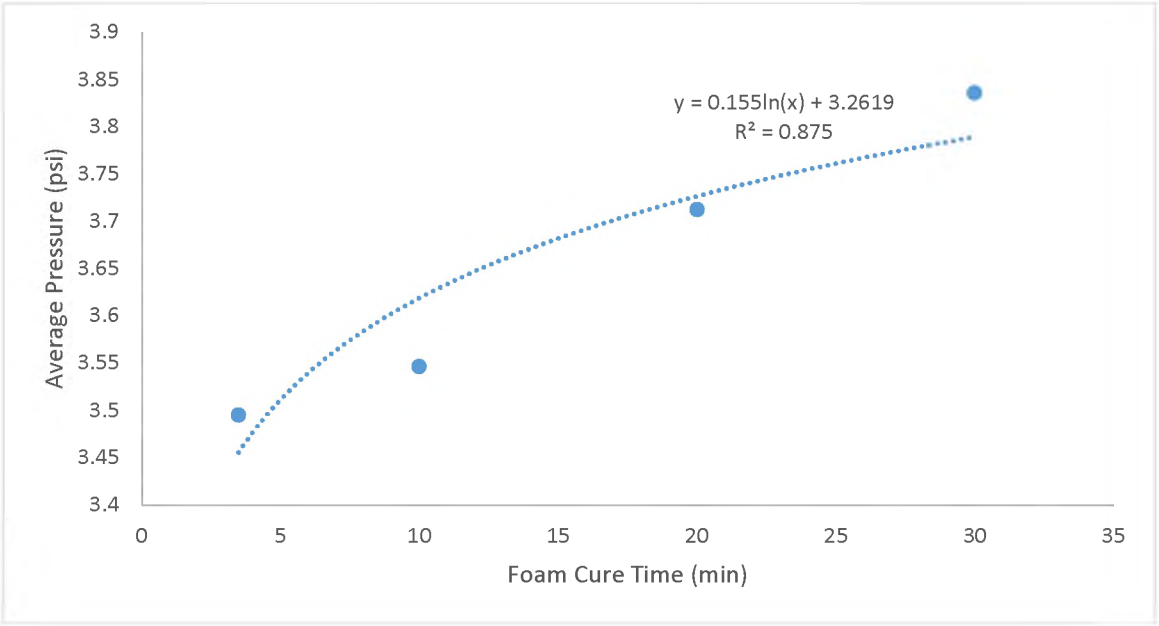

Figure D.4. C-4 averaged recorded positive peak pressure compared to the polyurethane-confinement foam cure time.

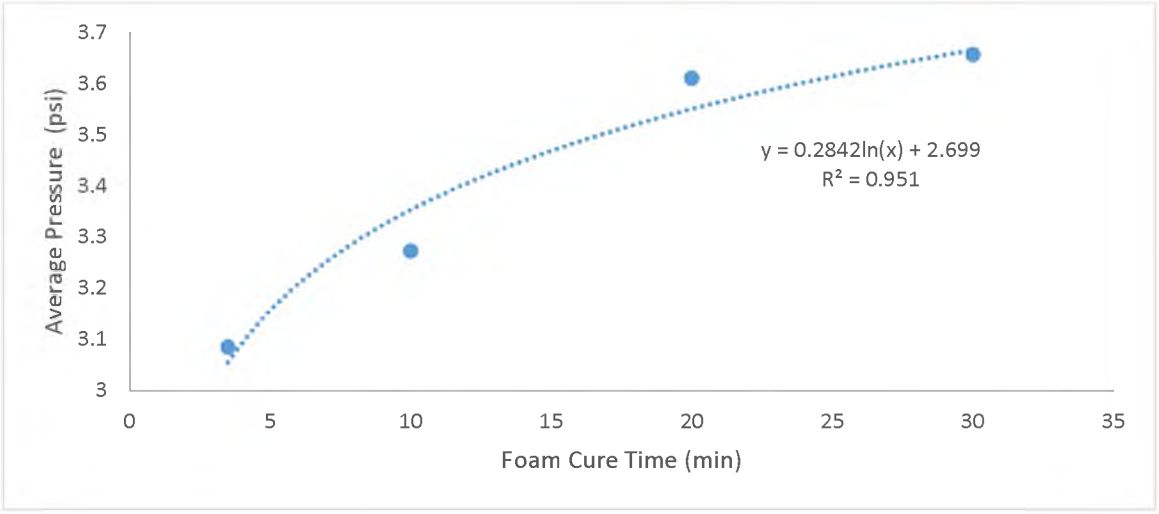

Figure D.5. DetaSheet recorded average positive peak pressure versus polyurethane-foam confinement cure time.

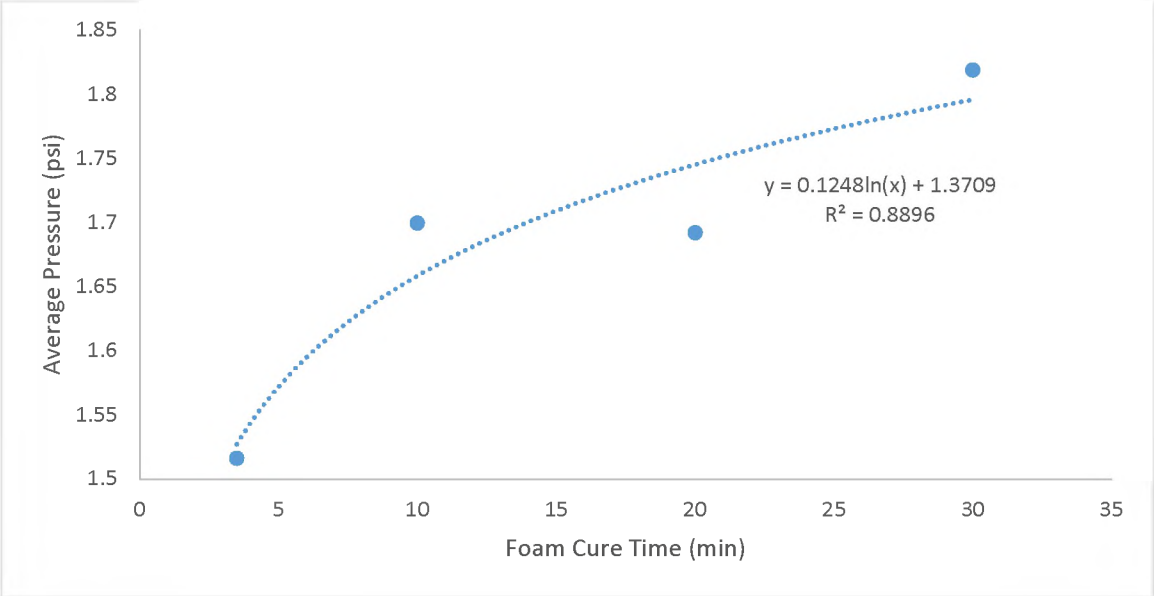

Figure D.6. Positive peak pressures measured of detonation of KineStik explosive with variable confining polyurethane foam cure time.

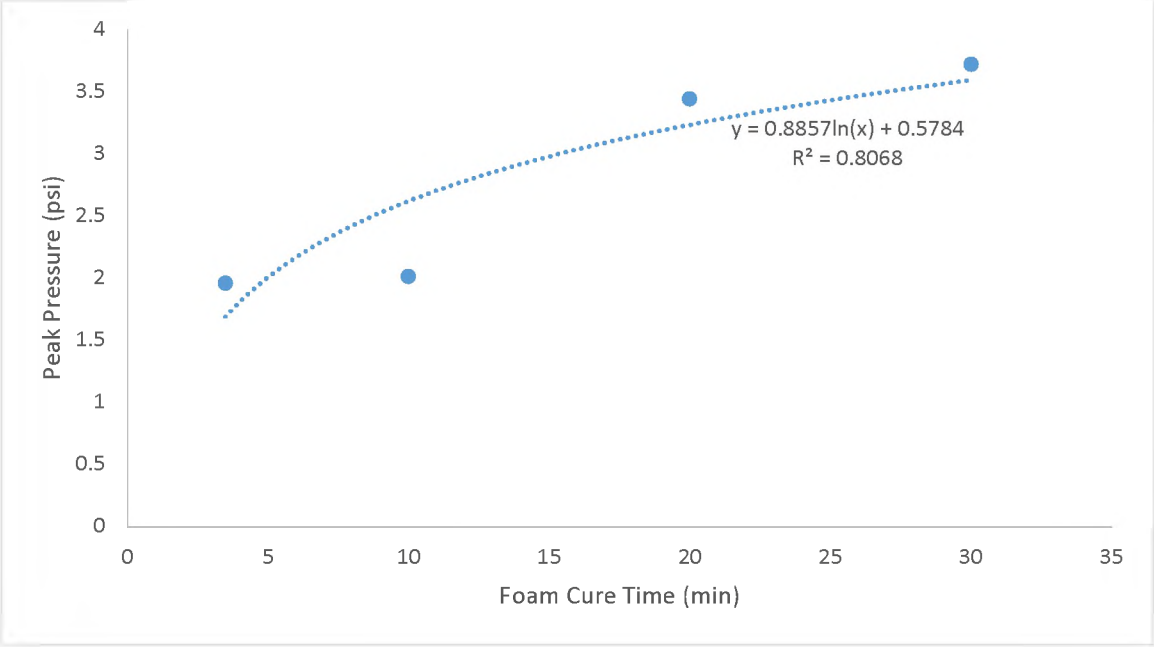

Figure D.7. TexPak positive peak pressure recorded in comparison to variable polyurethane foam cure time.

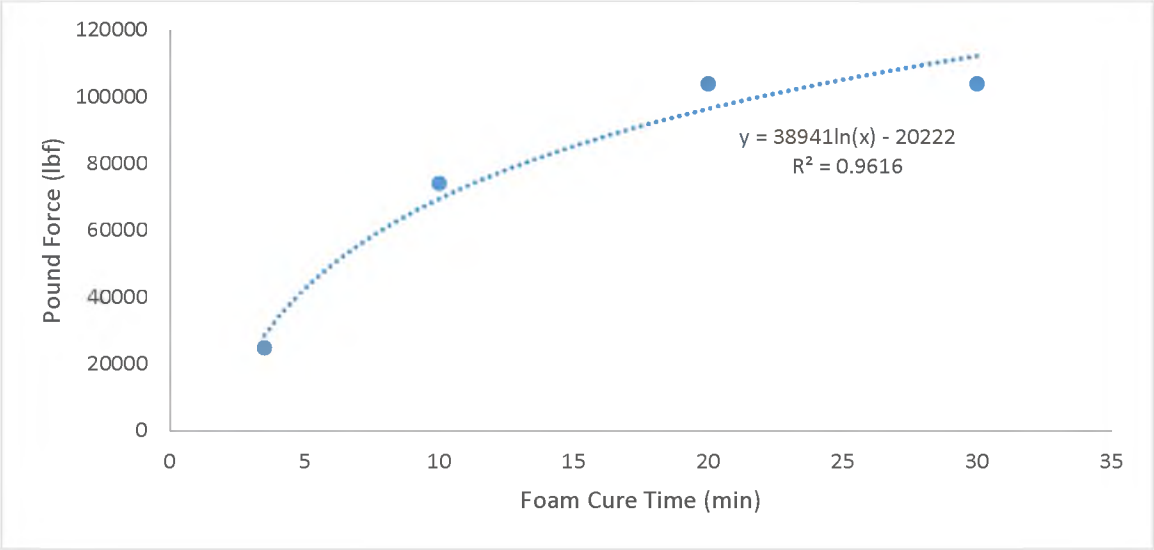

Figure D.8. C-4 compression force on load cell sensor as polyurethane-confinement foam cure time increased.

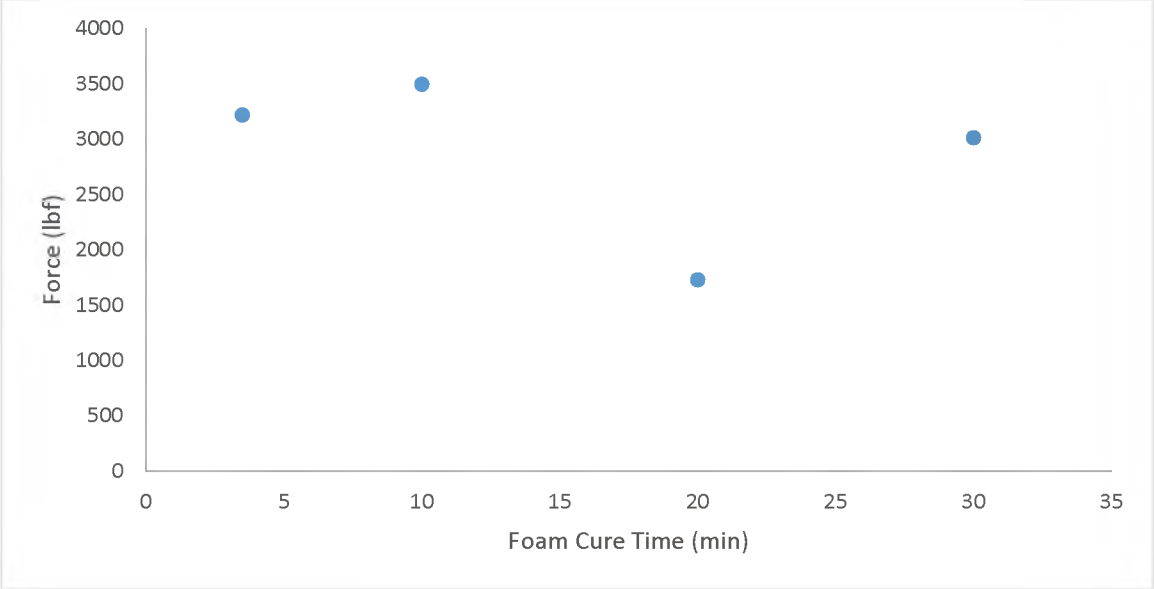

Figure D.9. The compression force of DetaSheet detonation with respect to the polyurethane foam cure time.

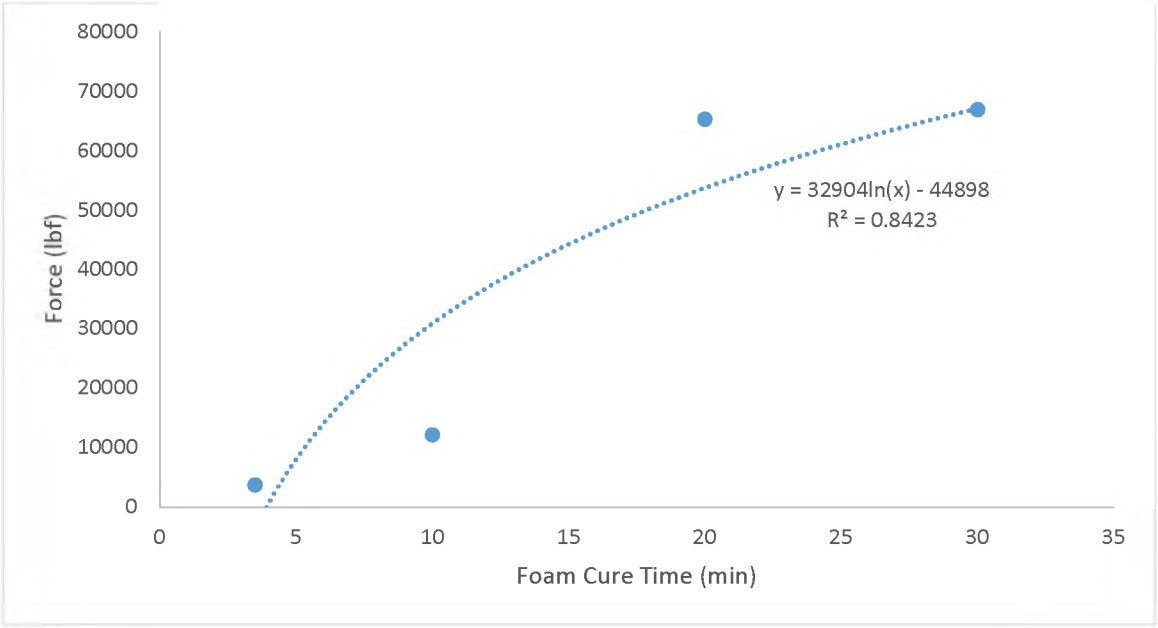

Figure D.10. Compression forces of KineStik explosive detonation with varying foam cure times of the polyurethane foam confining material.

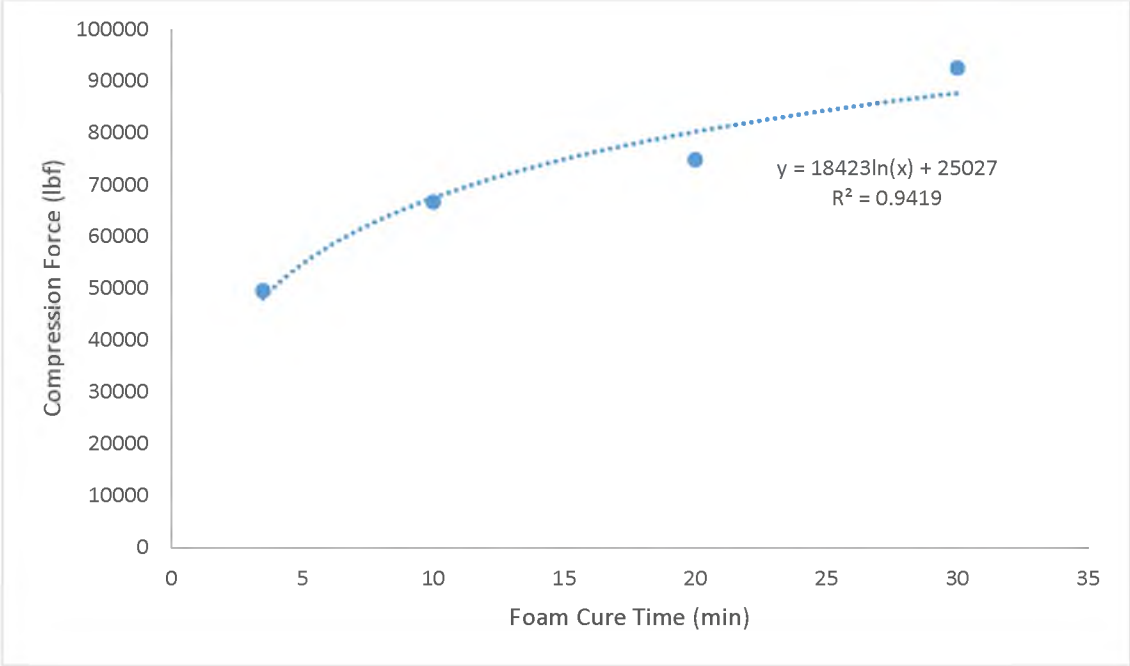

Figure D.11. TexPak recorded compression forces as the polyurethane foam cure time increased.

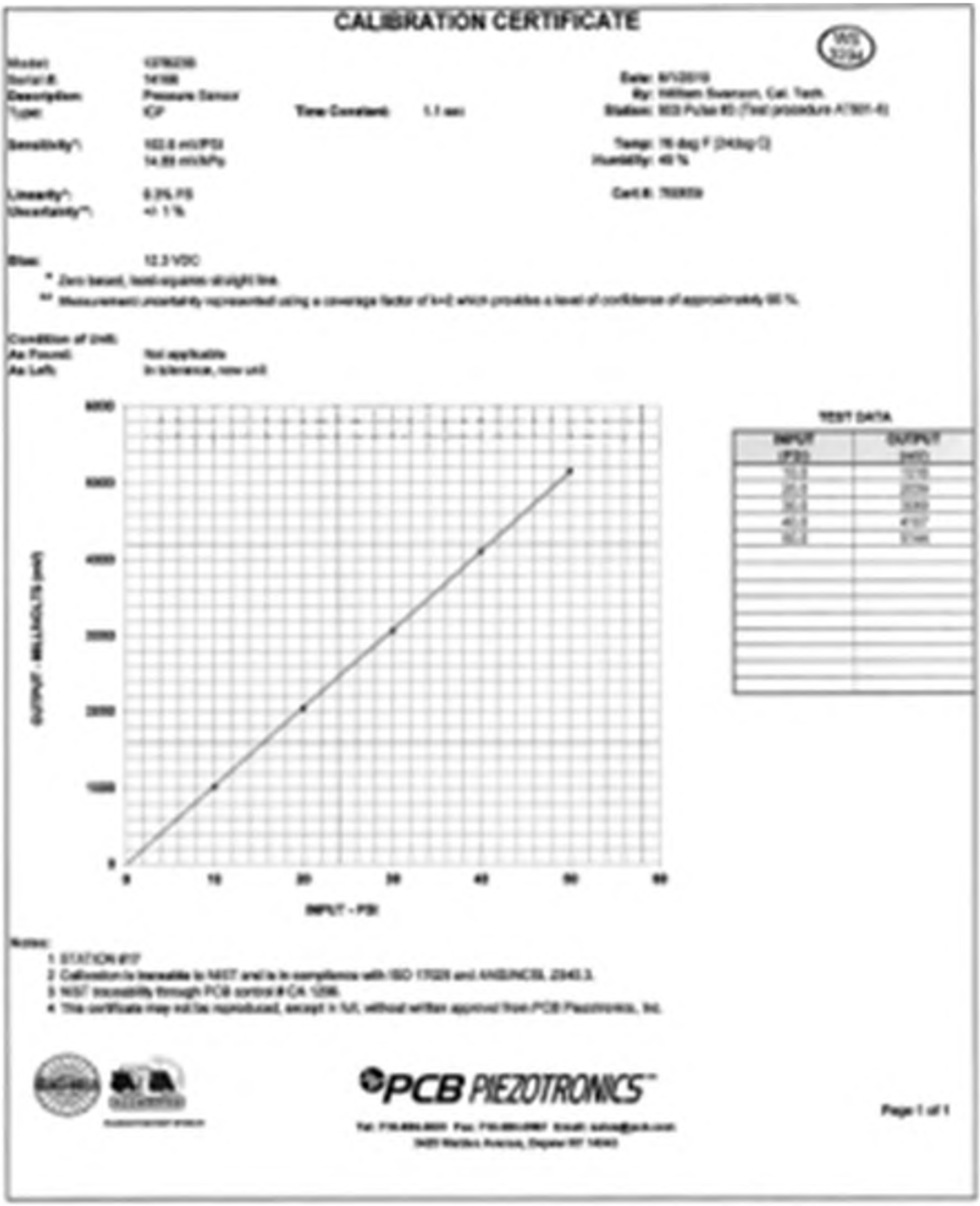

Figure D.12. Calibration sheet for pressure sensor probe S/N 14166.

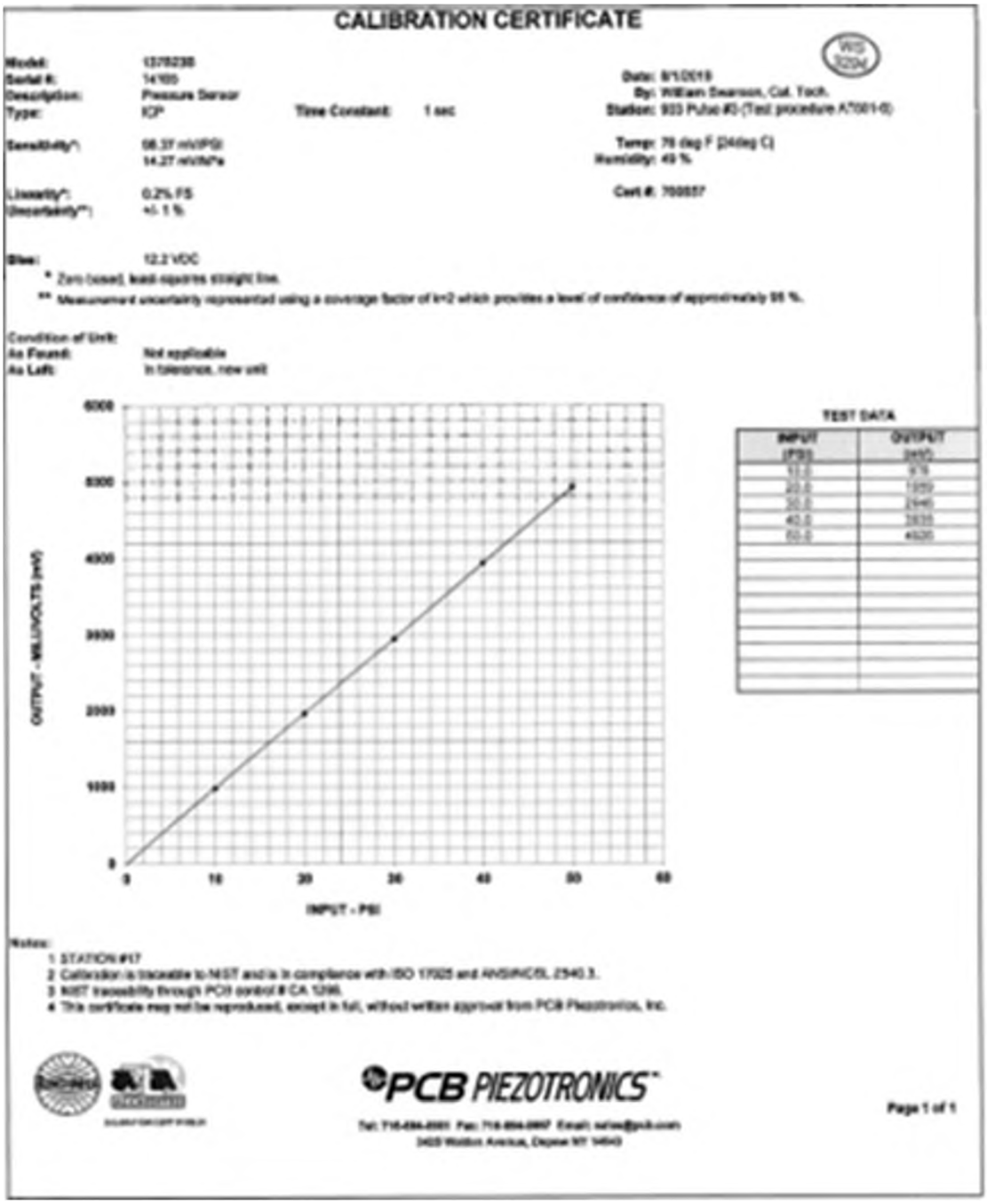

CALIBRATION CERTIFICATE

Model: 137B23B
Serial #: 14165
Description: Pressure Sensor
Type: ICP
Time Constant: 1 sec
Date: 8/1/2018
By: William Swanson, Cal. Tech.
Station: 933 Pulse #3 (Test procedure A7001-0)
Sensitivity*: 68.37 mV/PSI
14.27 mV/kPa
Temp: 76 deg F (24deg C)
Humidity: 49 %
Linearity*: 0.2% FS
(Uncertainty**): +/- 1 %
Cert #: 700557
Bias: 12.2 VDC

* Zero based, least-squares straight line.

** Measurement uncertainty represented using a coverage factor of k=2 which provides a level of confidence of approximately 95 %.

Condition of Unit:
As Found: Not applicable
As Left: In tolerance, new unit

TEST DATA

INPUT (PSI)	OUTPUT (mV)
10.0	678
20.0	1359
30.0	2040
40.0	2835
50.0	4520

OUTPUT - MILLIVOLTS (mV)

6000
5000
4000
3000
2000
1000
0

0 10 20 30 40 50 60

INPUT - PSI

Notes:
1. STATION #17
2. Calibration is traceable to NIST and is in compliance with ISO 17025 and ANSI/NCSL Z540.3.
3. NIST traceability through PCB control # CA 1298.
4. This certificate may not be reproduced, except in full, without written approval from PCB Piezotronics, Inc.

PCB PIEZOTRONICS

Page 1 of 1

Figure D.13. Calibration sheet for pressure sensor probe S/N 14165.

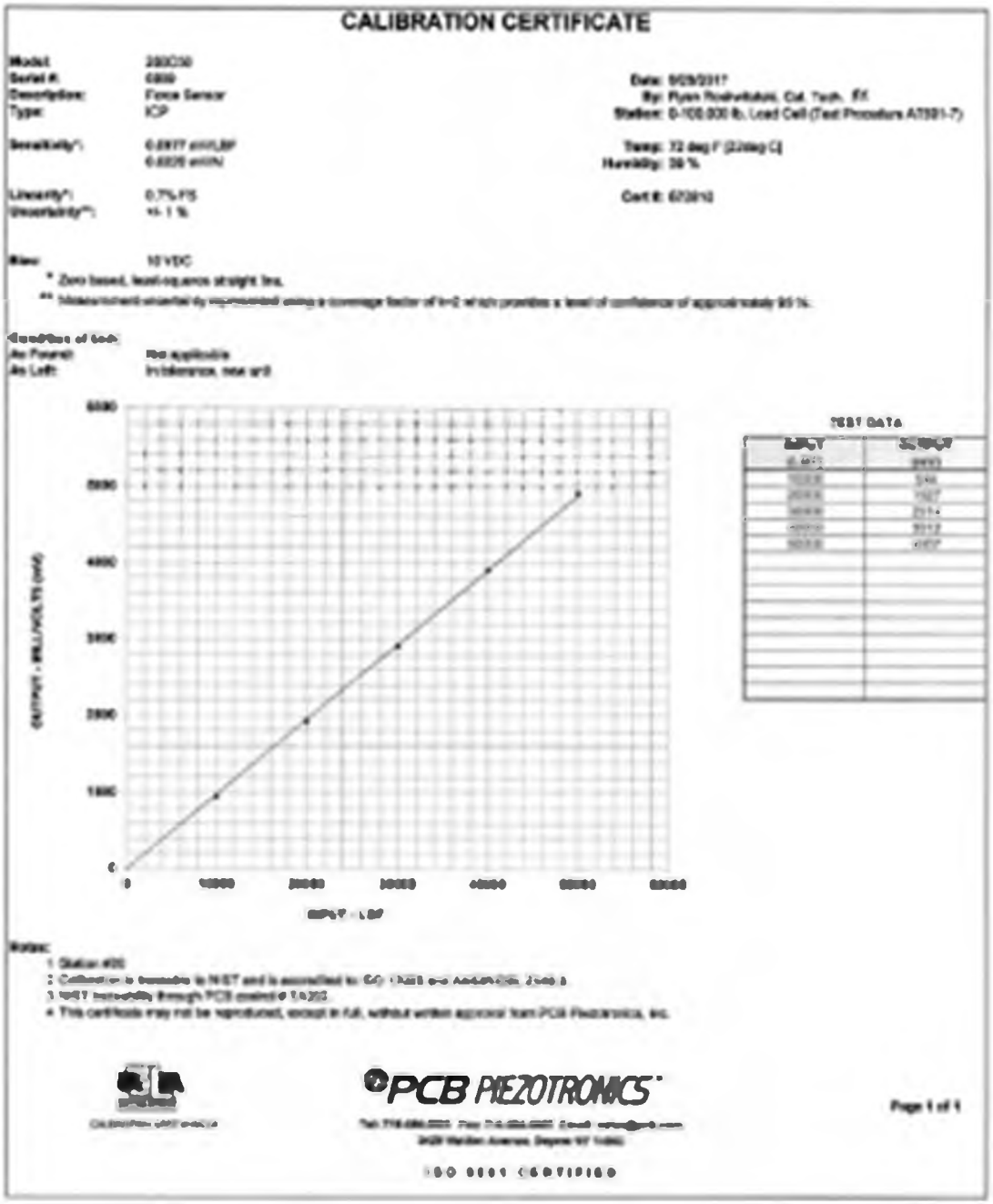

Figure D.14. The compression force load-cell sensor calibration sheet.

BIBLIOGRAPHY

A'Costa, A. (1999). *United States of America/ CO Patent No. 5883328.*

Akers, S. (2005). *Numerical Simulations of Explosive Wall Breaching.* Vicksburg: USACE Engineer Research and Development Center.

Akers, S. (2007). *Breaching of Triple-Brick Walls: Numerical Simulations.* Vicksburg: USACE Engineer Research and Development Center.

Alba, A. L. (1997). *The Use of Rigid Polyurethane Foam as a Landmine Breaching Technique.* Monterey: Naval Postgraduate School.

Atkins, P. (2010). *The Laws of Thermodynamics: A Very Short Introduction.* New York: Oxford University Press.

Boshoff, D. (2011). Testing stemming performance, possible or not? *The Journal of The Southern African Institute of Mining and Metallurgy*, Volume 111.

Bureau of Alcohol Tabacco and Firearms. (2014). ATF Law Enforcement Guide to Explosives Incident Reporting. Redstone, Alabama, United States of America.

Cantrell, M. (2020, March 3). *Five types of correctional breaching.* Retrieved from Correntions1: https://www.corrections1.com

Carpenter, C. (2011). *Neogard: N6 Building Envelope System.* Dallas: Neogard.

Cevizci, H. (2013). A New Stemming Application for Blasting. *Minas, Ouro Preto*, 513-519.

Chemring Energetics UK Limited. (n.d.). *C4 Mouldable Plastic Explosive.* Corsham: Chemring Energetics UK Limited.

Committee on Gulf War and Health: Long-Term Effects of Blast Exposures; Board on the Health of Select Populations; Institute of Medicine. (2014). *Gulf War and Health, Volume 9: Long-Term Effects of Blast Exposures.* Washington D.C.: National Academies Press (US).

Cooper, H. F. (1976). *Estimates of Crater Dimensions for Near-Surface Explosions of Nuclear and High-Explosives.* Livermore: Lawrence Livermore Laboratory.
Cooper, P. (1996). *Explosive Engineering.* Hoboken: Wiley.

Corrosion Pedia. (2017). Tack-free Time. *Corrosion Pedia.*

Department of Mining Engineering. (2017). *Experimental Mine Operating Procedure.* Rolla: University of Missouri Science and Technology.

Department of the Army. (2006). *Urban Operations.* Washington D.C.: Headquarters Department of the U.S. Army.

Dolah, R. .. (1961). *Relative Efficiency of Stemming Materials in Reducing Incendivity of Permissible Explosives.* United States Department of the Interior.

Elbeih, A. (2019). Preparation and Characterization of a New High-Performance Plastic Explosive in Comparison with Traditional Types. *International Journal of Chemical Engineering*.

Ezekiel Enterprises, LLC. (n.d.). Explosives. In L. Ezekiel Enterprises, *Rock Excavation Blasting Design Part 1* (pp. 14-25). New Smyrna Beach: EZ-pdh.

Feldgun, V. (2016). *Some Characteristics of Confined and Partially Confined Explosions.* Israel: National Building Research Institute.

Foster, J. S. (1983). *United States of America/ DC Patent No. 4418622.*

Grainger. (2020, October 1). *Great Stuff Insulating Foam Sealant.* Retrieved from Grainger: https://www.grainger.com/ec/pdf/48WK15_3.pdf

Hansen, A. J. (2017). Forcible Entry: The Frame Spreader. *Fire Prevention & Protection, Firefighter Training, Firefighting*, Issue 9, Volume 170.

Hetherington, J. (1994). *Blast and Ballistic Loading of Structures.* New York: Routledge.

Ingesson, L. (2014). *The United States of America. CA Patent No. 8794597B1.*

Jacobs, S. J. (1970). *United States of America/ MD Patent No. 3517615.*

Janssen, T. (2011). *Explosive Materials Classification, Composition, and Properties.* New York: Nova Science Publisher.

Kamimori, G. H. (2017). Occupational Overpressure Exposure of Breachers and Military. *Crossmark*.

Knepper, R. (2014). *Effects of Confinement on Detonation Behavior of Vapor-Deposited.* Albuquerque: Sandia National Laboratories.

Konya, C. J. (1990). *Surface Blast Design.* Englewood Cliffs: Prentice-Hall.

Lehman, M. D. (2010). *United States of America/ OH Patent No. 7819063B1.*

Licht, H.-H. (2000). *Propellants, Explosives, Pyrotechnics.* Germany: International Pyrotechnics Society.

Long, A. (2013). Breacher, You Have Control! *Marine Corps News.*

Lupoae, M. (2011). Aspects regarding the Water Jet Propulsion using Explosive Energy for Door Breaching. *Proceedings of the World Congress on Engineering.* London: World Congress on Engineering.

Lupoae, M. (2017). Metallic Doors Under Explosive Charges Detonation. *International Conference on Military Technologies (ICMT).* BRNO: ICMT.

Marques, P. D. (2014). *Guerrilla Warfare Tactics In Urban Environments.* Auckland: Pickle Partners Publishing.

Marz, H. F. (1985). *Canada Patent No. 4492165.*

MREL Blasting Instrumentation. (2020, October 15). *DAS Data Acquisition Suite*. Retrieved from MREL Blasting Instrumentation: http://mrel.com/blasting_instrumentation/supportdas.html

MREL Group of Companies Limited. (2021, January 22). *The World's Most Capable Data/VOD Recorder*. Retrieved from MREL Group of Companies Limited: http://mrel.com/blasting_instrumentation/datatrap.html

National Center for Biotechnology Information. (2021, January 22). *Cyclonite.* Retrieved from PubChem Compound Summary for CID 8490: https://pubchem.ncbi.nlm.nih.gov/compound/Cyclonite

National Center for Biotechnology Information. (2021, January 20). *Diethylenetriamine*. Retrieved from PubChem: https://pubchem.ncbi.nlm.nih.gov/compound/Diethylenetriamine

National Center for Biotechnology Information. (2021, January 22). *Pentaerythritol tetranitrate.* Retrieved from PubChem Compound Summary for CID 6518: https://pubchem.ncbi.nlm.nih.gov/compound/Pentaerythritol-tetranitrate

PCB Piezoelectonic. (2020). *Sensor Signal Conditioner.* Depew: PCB Piezoelectonic Inc.

PCB Piezoelectonics. (2020). *ICP Force Sensor.* Depew: PCB Piezoelectonics Inc.

PCB Piezoelectronics. (2020). *ICP Pressure Sensor.* Depew: PCB Piezoelectronics.

PCB Piezoelectronics. (2020). *Installation Drawing of Micro Sensor.* Depew: PCB Piezoelectronics Inc.

Persson, P.-A. (1994). *Rock Blasting and Explosive Engineering.* Boca Raton, Ann Arbor, London, Tokyo: CRC Press.

Pimbley, G. H. (1980). *Investigating Explosive and Material Properties by Use of the Plate Dent Test.* Los Alamos: Los Alamos Scientific Laboratory.

Pool, J. E. (1961). *United States of America/ VA Patent No. 2967099.*

Ranum, N. S. (2013, October 1). SRT MARINES CERTIFY CAPAB. The *United States Marine Corps Photograph*. Camp Hansen, Japan: United States Marine Corps.

Robbins, G. (1989). *Australia Patent No. 4846278.*

Sanai, M. (1995). *United States of America/ CA Patent No. 5417161.*

Sanai, M. (1995). *Unites States of Ameria/ Ca Patent No. 5417161.*

Snelling, W. O. (1912). *The Effect of Stemming on the Efficiency of Explosives.* Washington D.C.: Department of Commerce U.S. Government Printing Press.

Stark, H. J. (1954). *Low density cellular explosive foam and products made therefrom*. Retrieved 12 29, 2020, from http://freepatentsonline.com/2845025.html

Stewart, J. B. (2013). *Air Blast Calculations.* Aberdeen Proving Ground: Army Research Laboratory.

TACTICAL-LIFE.COM. (2007). Breaching Door. *Tactical Weapons Magazine*.

Thomas, R. (1965). *Unites States of America/ Va Patent No. 3198177.*

Tripwire Operations Group. (2021, January 15). *TexPak All-Liquid Binary.* Retrieved from Tripwire Operations Group: https://tripwireops.org/texpak/

TRZCINSKI, W. A. (2001). *Application of a Cylinder Test for Determining Energetic Characteristics of Explosives.* Warszawa: Military University of Technology.

Wunderli, J. M. (2014). Modeling the Source Strength of Explosions Under Consideration of the Ground Influence. *The Journal of the European Acta Acustica united with Acustica*, 5.

Yancik, J. J. (1970). Predicting Blasting Strengths Of Explosives From Underwater Tests. *The 12th U.S. Symposium on Rock Mechanics (USRMS).* Rolla: The U.S. Symposium on Rock Mechanics (USRMS).

Zillig, D. J. (2007). *United States of America/ MN Patent No. 2007/0125888.*

VITA

Nathan Paerschke-O'Brien enlisted in the United States Marine Corps directly out of graduating from Fruita Monument High School from 2010 to 2015 at seventeen. After five years of service and reaching the rank of sergeant, Nathan was honorably discharged from active-duty service in 2015. Nathan then attended Colorado Mesa University, where he was awarded a Bachelor of Science degree in Chemistry in 2019. He then enrolled in the Master of Science degree program of Explosives Engineering at Missouri Science and Technology in the Fall of 2019. Nathan received his Master of Science in Explosives Engineering from the Missouri University of Science and Technology in July of 2021.